

MAGNET DESIGN

Foundations of Electromagnetic Fields, Analytical and Numerical Field Computation, Design and Optimization in Magnet Technology

Stephan Russenschuck
CERN, TE-MSC, 1211 Geneva 23



The Nürnberg Funnel

No “cooking recipes”

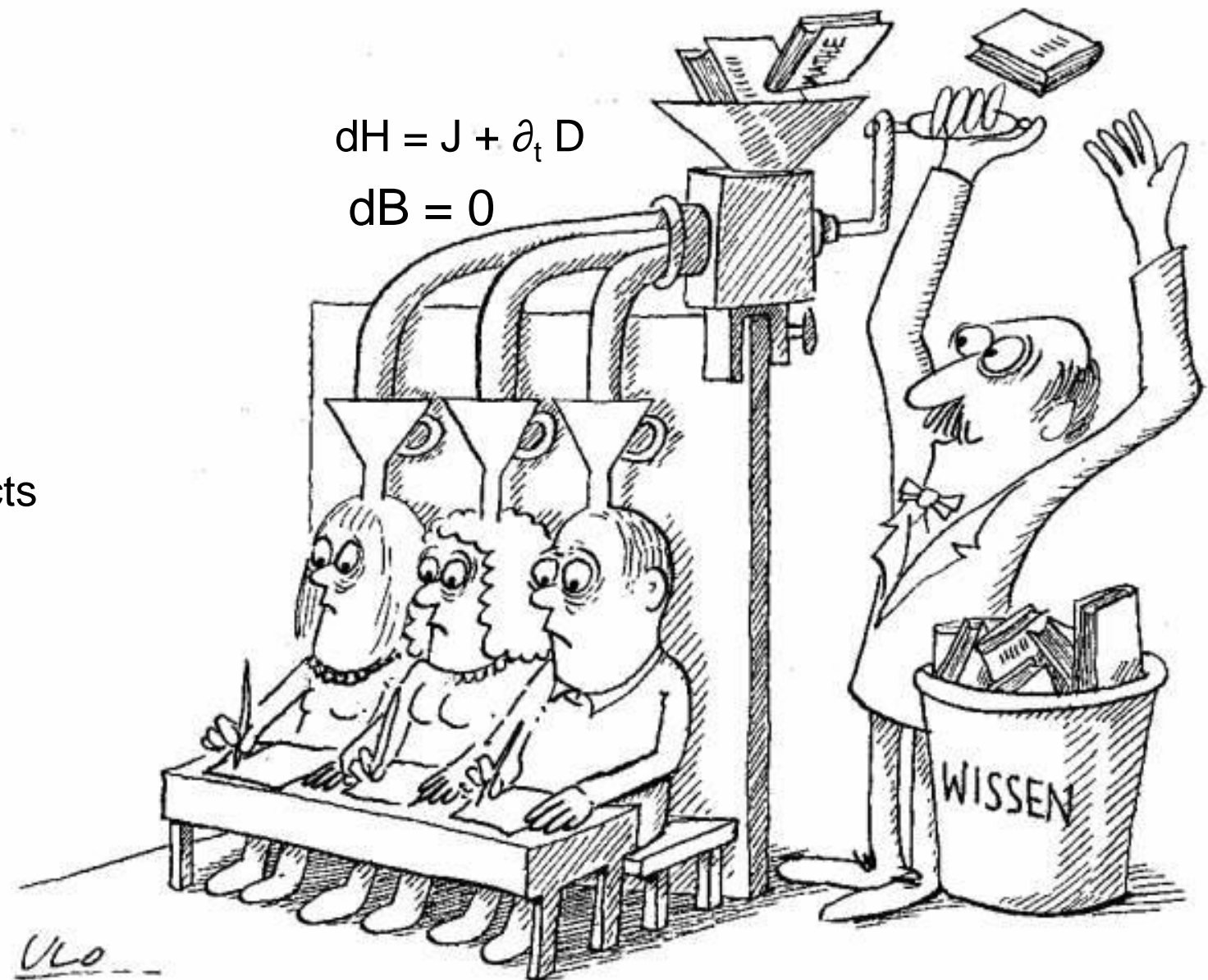
Less powerpoint

More interaction

If needed: Less subjects

$$dH = J + \partial_t D$$

$$dB = 0$$



Course Outline

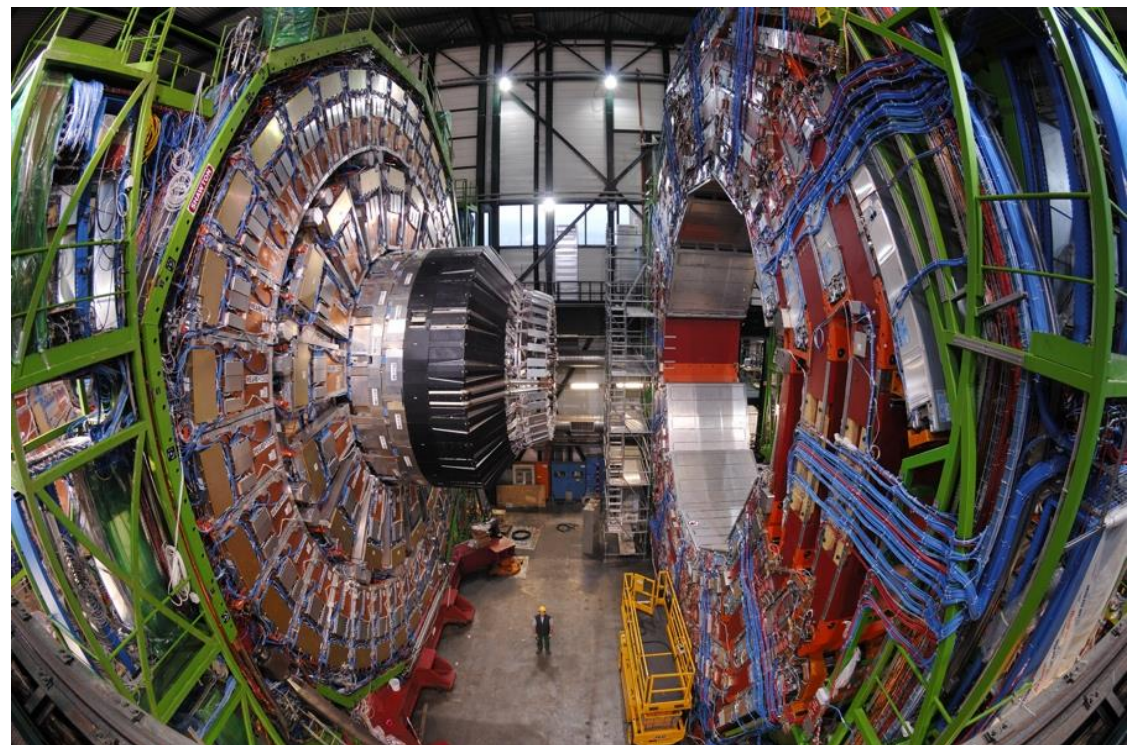
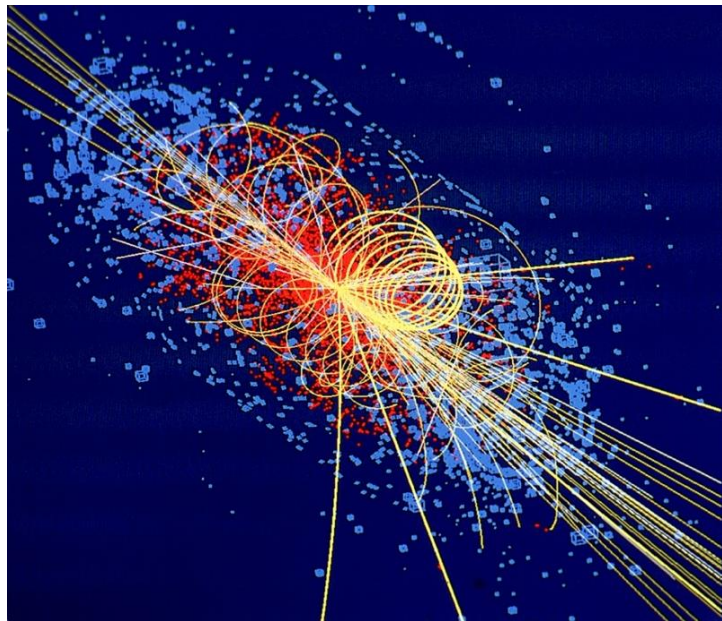
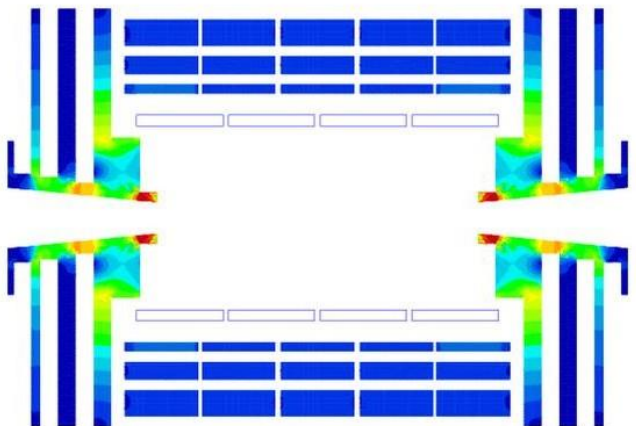
- ➔ Introduction and overview
- ➔ Mappings, Real functions, Linear algebra
- ➔ Vector analysis, Harmonic fields, Complex analysis
- ➔ Foundations of electromagnetic fields, the Maxwell equations

- ➔ Normal conducting magnets
- ➔ Magnetic field measurements
- ➔ Field of line-currents, Biot-Savart
- ➔ Coil fields of superconducting magnets, field harmonics

- ➔ Principles of numerical field computation
- ➔ Numerical field computation for accelerator magnets
- ➔ Post-processing: Inductances, persistent, interstrand coupling currents
- ➔ Quench simulation
- ➔ Mathematical Optimization techniques



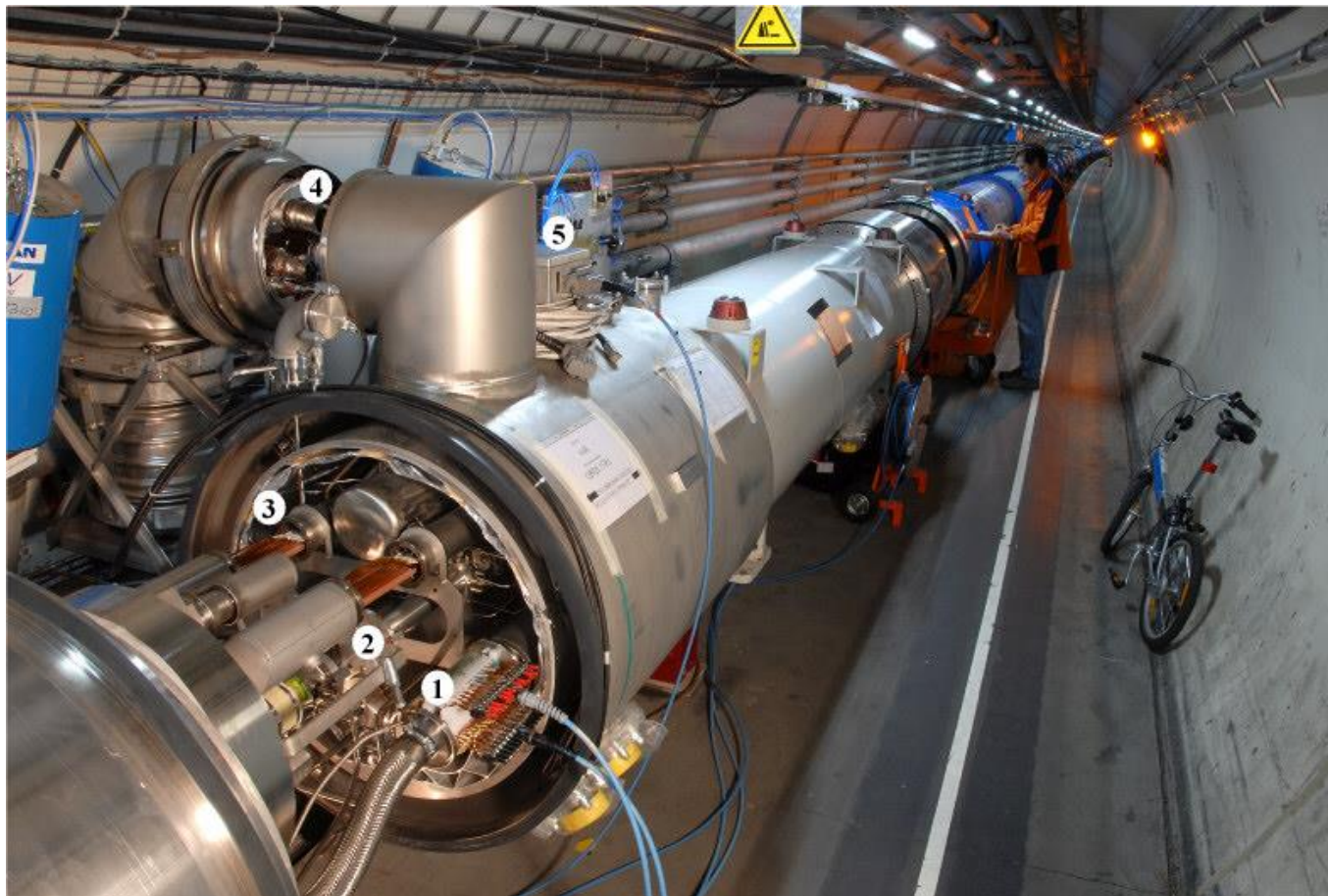
CMS (Class 1 Magnets)



$$S = R(1 - \cos \frac{\alpha}{2}) \approx \frac{R\alpha^2}{8} = \frac{QBL^2}{8p}$$

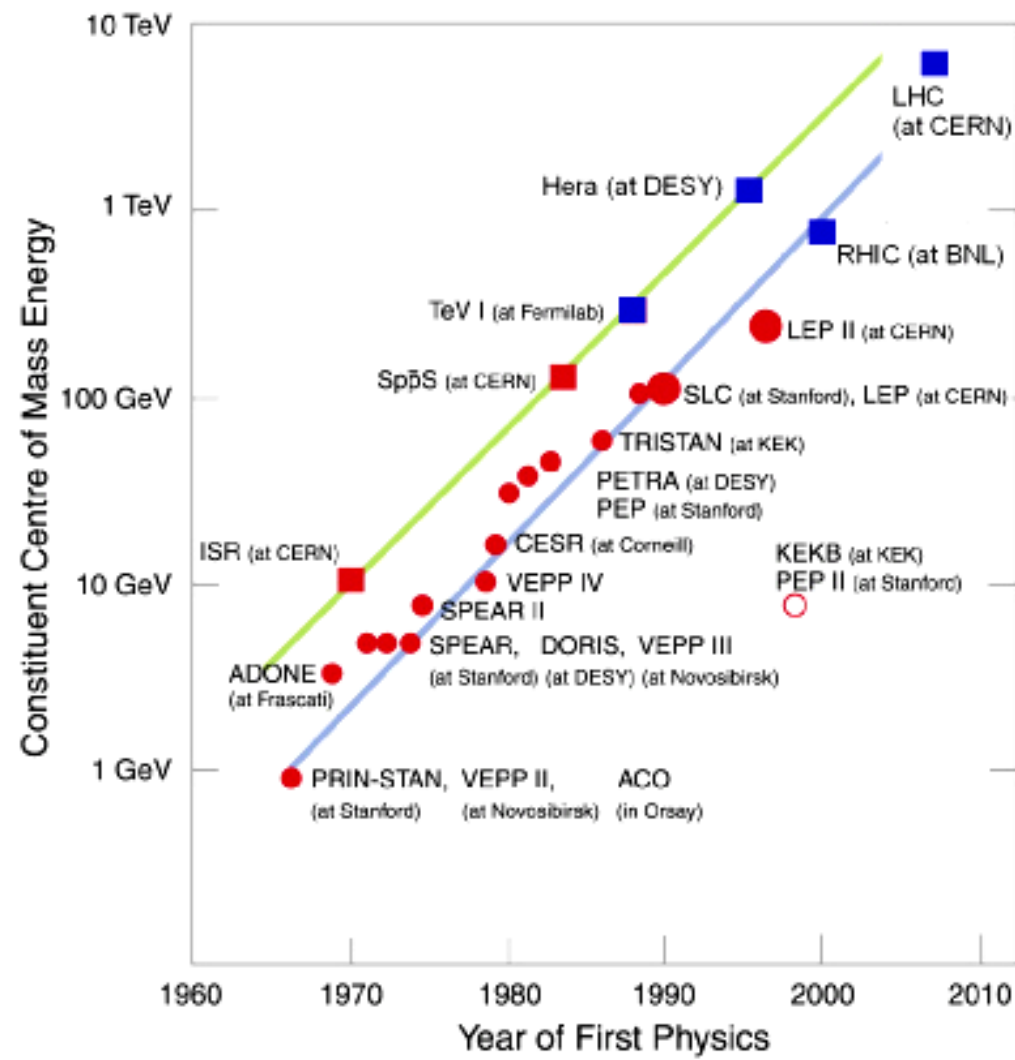
String of LHC Magnets in the Tunnel (Class 2 Magnets)

$$\{p\}_{\text{GeV}/c} \approx 0.3\{Q\}_e\{R\}_m\{B_0\}_T$$



High field and high current density

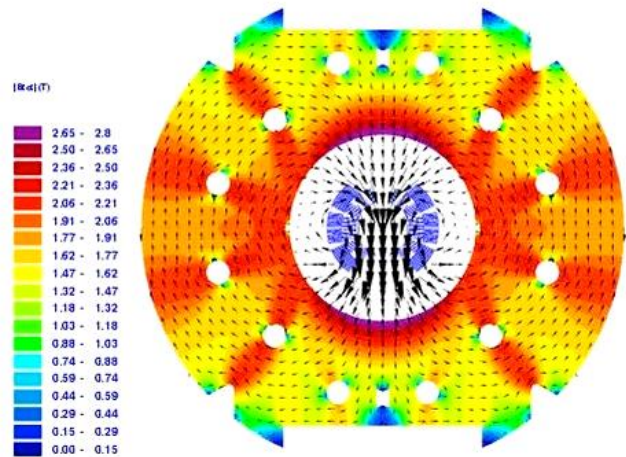
Livingston Plot



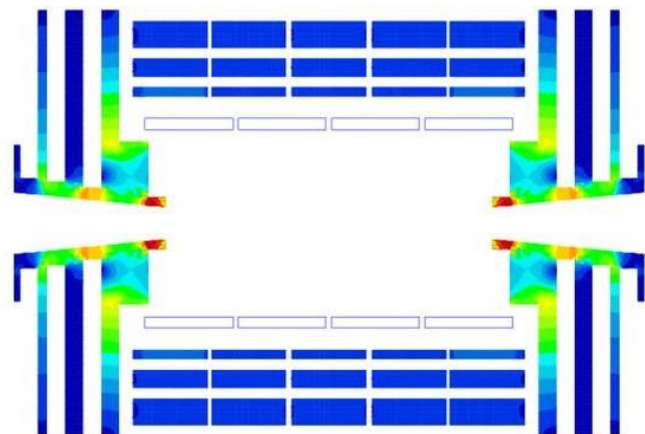
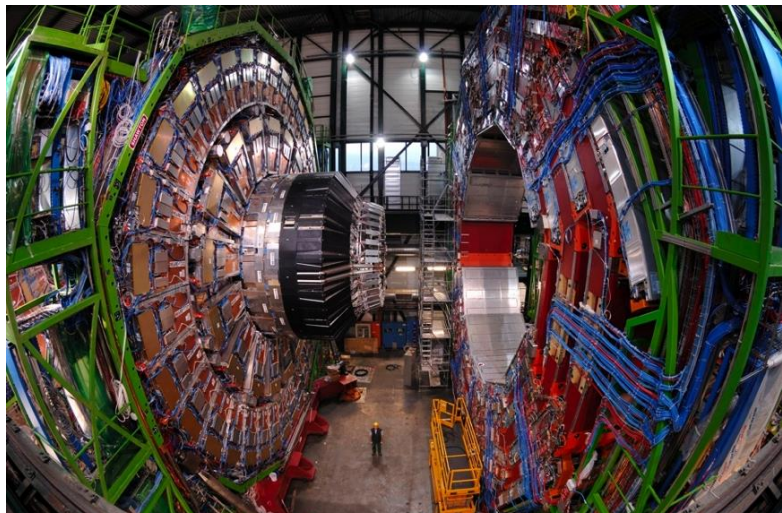
Blue: Accelerator project using SC technology



Coil Dominated Magnets

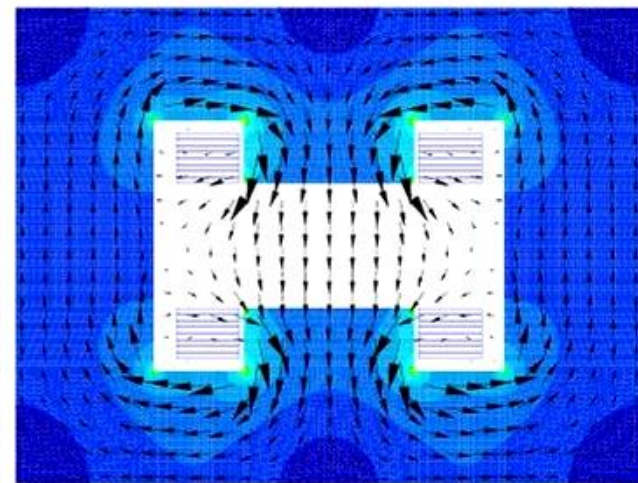
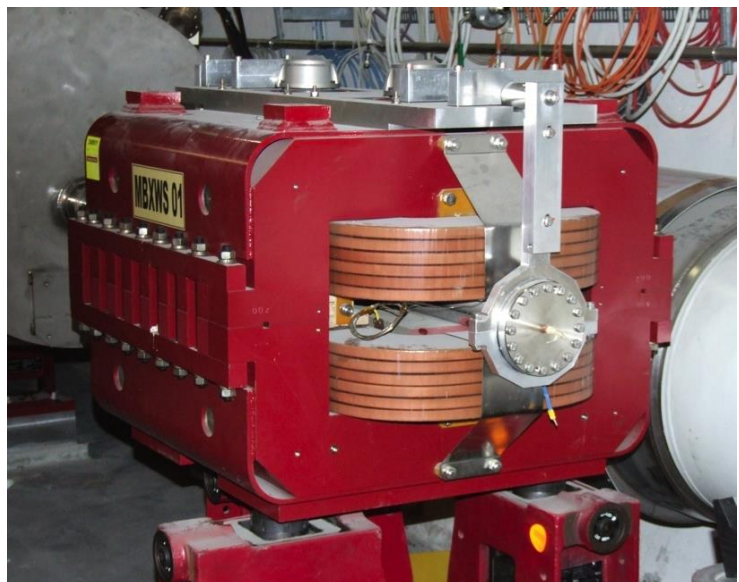
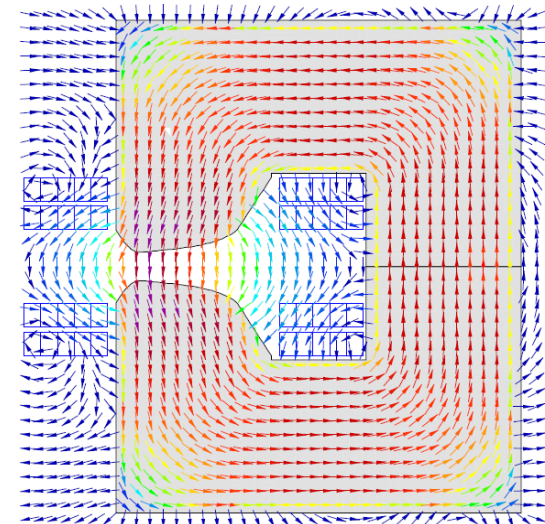


$$B = 8.33 \text{ T} \quad B_s = 7.77 \text{ T}$$



$$B = 4 \text{ T} \quad B_s = 3.69 \text{ T}$$

Iron Dominated Magnets



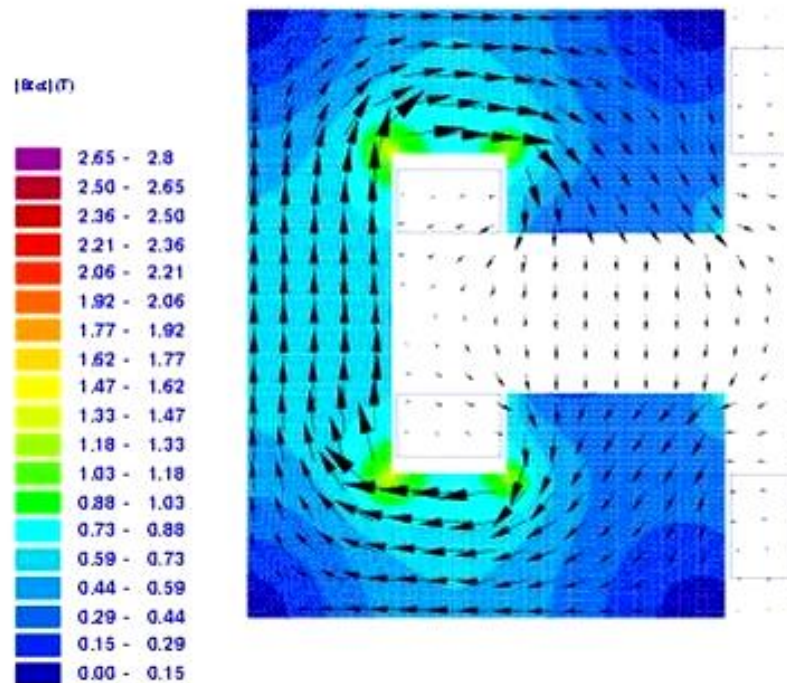
$N \cdot I = 24000 \text{ A}$

$B_1 = 0.3 \text{ T}$

$B_s = 0.065 \text{ T}$

Fill.fac. 0.98

LEP Dipole



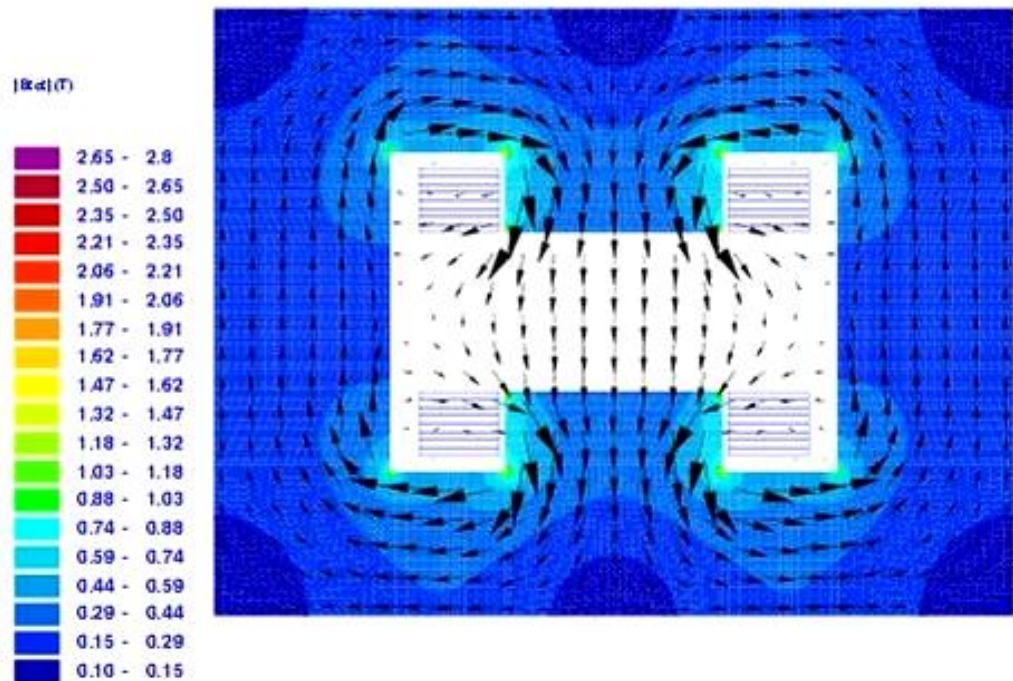
$$N \cdot I = 4480 \text{ A}$$

$$B_l = 0.13 \text{ T}$$

$$B_s = 0.042 \text{ T}$$

Fill.fac. 0.27

H Magnet (LHC transfer line)



$$N \cdot I = 24000 \text{ A}$$

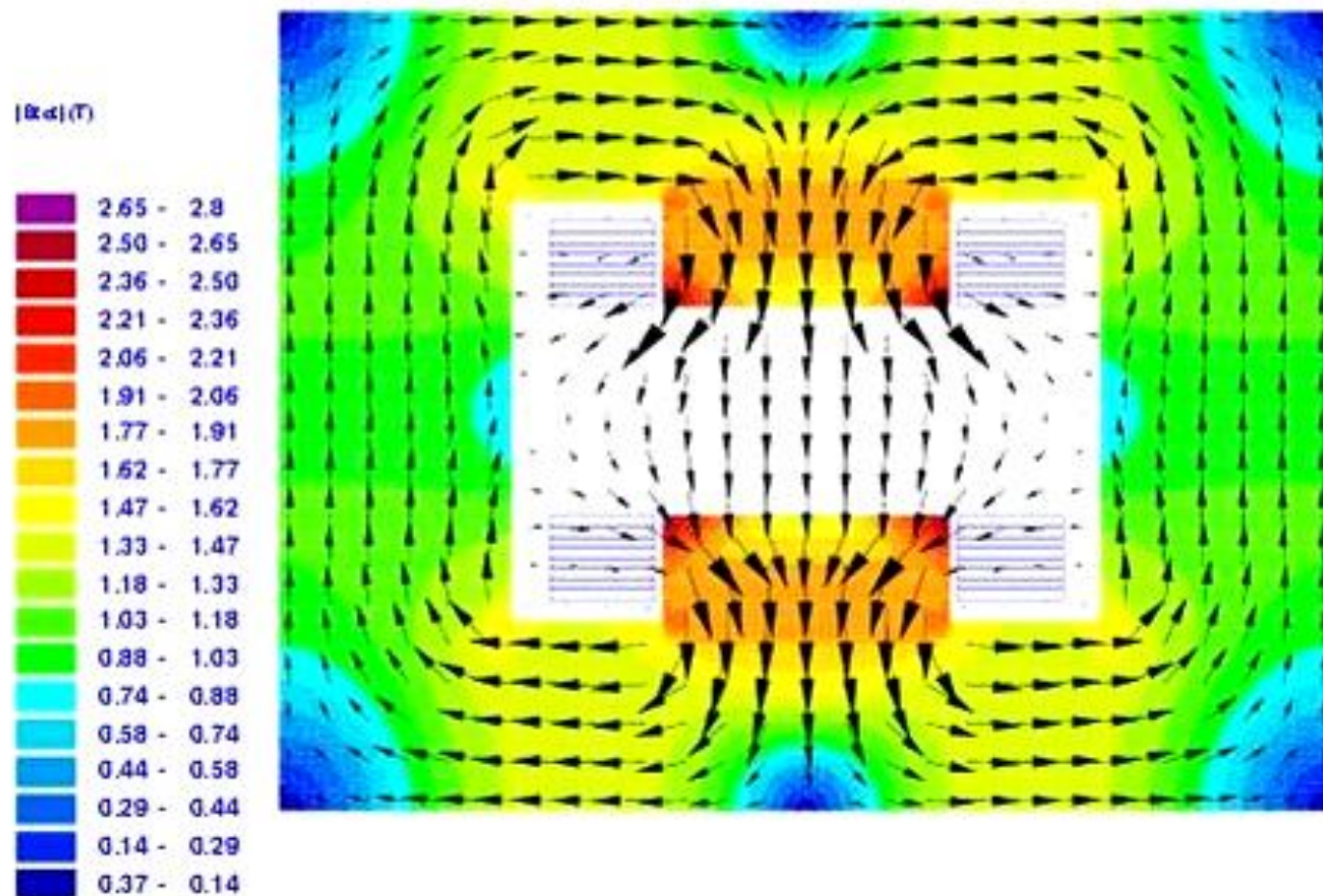
$$B_1 = 0.3 \text{ T}$$

$$B_s = 0.065 \text{ T}$$

Fill.fac. 0.98



Super-Ferric H Magnet

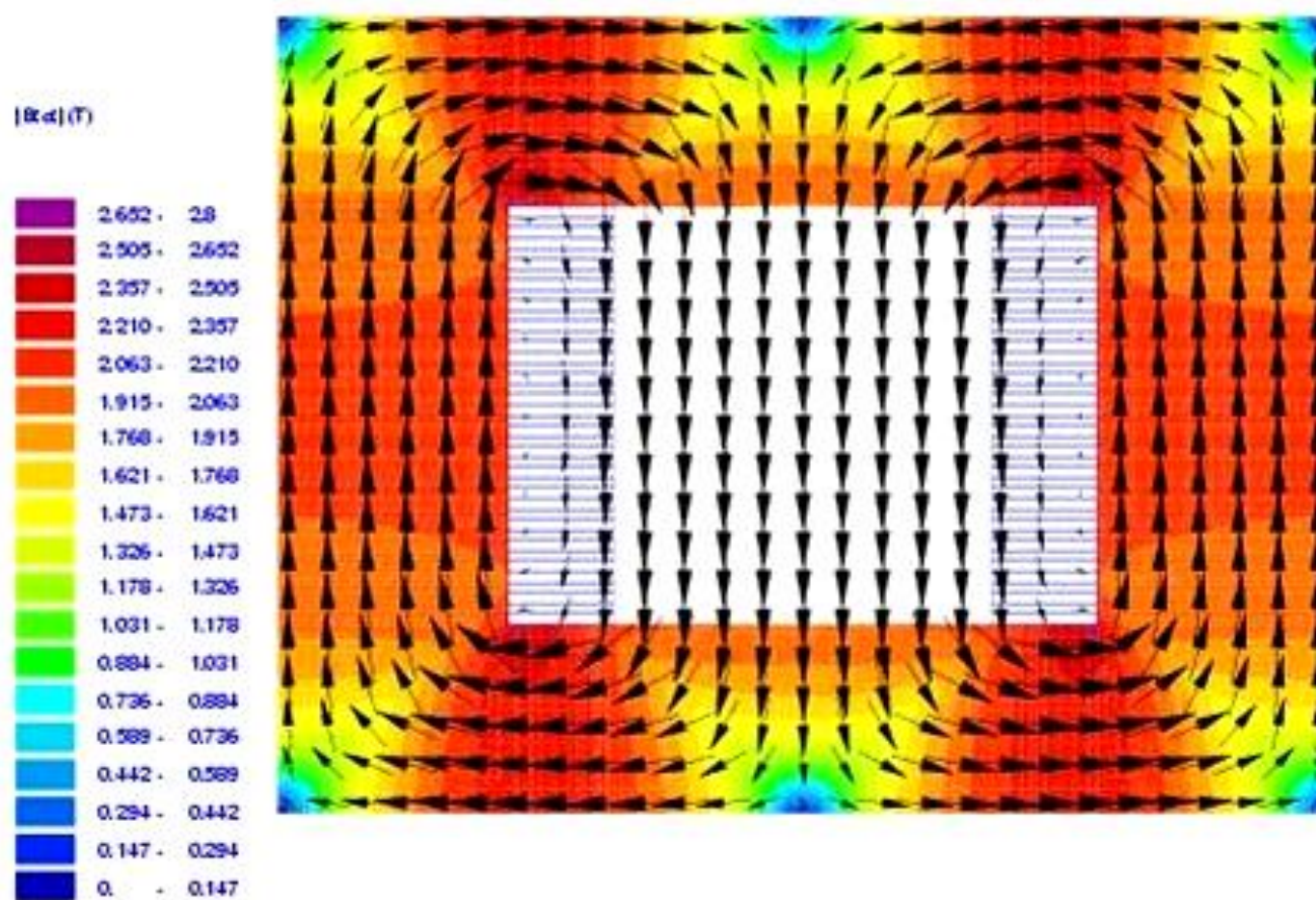


$$N \cdot I = 96000 \text{ A}$$

$$B_l = 1.18 \text{ T}$$

$$B_s = 0.26 \text{ T}$$

Window Frame Magnet

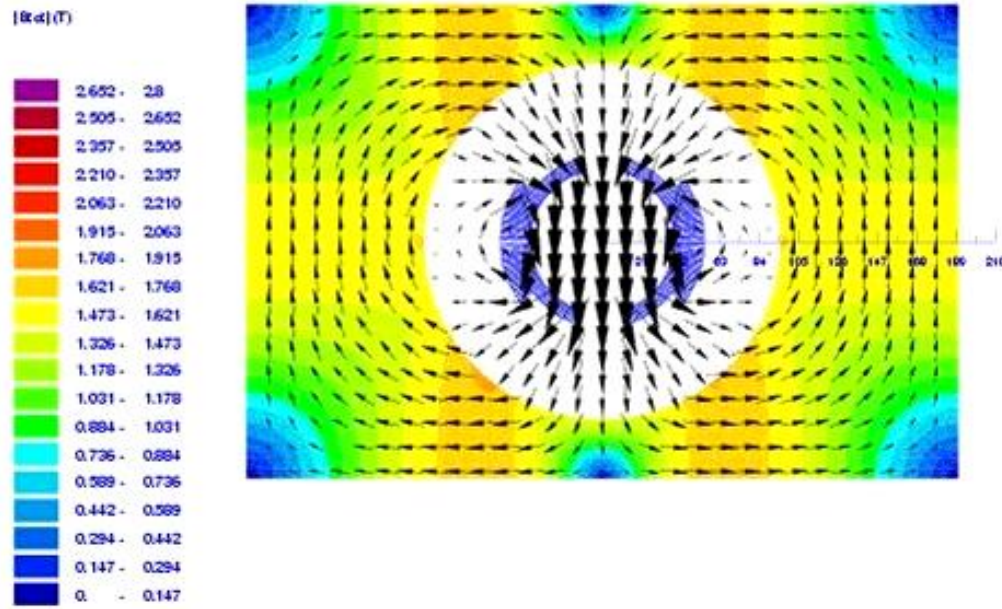


$$N \cdot I = 360000 \text{ A}$$

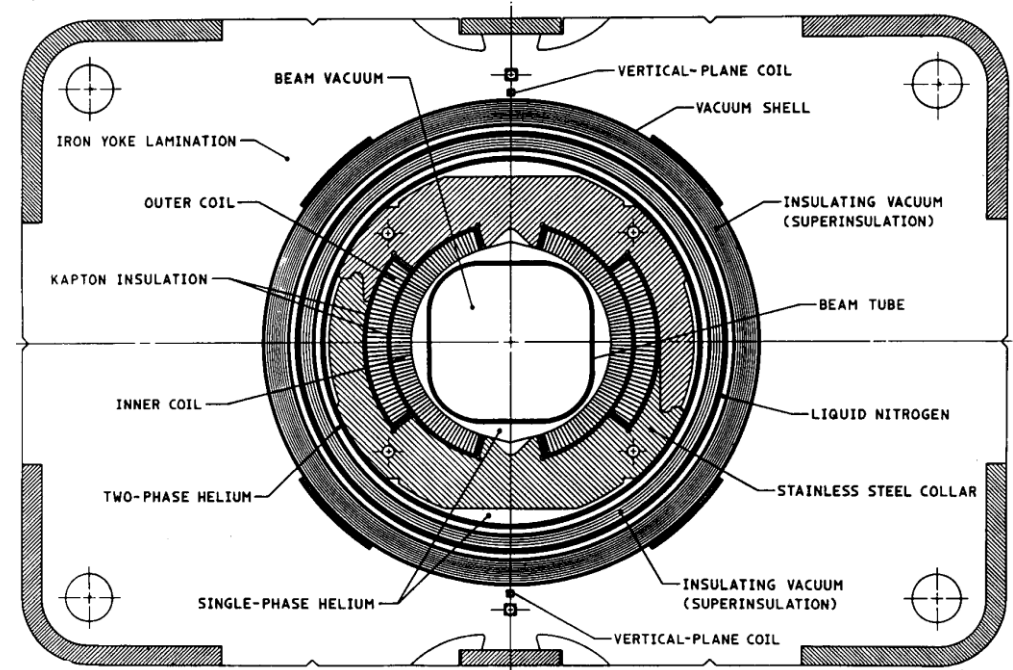
$$B_1 = 2.08 \text{ T}$$

$$B_s = 1.04 \text{ T}$$

$\cos \theta$ (Warm iron yoke) - Tevatron Dipole

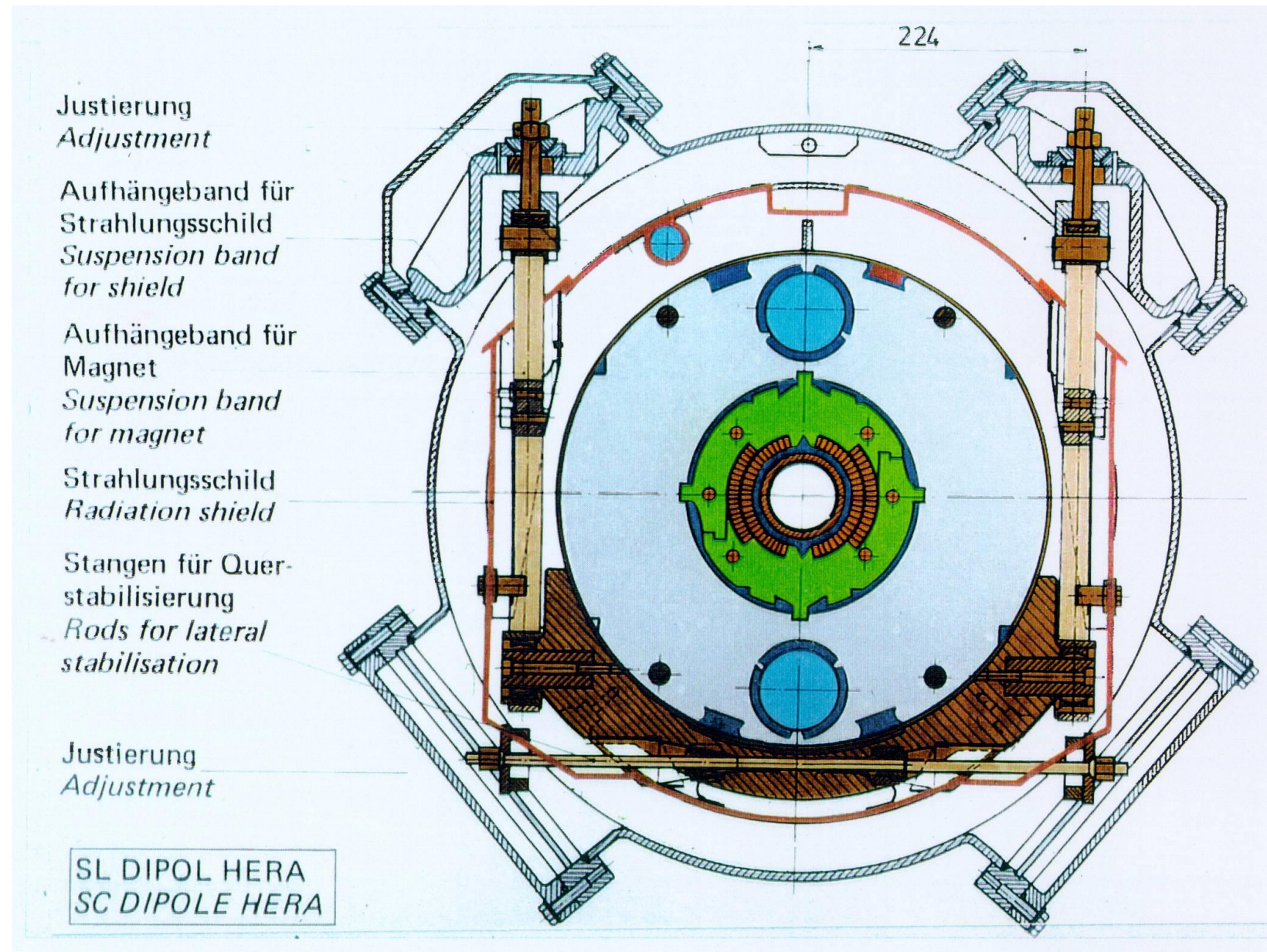


$$N \cdot I = 471000 \text{ A} \quad B_1 = 4.16 \text{ T} \quad B_s = 3.39 \text{ T}$$

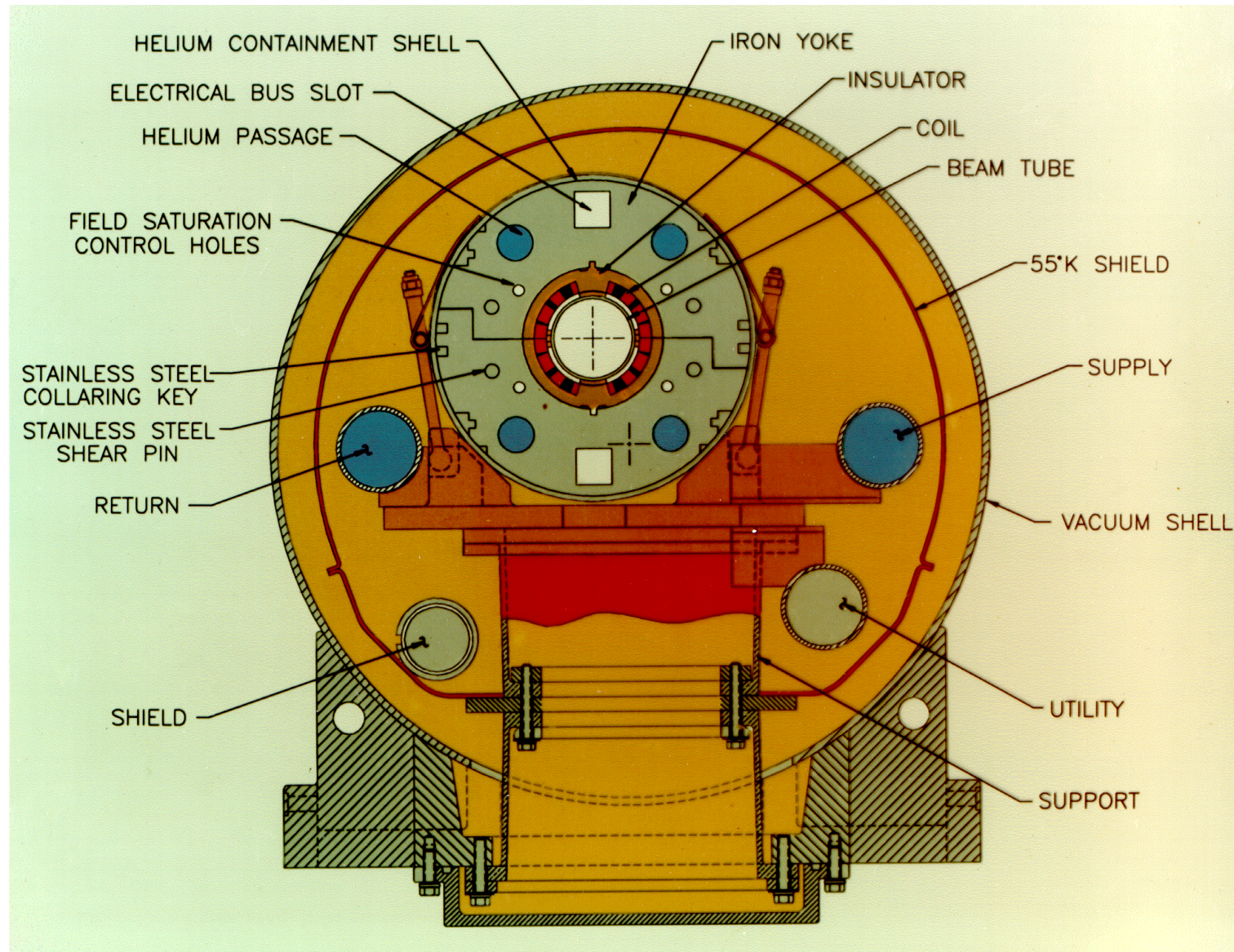


Notice the lower field in the iron yoke compared to the window frame

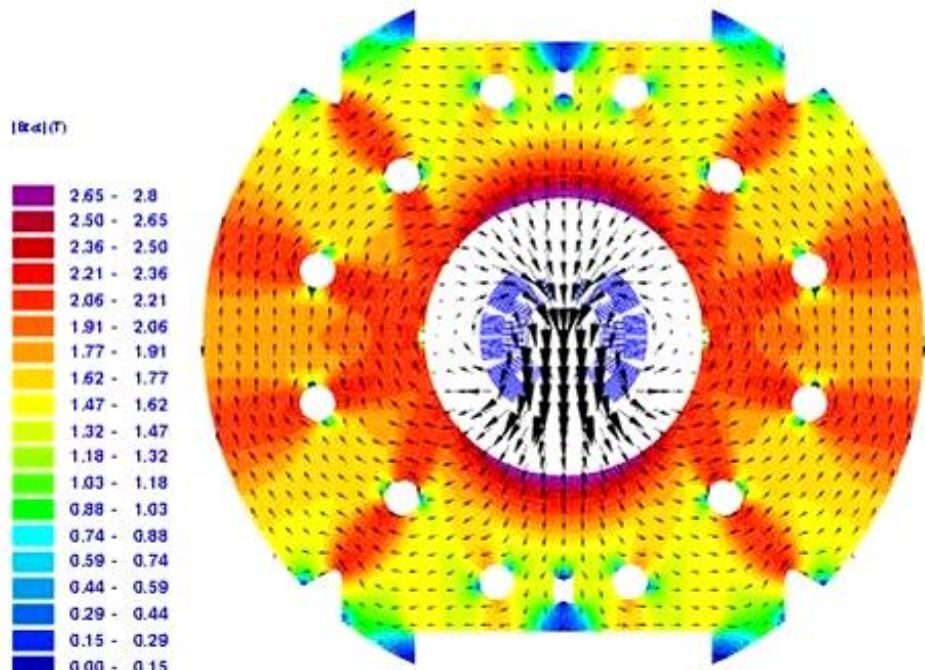
HERA Dipole in its Cryostat



RHIC Dipole in its Cryostat



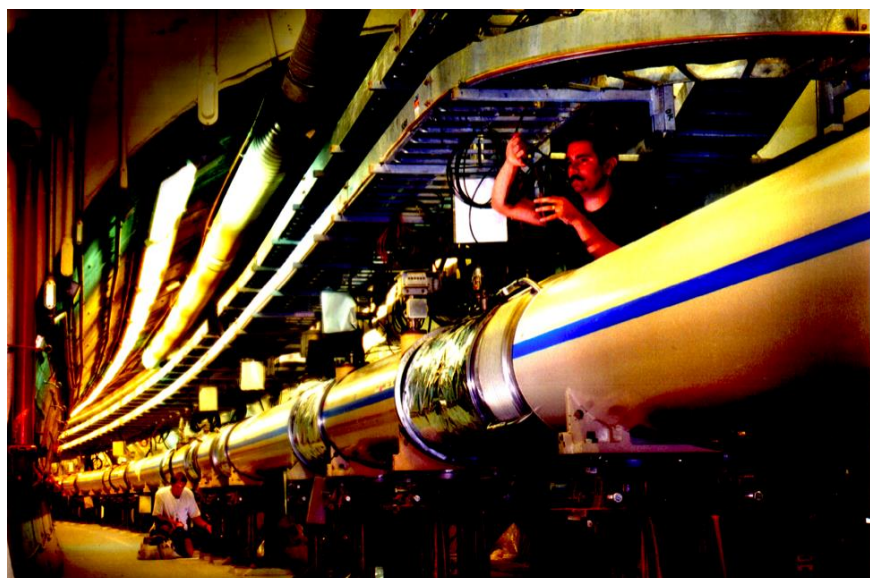
LHC Coil Test Facility for LHC (Based on HERA/RHIC Magnet Technology)



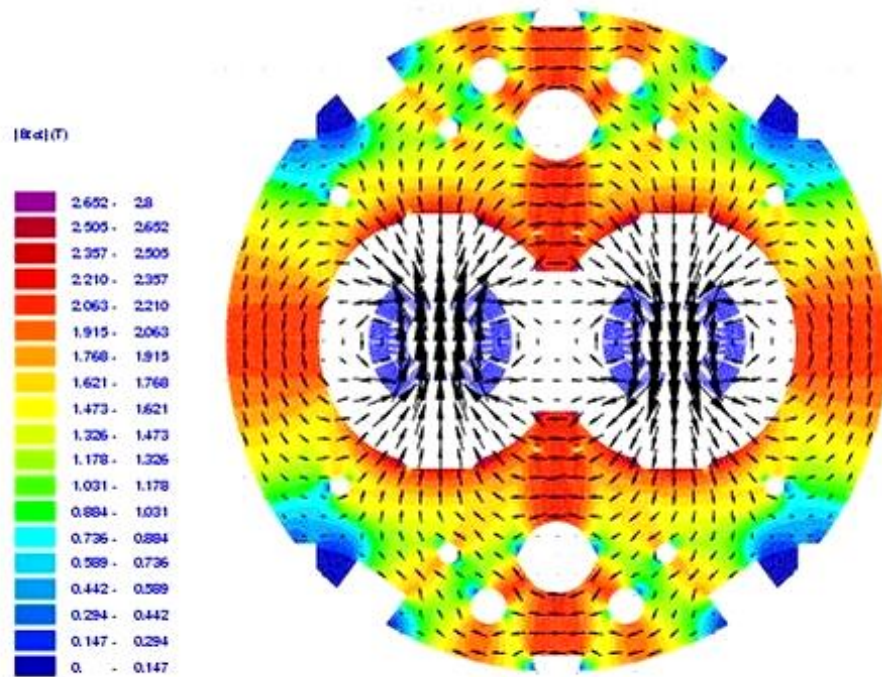
$$N \cdot I = 960000 \text{ A}$$

$$B_1 = 8.33 \text{ T}$$

$$B_s = 7.77 \text{ T}$$



LHC Two-in-one Dipole



$$N \cdot I = 2 \times 944000 \text{ A}$$

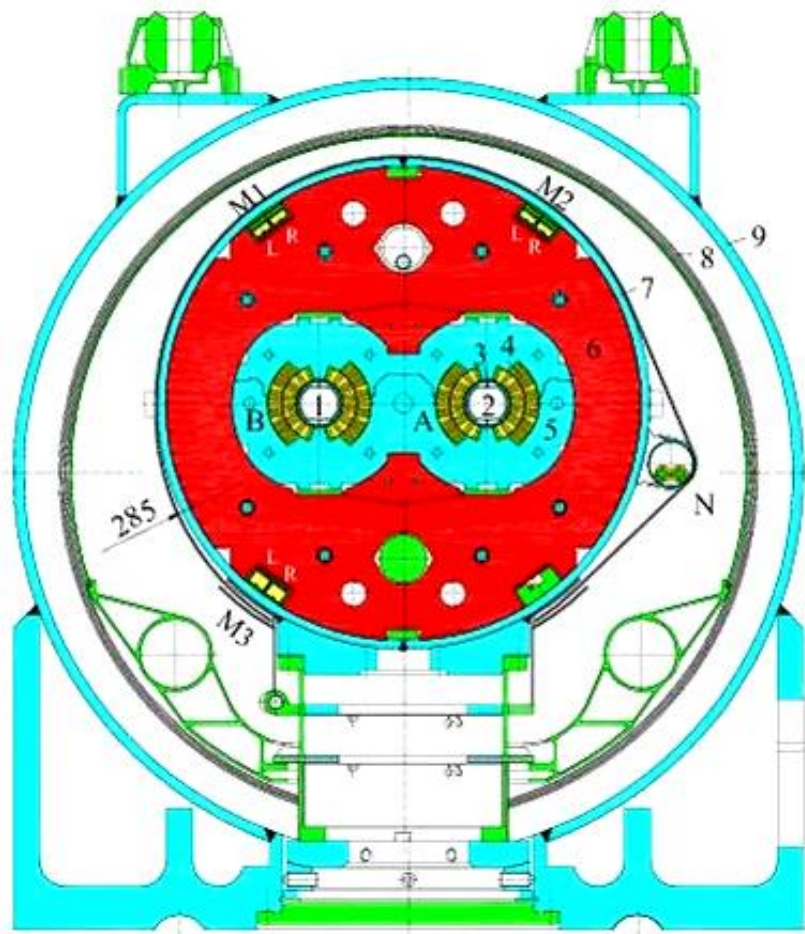
$$B_l = 8.32 \text{ T}$$

$$B_s = 7.44 \text{ T}$$

Storage of cold-masses



Cross-section of Cryodipole



Cryostat integration at CERN



Conventional and Superconducting Magnets

→ Conventional magnets

- Important ohmic losses require water cooling
- Field is defined by the iron pole shape (max 1.5 T)
- Easy electrical and beam-vacuum interconnections
- Voltage drop over one coil of the MBW magnets = 22 V

→ Superconducting magnets

- Field is defined by the coil layout
- Maximum field limited to 10 T (NbTi), 12 T (Nb₃Sn)
- Enormous electromagnetic forces (400 tons/m in MB for LHC)
- Quench protection system required
- Cryogenic installation (1.8 K)
- Electrical interconnections in cryo-lines
- Voltage drop on LHC magnet string (154 MB) 155 V



Comparison (EM-Design)

→ Conventional magnets

- Ideal pole shape known from potential theory
- One-dimensional (analytical) field computation for main field
- Commercial FEM software can be used as a black box (hysteresis modeling)

→ Superconducting magnets

- Decoupling of coil and yoke optimization
- Accuracy of the field solution
- Modeling of the coils
- Filament magnetization
- Quench simulations



A Multiphysics Problem

- Beam physics
- Material science: Superconducting cable, Steel, Insulation
- Mechanics and large-scale mechanical engineering
- Vacuum technology
- Cryogenics (Superfluid helium)
- Metrology and alignment
- Field measurements
- Electrical engineering (Power supplies, leads, buswork, quench detection and magnet protection)
- Analytical and numerical field computation



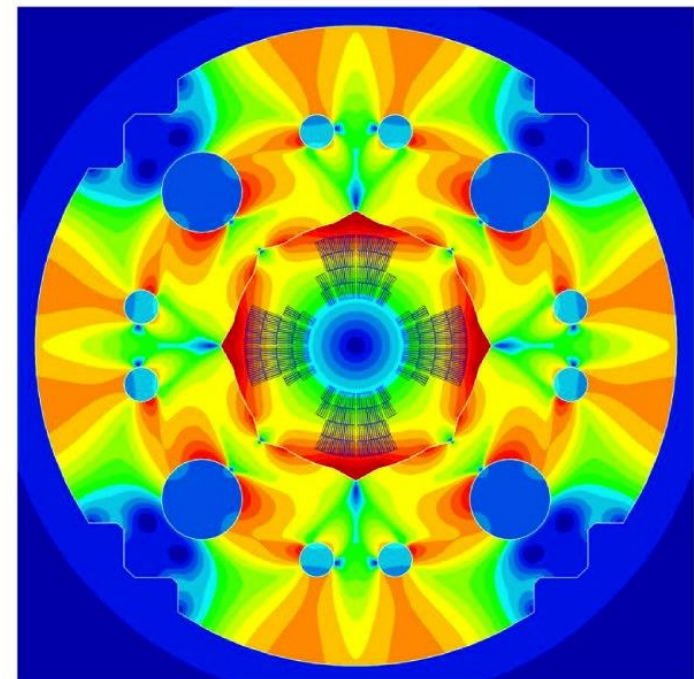
- Linear algebra
- Vector analysis
- Harmonic fields
- Green's functions and the method of images
- Complex analysis
- Differential geometry
- Numerical field computation
- Hysteresis modeling
- Coupled (thermo, magnetic, electric) systems
- Mathematical optimization

Stephan Russenschuck

Wiley-VCH

Field Computation for Accelerator Magnets

Analytical and Numerical Methods for Electromagnetic Design and Optimization

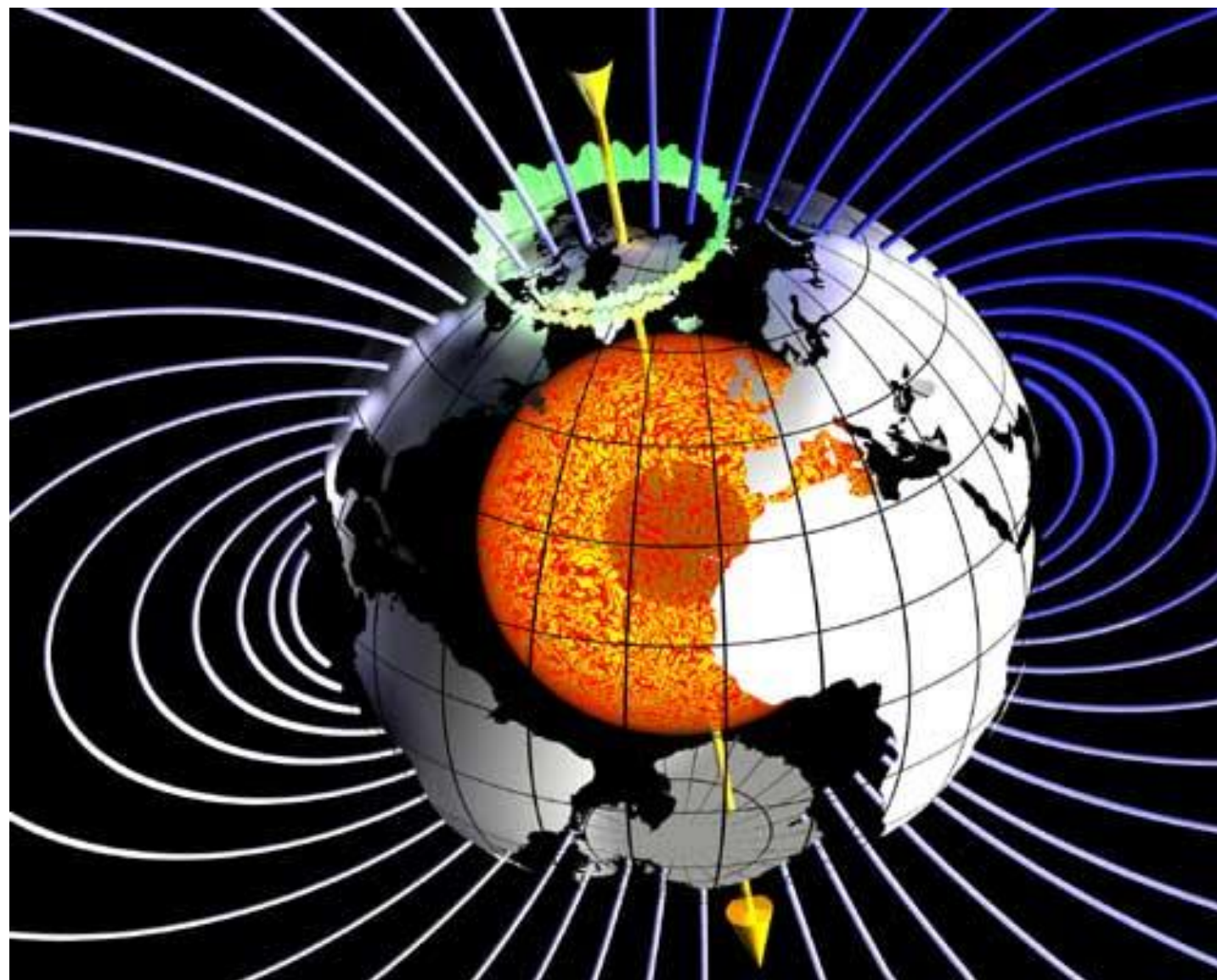


A Short Self-Test

- What is a vector? An arrow, a tuple of numbers, a quantity having direction and magnitude, a solution of a linear equation system, a contravariant tensor?
- What is more fundamental, \mathbf{B} or \mathbf{H} ?
- What is a (linear) field
- Is there a difference between coefficients, components, and coordinates?
- We know how to add vectors represented as arrows by means of the parallelogram law. Can we add a force vector at the tip of the position vector?
- What is between the field lines
- In Maxwell's equation we find $\mathbf{J} \cdot d\mathbf{a}$ and $\mathbf{B} \cdot d\mathbf{a}$. Is there a difference between these vectorial surface elements.
- What is a “convention recepteur”.

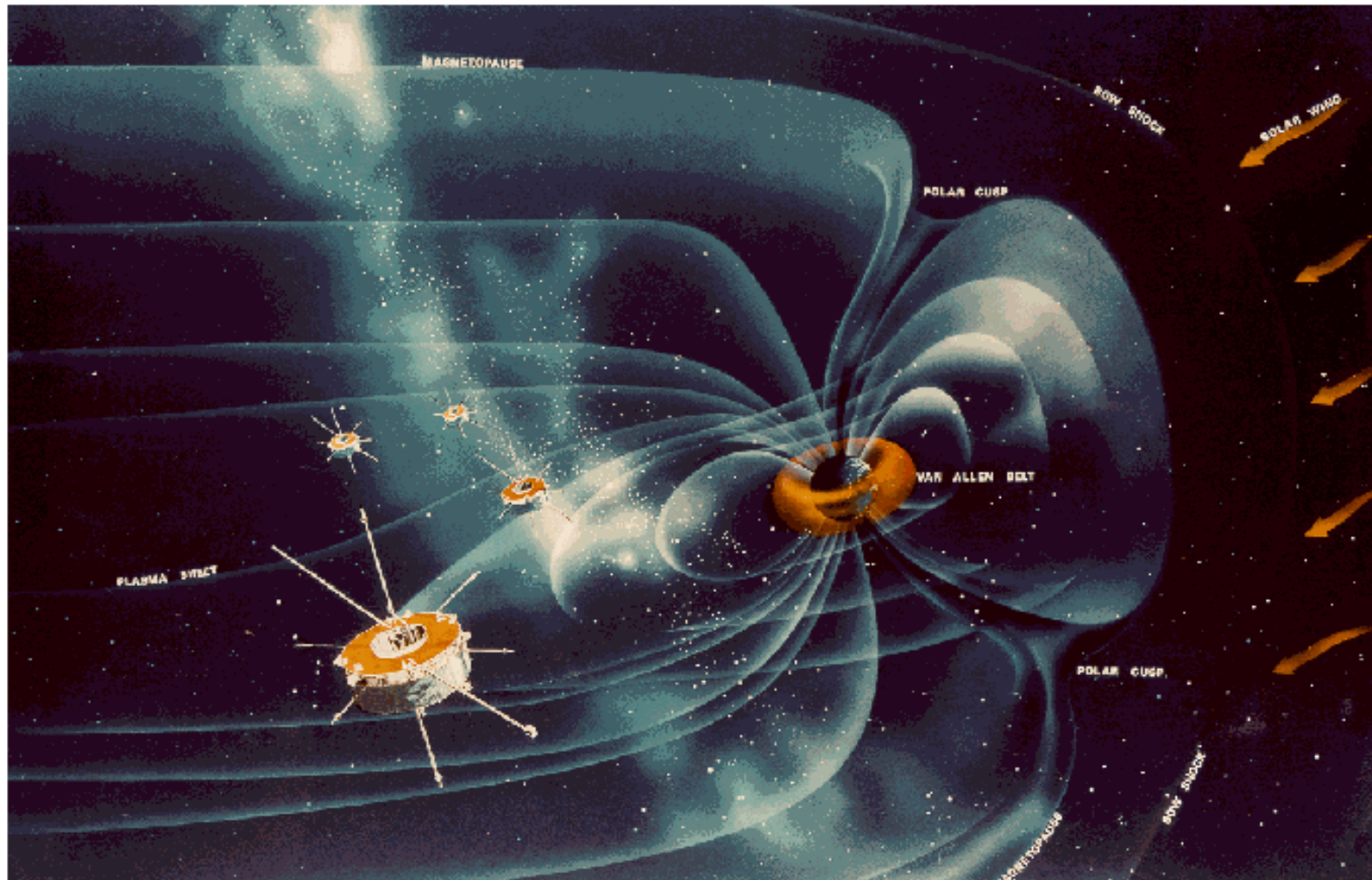


Flux Tubes of Mother Earth (or what is a magnetic field)

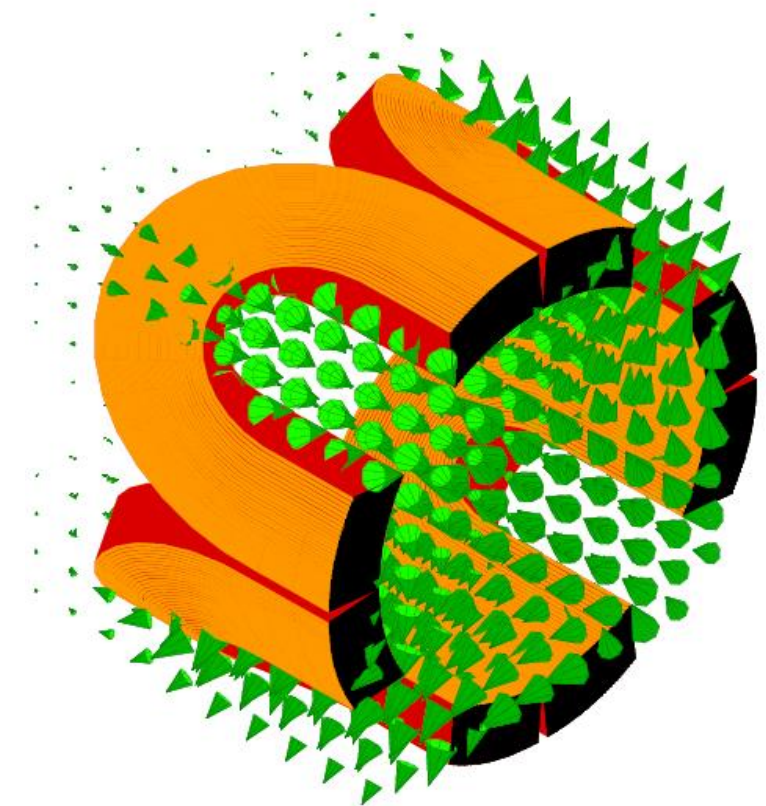
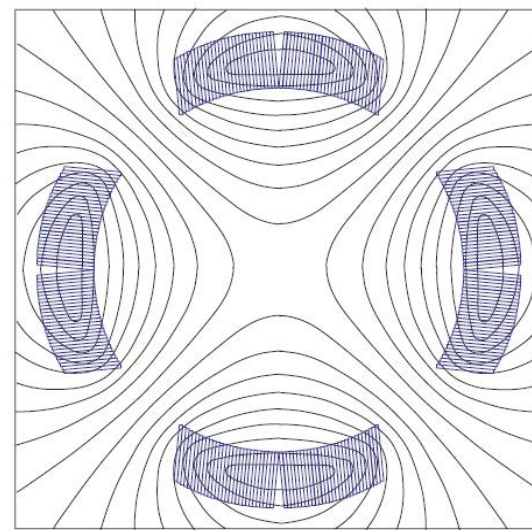
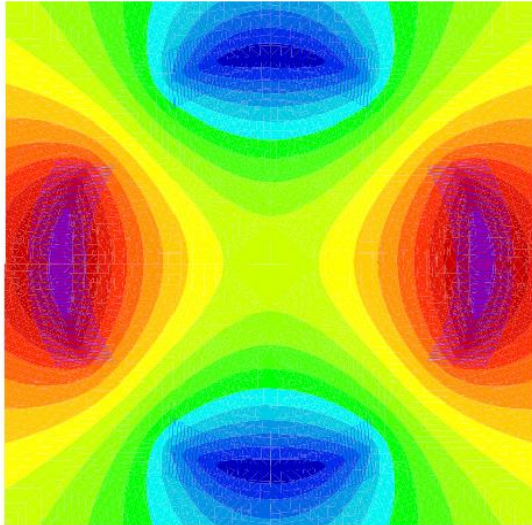
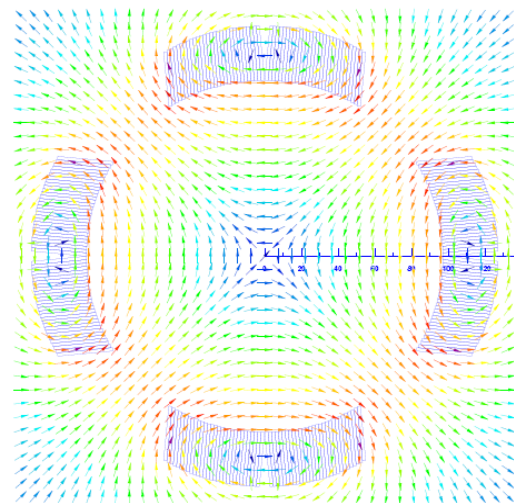
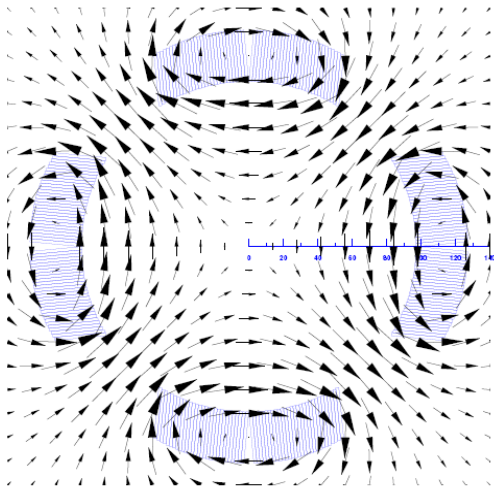


Erdmagnetfeld

PTB

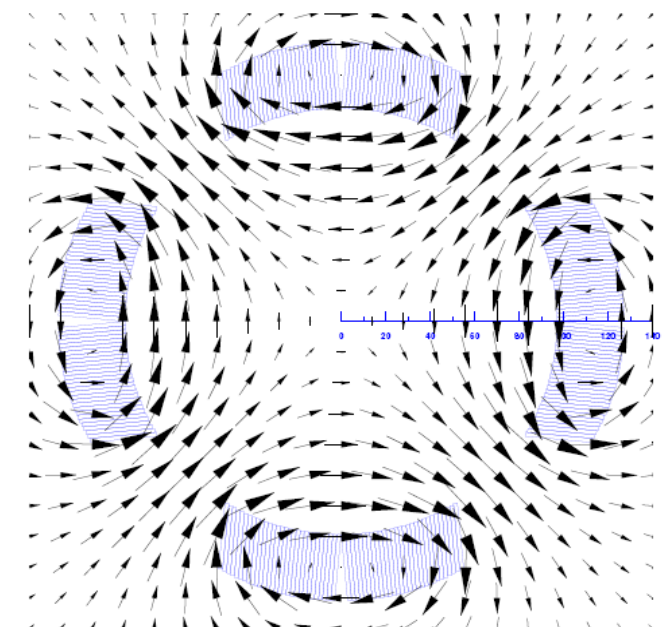


Different Renderings of the Same Vector Field



Framework of our Vectorfields E_3

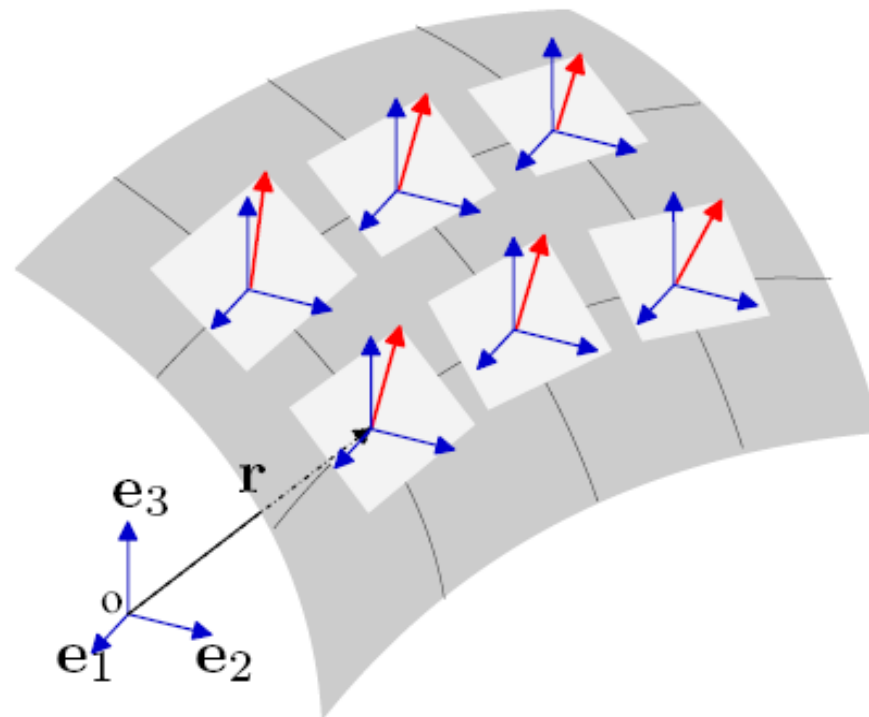
- E_3 has the structure of the affine point space
 - It carries the vector (linear) space structure of its associated vector space
 - It is equipped with a metric that gives rise to distance and angles
-
- If an origin and basis is selected, the projection of the position vector on the basis yields the coordinates (in \mathbb{R}^3)
 - The canonical basis can be made to a basis field by translation
 - The components of the field at some point are then the projection on this basis field



Vector and Scalar Fields

$$\mathbf{a} : \Omega \rightarrow \mathbb{R}^3 : \mathbf{r} \mapsto \mathbf{a}(\mathbf{r}) : \mathbf{a}(\mathbf{r}) = (a^1(\mathbf{r}), a^2(\mathbf{r}), a^3(\mathbf{r}))$$

$$\Omega \subset \mathbb{R}^3$$



$$\phi : \Omega \rightarrow \mathbb{R} : \phi \mapsto \phi(\mathbf{r})$$

Different Incarnations of Maxwell's Equations

$$\int_{\partial \mathcal{A}} \mathbf{H} \cdot d\mathbf{r} = \int_{\mathcal{A}} \mathbf{J} \cdot d\mathbf{a} + \frac{d}{dt} \int_{\mathcal{A}} \mathbf{D} \cdot d\mathbf{a},$$

$$\int_{\partial \mathcal{A}} \mathbf{E} \cdot d\mathbf{r} = -\frac{d}{dt} \int_{\mathcal{A}} \mathbf{B} \cdot d\mathbf{a},$$

$$\int_{\partial \mathcal{V}} \mathbf{B} \cdot d\mathbf{a} = 0,$$

$$\int_{\partial \mathcal{V}} \mathbf{D} \cdot d\mathbf{a} = \int_{\mathcal{V}} \rho \, dV.$$

$$V_m(\partial \mathcal{A}) = I(\mathcal{A}) + \frac{d}{dt} \Psi(\mathcal{A}),$$

$$U(\partial \mathcal{A}) = -\frac{d}{dt} \Phi(\mathcal{A}),$$

$$\Phi(\partial \mathcal{V}) = 0,$$

$$\Psi(\partial \mathcal{V}) = Q(\mathcal{V}).$$

$$\text{curl } \mathbf{H} = \mathbf{J} + \frac{\partial}{\partial t} \mathbf{D},$$

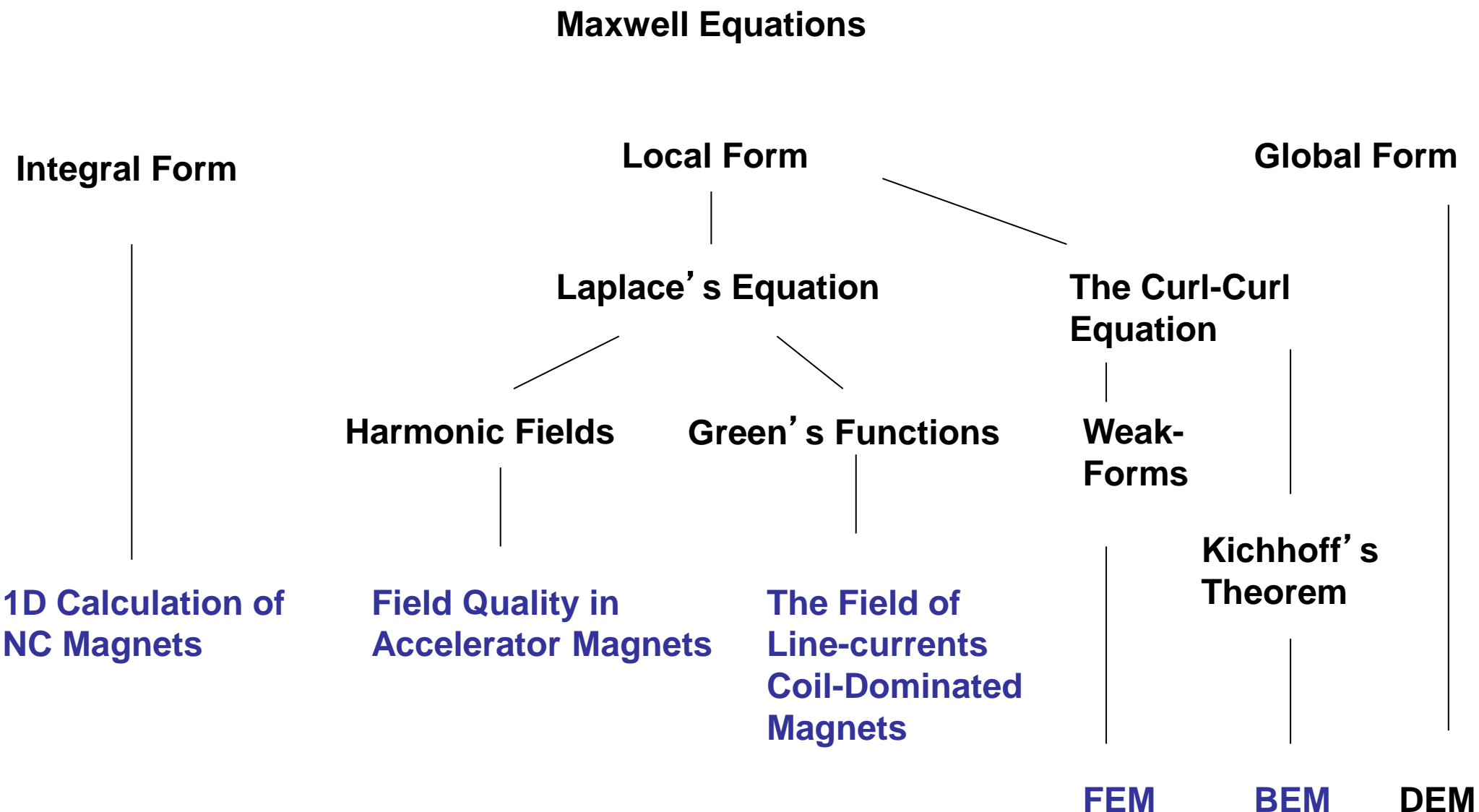
$$\text{curl } \mathbf{E} = -\frac{\partial}{\partial t} \mathbf{B},$$

$$\text{div } \mathbf{B} = 0,$$

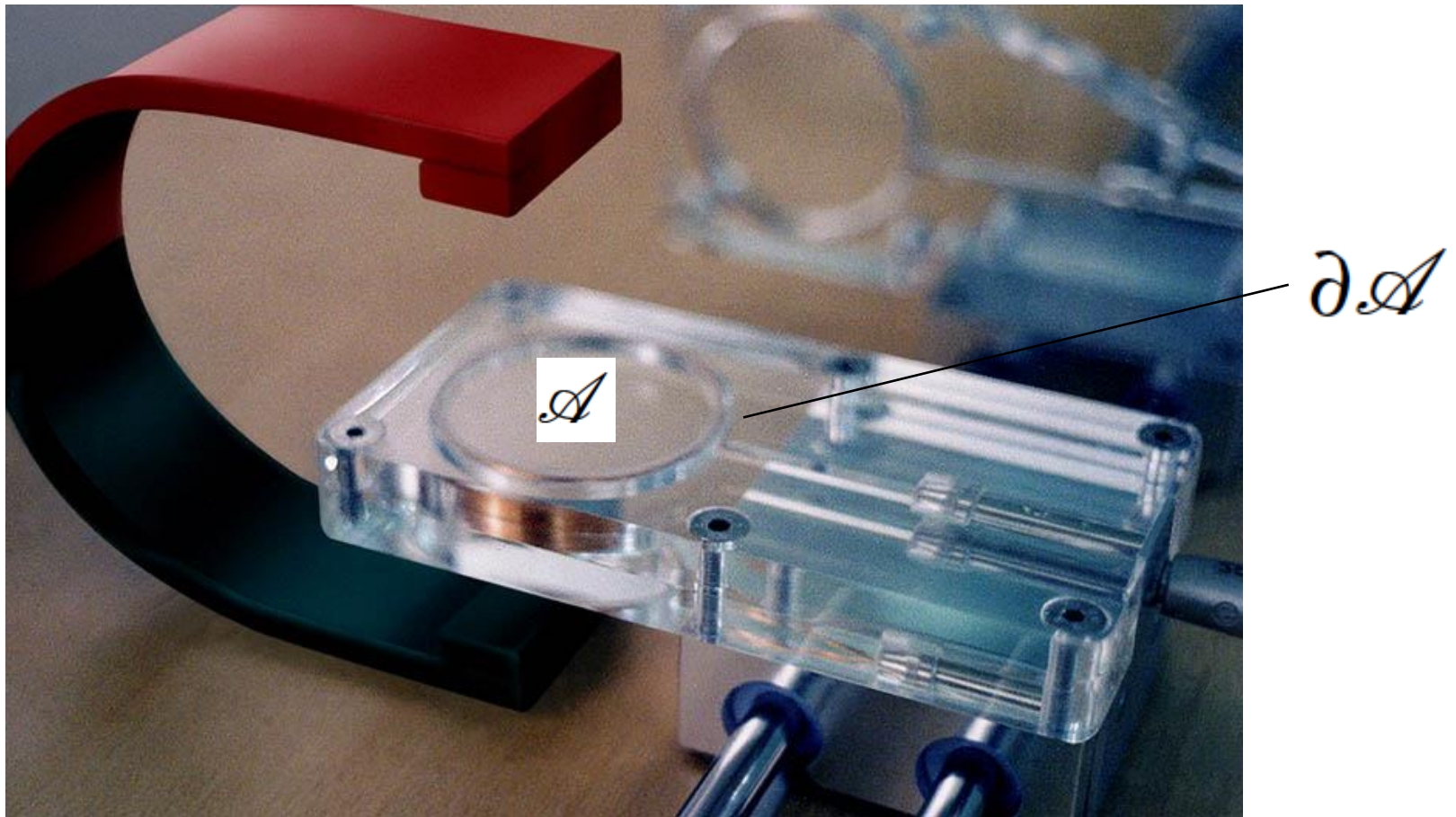
$$\text{div } \mathbf{D} = \rho.$$



Mathematical Foundations of Magnet Design



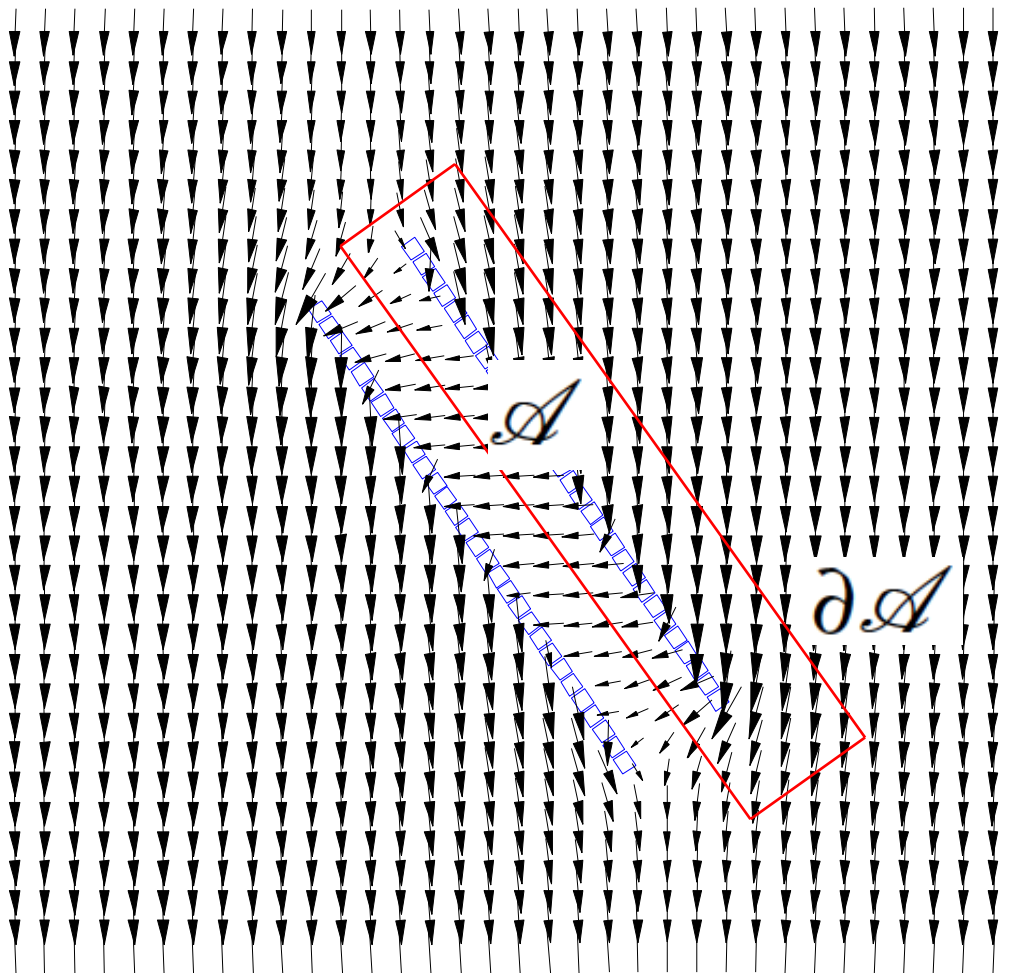
Faraday's Law (Inner Oriented Surface, Voltage along its Rim)



$$U(\partial\mathcal{A}) = -\frac{d}{dt}\Phi(\mathcal{A})$$

The potential to induce a voltage

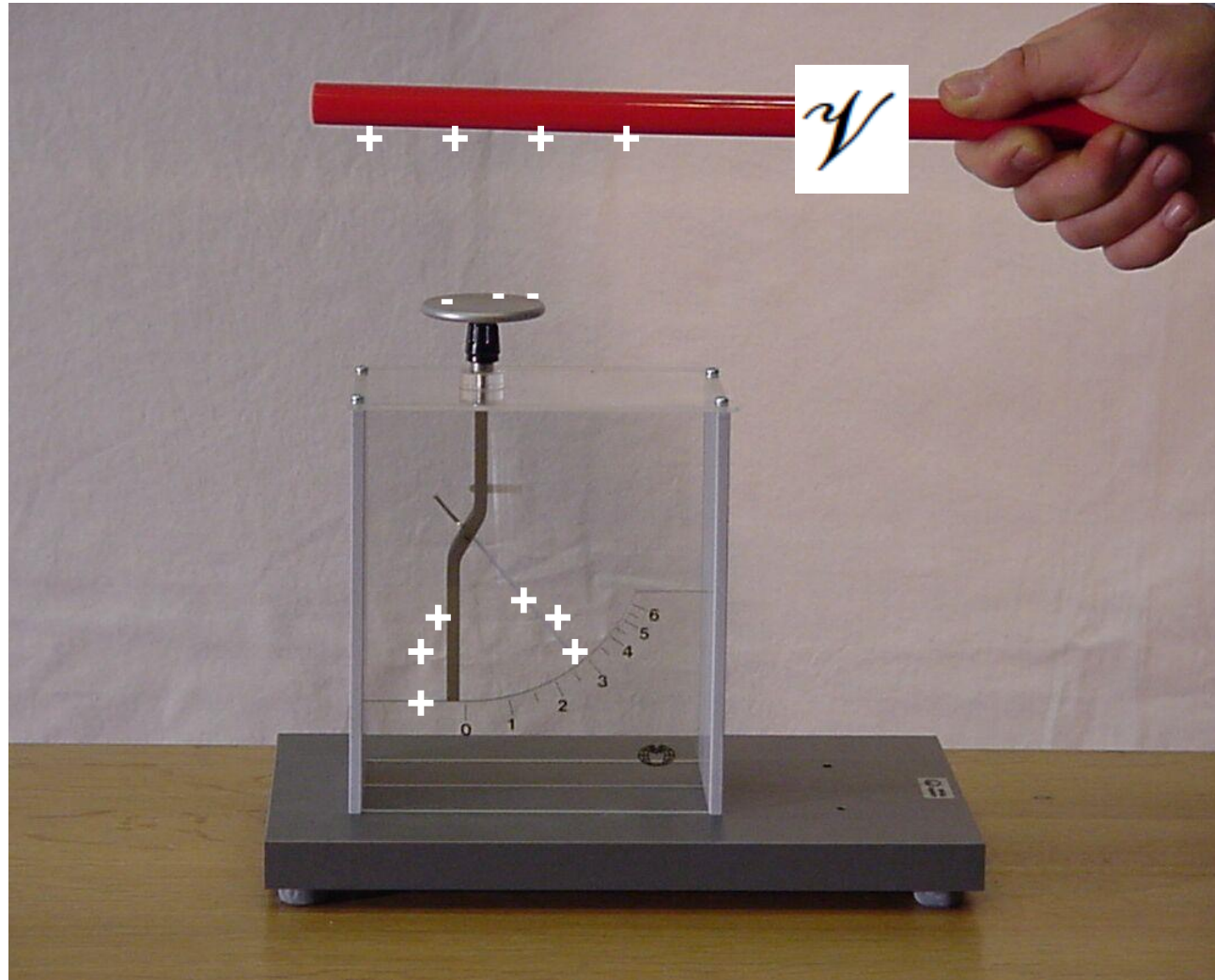
Ampere's Law (Outer Oriented Surface; Current crossing)



$$V_m(\partial\mathcal{A}) = I(\mathcal{A})$$

The current needed to cancel the longitudinal field component

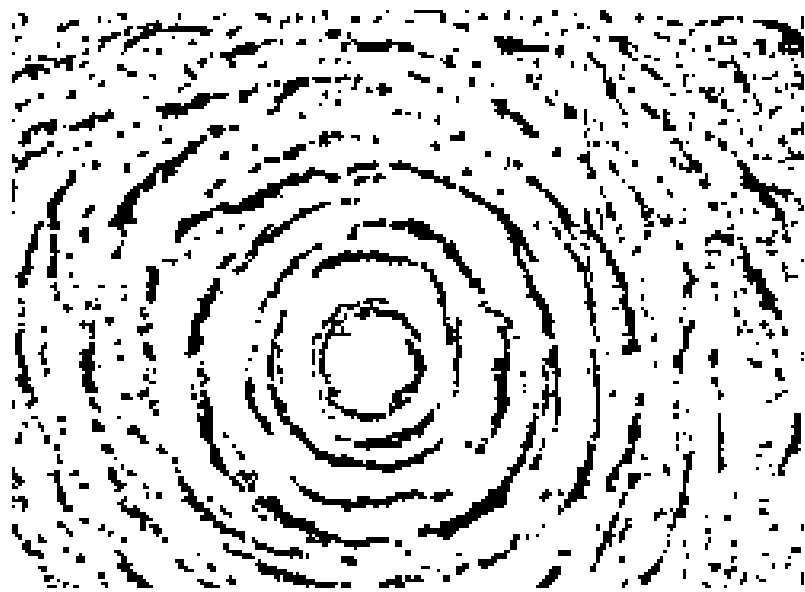
Gauss Law (Outer Oriented Volume; Electric Charge that can be influenced)



$$\Psi(\partial\mathcal{V}) = Q(\mathcal{V})$$

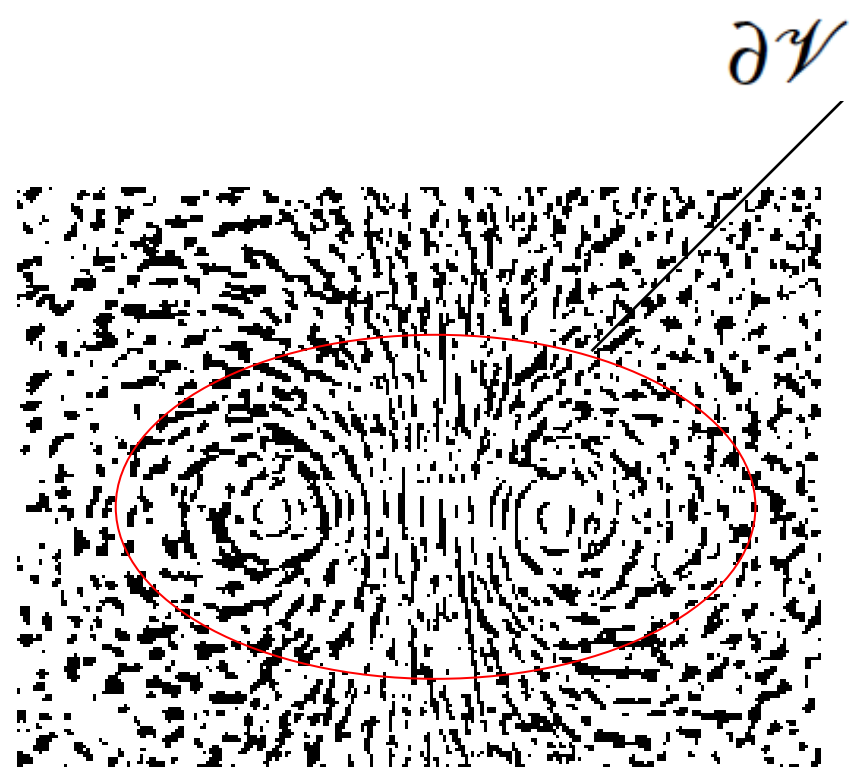
The capacity to induce charge

Magnetic Flux Conservation Law (Inner Oriented Volume)

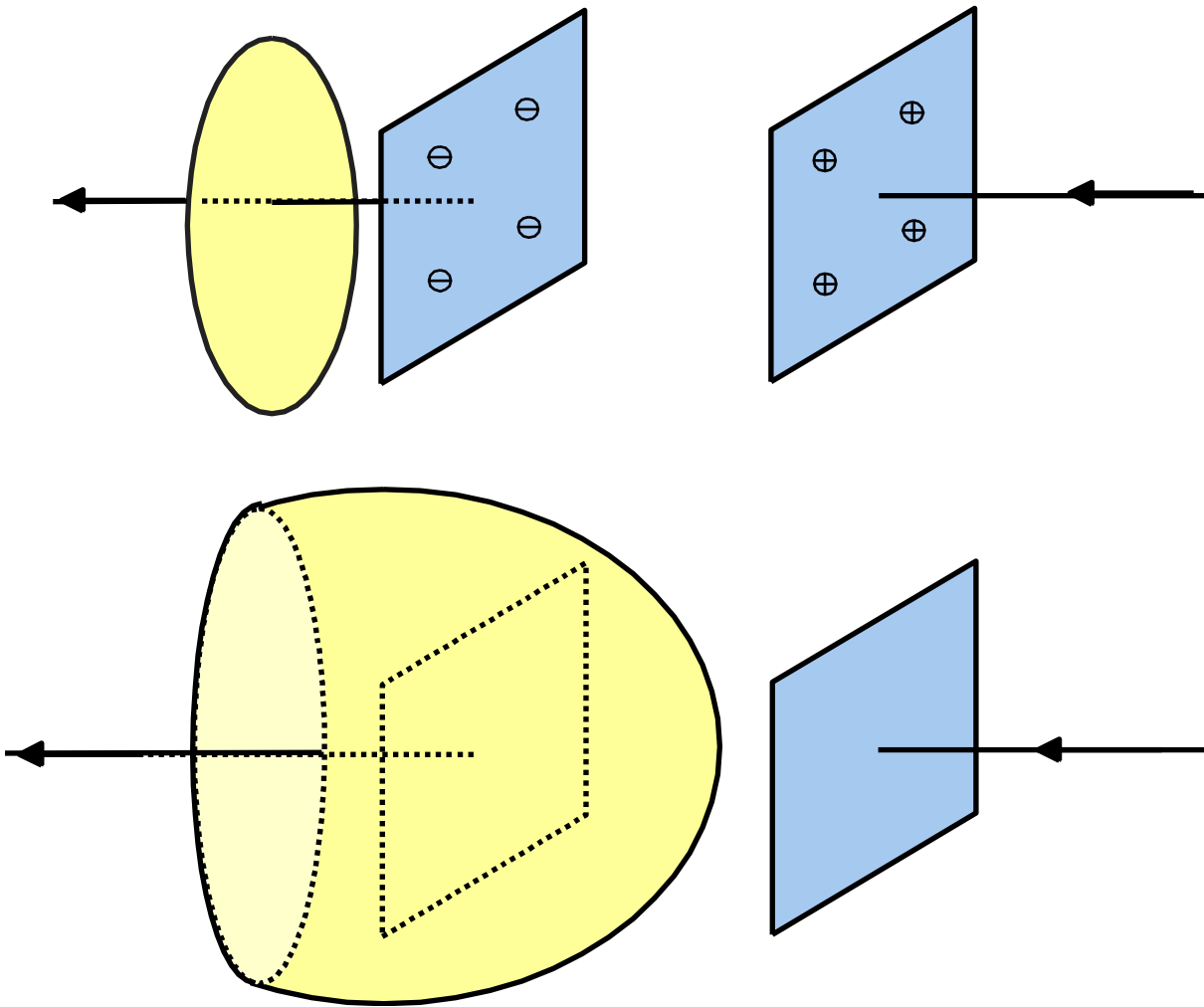


$$\Phi(\partial\mathcal{V}) = 0$$

Conservation of flux



Maxwell's Extension



Ampere

$$V_m(\partial \mathcal{A}) = I(\mathcal{A}) + \frac{d}{dt} \Psi(\mathcal{A})$$

Rate of change of
charge

Maxwell's Equations in Global Form

Ampere	$V_m(\partial a) = I(a) + \frac{d}{dt}\Psi(a)$
Faraday	$U(\partial a) = -\frac{d}{dt}\Phi(a)$
Flux conservation	$\Phi(\partial V) = 0$
Gauss	$\Psi(\partial V) = Q(V)$

Conservation of charge / Kirchhoff law

$$V_m(\partial(\partial V)) = 0 = I(\partial V) + \frac{d}{dt}Q(V)$$

In words: The current exiting a volume is equal to the negative rate of the charge in that volume



Electromagnetic Fields

Global quantity	SI unit	Relation	SI unit	Field
MMF	1 A	$V_m(\mathcal{S}) = \int_{\mathcal{S}} \mathbf{H} \cdot d\mathbf{r}$	1 A m ⁻¹	Magnetic field
Electric voltage	1 V	$U(\mathcal{S}) = \int_{\mathcal{S}} \mathbf{E} \cdot d\mathbf{r}$	1 V m ⁻¹	Electric field
Magnetic flux	1 V s	$\Phi(\mathcal{A}) = \int_{\mathcal{A}} \mathbf{B} \cdot d\mathbf{a}$	1 V s m ⁻²	Magnetic flux density
Electric flux	1 A s	$\Psi(\mathcal{A}) = \int_{\mathcal{A}} \mathbf{D} \cdot d\mathbf{a}$	1 A s m ⁻²	Electric flux density
Electric current	1 A	$I(\mathcal{A}) = \int_{\mathcal{A}} \mathbf{J} \cdot d\mathbf{a}$	1 A m ⁻²	Electric current density
Electric charge	1 A s	$Q(\mathcal{V}) = \int_{\mathcal{V}} \rho \cdot dV$	1 A s m ⁻³	Electric charge density

Interrupt: The vectorial line and surface elements, and the volume element



Maxwell's Equations in Integral Form

$$\int_{\partial \mathcal{A}} \mathbf{H} \cdot d\mathbf{r} = \int_{\mathcal{A}} \mathbf{J} \cdot d\mathbf{a} + \frac{d}{dt} \int_{\mathcal{A}} \mathbf{D} \cdot d\mathbf{a},$$

$$\int_{\partial \mathcal{A}} \mathbf{E} \cdot d\mathbf{r} = -\frac{d}{dt} \int_{\mathcal{A}} \mathbf{B} \cdot d\mathbf{a},$$

$$\int_{\partial \mathcal{V}} \mathbf{B} \cdot d\mathbf{a} = 0,$$

$$\int_{\partial \mathcal{V}} \mathbf{D} \cdot d\mathbf{a} = \int_{\mathcal{V}} \rho dV.$$

Contains the
Kirchhoff laws



$$V_m(\partial \mathcal{A}) = I(\mathcal{A}) + \frac{d}{dt} \Psi(\mathcal{A}),$$

$$U(\partial \mathcal{A}) = -\frac{d}{dt} \Phi(\mathcal{A}),$$

$$\Phi(\partial \mathcal{V}) = 0,$$

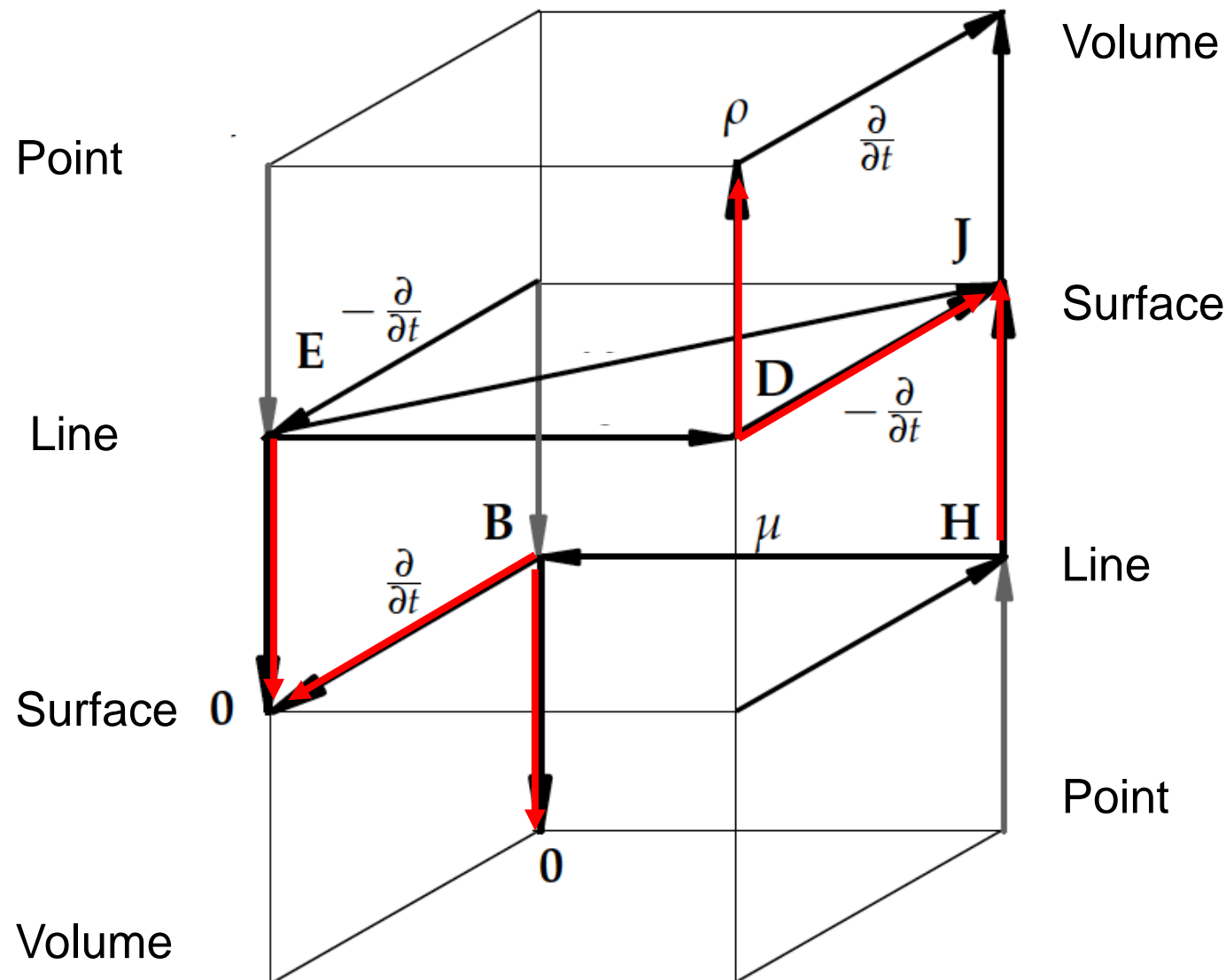
$$\Psi(\partial \mathcal{V}) = Q(\mathcal{V}).$$

8 Equations
16 Unknowns

Exercise: Ampere's law in integral form



Maxwell's House



Constitutive Equations

$$\mathbf{B} = \mu \mathbf{H}, \quad \mathbf{D} = \varepsilon \mathbf{E}, \quad \mathbf{J} = \kappa \mathbf{E},$$

$$[\mu] = 1 \text{ VsA}^{-1} \text{ m}^{-1} = 1 \text{ Hm}^{-1},$$

$$[\varepsilon] = 1 \text{ AsV}^{-1} \text{ m}^{-1},$$

$$[\kappa] = 1 \text{ AV}^{-1} \text{ m}^{-1} = 1 \Omega^{-1} \text{ m}^{-1}.$$

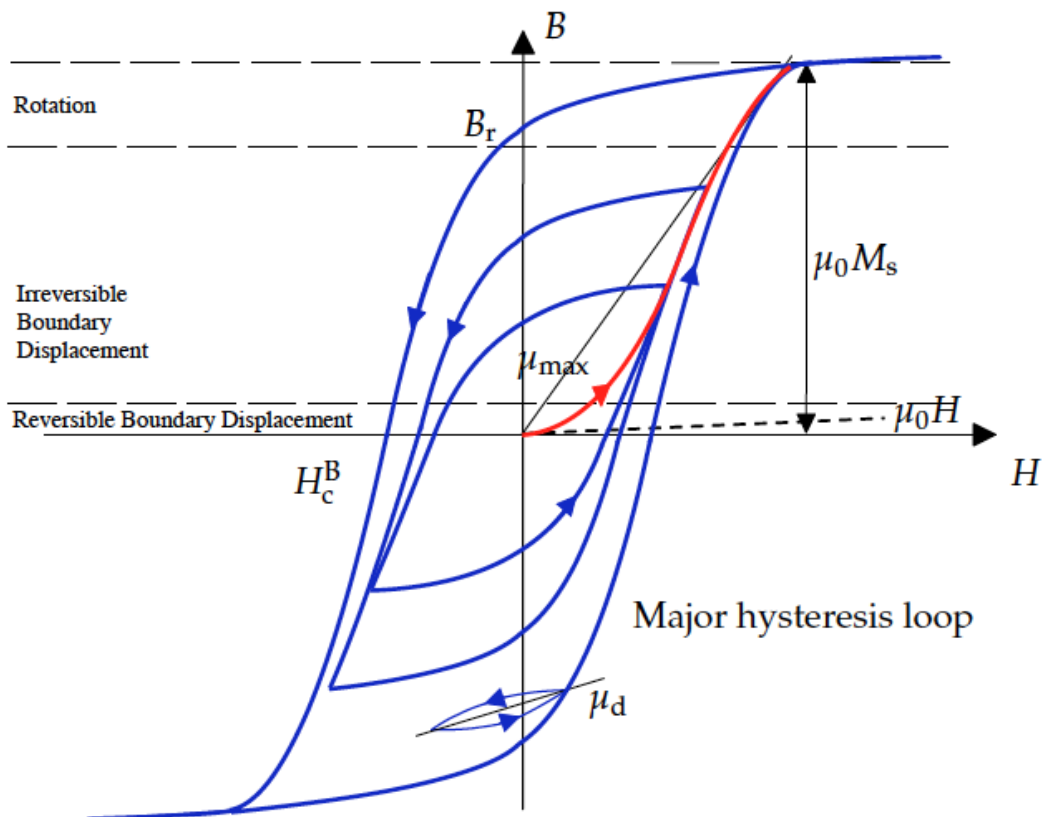
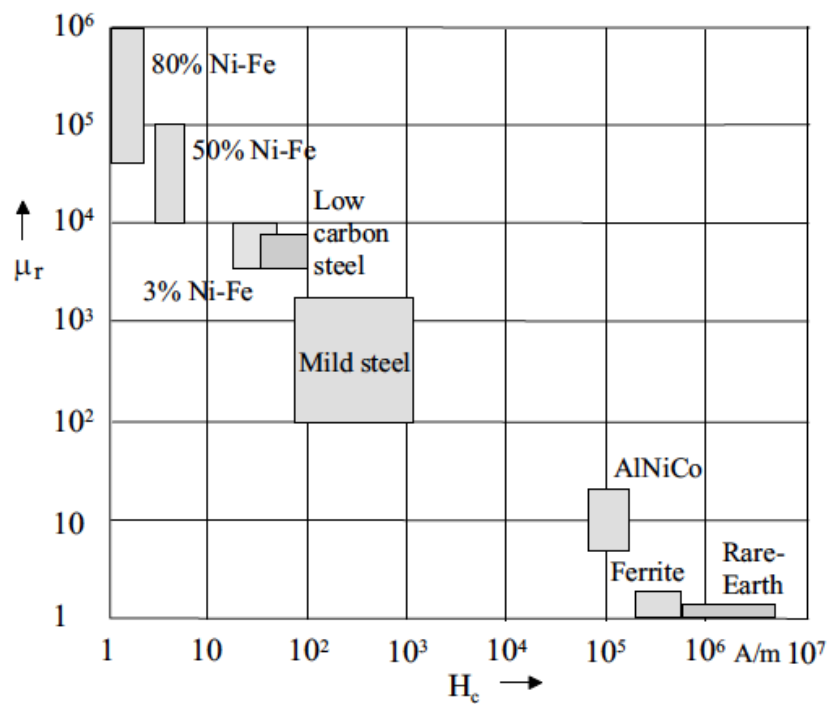
Linear (field independent, homogeneous (position independent), lossless, isotropic (direction independent, stationary

$$\mu = \mu_r \mu_0, \quad \varepsilon = \varepsilon_r \varepsilon_0,$$

$$\mu_0 = 4\pi \times 10^{-7} \text{ Hm}^{-1}, \quad \varepsilon_0 = 8.8542\dots \times 10^{-12} \text{ Fm}^{-1},$$

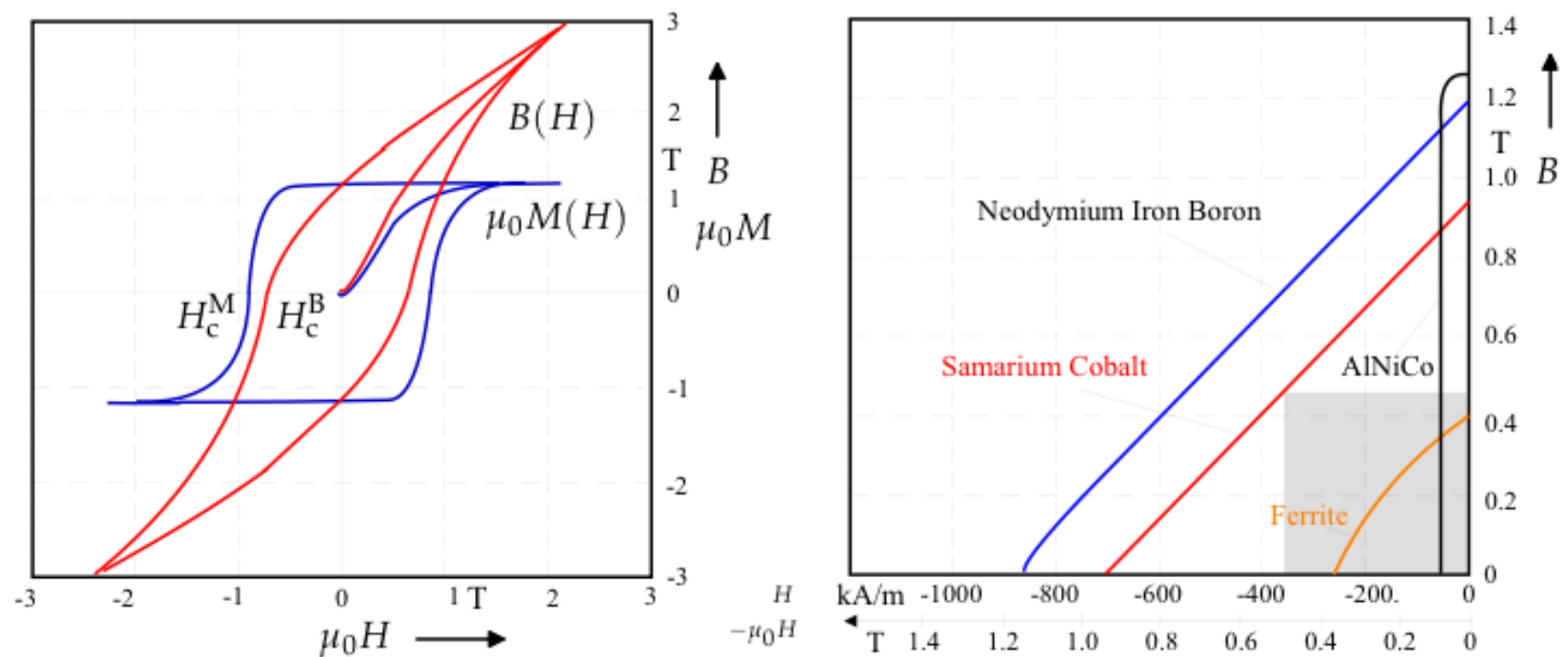


Hysteresis



$$\mathbf{B} = \mu_0 \mathbf{H} + \mathbf{P}_m(\mathbf{H}) = \mu_0 (\mathbf{H} + \mathbf{M}(\mathbf{H})),$$

$M(H)$ and $B(H)$ for Permanent Magnets



	B_r	$\mu_0 H_c^M$	H_c^B	$(BH)_{\max}$	$(BH)_{\max}^{\text{id}}$	T_c
	T	T	T	kJ m^{-3}	kJ m^{-3}	°C
AlNiCo	1.3	0.06	0.06	50	336	857
Ferrite	0.4	0.4	0.37	30	32	447
SmCo_5	0.9	2.5	0.87	160	161	727
$\text{Sm}_2\text{Co}_{17}$	1.1	1.3	0.97	220	241	827
NdFeB	1.3	1.5	1.25	320	336	313

B(H) Measurement

$H = NI/2\pi r$ within the specimen, which is

$$\bar{H} = \frac{NI}{2\pi(r_2 - r_1)} \ln \left(\frac{r_2}{r_1} \right).$$

$$U = \frac{d}{dt} \Phi = \frac{d}{dt} \bar{B} a,$$

$$\int U dt = \bar{B} a \quad \mu = \bar{B}/\bar{H}$$

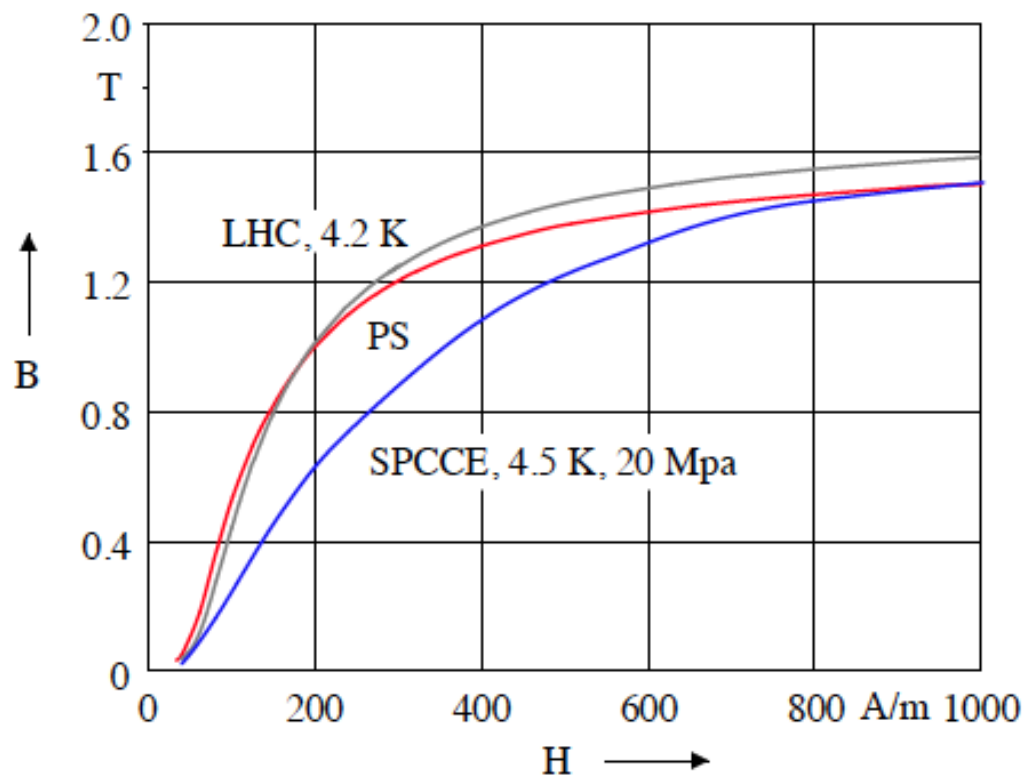
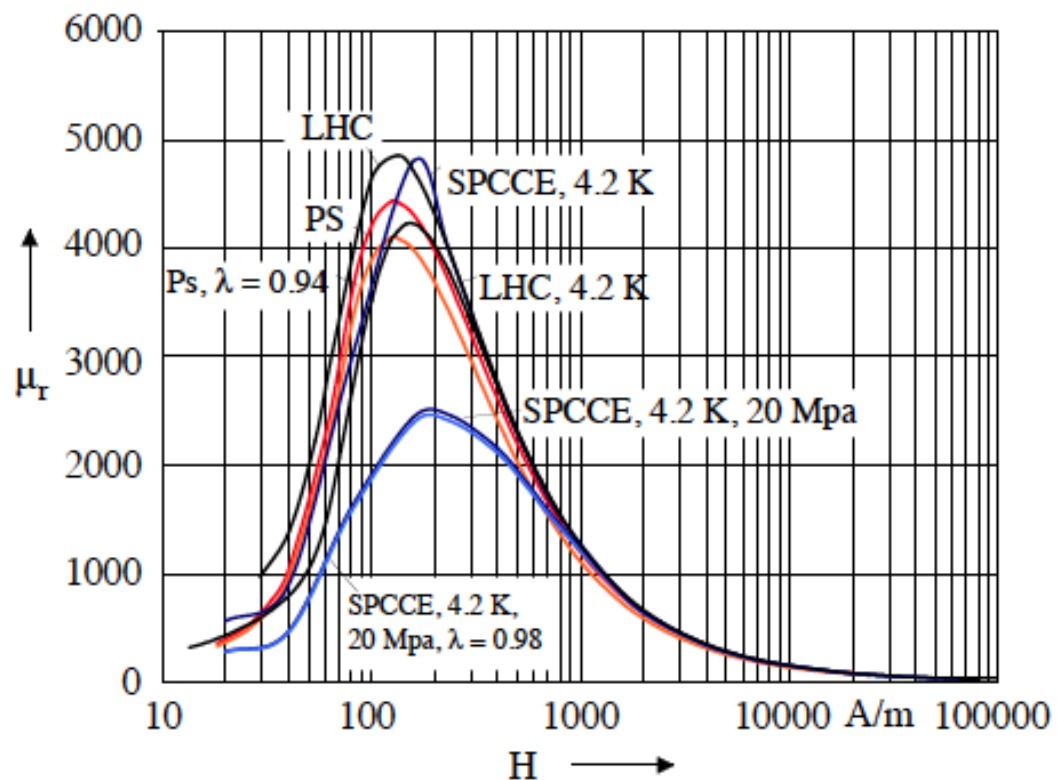
$$\bar{B} = \bar{B}_{\text{meas}} + B_{\text{corr.}}$$



Always check conditions of measurements

Temperature T	Stress	Coercive field H_c^B	Remanence B_r	max μ_r
K	MPa	A m ⁻¹	T	
300	0	68.4	1.07	5900
77	0	79.6	1.12	5600
4.2	0	85.1	1.06	4800
4.2	20	110	0.67	2460

Nonlinear Iron Magnetization



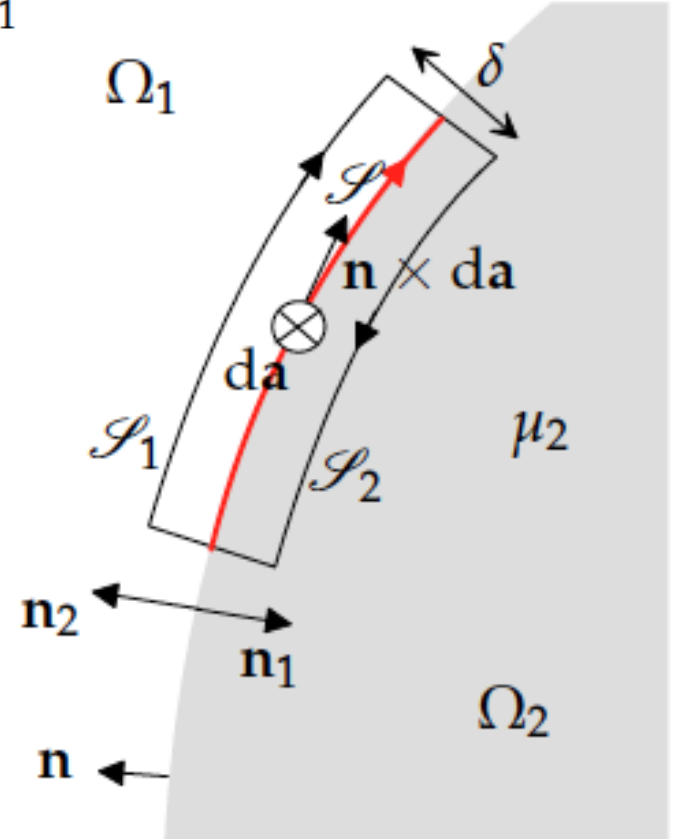
Continuity Conditions (1)

Applying Ampère's law $\int_{\partial\mathcal{A}} \mathbf{H} \cdot d\mathbf{r} = \int_{\mathcal{A}} \mathbf{J} \cdot d\mathbf{a}$ to the rectangular loop, yields for $\delta \rightarrow 0$

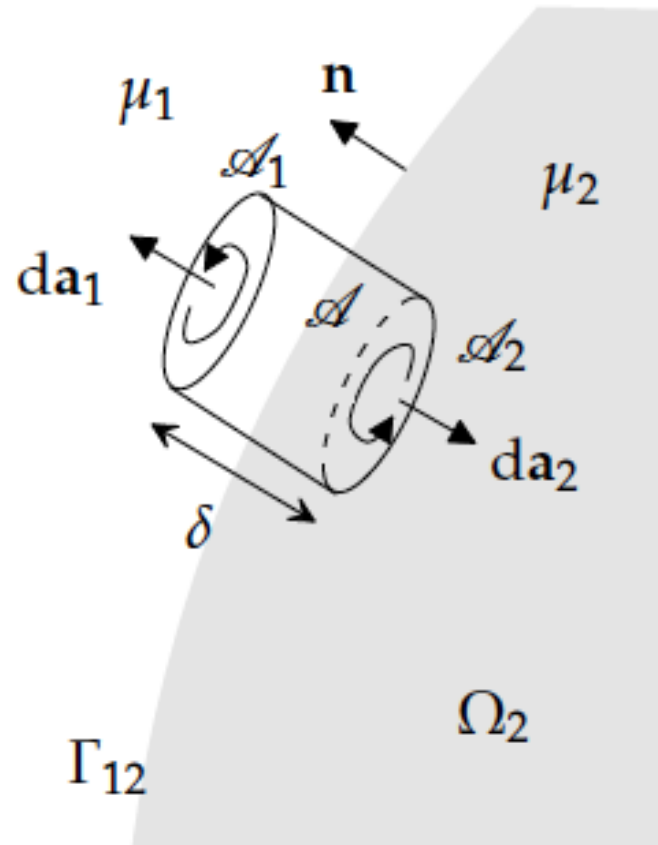
$$\int_{\mathcal{S}_2} \mathbf{H}_2 \cdot d\mathbf{r} + \int_{\mathcal{S}_1} \mathbf{H}_1 \cdot d\mathbf{r} = \int_{\mathcal{S}} (\mathbf{H}_1 - \mathbf{H}_2) \cdot d\mathbf{r} = - \int_{\mathcal{S}} (\mathbf{n} \times \boldsymbol{\alpha}) \cdot d\mathbf{r},$$

where the surface normal vector \mathbf{n} points from Ω_2 to Ω_1

$$H_{t1} = H_{t2} \quad \equiv \quad \mathbf{n} \times (\mathbf{H}_1 - \mathbf{H}_2) = 0$$



Continuity Conditions (2)



$$\int_{\partial V} \mathbf{B} \cdot d\mathbf{a} = 0 \quad \delta \rightarrow 0$$

$$\begin{aligned} \int_a \sigma_{\text{mag}} d\mathbf{a} &= \int_a \mathbf{B}_1 \cdot d\mathbf{a}_1 + \mathbf{B}_2 \cdot d\mathbf{a}_2 \\ &= \int_a (\mathbf{B}_1 - \mathbf{B}_2) \cdot \mathbf{n}_1 d\mathbf{a} \end{aligned}$$

Holds for any surface a if

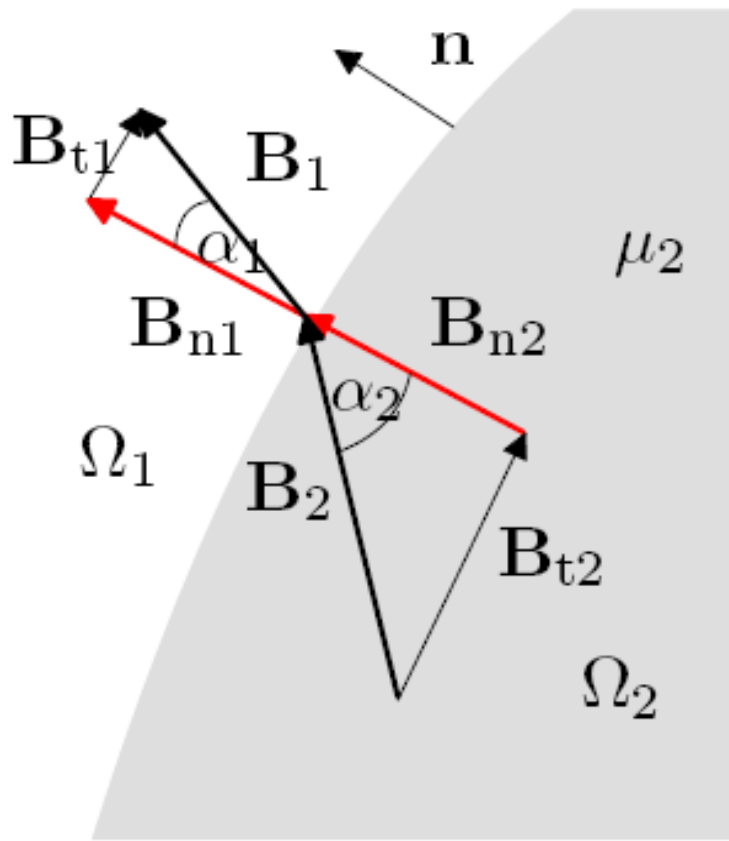
$$\begin{aligned} \sigma_{\text{mag}} &= (\mathbf{B}_1 - \mathbf{B}_2) \cdot \mathbf{n} \\ &= [\mathbf{B} \cdot \mathbf{n}]_{12} \end{aligned}$$

$$B_{n1} = B_{n2} \equiv (\mathbf{B}_1 - \mathbf{B}_2) \cdot \mathbf{n} = 0 \equiv [\mathbf{B} \cdot \mathbf{n}]_{12} = 0$$

Continuity Conditions (3)

No surface currents:

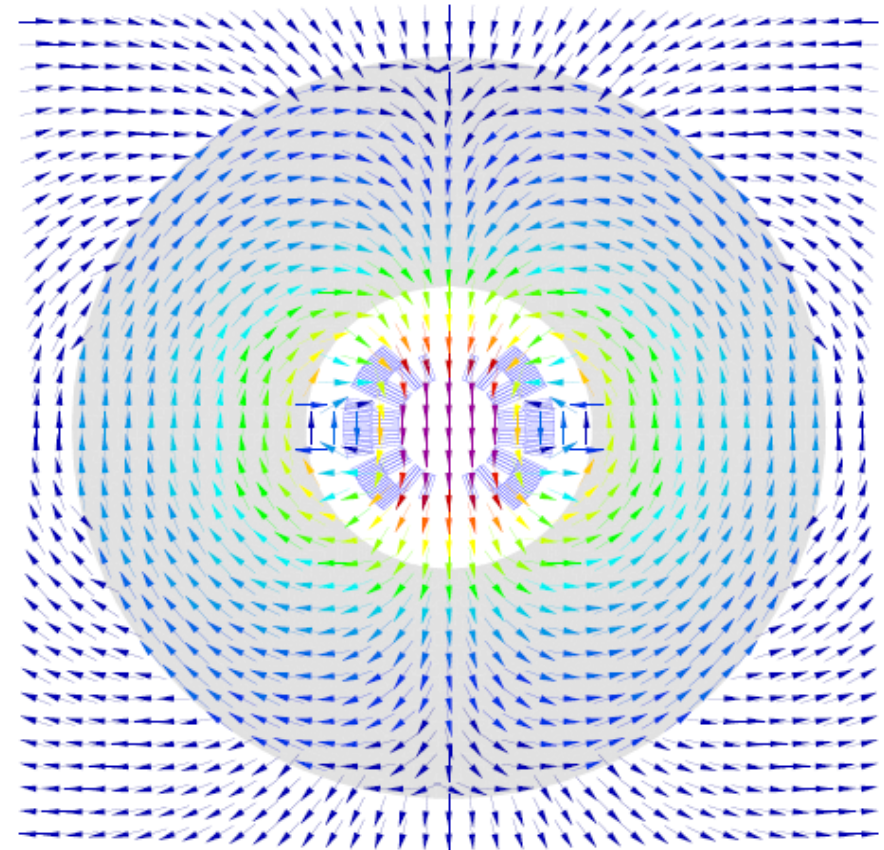
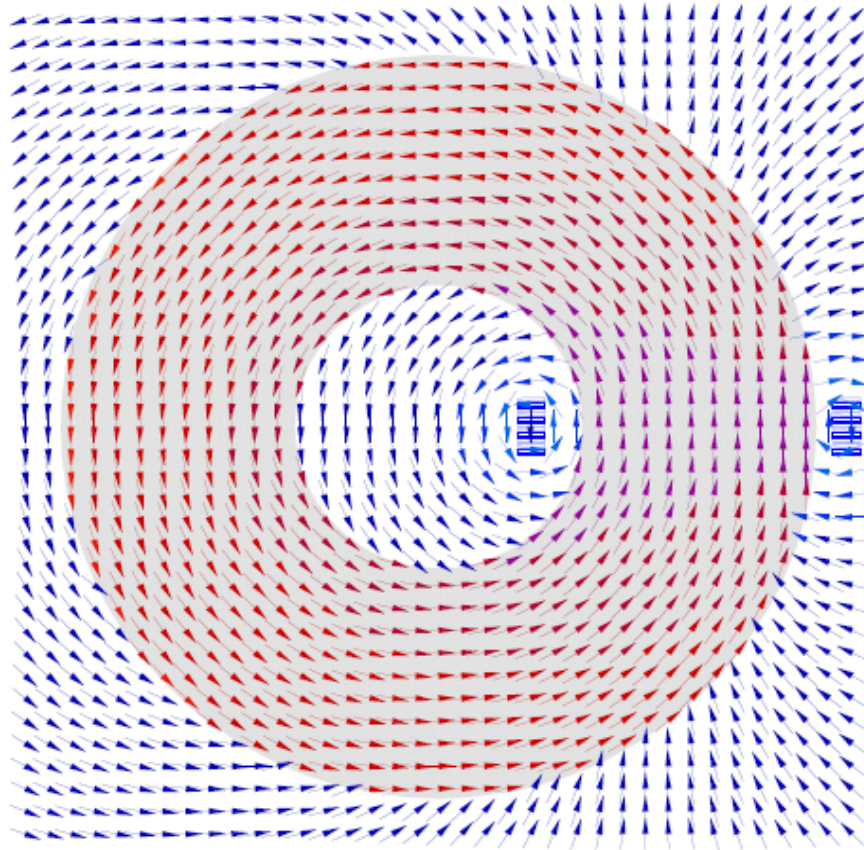
$$\frac{\tan \alpha_1}{\tan \alpha_2} = \frac{\frac{B_{t1}}{B_{n1}}}{\frac{B_{t2}}{B_{n2}}} = \frac{\mu_1 \frac{H_{t1}}{B_{n1}}}{\mu_2 \frac{H_{t2}}{B_{n2}}} = \frac{\mu_1 H_{t1}}{\mu_2 H_{t2}} = \frac{\mu_1}{\mu_2}$$



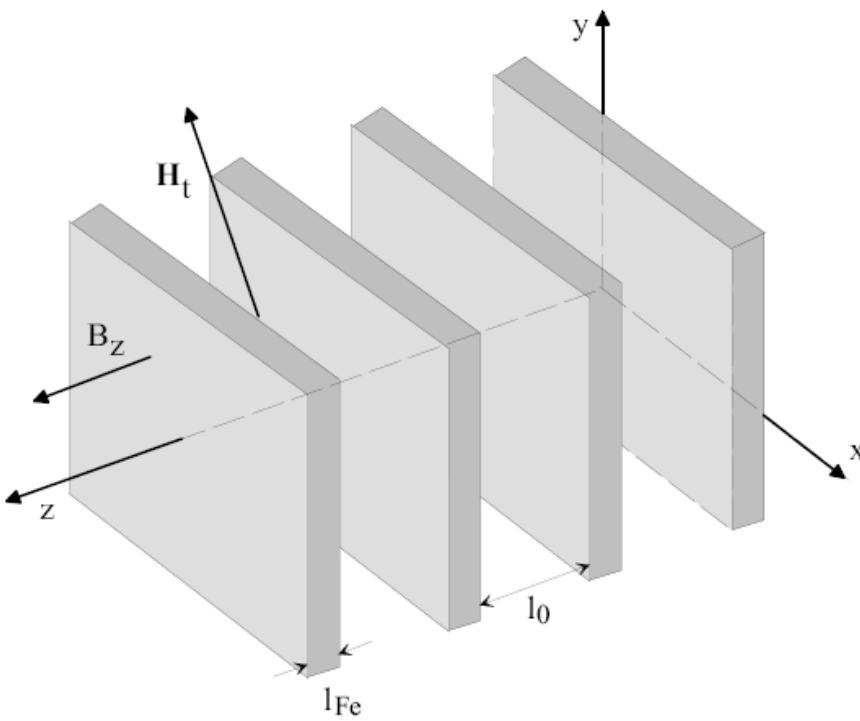
$$\mu_2 \gg \mu_1$$

$$\alpha_1 \approx 0, \quad \text{or} \quad \alpha_2 \approx \pi/2,$$

Continuity at Iron Boundaries



Stacking Factor for Yoke Laminations



$$H_t^0 = H_t^{Fe} = \bar{H}_t$$

$$\bar{B}_t = \frac{1}{l_{Fe} + l_0} (l_{Fe}\mu\bar{H}_t + l_0\mu_0\bar{H}_t)$$

$$B_z^0 = B_z^{Fe} = \bar{B}_z$$

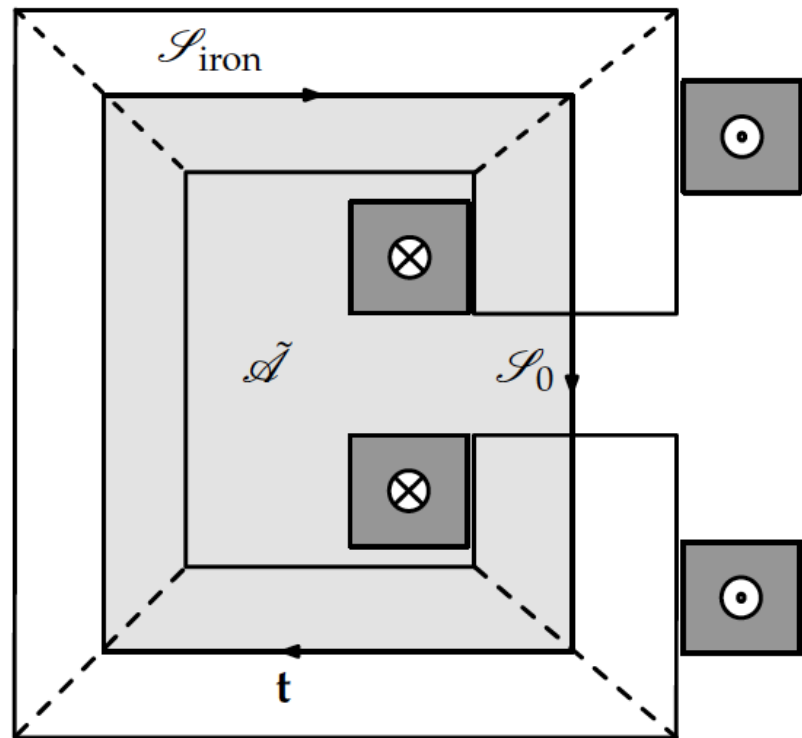
$$\bar{H}_z = \frac{1}{l_{Fe} + l_0} \left(l_{Fe} \frac{\bar{B}_z}{\mu} + l_0 \frac{\bar{B}_z}{\mu_0} \right)$$

$$\lambda = \frac{l_{Fe}}{l_{Fe} + l_0}$$

$$\bar{\mu}_t = \lambda\mu + (1 - \lambda)\mu_0$$

$$\bar{\mu}_z = \left(\frac{\lambda}{\mu} + \frac{1 - \lambda}{\mu_0} \right)^{-1}$$

Main Field in Normal Conducting Dipole



$$\int_{\partial \tilde{\mathcal{A}}} \mathbf{H} \cdot d\mathbf{r} = \int_{\tilde{\mathcal{A}}} \mathbf{J} \cdot \mathbf{n} da,$$

$$\int_{\mathcal{S}_{\text{iron}}} \mathbf{H} \cdot d\mathbf{r} + \int_{\mathcal{S}_0} \mathbf{H} \cdot d\mathbf{r} = \int_{\tilde{\mathcal{A}}_{\text{coil}}} \mathbf{J} \cdot \mathbf{n} da,$$

$$H_{\text{iron}} s_{\text{iron}} + H_0 s_0 = NI,$$

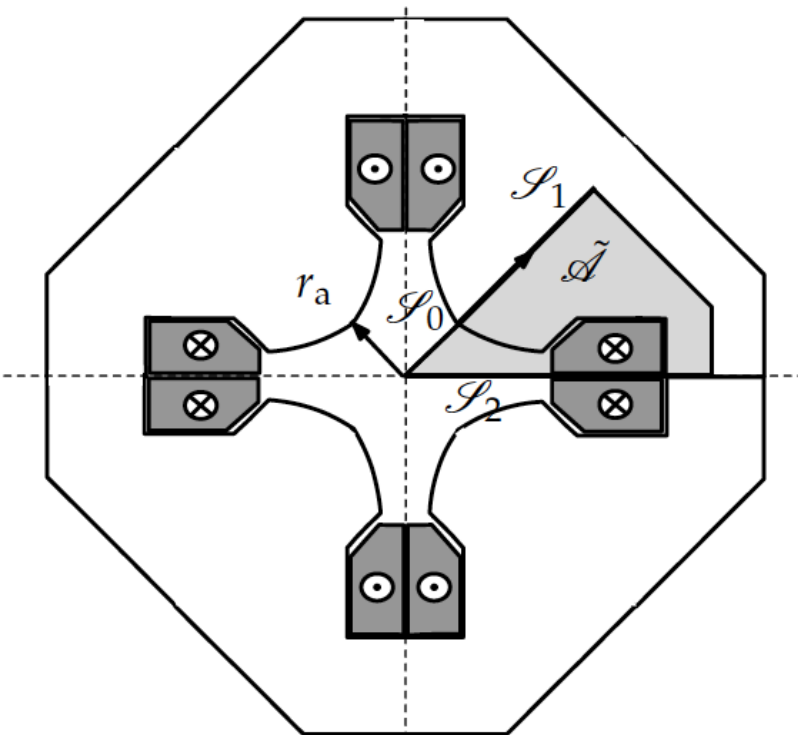
$$\frac{1}{\mu_0 \mu_r} B_{\text{iron}} s_{\text{iron}} + \frac{1}{\mu_0} B_0 s_0 = NI,$$

$$B_0 = \frac{\mu_0 NI}{s_0}.$$

Interrupt: Ampere-turns

Gradient in Normal Conducting Quadrupole

$$\int_{\partial \tilde{\mathcal{A}}} \mathbf{H} \cdot d\mathbf{r} = \int_{\mathcal{S}_0} \mathbf{H}_0 \cdot d\mathbf{r} + \int_{\mathcal{S}_1} \mathbf{H}_1 \cdot d\mathbf{r} + \int_{\mathcal{S}_2} \mathbf{H}_2 \cdot d\mathbf{r} = NI.$$



$$B_x = gy, \quad B_y = gx;$$

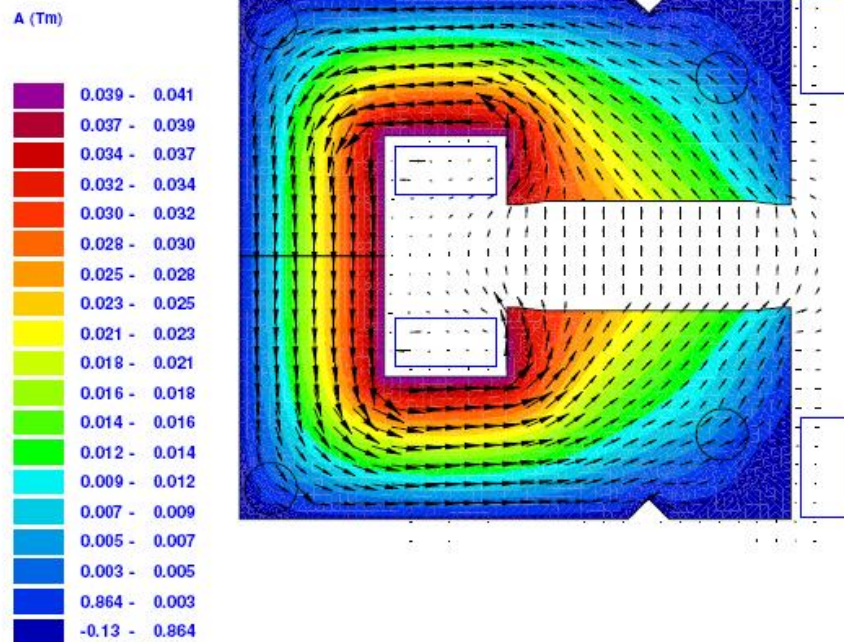
$$H = \frac{g}{\mu_0} \sqrt{x^2 + y^2} = \frac{g}{\mu_0} r.$$

$$\int_0^{r_a} H dr = \frac{g}{\mu_0} \int_0^{r_a} r dr = \frac{g}{\mu_0} \frac{r_a^2}{2} = NI,$$

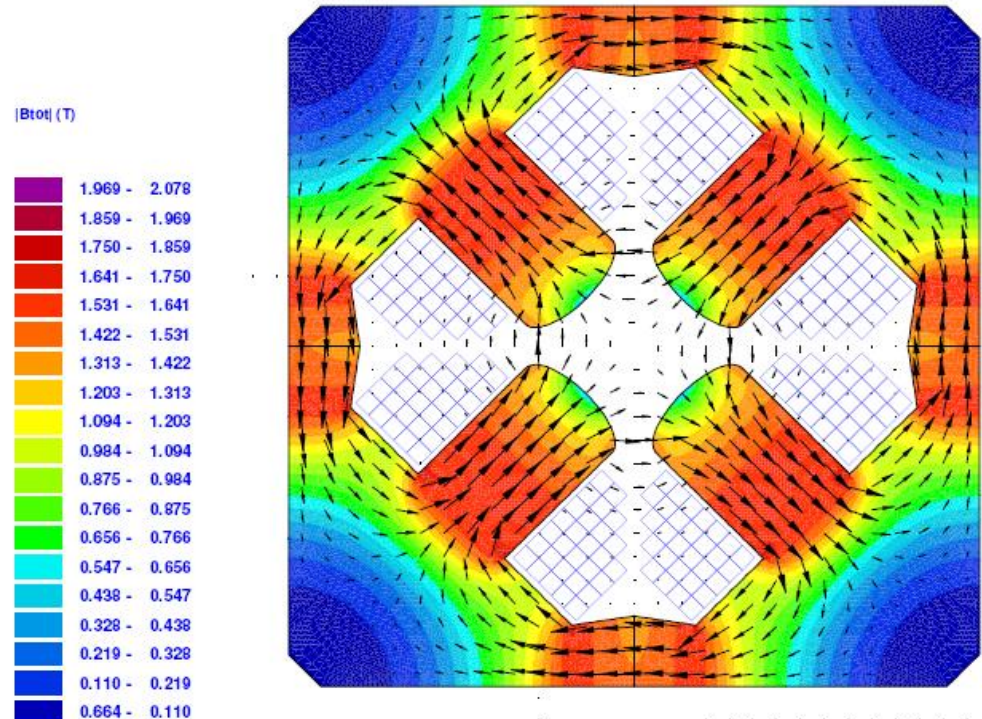
or

$$g = \frac{2\mu_0 NI}{r_a^2}.$$

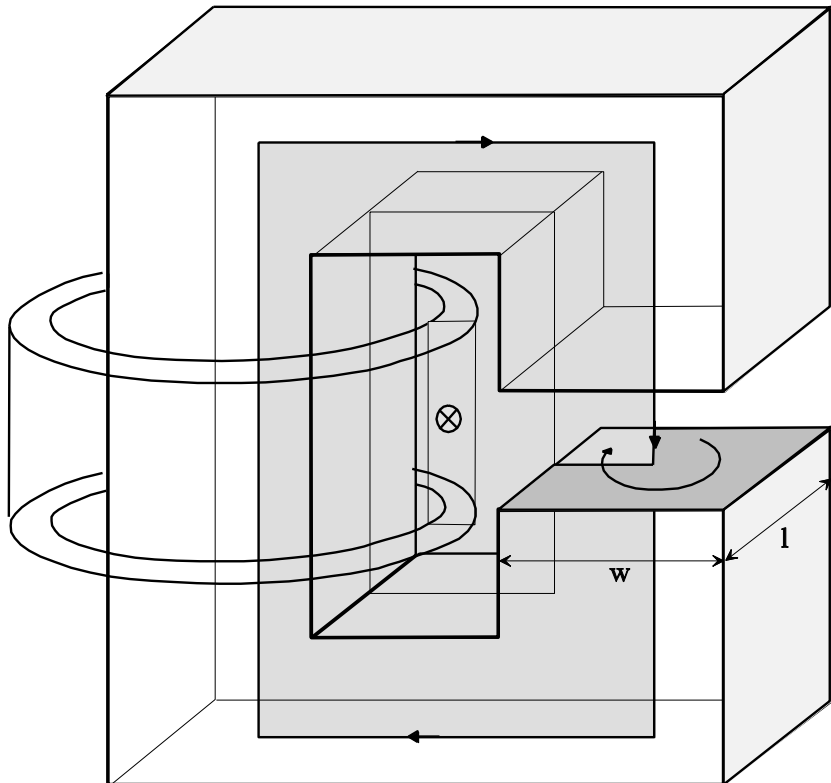
LEP Dipole and Quadrupole



Interrupt: Exercise c-core
dipole; comparison to
ROXIE simulations



Dipole with Varying Cut-Section



$$\sum_{i=0}^n H_i s_i = N I$$

$$H_i = \frac{B_i}{\mu_i} = \frac{\Phi}{a_i \mu_i}$$

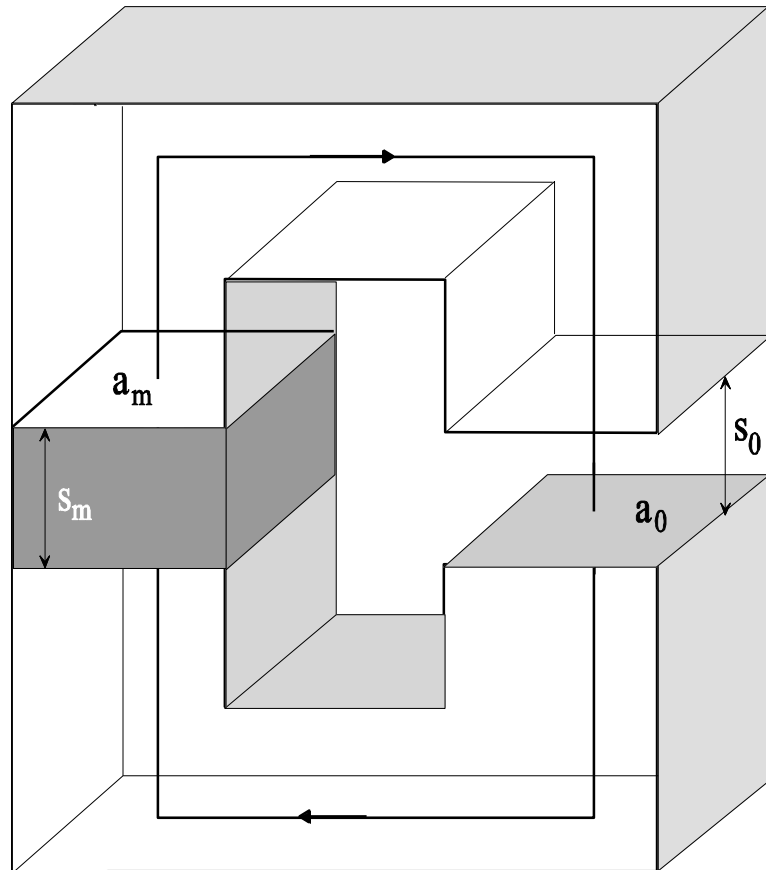
$$\Phi \sum_{i=0}^n \frac{s_i}{a_i \mu_i} = N I = V_m$$

$$\text{Ohm's law: } I \sum_{i=0}^n \frac{s_i}{a_i \kappa_i} = U$$

$$N I = \Phi \sum_{i=0}^n \frac{s_i}{a_i \mu_i} = \Phi \left(\frac{s_0}{a_0 \mu_0} + \sum_{i=1}^n \frac{s_i}{a_i \mu_i} \right)$$

Conclusion: Magnet with large air-gap is stabilized against variations in permeability

Permanent Magnet Excitation



$$H_0 s_0 + H_m s_m = 0$$

$$B_m a_m = B_0 a_0 = \mu_0 H_0 a_0$$

$$H_0 s_0 = -H_m s_m,$$

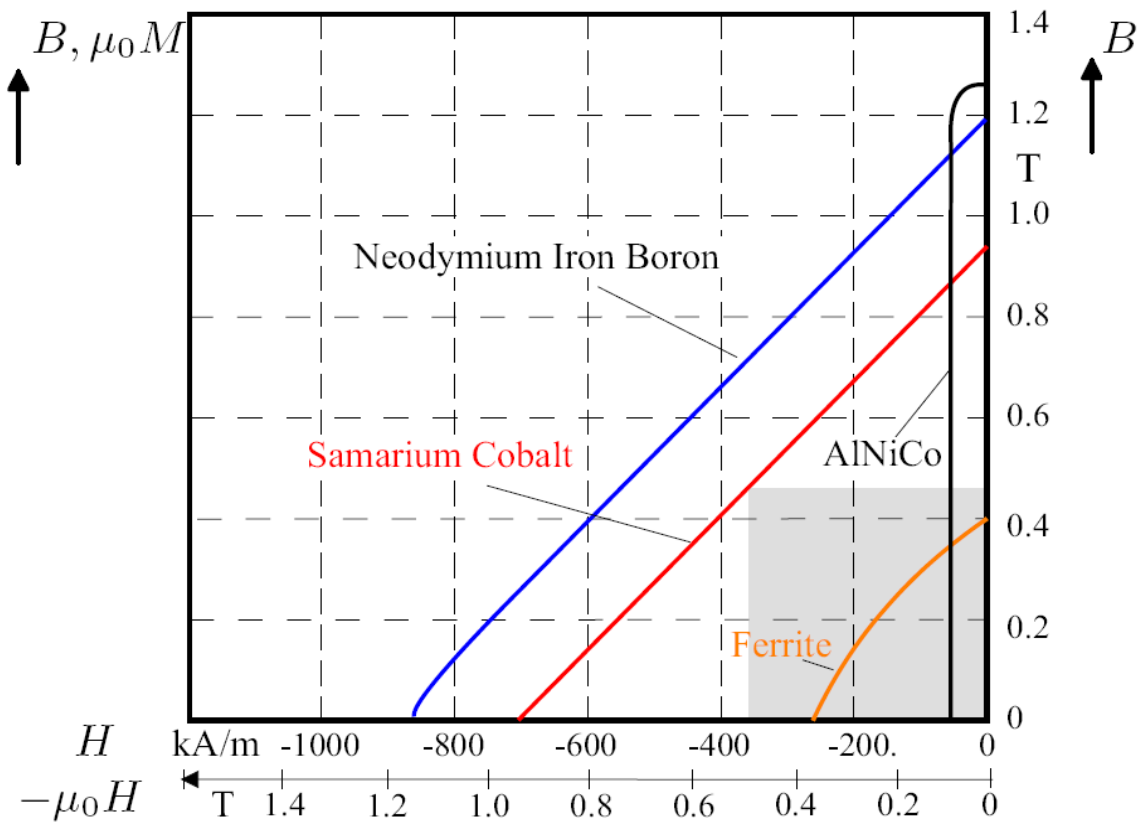
$$\frac{1}{\mu_0} B_m \frac{a_m}{a_0} s_0 = -H_m s_m,$$

$$B_m = -\mu_0 \frac{s_m a_0}{s_0 a_m} H_m,$$

$$\frac{B_m}{\mu_0 H_m} = -\frac{s_m a_0}{s_0 a_m} = P$$

$$s = \frac{B_m}{H_m} = \mu_0 P = -\mu_0 \frac{s_m a_0}{s_0 a_m} = \mu_0 \frac{M(1-N)}{H_m - N M}$$

BH Maximum



$$B_{\text{max}} = B_0 a_0 = \mu_0 H_0 a_0$$

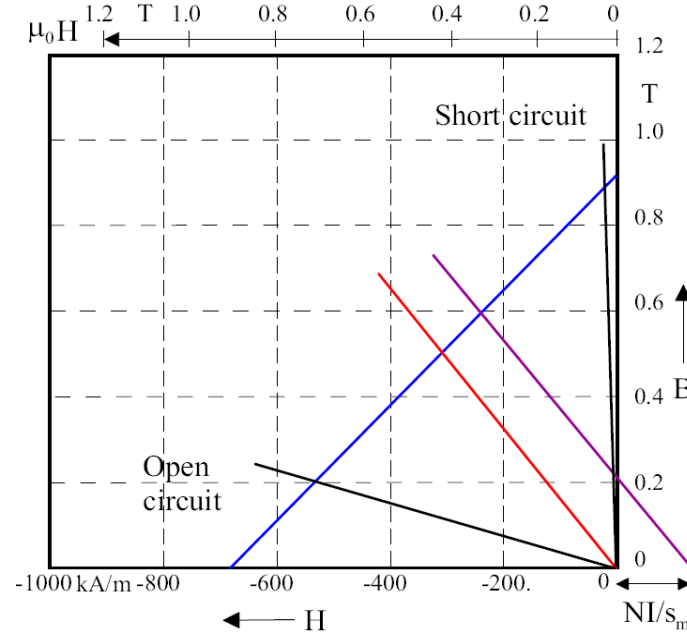
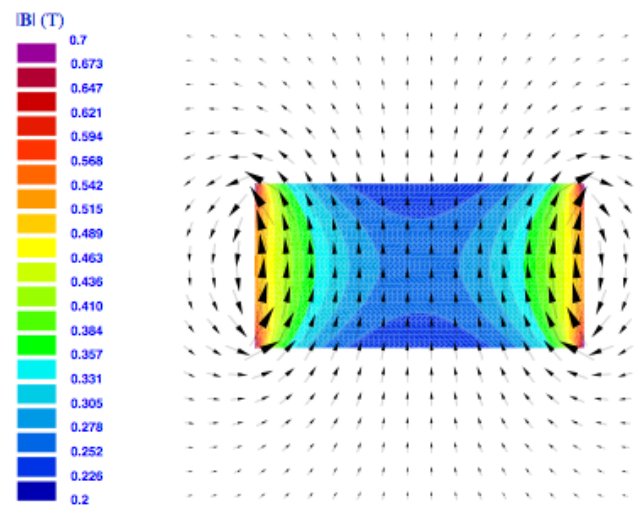
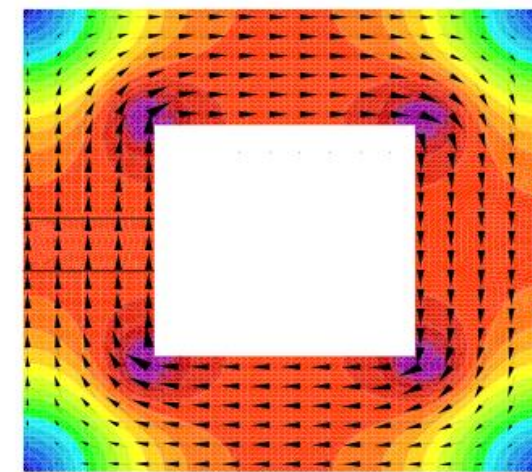
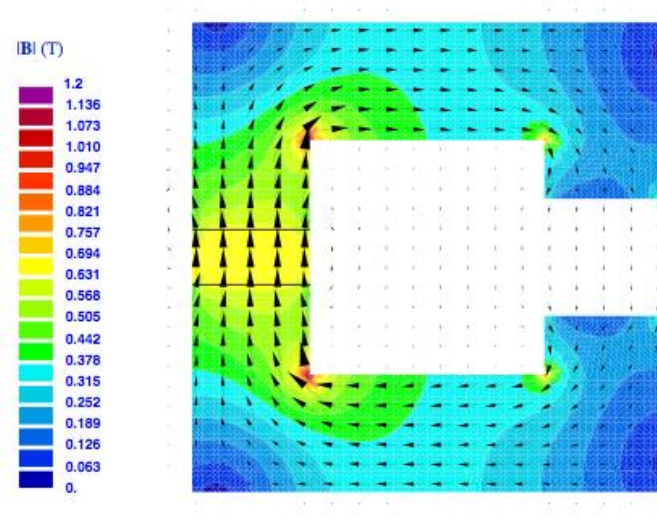
$$H_0 s_0 = -H_{\text{msm}}$$

$$B_{\text{maxsm}} = \mu_0 H_0 a_0 \frac{-H_0 s_0}{H_m}$$

$$(BH)_{\text{max}}^{\text{id}} := \frac{B_r^2}{4\mu_0},$$

$$H_0 = \sqrt{\frac{(a_{\text{msm}})(-B_m H_m)}{\mu_0 (a_0 s_0)}} = \sqrt{\frac{V_m (-B_m H_m)}{\mu_0 V_0}}$$

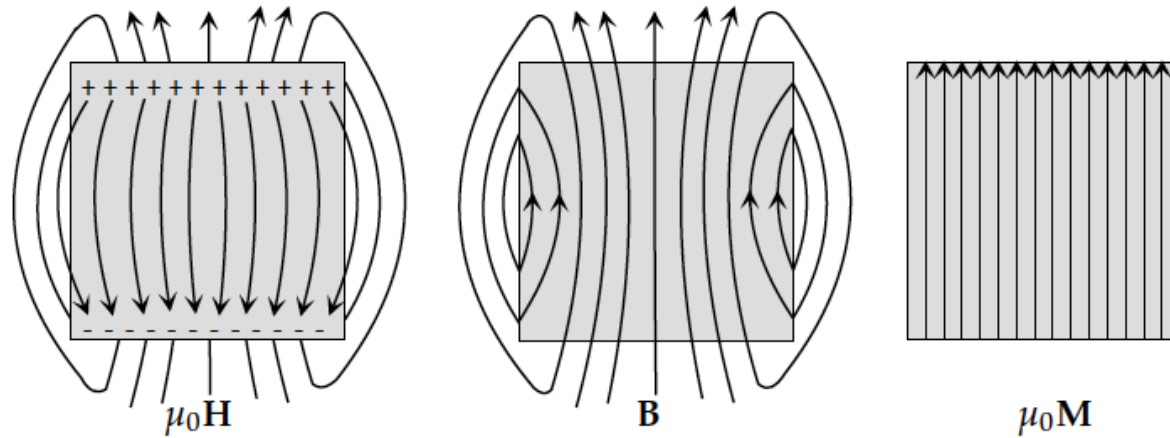
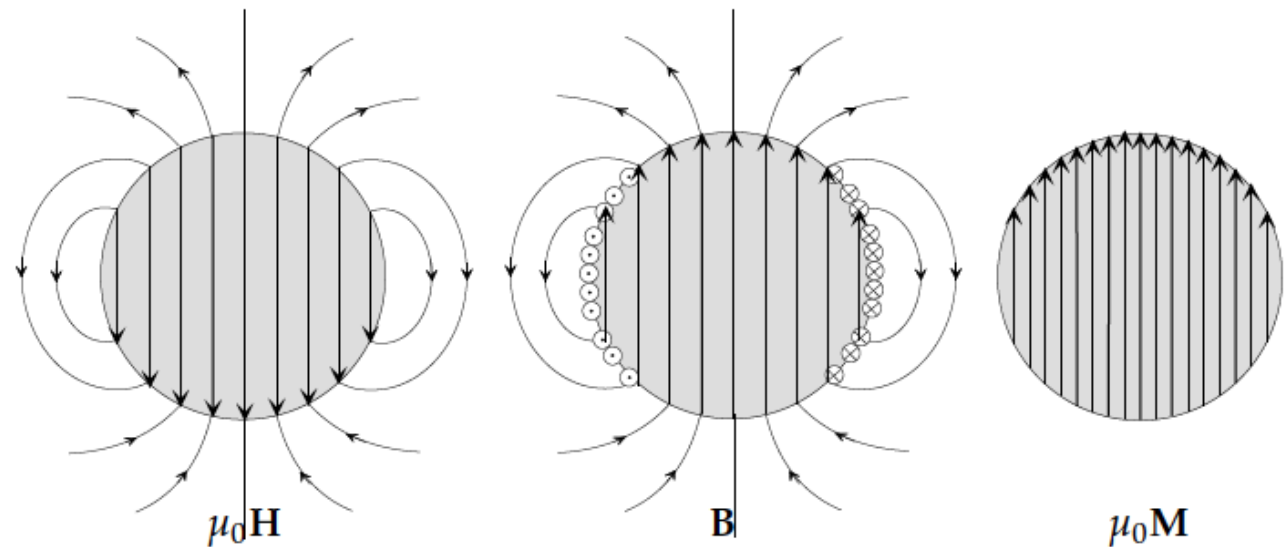
Permanent Magnet Circuits



$$s = \frac{B_m}{H_m} = \mu_0 P = -\mu_0 \frac{s_m a_0}{s_0 a_m}$$

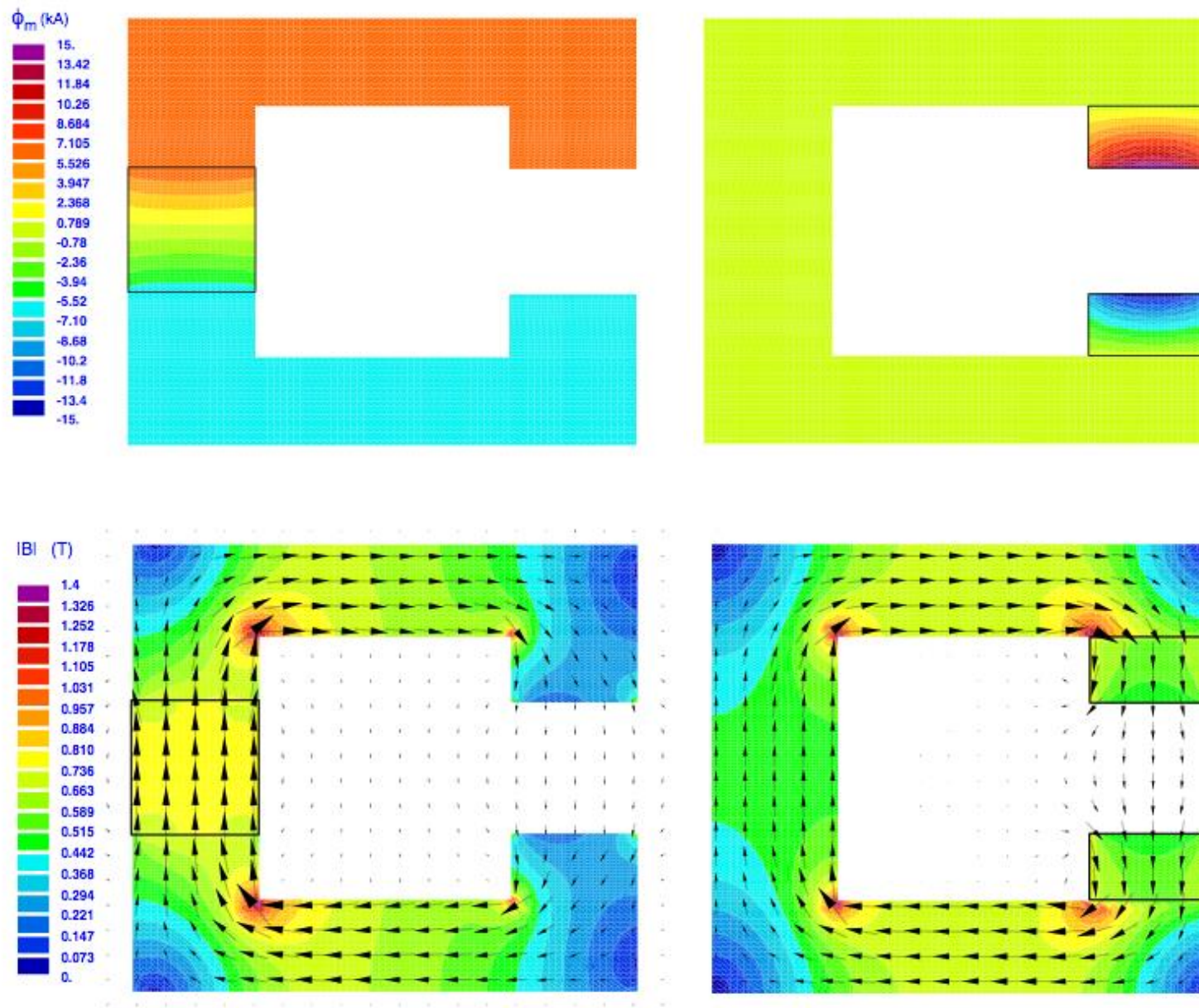
Surface charges and Surface Currents

$$\alpha = -\mathbf{n} \times [\mathbf{M}]_{12}$$

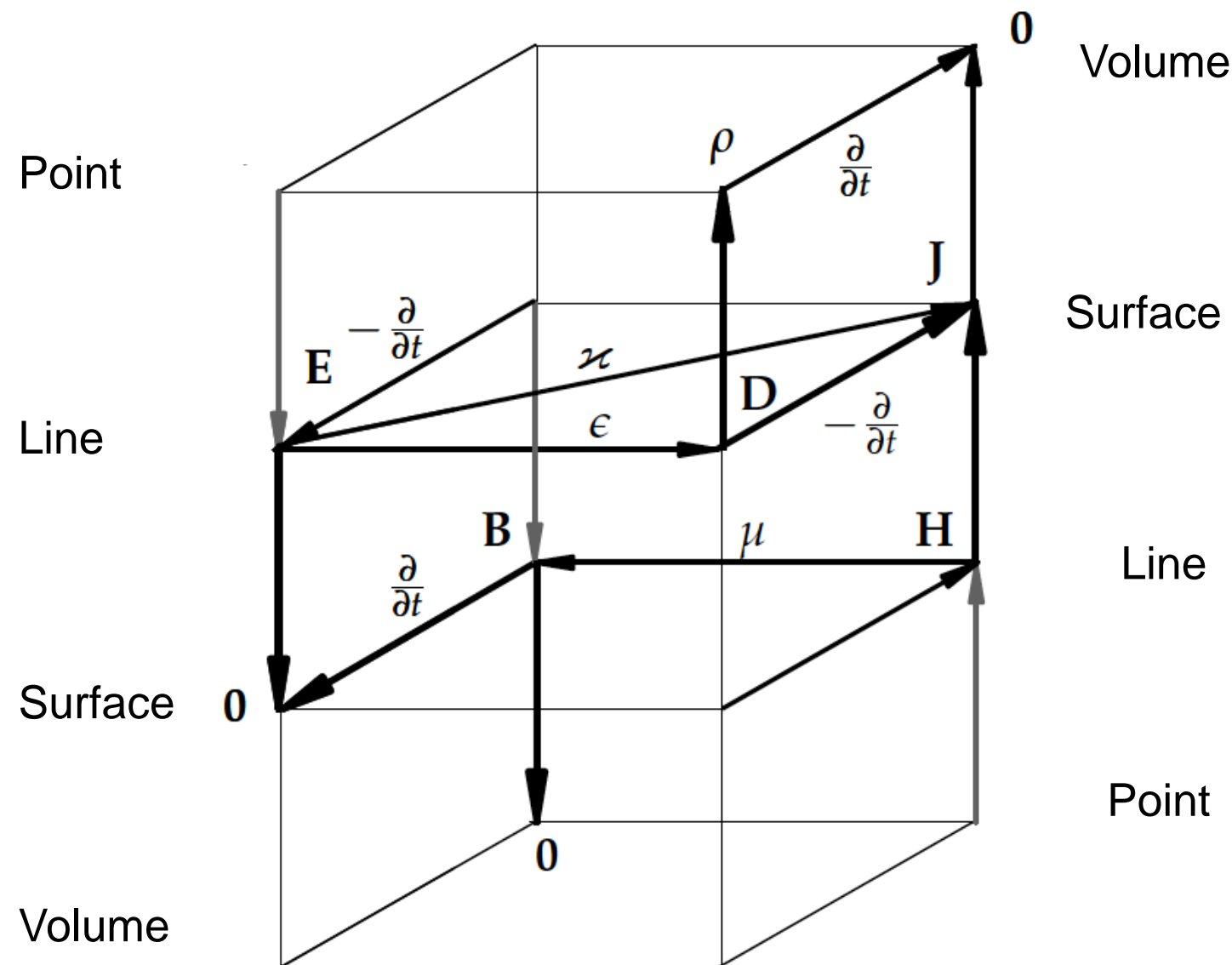


$$\sigma_m = -\mu_0 \mathbf{n} \cdot [\mathbf{M}]_{12}$$

Optimal Position of Permanent Magnets



Maxwell's House Again



Coordinate Free Definition of Grad, Curl, and Div

$$\int_{\mathcal{P}_1}^{\mathcal{P}_2} \mathbf{a} \cdot d\mathbf{r} = \int_{\mathcal{P}_1}^{\mathcal{P}_2} \text{grad } \phi \cdot d\mathbf{r} = \int_{\mathcal{P}_1}^{\mathcal{P}_2} d\phi = \phi(\mathcal{P}_2) - \phi(\mathcal{P}_1),$$

-

$$\mathbf{n} \cdot \text{curl } \mathbf{g} = \lim_{a \rightarrow 0} \frac{\int_{\partial \mathcal{A}} \mathbf{g} \cdot d\mathbf{r}}{a},$$

$$\text{div } \mathbf{g} = \lim_{V \rightarrow 0} \frac{\int_{\partial V} \mathbf{g} \cdot d\mathbf{a}}{V},$$



Grad, Curl and Div in Cartesian Coordinates

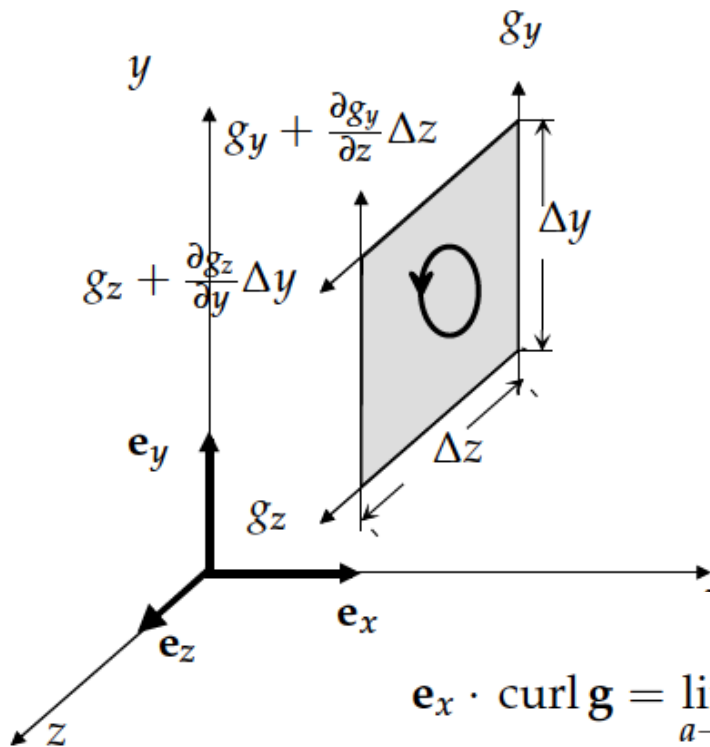
$$\text{grad } \phi := \frac{\partial \phi}{\partial x} \mathbf{e}_x + \frac{\partial \phi}{\partial y} \mathbf{e}_y + \frac{\partial \phi}{\partial z} \mathbf{e}_z$$

$$\text{curl } \mathbf{g} = \left(\frac{\partial g_z}{\partial y} - \frac{\partial g_y}{\partial z} \right) \mathbf{e}_x + \left(\frac{\partial g_x}{\partial z} - \frac{\partial g_z}{\partial x} \right) \mathbf{e}_y + \left(\frac{\partial g_y}{\partial x} - \frac{\partial g_x}{\partial y} \right) \mathbf{e}_z.$$

$$\text{div } \mathbf{g} = \frac{\partial g_x}{\partial x} + \frac{\partial g_y}{\partial y} + \frac{\partial g_z}{\partial z}.$$



Curl in Cartesian Coordinates



$$\mathbf{e}_x \cdot \operatorname{curl} \mathbf{g} = \lim_{a \rightarrow 0} \frac{\int_{\partial \mathcal{A}} \mathbf{g} \cdot d\mathbf{r}}{a}$$

$$\begin{aligned}
 &= \lim_{\Delta y, \Delta z \rightarrow 0} \frac{g_y \Delta y + \left(g_z + \frac{\partial g_z}{\partial y} \Delta y\right) \Delta z - \left(g_y + \frac{\partial g_y}{\partial z} \Delta z\right) \Delta y - g_z \Delta z}{\Delta y \Delta z} \\
 &= \frac{\partial g_z}{\partial y} - \frac{\partial g_y}{\partial z}.
 \end{aligned}$$

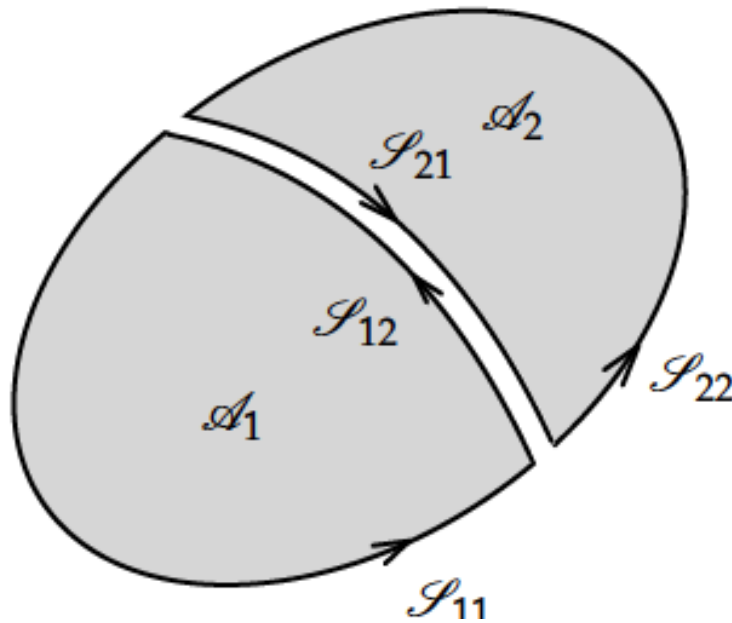
$$\operatorname{curl} \mathbf{g} = \left(\frac{\partial g_z}{\partial y} - \frac{\partial g_y}{\partial z} \right) \mathbf{e}_x + \left(\frac{\partial g_x}{\partial z} - \frac{\partial g_z}{\partial x} \right) \mathbf{e}_y + \left(\frac{\partial g_y}{\partial x} - \frac{\partial g_x}{\partial y} \right) \mathbf{e}_z.$$

Differential Operators in Coordinates

	Cartesian	Cylindrical
u^1, u^2, u^3	x, y, z	r, φ, z
ds^2	$dx^2 + dy^2 + dz^2$	$dr^2 + r^2 d\varphi^2 + dz^2$
dV	$dxdydz$	$rdrd\varphi dz$
$\text{grad } \phi$	$\frac{\partial \phi}{\partial x} \mathbf{e}_x + \frac{\partial \phi}{\partial y} \mathbf{e}_y + \frac{\partial \phi}{\partial z} \mathbf{e}_z$	$\frac{\partial \phi}{\partial r} \mathbf{e}_r + \frac{1}{r} \frac{\partial \phi}{\partial \varphi} \mathbf{e}_\varphi + \frac{\partial \phi}{\partial z} \mathbf{e}_z$
$\text{div } \mathbf{g}$	$\frac{\partial g_x}{\partial x} + \frac{\partial g_y}{\partial y} + \frac{\partial g_z}{\partial z}$	$\frac{1}{r} \frac{\partial}{\partial r} (rg_r) + \frac{1}{r} \frac{\partial g_\varphi}{\partial \varphi} + \frac{\partial g_z}{\partial z}$
$\text{curl } \mathbf{g}$	$\begin{aligned} & \left(\frac{\partial g_z}{\partial y} - \frac{\partial g_y}{\partial z} \right) \mathbf{e}_x \\ & + \left(\frac{\partial g_x}{\partial z} - \frac{\partial g_z}{\partial x} \right) \mathbf{e}_y \\ & + \left(\frac{\partial g_y}{\partial x} - \frac{\partial g_x}{\partial y} \right) \mathbf{e}_z \end{aligned}$	$\begin{aligned} & \left(\frac{1}{r} \frac{\partial g_z}{\partial \varphi} - \frac{\partial g_\varphi}{\partial z} \right) \mathbf{e}_r \\ & + \left(\frac{\partial g_r}{\partial z} - \frac{\partial g_z}{\partial r} \right) \mathbf{e}_\varphi \\ & + \left(\frac{1}{r} \frac{\partial}{\partial r} (rg_\varphi) - \frac{1}{r} \frac{\partial g_r}{\partial \varphi} \right) \mathbf{e}_z \end{aligned}$
$\nabla^2 \phi$	$\frac{\partial^2 \phi}{\partial x^2} + \frac{\partial^2 \phi}{\partial y^2} + \frac{\partial^2 \phi}{\partial z^2}$	$\frac{1}{r} \frac{\partial}{\partial r} \left(r \frac{\partial \phi}{\partial r} \right) + \frac{1}{r^2} \frac{\partial^2 \phi}{\partial \varphi^2} + \frac{\partial^2 \phi}{\partial z^2}$



Kelvin-Stokes Theorem

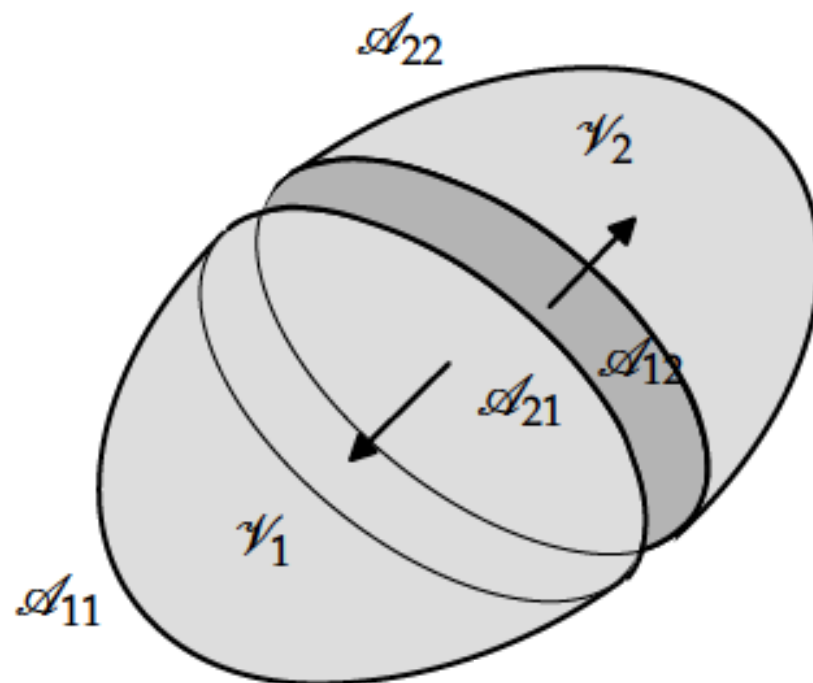


Smooth vector fields, smooth surfaces with simply connected, closed, piecewise-smooth and consistently oriented boundaries, and volumes with piecewise-smooth, closed and consistently oriented surfaces.

$$\int_{\partial \mathcal{A}} \mathbf{g} \cdot d\mathbf{r} = \int_{S_1} \mathbf{g} \cdot d\mathbf{r} + \int_{S_2} \mathbf{g} \cdot d\mathbf{r} = \int_{S_{11}} \mathbf{g} \cdot d\mathbf{r} + \int_{S_{22}} \mathbf{g} \cdot d\mathbf{r},$$

$$\begin{aligned}\int_{\partial \mathcal{A}} \mathbf{g} \cdot d\mathbf{r} &= \lim_{I \rightarrow \infty} \sum_{i=1}^I \int_{\partial \mathcal{A}_i} \mathbf{g} \cdot d\mathbf{r} = \lim_{I \rightarrow \infty} \sum_{i=1}^I \Delta a_i \frac{1}{\Delta a_i} \int_{\partial \mathcal{A}_i} \mathbf{g} \cdot d\mathbf{r} \\ &= \lim_{I \rightarrow \infty} \sum_{i=1}^I (\operatorname{curl} \mathbf{g})_i \cdot \mathbf{n} \Delta a_i = \int_{\mathcal{A}} \operatorname{curl} \mathbf{g} \cdot d\mathbf{a}.\end{aligned}$$

Gauss' Theorem



Smooth vector fields, smooth surfaces with simply connected, closed, piecewise-smooth and consistently oriented boundaries, and volumes with piecewise-smooth, closed and consistently oriented surfaces.

$$\int_{\partial V} \mathbf{g} \cdot d\mathbf{a} = \int_{\mathcal{A}_1} \mathbf{g} \cdot d\mathbf{a} + \int_{\mathcal{A}_2} \mathbf{g} \cdot d\mathbf{a} = \int_{\mathcal{A}_{11}} \mathbf{g} \cdot d\mathbf{a} + \int_{\mathcal{A}_{22}} \mathbf{g} \cdot d\mathbf{a}$$

$$\begin{aligned}\int_{\partial V} \mathbf{g} \cdot d\mathbf{a} &= \lim_{I \rightarrow \infty} \sum_{i=1}^I \int_{\partial \gamma_i} \mathbf{g} \cdot d\mathbf{a} = \lim_{I \rightarrow \infty} \sum_{i=1}^I \Delta V_i \frac{1}{\Delta V_i} \int_{\partial \gamma_i} \mathbf{g} \cdot d\mathbf{a} \\ &= \lim_{I \rightarrow \infty} \sum_{i=1}^I (\operatorname{div} \mathbf{g})_i \Delta V_i = \int_V \operatorname{div} \mathbf{g} dV.\end{aligned}$$

Maxwell's Equations in Differential Form

$$\int_{\mathcal{A}} \operatorname{curl} \mathbf{g} \cdot d\mathbf{a} = \int_{\partial\mathcal{A}} \mathbf{g} \cdot d\mathbf{r}, \quad \begin{cases} \int_{\partial\mathcal{A}} \mathbf{H} \cdot d\mathbf{r} = \int_{\mathcal{A}} \mathbf{J} \cdot d\mathbf{a} + \frac{d}{dt} \int_{\mathcal{A}} \mathbf{D} \cdot d\mathbf{a}, \\ \int_{\partial\mathcal{A}} \mathbf{E} \cdot d\mathbf{r} = -\frac{d}{dt} \int_{\mathcal{A}} \mathbf{B} \cdot d\mathbf{a}, \\ \int_{\partial\mathcal{A}} \mathbf{B} \cdot d\mathbf{a} = 0, \\ \int_{\partial\mathcal{A}} \mathbf{D} \cdot d\mathbf{a} = \int_{\mathcal{V}} \rho dV. \end{cases}$$
$$\int_{\mathcal{V}} \operatorname{div} \mathbf{g} dV = \int_{\partial\mathcal{V}} \mathbf{g} \cdot d\mathbf{a}, \quad \begin{cases} \int_{\partial\mathcal{V}} \mathbf{H} \cdot d\mathbf{a} = \int_{\mathcal{A}} \left(\mathbf{J} + \frac{\partial}{\partial t} \mathbf{D} \right) \cdot d\mathbf{a}, \\ \int_{\mathcal{V}} \operatorname{curl} \mathbf{E} \cdot d\mathbf{a} = -\int_{\mathcal{A}} \frac{\partial}{\partial t} \mathbf{B} \cdot d\mathbf{a}, \\ \int_{\mathcal{V}} \operatorname{div} \mathbf{B} dV = 0, \\ \int_{\mathcal{V}} \operatorname{div} \mathbf{D} dV = \int_{\mathcal{V}} \rho dV. \end{cases}$$

$$\begin{array}{ccc} \int_{\mathcal{A}} \operatorname{curl} \mathbf{H} \cdot d\mathbf{a} = \int_{\mathcal{A}} \left(\mathbf{J} + \frac{\partial}{\partial t} \mathbf{D} \right) \cdot d\mathbf{a}, & & \operatorname{curl} \mathbf{H} = \mathbf{J} + \frac{\partial}{\partial t} \mathbf{D}, \\ \int_{\mathcal{A}} \operatorname{curl} \mathbf{E} \cdot d\mathbf{a} = -\int_{\mathcal{A}} \frac{\partial}{\partial t} \mathbf{B} \cdot d\mathbf{a}, & \xrightarrow{\text{red arrow}} & \operatorname{curl} \mathbf{E} = -\frac{\partial}{\partial t} \mathbf{B}, \\ \int_{\mathcal{V}} \operatorname{div} \mathbf{B} dV = 0, & & \operatorname{div} \mathbf{B} = 0, \\ \int_{\mathcal{V}} \operatorname{div} \mathbf{D} dV = \int_{\mathcal{V}} \rho dV. & \xrightarrow{\text{red arrow}} & \operatorname{div} \mathbf{D} = \rho. \end{array}$$



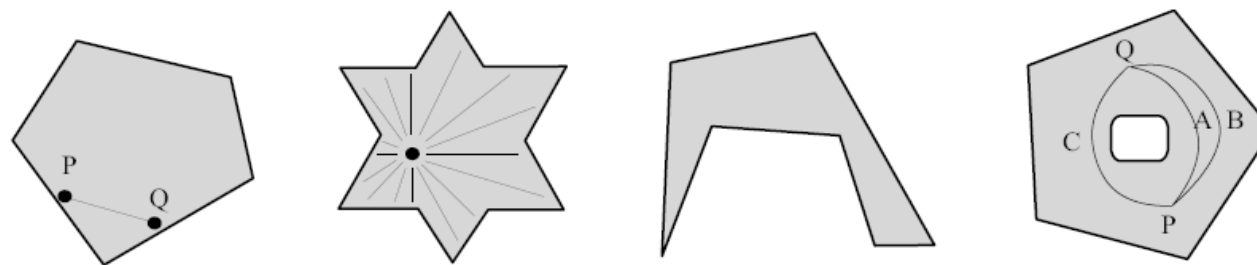
Lemmas of Poincare

$$\operatorname{div} \operatorname{curl} \mathbf{g} = 0, \quad \operatorname{curl} \operatorname{grad} \phi = 0,$$

$$\partial(\partial\mathcal{V}) = \emptyset, \quad \partial(\partial\mathcal{A}) = \emptyset,$$

$$\int_{\mathcal{A}} \operatorname{curl} \operatorname{grad} \phi \cdot d\mathbf{a} = \int_{\partial\mathcal{A}} \operatorname{grad} \phi \cdot d\mathbf{r} = \phi|_{\partial(\partial\mathcal{A})} = 0,$$

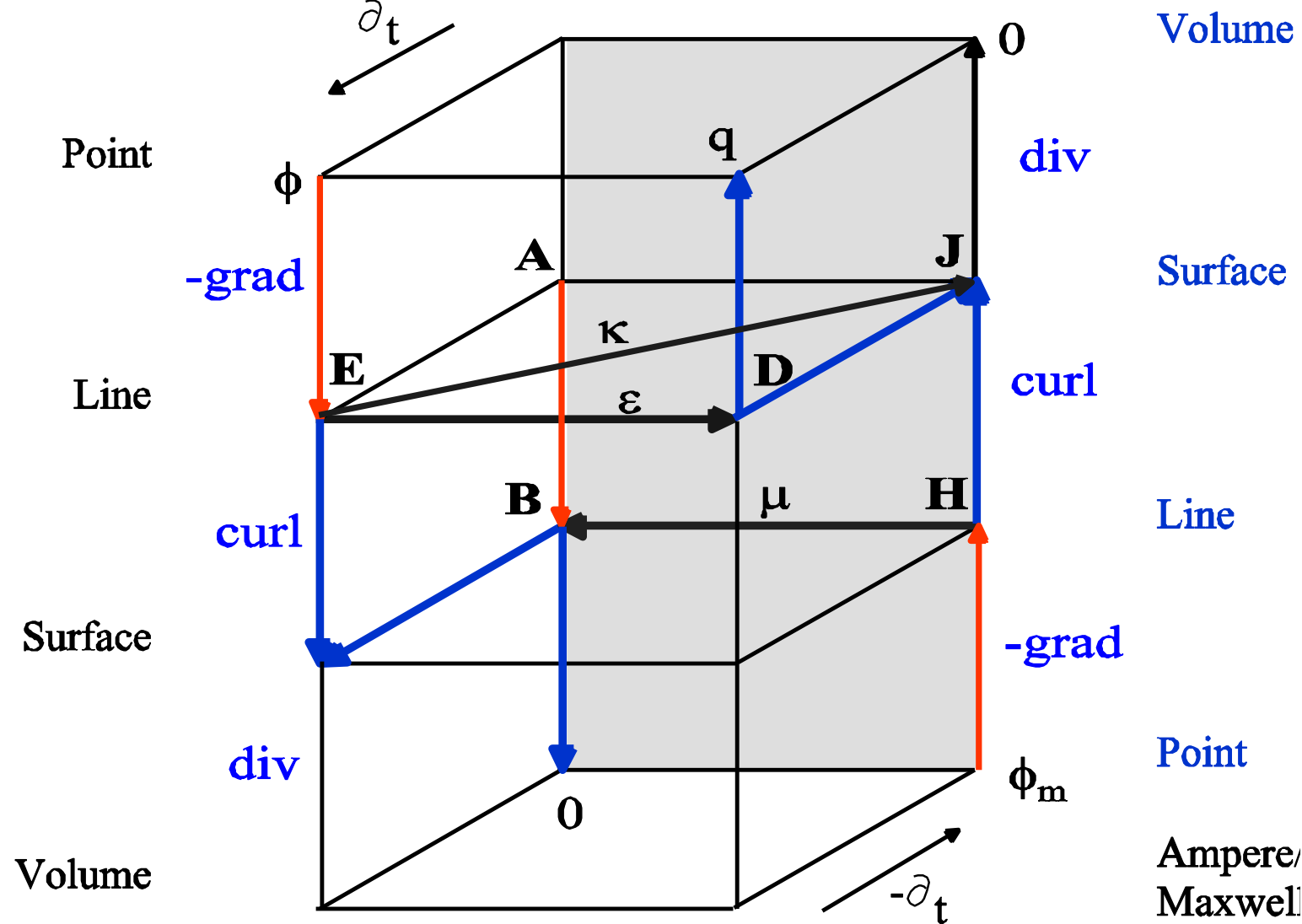
$$\int_{\mathcal{V}} \operatorname{div} \operatorname{curl} \mathbf{g} dV = \int_{\partial\mathcal{V}} \operatorname{curl} \mathbf{g} \cdot d\mathbf{a} = \int_{\partial(\partial\mathcal{V})} \mathbf{g} \cdot d\mathbf{r} = 0,$$



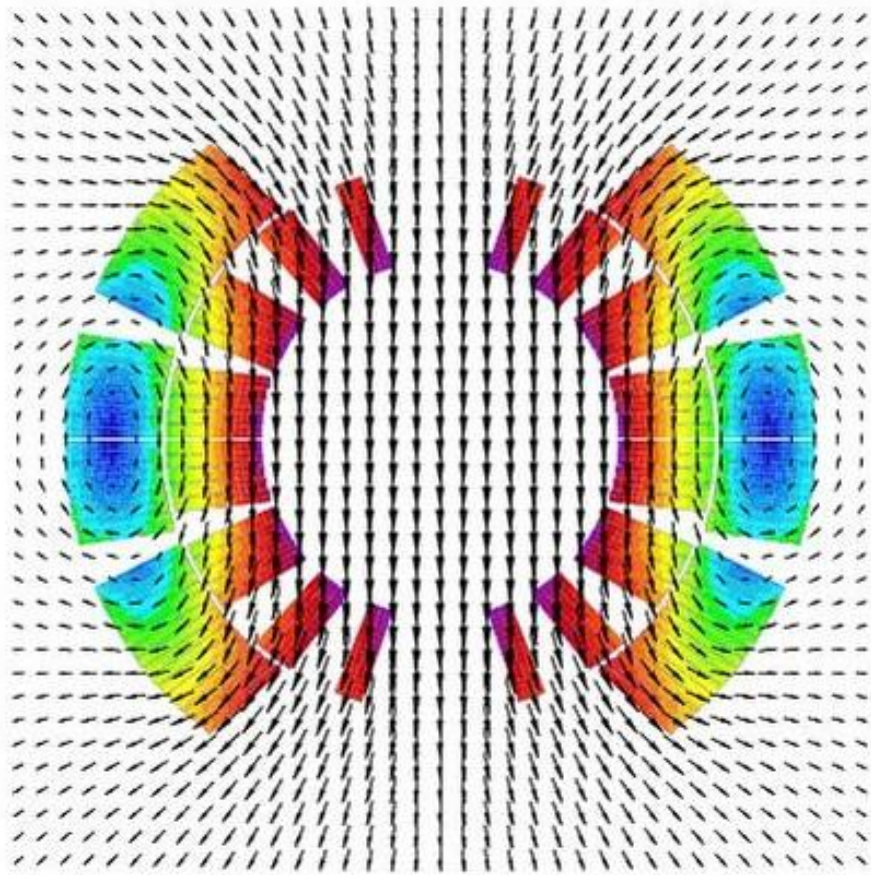
In 3D: also connected boundaries

Maxwell's House

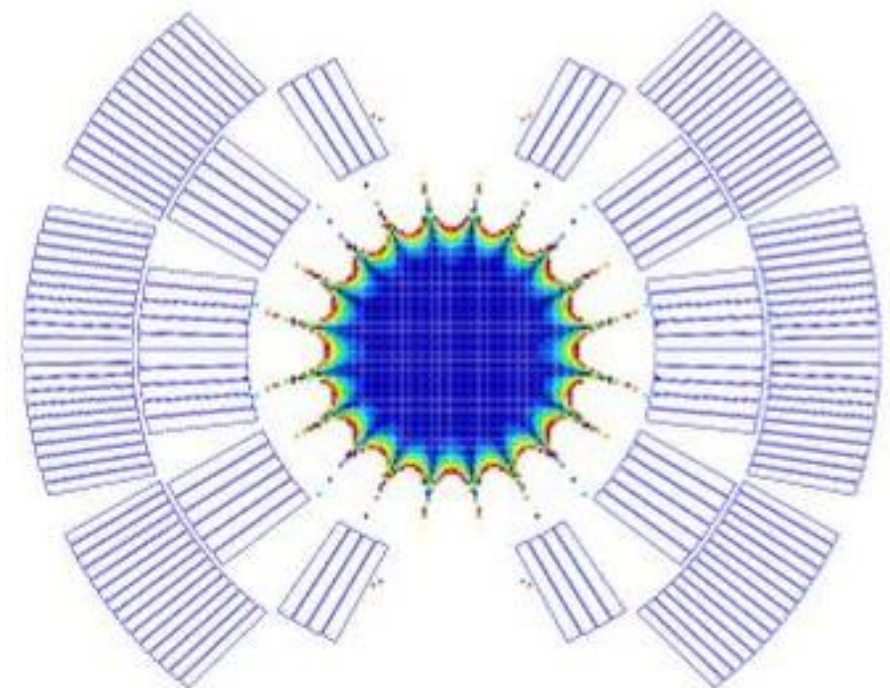
Faraday



Field Quality



Field map



Good field region

Maxwell's Facade

$$\operatorname{curl} \frac{1}{\mu} \operatorname{curl} \mathbf{A} = \mathbf{J}$$

$$\frac{1}{\mu_0} \operatorname{curl} \operatorname{curl} \mathbf{A} = \mathbf{J}$$

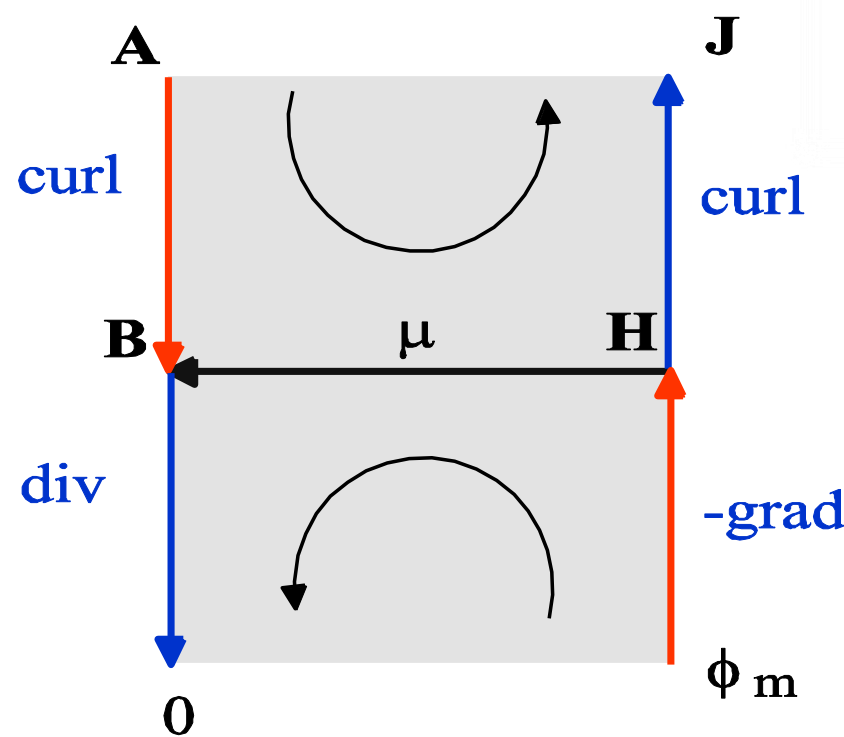
$$\nabla^2 \mathbf{A} - \operatorname{grad} \operatorname{div} \mathbf{A} = 0$$

$$\nabla^2 A_z = 0$$

$$\operatorname{div} \mu \operatorname{grad} \phi_m = 0$$

$$\mu_0 \operatorname{div} \operatorname{grad} \phi_m = 0$$

$$\nabla^2 \phi_m = 0$$



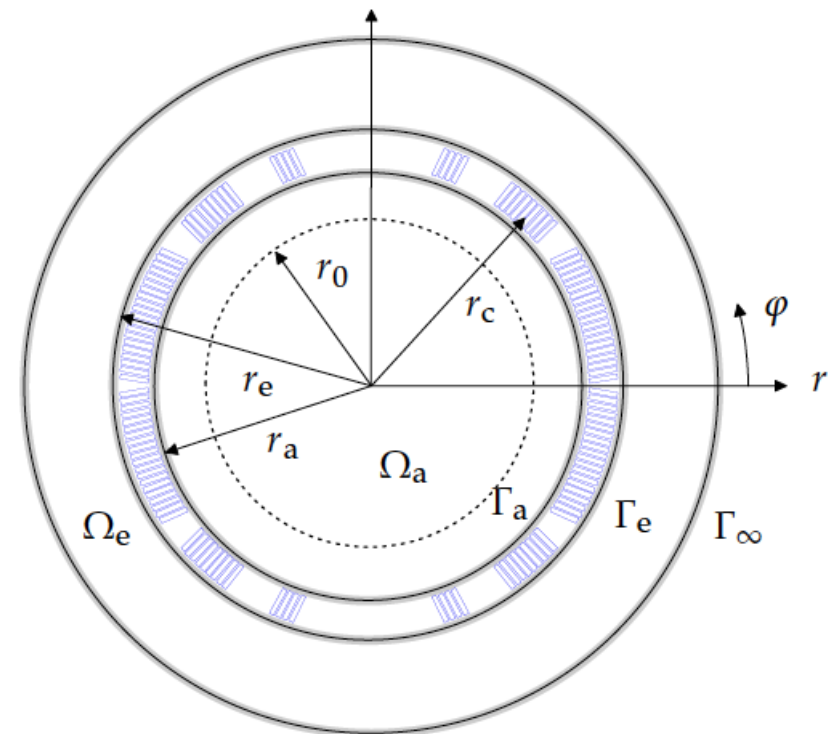
Solving of Boundary Value Problems

1. Governing equation in the air domain

$$\nabla^2 A_z = 0,$$

2. Chose a suitable coordinate system

$$r^2 \frac{\partial^2 A_z}{\partial r^2} + r \frac{\partial A_z}{\partial r} + \frac{\partial^2 A_z}{\partial \varphi^2} = 0,$$



3. Make a guess, look it up in a book, use the method of separation:
That is: find eigenfunctions. Coefficients are not known yet

$$A_z(r, \varphi) = \sum_{n=1}^{\infty} (\mathcal{E}_n r^n + \mathcal{F}_n r^{-n})(\mathcal{G}_n \sin n\varphi + \mathcal{H}_n \cos n\varphi).$$

Solving of Boundary Value Problems

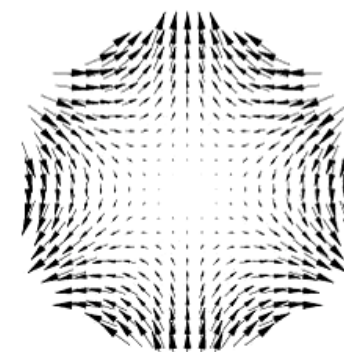
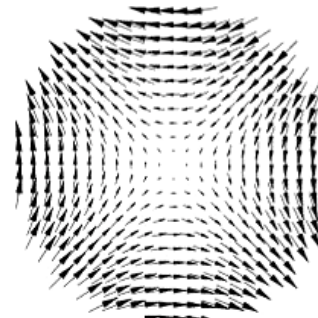
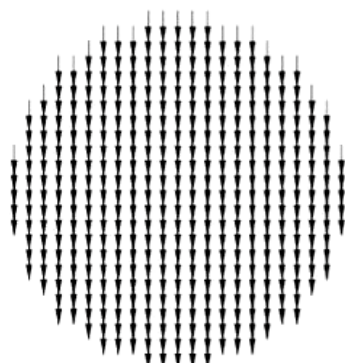
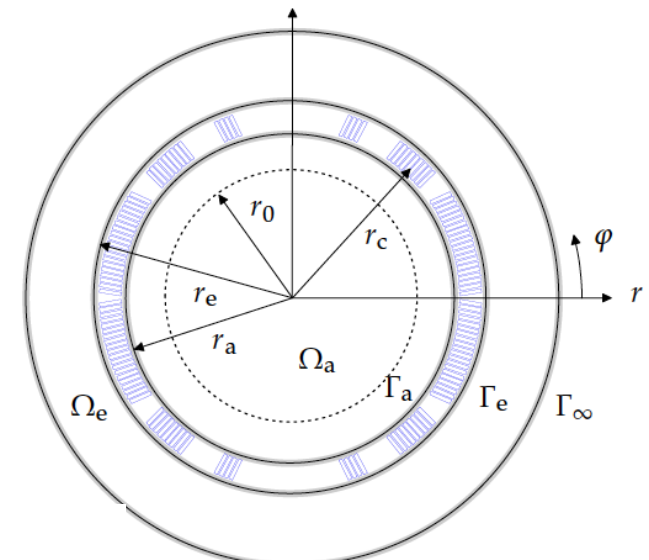
4. Incorporate a bit of knowledge and rename

$$A_z(r, \varphi) = \sum_{n=1}^{\infty} r^n (\mathcal{A}_n \sin n\varphi + \mathcal{B}_n \cos n\varphi).$$

2. Calculate a field component

$$B_r(r, \varphi) = \frac{1}{r} \frac{\partial A_z}{\partial \varphi} = \sum_{n=1}^{\infty} nr^{n-1} (\mathcal{A}_n \cos n\varphi - \mathcal{B}_n \sin n\varphi),$$

$$B_\varphi(r, \varphi) = -\frac{\partial A_z}{\partial r} = -\sum_{n=1}^{\infty} nr^{n-1} (\mathcal{A}_n \sin n\varphi + \mathcal{B}_n \cos n\varphi),$$

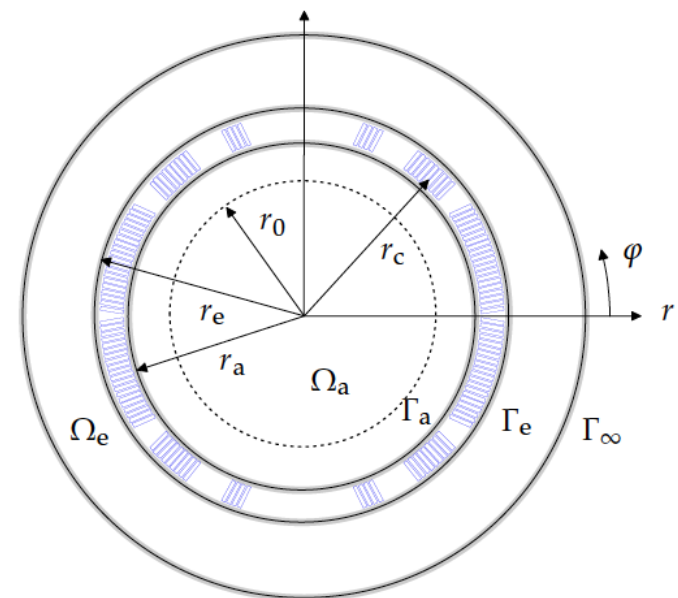


Solving of Boundary Value Problems

$$B_r(r, \varphi) = \frac{1}{r} \frac{\partial A_z}{\partial \varphi} = \sum_{n=1}^{\infty} n r^{n-1} (\mathcal{A}_n \cos n\varphi - \mathcal{B}_n \sin n\varphi),$$

3. Measure or calculate the field on a reference radius and perform Fourier analysis (develop into the eigenfunctions). **Coefficients known here.**

$$B_r(r_0, \varphi) = \sum_{n=1}^{\infty} (B_n(r_0) \sin n\varphi + A_n(r_0) \cos n\varphi),$$



Solving the Boundary Value Problem

4: Compare the known and unknown coefficients

$$B_r(r, \varphi) = \frac{1}{r} \frac{\partial A_z}{\partial \varphi} = \sum_{n=1}^{\infty} n r^{n-1} (\mathcal{A}_n \cos n\varphi - \mathcal{B}_n \sin n\varphi),$$

$$B_r(r_0, \varphi) = \sum_{n=1}^{\infty} (B_n(r_0) \sin n\varphi + A_n(r_0) \cos n\varphi),$$

$$\mathcal{A}_n = \frac{1}{n r_0^{n-1}} A_n(r_0), \quad \mathcal{B}_n = \frac{-1}{n r_0^{n-1}} B_n(r_0).$$

5. Put this into the original solution for the entire air domain

$$A_z(r, \varphi) = - \sum_{n=1}^{\infty} \frac{r_0}{n} \left(\frac{r}{r_0} \right)^n (B_n(r_0) \cos n\varphi - A_n(r_0) \sin n\varphi).$$



Solving the Boundary Value Problem

6: Calculate fields and potential in the entire air domain

$$A_z(r, \varphi) = - \sum_{n=1}^{\infty} \frac{r_0}{n} \left(\frac{r}{r_0} \right)^n (B_n(r_0) \cos n\varphi - A_n(r_0) \sin n\varphi).$$

$$B_r(r, \varphi) = \sum_{n=1}^{\infty} \left(\frac{r}{r_0} \right)^{n-1} (B_n(r_0) \sin n\varphi + A_n(r_0) \cos n\varphi)$$

$$B_\varphi(r, \varphi) = \sum_{n=1}^{\infty} \left(\frac{r}{r_0} \right)^{n-1} (B_n(r_0) \cos n\varphi - A_n(r_0) \sin n\varphi)$$

$$B_x(r, \varphi) = \sum_{n=1}^{\infty} \left(\frac{r}{r_0} \right)^{n-1} (B_n(r_0) \sin(n-1)\varphi + A_n(r_0) \cos(n-1)\varphi)$$

$$B_y(r, \varphi) = \sum_{n=1}^{\infty} \left(\frac{r}{r_0} \right)^{n-1} (B_n(r_0) \cos(n-1)\varphi - A_n(r_0) \sin(n-1)\varphi)$$



Fourier Series (an Infinite Dimensional Vector Space)

$$B_r(r_0, \varphi) = \sum_{n=1}^{\infty} (B_n(r_0) \sin n\varphi + A_n(r_0) \cos n\varphi),$$

$$A_n(r_0) = \frac{1}{\pi} \int_0^{2\pi} B_r(r_0, \varphi) \cos n\varphi \, d\varphi, \quad n = 1, 2, 3, \dots,$$

$$B_n(r_0) = \frac{1}{\pi} \int_0^{2\pi} B_r(r_0, \varphi) \sin n\varphi \, d\varphi, \quad n = 1, 2, 3, \dots.$$

And on the computer: Discrete setting (don't bother with the FFT)

$$\varphi_k = \frac{2\pi k}{N}, \quad k = 0, 1, 2, \dots, N-1.$$

$$A_n(r_0) \approx \frac{2}{N} \sum_{k=0}^{N-1} B_r(r_0, \varphi_k) \cos n\varphi_k,$$

$$B_n(r_0) \approx \frac{2}{N} \sum_{k=0}^{N-1} B_r(r_0, \varphi_k) \sin n\varphi_k.$$

Interrupt: Expansions; orthogonality, completeness, convergence

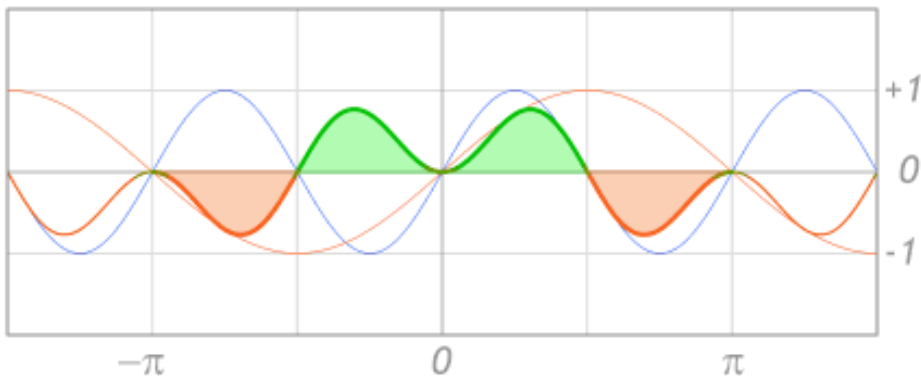


The Road Map to Convergence of Fourier Series

- The trigonometric functions are orthogonal
- The Fourier polynomial P_n of grade n is the best approximation of f in V_n
- The projections onto the trigonometric functions (scalar product) induces a norm (the RMS error)
- Riemann Lebesgue Lemma: Within this norm, the coefficients converge to zero.
- 3 Convergence theorems
 - For a C^1 function P_n converges uniformly to $f(x)$
 - For “clean jumps” P_n converges pointwise to $0.5 (f_+(x) + f_-(x))$
 - The P_n converges for every square integrable function in the RMS sense



Trigonometric Functions as Orthogonal Function Set (from Wikipedia)



$$\int_{-\pi}^{+\pi} \sin(2x) \sin(1x) dx = 0$$

$$\int_{-\pi}^{\pi} \cos(mx) \cos(nx) dx = \pi \delta_{mn},$$
$$\int_{-\pi}^{\pi} \sin(mx) \sin(nx) dx = \pi \delta_{mn},$$

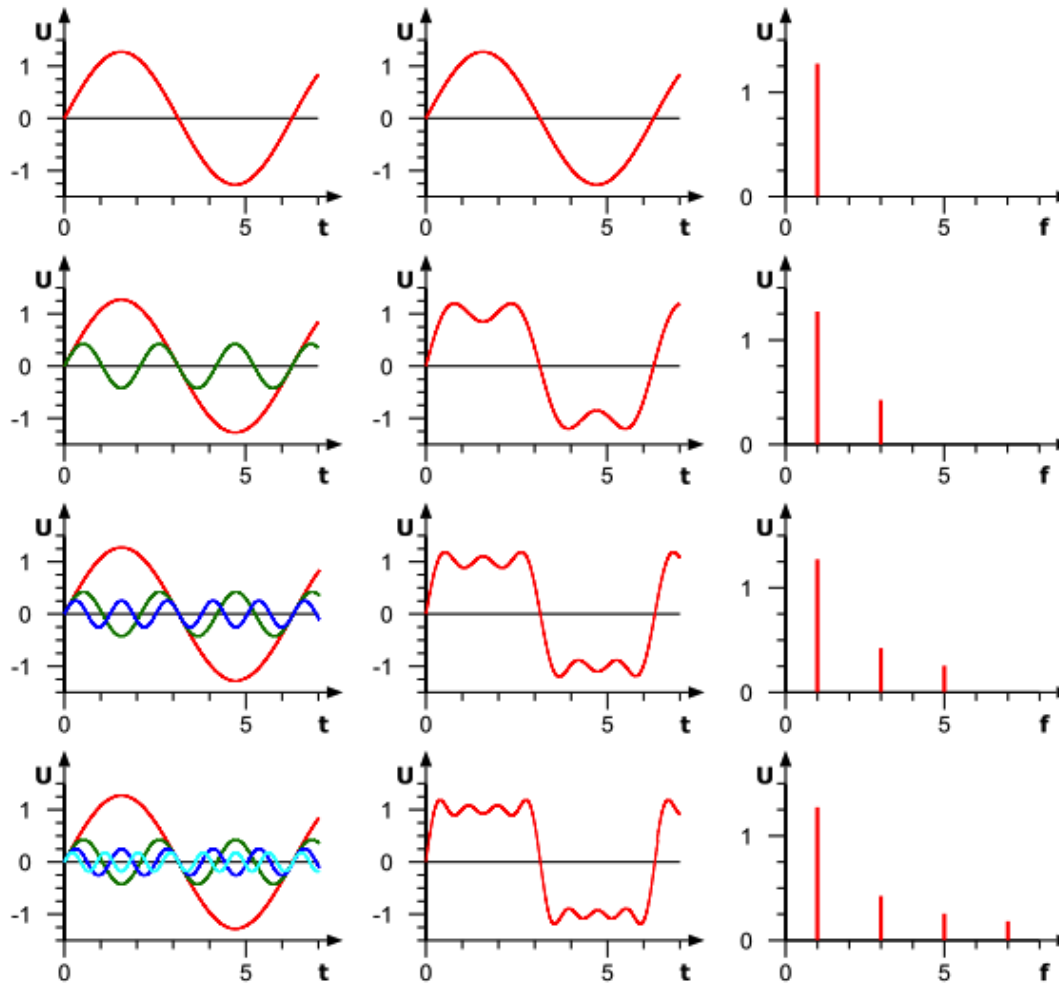
(where δ_{mn} is the Kronecker delta), and

$$\int_{-\pi}^{\pi} \cos(mx) \sin(nx) dx = 0 ;$$

$$\cos \alpha \sin \beta = \frac{1}{2} (\sin(\alpha + \beta) - \sin(\alpha - \beta))$$

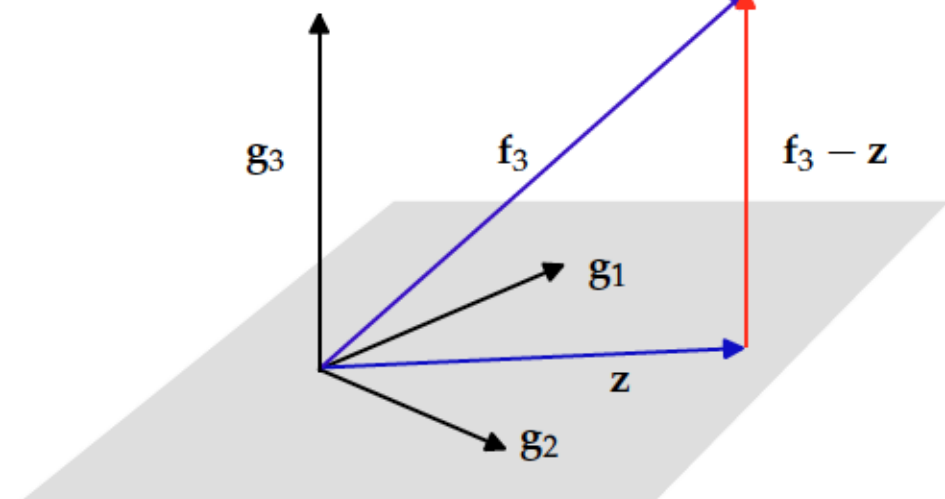
$$\begin{aligned} \int_{-L}^L \cos \frac{m\pi x}{L} \sin \frac{n\pi x}{L} dx &= \frac{1}{2} \int_{-L}^L \sin \frac{(m+n)\pi x}{L} dx - \frac{1}{2} \int_{-L}^L \sin \frac{(m-n)\pi x}{L} dx \\ &= \frac{1}{2} \left(\frac{-\cos \frac{(m+n)\pi x}{L}}{\frac{(m+n)\pi}{L}} \right) \Big|_{-L}^L - \frac{1}{2} \left(\frac{-\cos \frac{(m-n)\pi x}{L}}{\frac{(m-n)\pi}{L}} \right) \Big|_{-L}^L = 0 \end{aligned}$$

The Fourier Polynomial P_n is the best Approximation in V_n



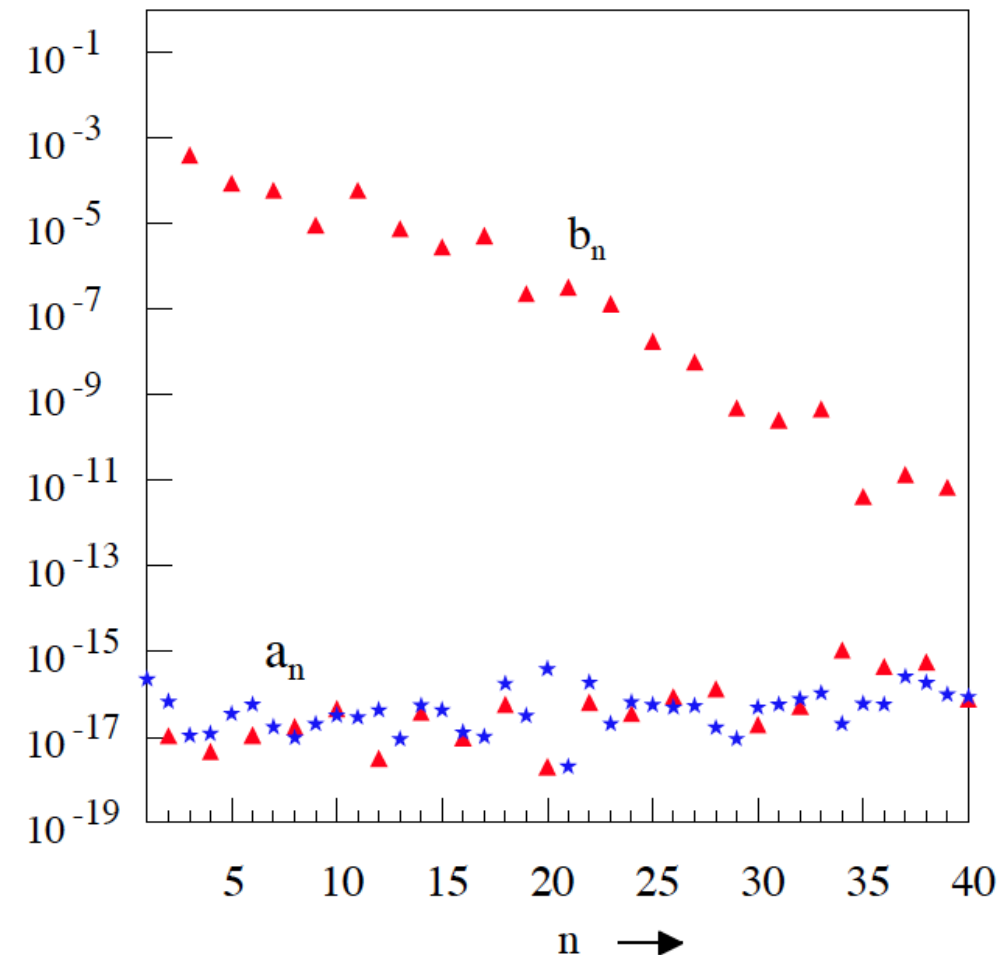
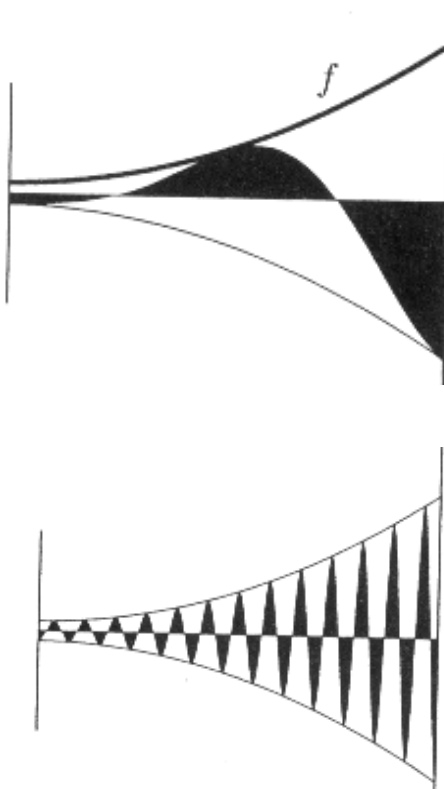
Projection of the square wave onto the “shape” of the trigonometric functions

f_3-z is the shortest distance to the projective plane



The Riemann Lebesgue Lemma

The Fourier coefficients
tend to zero as n goes to
infinity

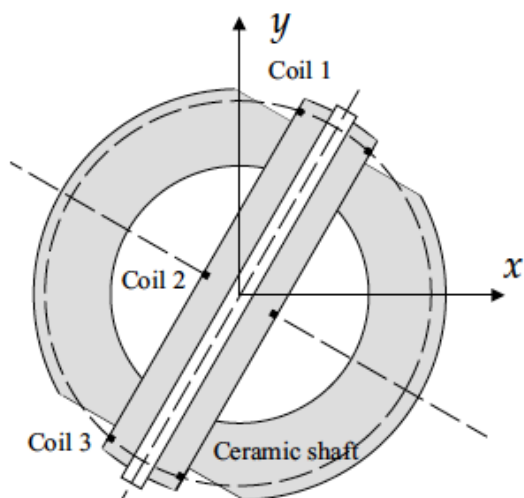
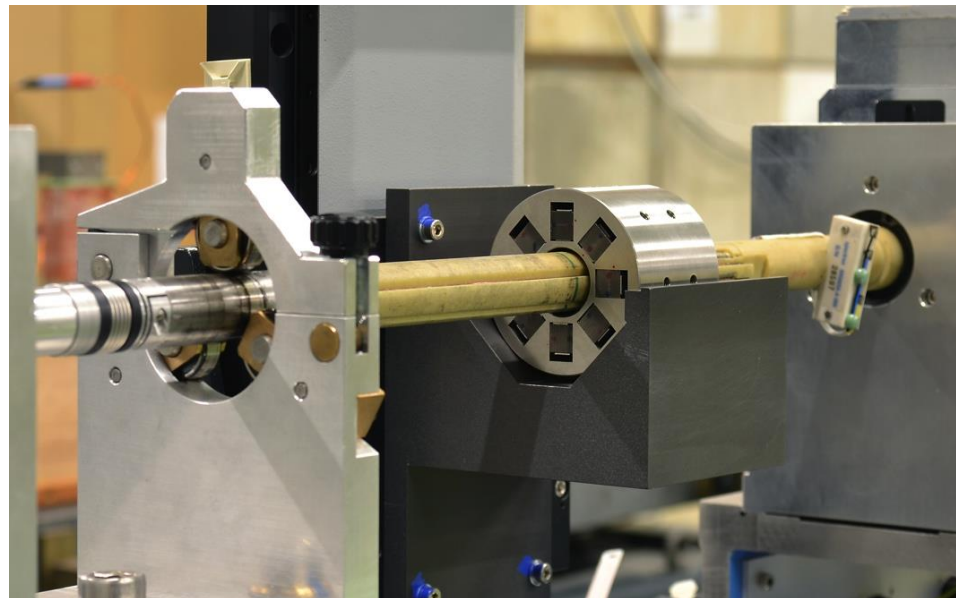


Series Measurements of the LHC Magnets

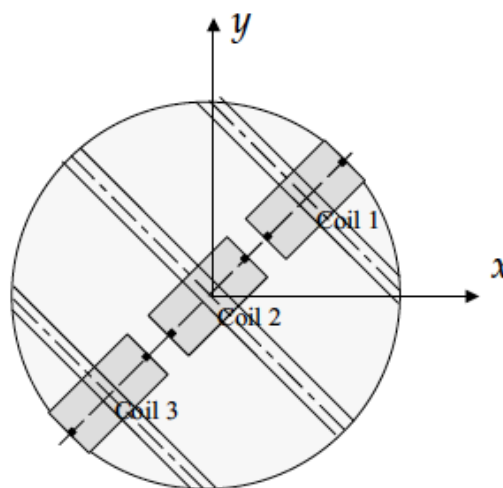


Stephan Russenschuck, CERN TE-MSC-MM, 1211 Geneva 23
JUAS-2013

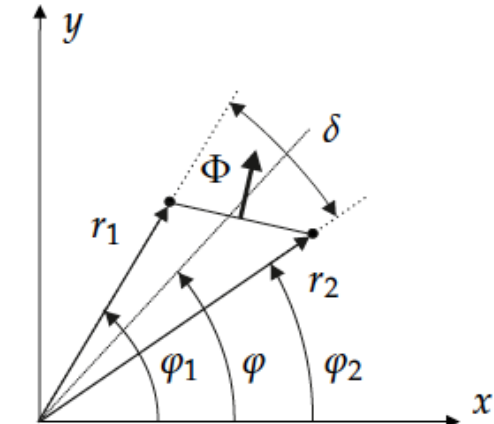
Rotating Coil Measurements



Tangential coil
Radial flux



Radial coil
Tangential flux

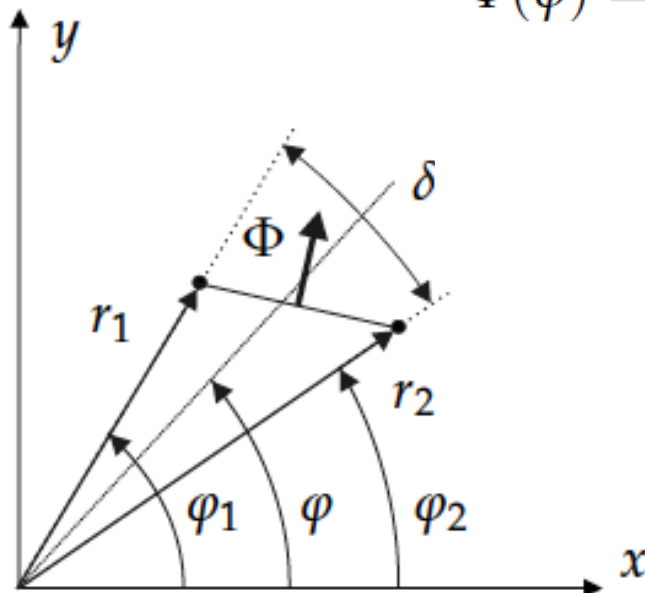


Rotating Coil Measurements

$$\varphi = \omega t + \Theta, \quad \Phi(\varphi) = N \int_{\mathcal{A}} \mathbf{B} \cdot d\mathbf{a} = N \int_{\mathcal{A}} \operatorname{curl} \mathbf{A} \cdot d\mathbf{a} = N \int_{\partial \mathcal{A}} \mathbf{A} \cdot d\mathbf{r}$$
$$= N\ell [A_z(\mathcal{P}_1) - A_z(\mathcal{P}_2)],$$

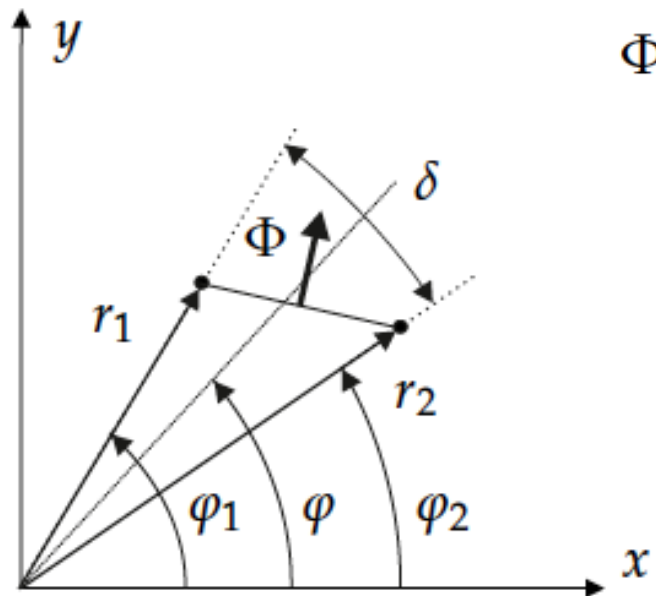
2 Dim version of Stoke's Theorem

$$\Phi(\varphi) = N\ell \left[\sum_{n=1}^{\infty} \frac{r_0}{n} \left(\frac{r_2}{r_0} \right)^n (B_n(r_0) \cos n\varphi_2 - A_n(r_0) \sin n\varphi_2) \right.$$
$$\left. - \sum_{n=1}^{\infty} \frac{r_0}{n} \left(\frac{r_1}{r_0} \right)^n (B_n(r_0) \cos n\varphi_1 - A_n(r_0) \sin n\varphi_1) \right],$$



Rotating Coil Measurements

$$\Phi(\varphi) = N\ell \left[\sum_{n=1}^{\infty} \frac{r_0}{n} \left(\frac{r_2}{r_0} \right)^n (B_n(r_0) \cos n\varphi_2 - A_n(r_0) \sin n\varphi_2) - \sum_{n=1}^{\infty} \frac{r_0}{n} \left(\frac{r_1}{r_0} \right)^n (B_n(r_0) \cos n\varphi_1 - A_n(r_0) \sin n\varphi_1) \right],$$

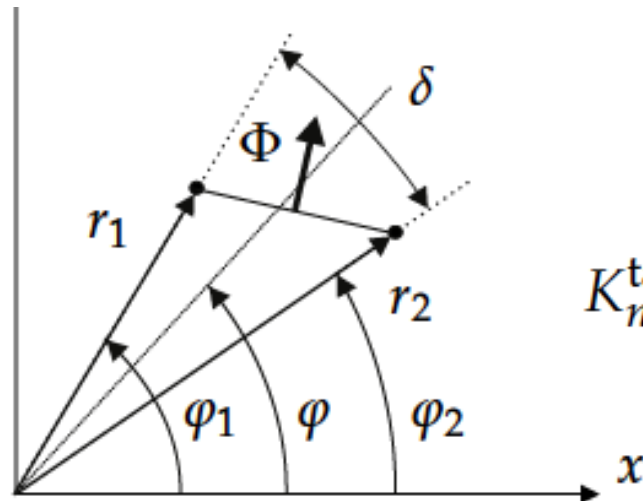


$$\Phi(\varphi) = \sum_{n=1}^{\infty} \frac{\ell}{r_0^{n-1}} \left[K_n^{\text{rad}} (B_n(r_0) \cos n\varphi - A_n(r_0) \sin n\varphi) + K_n^{\tan} (B_n(r_0) \sin n\varphi + A_n(r_0) \cos n\varphi) \right],$$

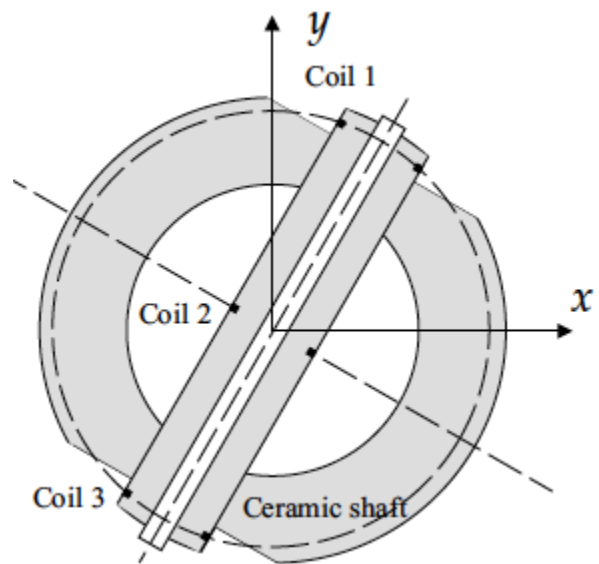
$$K_n^{\text{rad}} = \frac{N}{n} \left[r_2^n \cos n(\varphi_2 - \varphi) - r_1^n \cos n(\varphi_1 - \varphi) \right],$$

$$K_n^{\tan} = -\frac{N}{n} \left[r_2^n \sin n(\varphi_2 - \varphi) - r_1^n \sin n(\varphi_1 - \varphi) \right],$$

Rotating Coil Measurements



$$K_n^{\tan} = \frac{2N}{n} r_c^n \sin\left(\frac{n\delta}{2}\right),$$



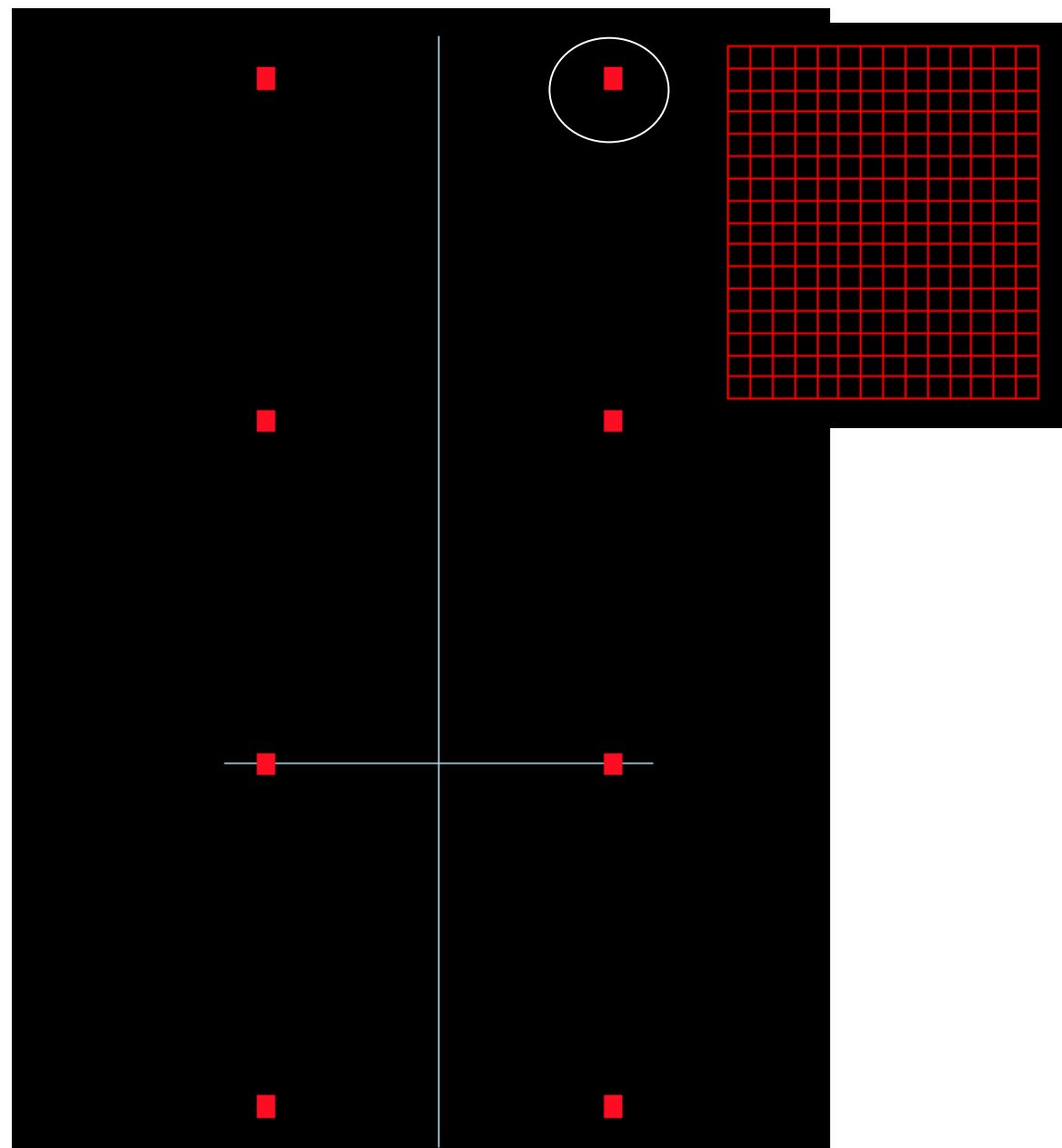
$$\Phi = N\ell \int_{\varphi-\delta/2}^{\varphi+\delta/2} B_r(r_c, \varphi) r_c d\varphi$$

$$= \sum_{n=1}^{\infty} K_n^{\tan} \frac{\ell}{r_0^{n-1}} \left[B_n(r_0) \sin(n\omega t + n\Theta) + A_n(r_0) \cos(n\omega t + n\Theta) \right],$$

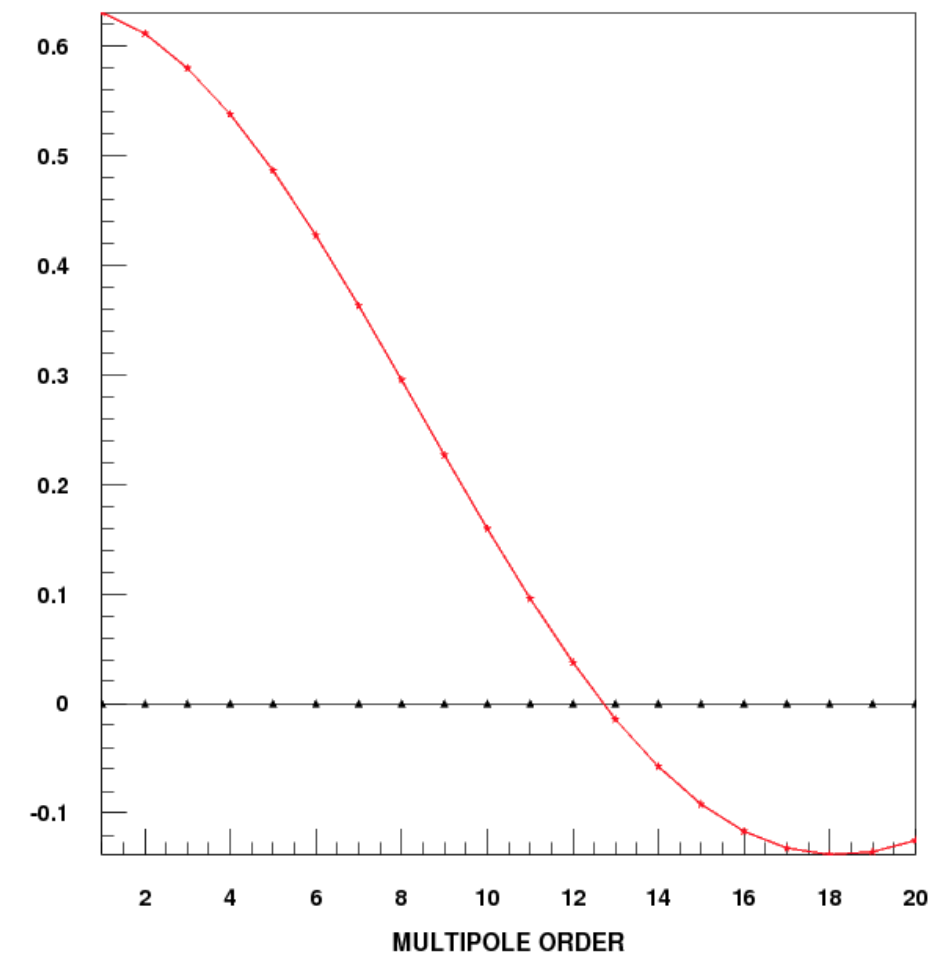
$$U = -\frac{d\Phi}{dt}$$

$$= \sum_{n=1}^{\infty} K_n^{\tan} \frac{n\omega\ell}{r_0^{n-1}} \left[-B_n(r_0) \cos(n\omega t + n\Theta) + A_n(r_0) \sin(n\omega t + n\Theta) \right].$$

Rotating Coil Measurements



$$S_n := \frac{\ell}{r_0^{n-1}} K_n .$$



Multipoles and Scaling Laws

$$B_r(r, \varphi) = \sum_{n=1}^{\infty} \left(\frac{r}{r_0} \right)^{n-1} (B_n(r_0) \sin n\varphi + A_n(r_0) \cos n\varphi)$$

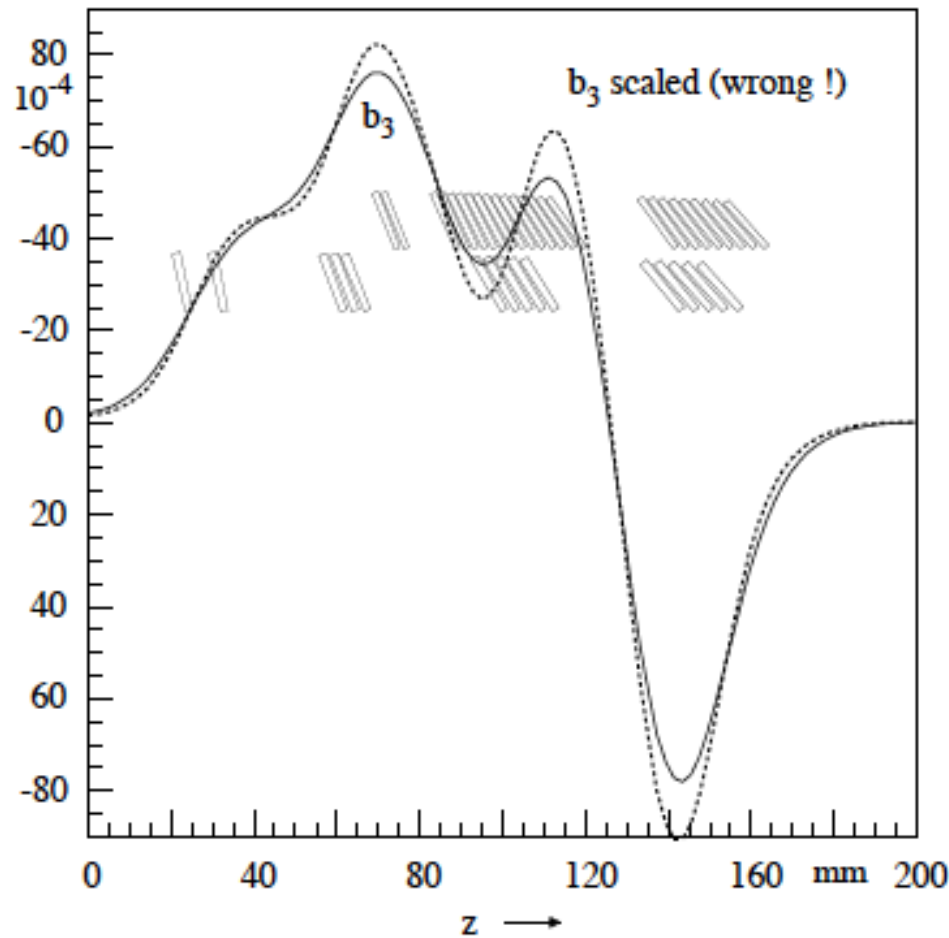
$$B_r(r, \varphi) = B_N \sum_{n=1}^{\infty} \left(\frac{r}{r_0} \right)^{n-N} (b_n(r_0) \sin n\varphi + a_n(r_0) \cos n\varphi).$$

$$A_n(r_1) = \left(\frac{r_1}{r_0} \right)^{n-1} A_n(r_0), \quad B_n(r_1) = \left(\frac{r_1}{r_0} \right)^{n-1} B_n(r_0),$$

$$b_n(r_1) = \frac{B_n(r_1)}{B_N(r_1)} = \frac{\left(\frac{r_1}{r_0} \right)^{n-1} B_n(r_0)}{\left(\frac{r_1}{r_0} \right)^{N-1} B_N(r_0)} = \left(\frac{r_1}{r_0} \right)^{n-N} b_n(r_0),$$



Integrated Harmonics



Local transverse
harmonics calculated at
different reference radii
and scaled with the 2D
laws

$$b_n(r_1) = \left(\frac{r_1}{r_0}\right)^{n-N} b_n(r_0),$$

wrong

Integrated Harmonics

$$\nabla^2 \phi_m(x, y, z) = \frac{\partial^2 \phi_m(x, y, z)}{\partial x^2} + \frac{\partial^2 \phi_m(x, y, z)}{\partial y^2} + \frac{\partial^2 \phi_m(x, y, z)}{\partial z^2} = 0.$$

$$\bar{\phi}_m(x, y) := \int_{-z_0}^{z_0} \phi_m(x, y, z) dz.$$

$$\begin{aligned} \frac{\partial^2 \bar{\phi}_m(x, y)}{\partial x^2} + \frac{\partial^2 \bar{\phi}_m(x, y)}{\partial y^2} &= \int_{-z_0}^{z_0} \left(\frac{\partial^2 \phi_m}{\partial x^2} + \frac{\partial^2 \phi_m}{\partial y^2} \right) dz \\ &= \int_{-z_0}^{z_0} \left(-\frac{\partial^2 \phi_m}{\partial z^2} \right) dz = -\left. \frac{\partial \phi_m}{\partial z} \right|_{-z_0}^{z_0} \\ &= H_z(-z_0) - H_z(z_0) \stackrel{!}{=} 0. \end{aligned}$$

The 2D scaling laws hold for the integrated harmonics



Separation (in Cylindrical Coordinates)

$$\nabla^2 A_z = 0,$$



$$A_z = \rho(r)\phi(\varphi)$$



$$\frac{\partial A_z}{\partial r} = \frac{d\rho(r)}{dr} \phi(\varphi),$$

$$\frac{\partial^2 A_z}{\partial r^2} = \frac{d^2\rho(r)}{dr^2} \phi(\varphi),$$

$$\frac{\partial^2 A_z}{\partial \varphi^2} = \frac{d^2\phi(\varphi)}{d\varphi^2} \rho(r).$$



$$r^2 \frac{\partial^2 A_z}{\partial r^2} + r \frac{\partial A_z}{\partial r} + \frac{\partial^2 A_z}{\partial \varphi^2} = 0,$$



$$\underbrace{\frac{1}{\rho(r)} \left(r^2 \frac{d^2\rho(r)}{dr^2} + r \frac{d\rho(r)}{dr} \right)}_{n^2} = - \underbrace{\frac{1}{\phi(\varphi)} \frac{d^2\phi(\varphi)}{d\varphi^2}}_{n^2}.$$



$$r^2 \frac{d^2\rho(r)}{dr^2} + r \frac{d\rho(r)}{dr} - n^2 \rho(r) = 0,$$



$$\frac{d^2\phi(\varphi)}{d\varphi^2} + n^2 \phi(\varphi) = 0,$$

$$\rho_n(r) = \mathcal{A}_n r^n + \mathcal{B}_n r^{-n},$$

$$\phi_n(\varphi) = \mathcal{C}_n \sin n\varphi + \mathcal{D}_n \cos n\varphi.$$

Cartesian Components

$$\nabla^2 \phi_m = 0.$$

$$\phi_m = X(x)Y(y).$$



$$\frac{\partial^2 \phi_m}{\partial x^2} + \frac{\partial^2 \phi_m}{\partial y^2} + \frac{\partial^2 \phi_m}{\partial z^2} = 0$$



$$\underbrace{\frac{1}{X(x)} \frac{d^2 X(x)}{dx^2}}_{p^2} + \underbrace{\frac{1}{Y(y)} \frac{d^2 Y(y)}{dy^2}}_{-p^2} = 0.$$



$$p = n \frac{2\pi}{\lambda} =: nk_0,$$

$$X_p(x) = \mathcal{C}_p \cos px + \mathcal{D}_p \sin px, \\ Y_p(y) = \mathcal{E}_p \cosh py + \mathcal{F}_p \sinh py,$$

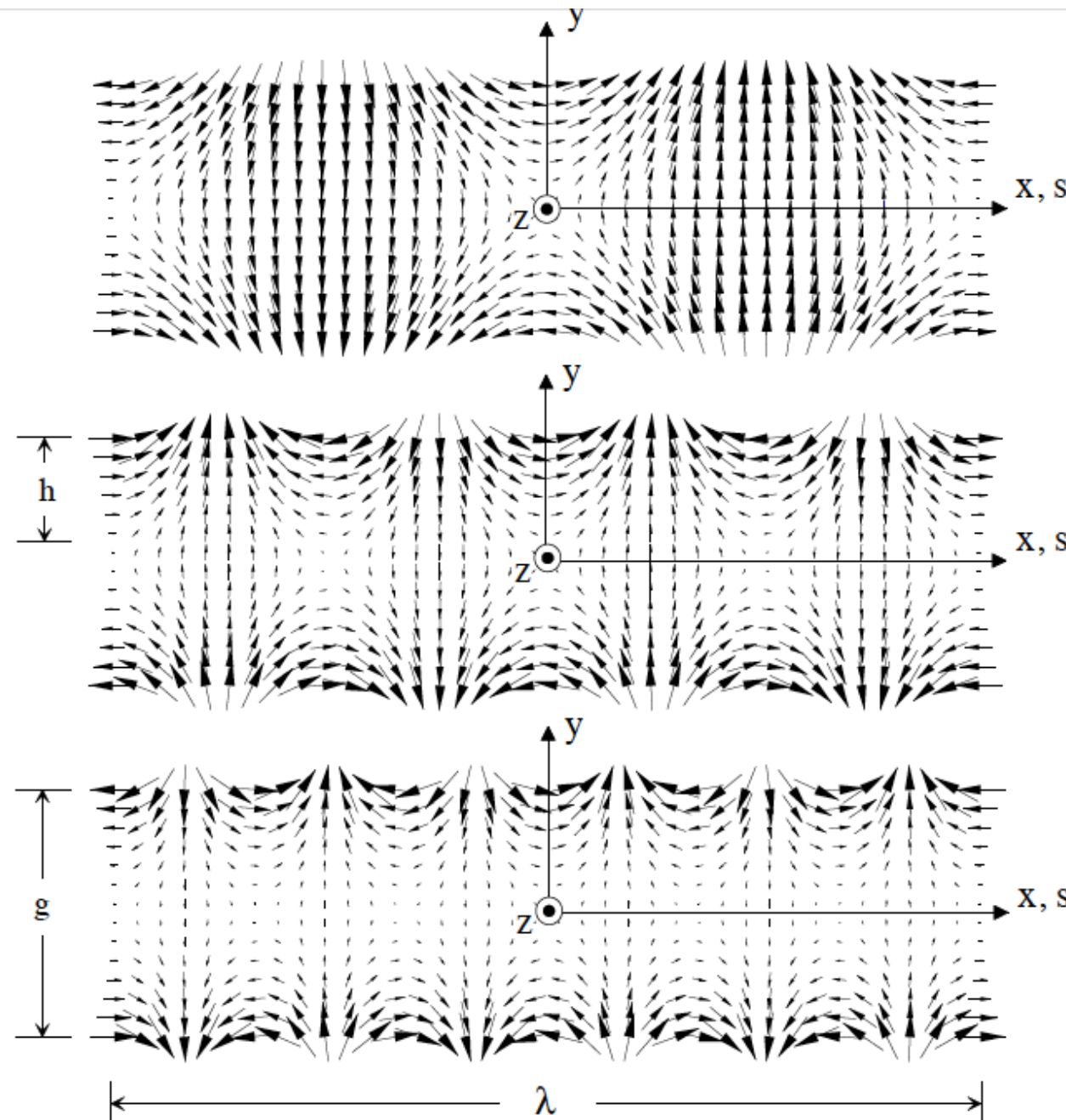


$$B_x(x, y) = \mu_0 \sum_{n=1}^{\infty} (-\mathcal{A}_n \sin(nk_0x) + \mathcal{B}_n \cos(nk_0x)) \sinh(nk_0y),$$

$$B_y(x, y) = \mu_0 \sum_{n=1}^{\infty} (\mathcal{A}_n \cos(nk_0x) + \mathcal{B}_n \sin(nk_0x)) \cosh(nk_0y).$$



Cartesian Components (Eigenfunctions of the Wiggler Magnet)



Ideal Pole Shape of Conventional Magnets

Cauchy Schwarz inequality

$$|\langle \mathbf{a}, \mathbf{b} \rangle| \leq \|\mathbf{a}\| \|\mathbf{b}\|,$$

Thus for the directional derivative

$$|\partial_{\mathbf{v}} \phi| \leq |\operatorname{grad} \phi| |\mathbf{v}|.$$

This implies that the directional derivative is maximal when \mathbf{v} points in the direction of the gradient. But the gradient points in the direction of the steepest ascent of Φ and is thus normal to the surface of equipotential.

Remember also, that \mathbf{B} exits a highly permeable surface in normal direction. Therefore the pole shape can be seen as an equipotential of the magnetic scalar potential.

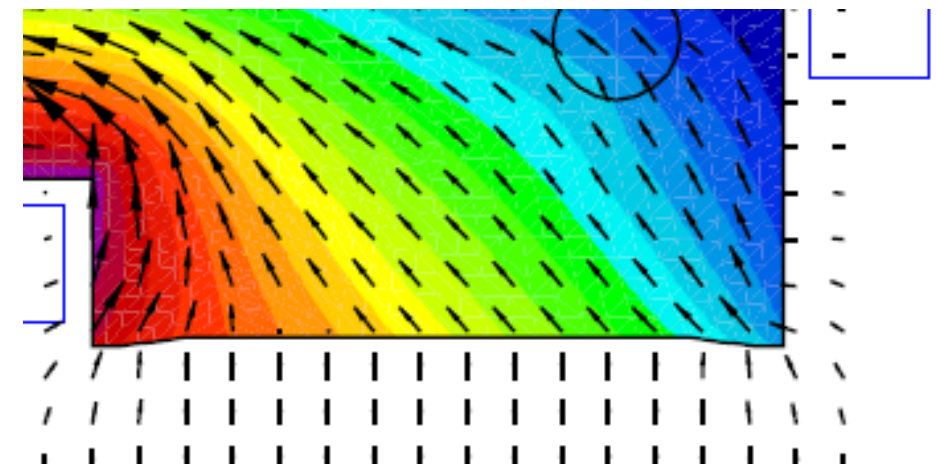
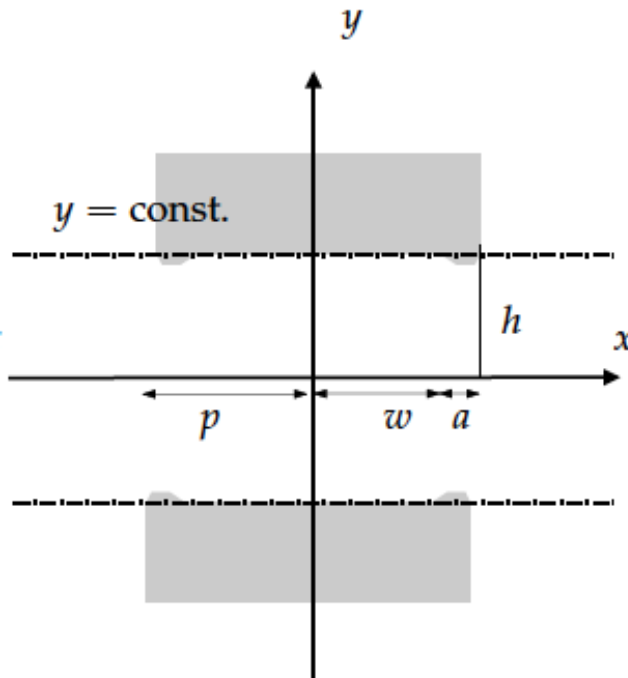


Ideal Pole Shape of Conventional Magnets

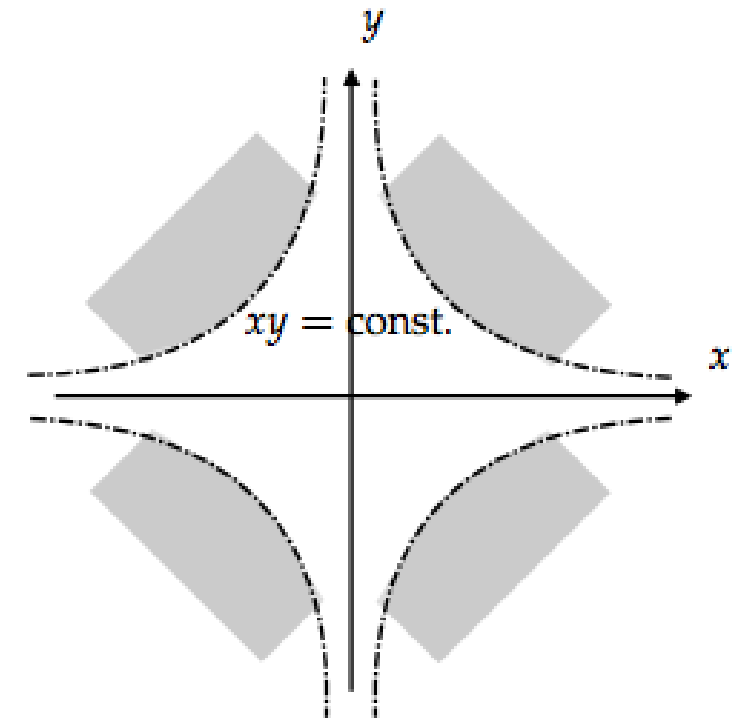
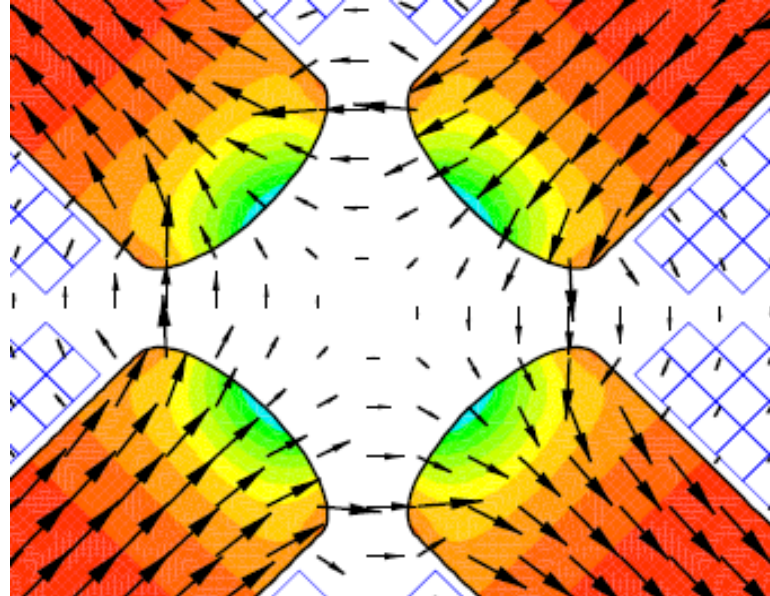
$$\phi_m(r, \varphi) = - \sum_{n=1}^{\infty} \frac{r^n}{\mu_0} (A_n \cos n\varphi - B_n \sin n\varphi).$$

$$\phi_m(r, \varphi) = - \sum_{n=1}^{\infty} \frac{r_0}{n\mu_0} \left(\frac{r}{r_0} \right)^n (A_n(r_0) \cos n\varphi + B_n(r_0) \sin n\varphi).$$

$$\phi_m(x, y) = - \frac{1}{\mu_0} (B_1 y + A_1 x).$$



Ideal Pole Shape of Conventional Magnets



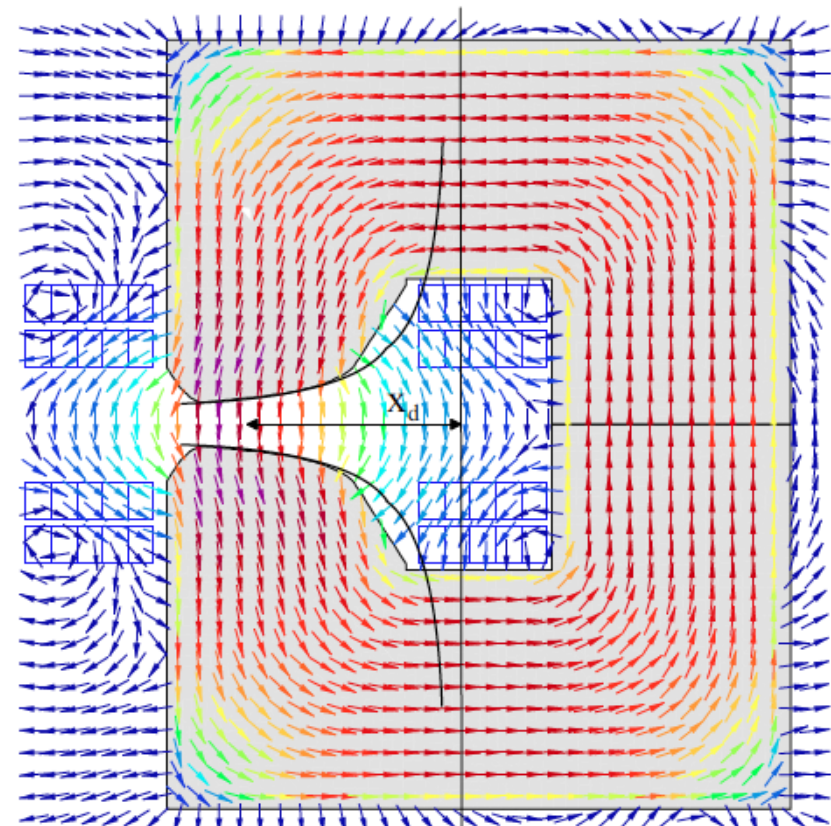
$$\phi_m(r, \varphi) = \frac{1}{2\mu_0 r_0} \left(B_2(r_0) 2xy + A_2(r_0) (x^2 - y^2) \right).$$

Combined Function Magnet (Feed Down)

The magnet has a field gradient of 5 T m^{-1} and a dipole field of 1.5 T at nominal excitation of 6000 A.

$$x' = x - x_d:$$

$$B_y(x') = \frac{1}{r_0} (B_2(r_0)x' + B_2(r_0)x_d).$$



Theorem 9.2 *Real and imaginary parts of a holomorphic function are harmonic functions.*

Proof. If $f(z) = f(x, y) = u(x, y) + iv(x, y)$ is holomorphic, the Cauchy–Riemann equations yield

$$\nabla^2 u = \frac{\partial}{\partial x} \left(\frac{\partial u}{\partial x} \right) + \frac{\partial}{\partial y} \left(\frac{\partial u}{\partial y} \right) = \frac{\partial}{\partial x} \left(\frac{\partial v}{\partial y} \right) + \frac{\partial}{\partial y} \left(-\frac{\partial v}{\partial x} \right) = 0, \quad (9.55)$$

$$\nabla^2 v = \frac{\partial}{\partial x} \left(\frac{\partial v}{\partial x} \right) + \frac{\partial}{\partial y} \left(\frac{\partial v}{\partial y} \right) = \frac{\partial}{\partial x} \left(-\frac{\partial u}{\partial y} \right) + \frac{\partial}{\partial y} \left(\frac{\partial u}{\partial x} \right) = 0.$$

$$\frac{\partial u}{\partial x} = \frac{\partial v}{\partial y}, \quad \frac{\partial u}{\partial y} = -\frac{\partial v}{\partial x}, \quad f^{(1)}(z_0) = \frac{\partial f}{\partial x} = \frac{\partial f}{\partial y} \frac{1}{i}$$

Complex Potentials

$$\mathbf{H} = -\operatorname{grad} \phi = -\frac{\partial \phi}{\partial x} \mathbf{e}_x - \frac{\partial \phi}{\partial y} \mathbf{e}_y,$$

$$\mathbf{B} = \operatorname{curl} (\mathbf{e}_z A_z) = \frac{\partial A_z}{\partial y} \mathbf{e}_x - \frac{\partial A_z}{\partial x} \mathbf{e}_y.$$

This implies

$$\frac{\partial A_z}{\partial y} = -\mu_0 \frac{\partial \phi}{\partial x} \quad \text{and} \quad \frac{\partial A_z}{\partial x} = \mu_0 \frac{\partial \phi}{\partial y},$$

Which are the Cauchy Riemann equations of

$$w(z) := u(x, y) + iv(x, y) = A_z(x, y) + i\mu_0\phi(x, y).$$

$$-\frac{dw}{dz} = -\frac{\partial A_z}{\partial x} - i\mu_0 \frac{\partial \phi}{\partial x} = i\frac{\partial A_z}{\partial y} - \mu_0 \frac{\partial \phi}{\partial y} = B_y(x, y) + iB_x(x, y) =: B(z).$$



Complex Representation of the Field in Accelerator Magnets

$$B_x = B_r \cos \varphi - B_\varphi \sin \varphi, \quad B_y = B_r \sin \varphi + B_\varphi \cos \varphi,$$

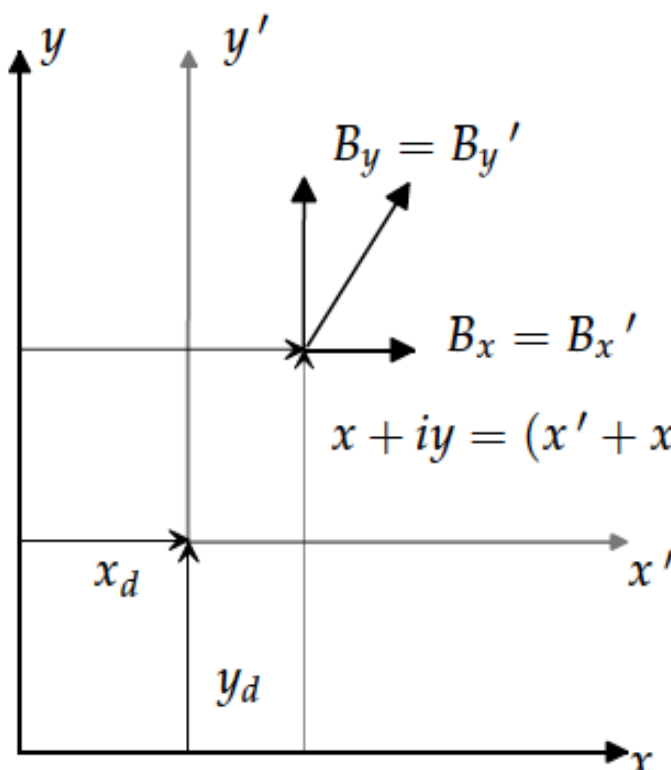
$$B_y + iB_x = (B_\varphi + iB_r)e^{-i\varphi}.$$

$$\begin{aligned} B_y + iB_x &= \sum_{n=1}^{\infty} (B_n(r_0) + i A_n(r_0)) \left(\frac{r}{r_0}\right)^{n-1} e^{i(n-1)\varphi} \\ &= \sum_{n=1}^{\infty} (B_n(r_0) + i A_n(r_0)) \left(\frac{z}{r_0}\right)^{n-1} \\ &= B_N \sum_{n=1}^{\infty} (b_n(r_0) + i a_n(r_0)) \left(\frac{z}{r_0}\right)^{n-1}, \end{aligned}$$



Feed-down (Holomorphic Continuation)

$$\sum_{n=1}^{\infty} C_n \left(\frac{z}{r_0} \right)^{n-1} \stackrel{!}{=} \sum_{n=1}^{\infty} C'_n \left(\frac{z'}{r_0} \right)^{n-1},$$



$$C'_n = \sum_{k=n}^{\infty} C_k \binom{k-1}{n-1} \left(\frac{z_d}{r_0} \right)^{k-n}.$$

$$\binom{n}{p} = \frac{n!}{p!(n-p)!} \text{ for } 0 \leq p \leq n$$

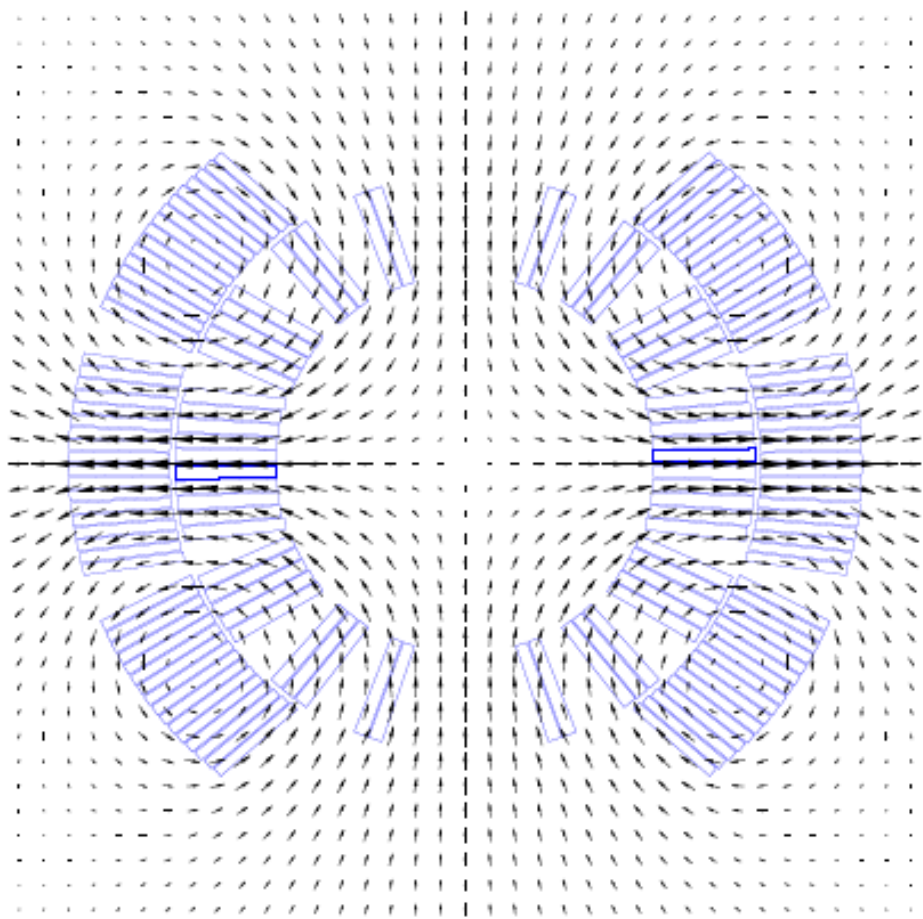
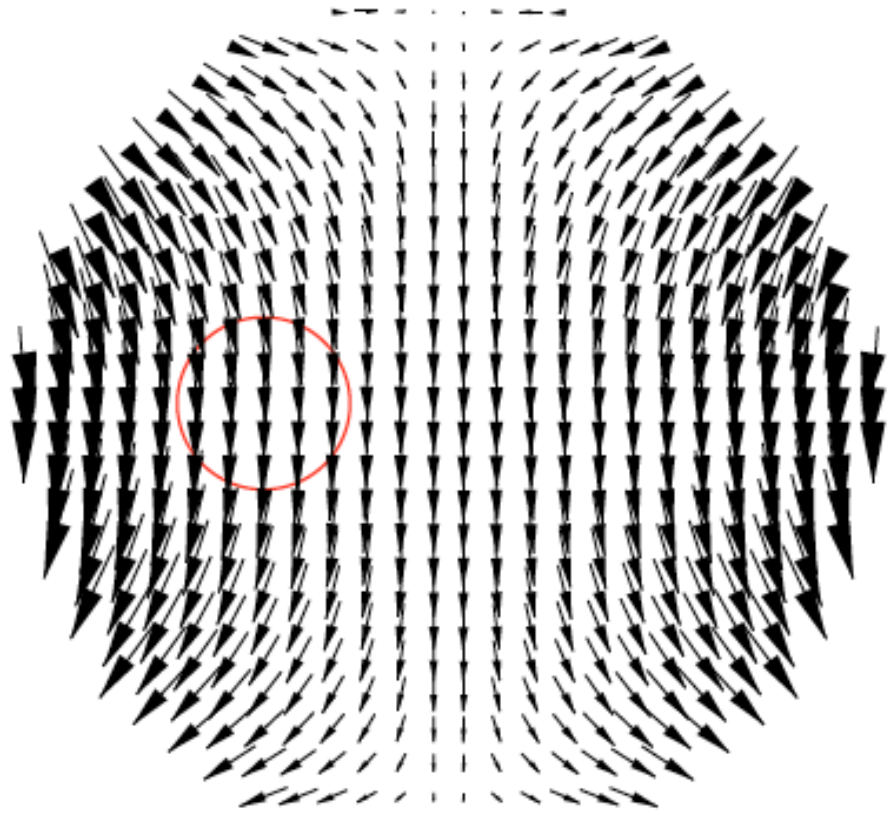
$$C'_2 = C_2 + 2 C_3 \left(\frac{z_d}{r_0} \right) + 3 C_4 \left(\frac{z_d}{r_0} \right)^2 + \dots,$$

Feed-down: Proof

$$\begin{aligned} \sum_{n=1}^{\infty} C_n \left(\frac{z}{r_0} \right)^{n-1} &= \sum_{n=1}^{\infty} \frac{C_n}{r_0^{n-1}} (z' + z_d)^{n-1} \\ &= \sum_{n=1}^{\infty} \frac{C_n}{r_0^{n-1}} \sum_{k=1}^n \binom{n-1}{k-1} (z')^{k-1} z_d^{n-k} \\ &= \sum_{k=1}^{\infty} \left[\sum_{n=1}^k \frac{C_n}{r_0^{n-1}} \binom{n-1}{k-1} z_d^{n-k} \right] (z')^{k-1} \\ &= \sum_{k=1}^{\infty} \left[\sum_{n=k}^{\infty} C_n \binom{n-1}{k-1} \left(\frac{z_d}{r_0} \right)^{n-k} \right] \left(\frac{z'}{r_0} \right)^{k-1} \\ &= \sum_{n=1}^{\infty} \left[\sum_{k=n}^{\infty} C_k \binom{k-1}{n-1} \left(\frac{z_d}{r_0} \right)^{k-n} \right] \left(\frac{z'}{r_0} \right)^{n-1}. \end{aligned}$$



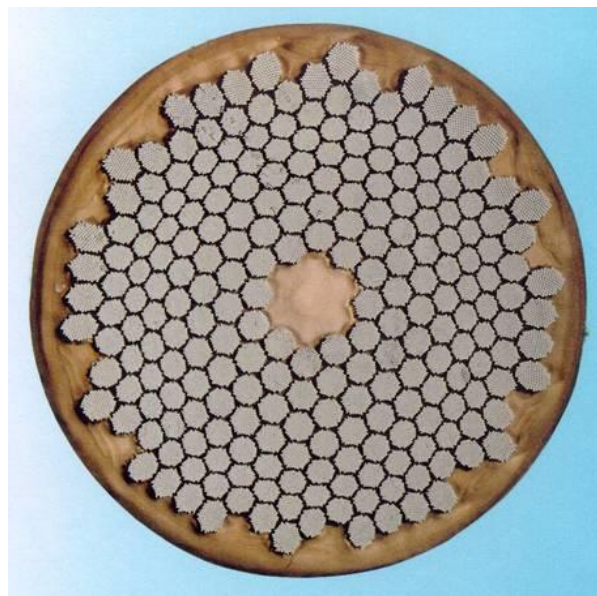
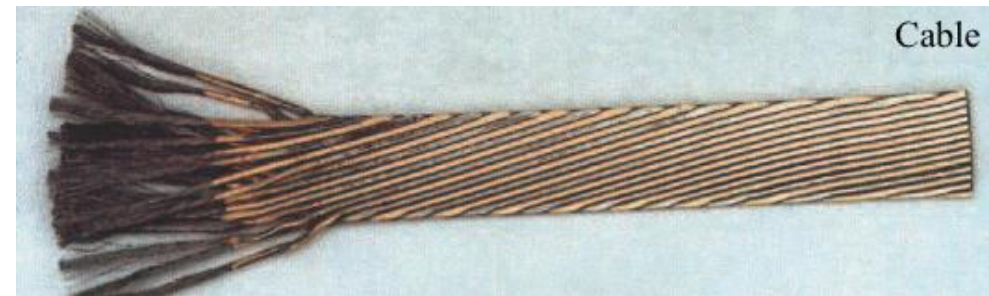
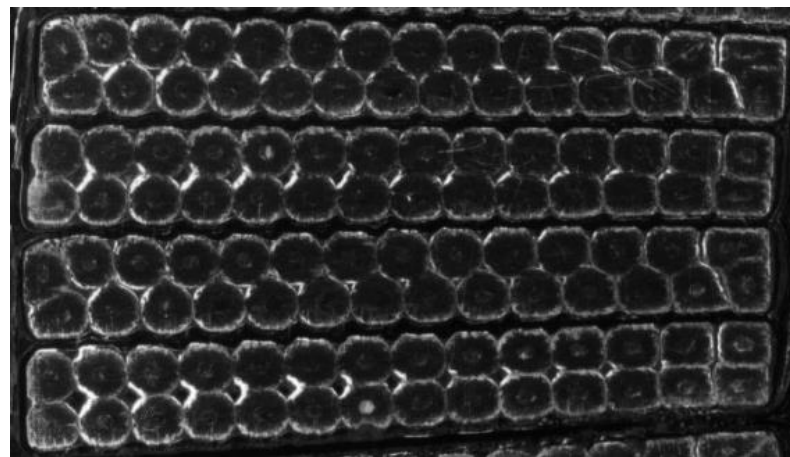
Feed-down: Enemy and Friend



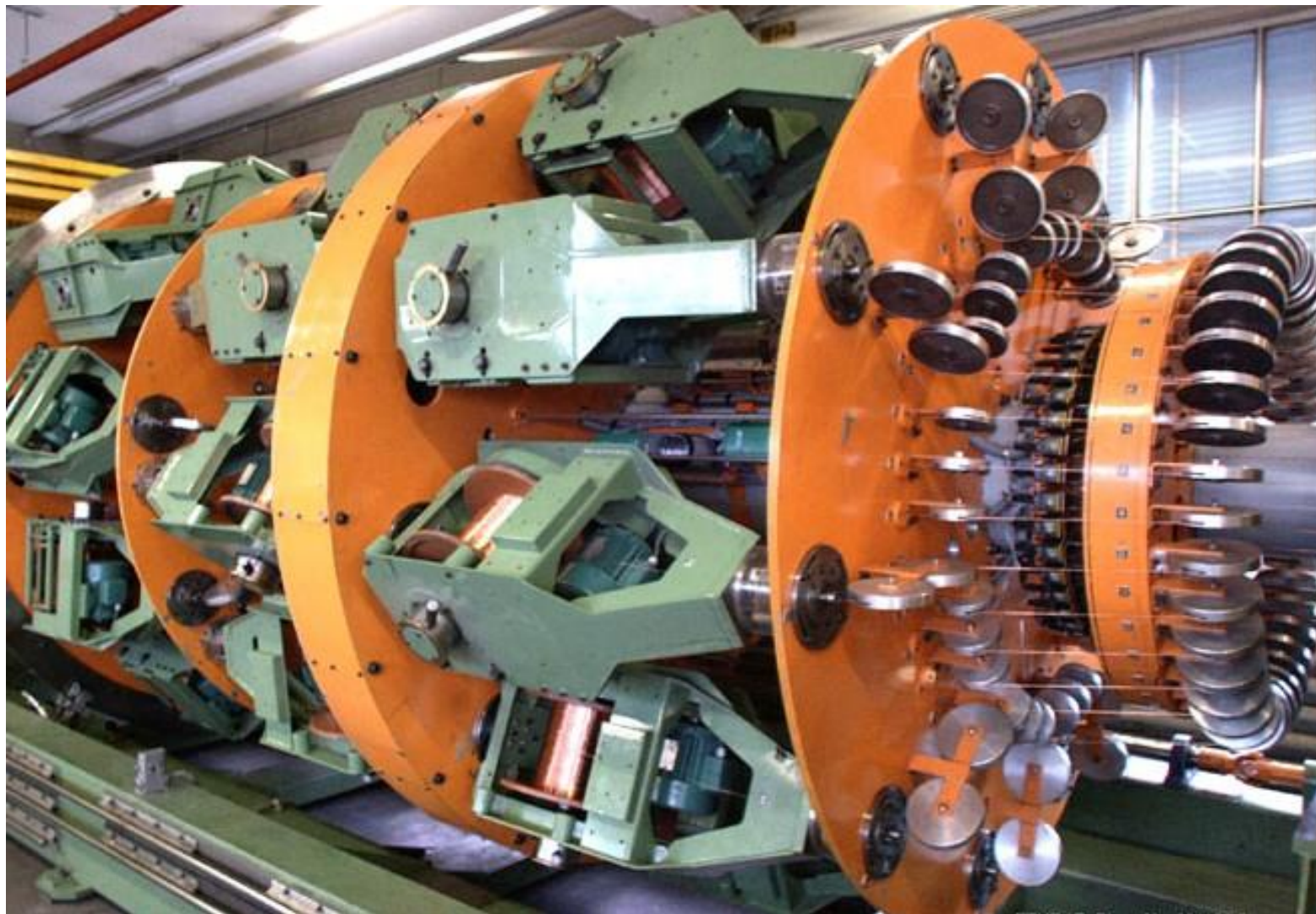
Where we are

- We have studied the mathematical foundations of magnetic fields
 - Vectorfields
 - One dimensional techniques for normal conducting magnets
 - The Laplace equation
 - Field harmonics in accelerator magnets
- So far we assumed that the fields on the domain boundary were known (from measurements or calculations)
- Now we need to address how to calculate these fields
 - The field of line currents and the Biot Savart law
 - Development of these field solutions into the Eigenfunctions

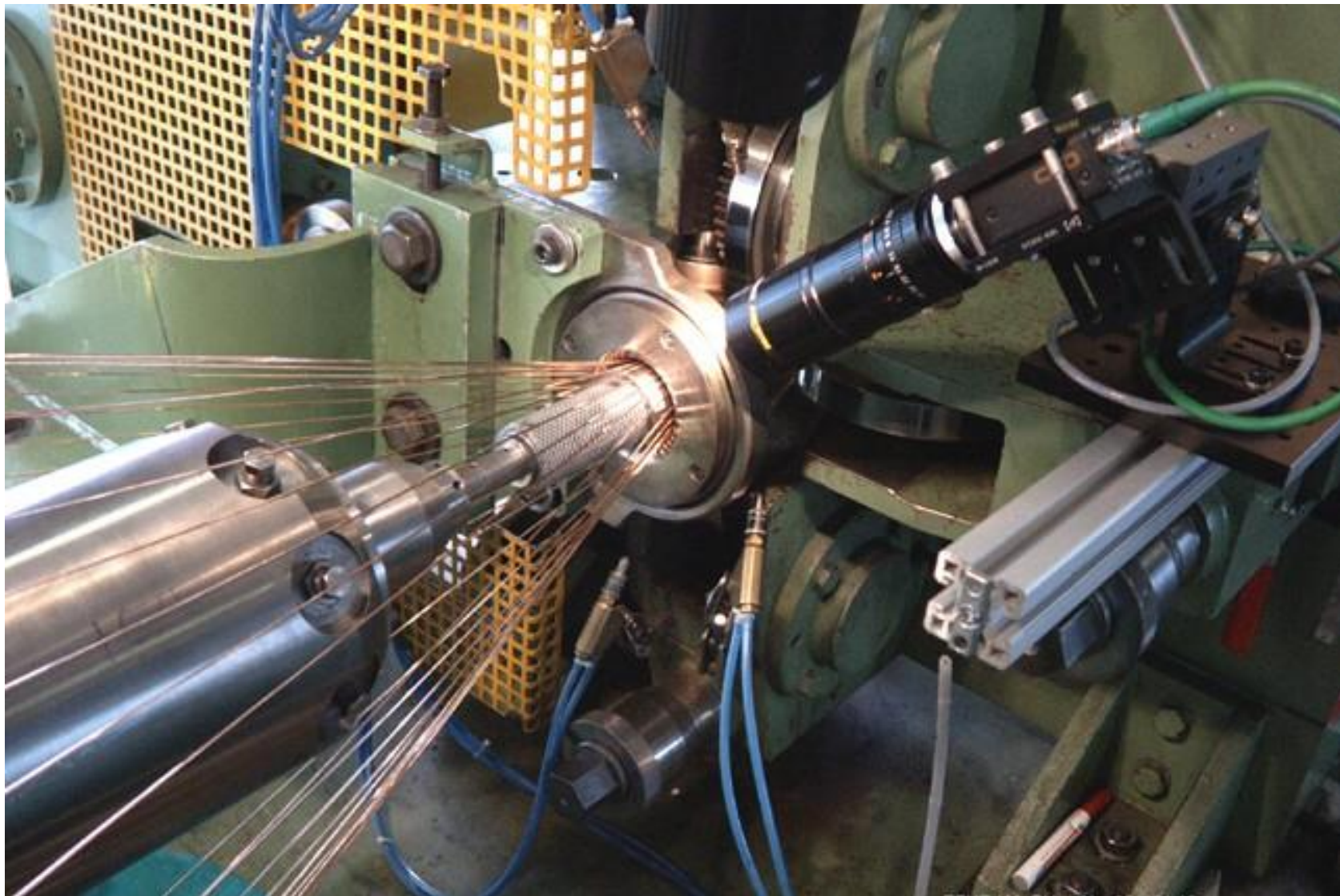
Rutherford (Roebel) Kabel, Strand, Nb-Ti Filament



Cabling Machine for Rutherford Cables



Turk's Head



The Field of Line Currents

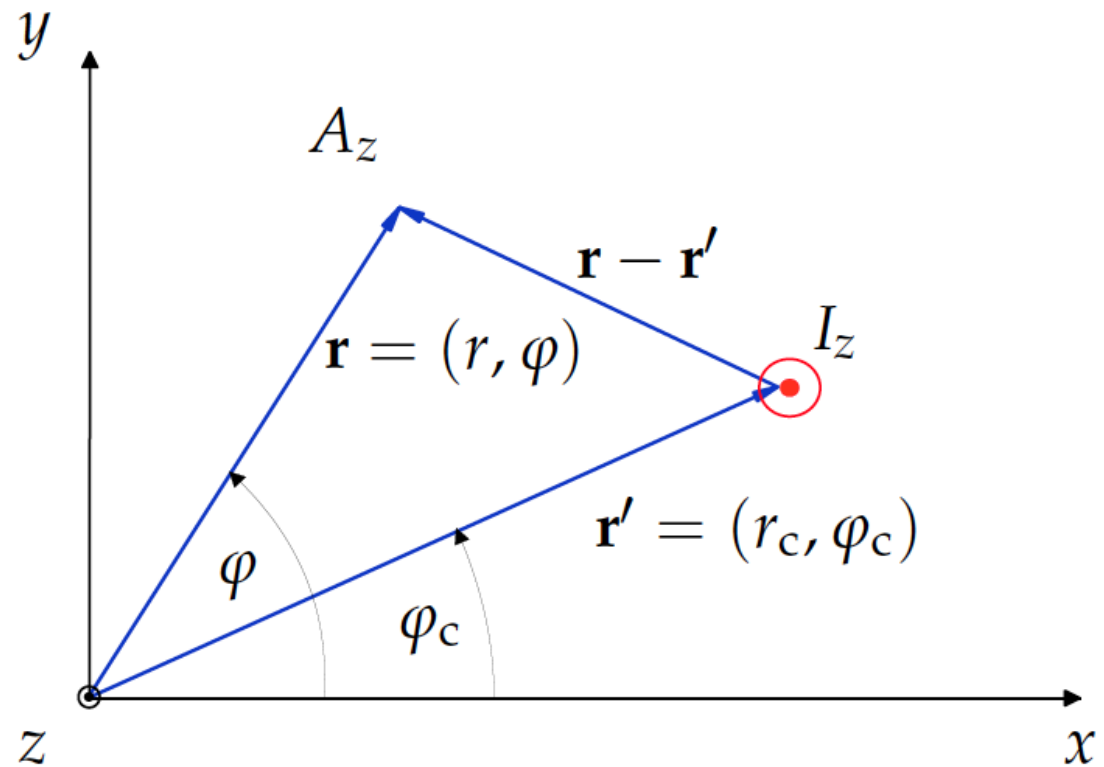
$$\begin{aligned}\mathbf{r} &\mapsto \phi(|\mathbf{r} - \mathbf{r}'|) \\ \mathbf{r}' &\mapsto \phi(|\mathbf{r} - \mathbf{r}'|)\end{aligned}$$

$$\begin{aligned}\operatorname{grad} \phi(|\mathbf{r} - \mathbf{r}'|) &= -\operatorname{grad}_{\mathbf{r}'} \phi(|\mathbf{r} - \mathbf{r}'|), \\ \operatorname{div} \mathbf{a}(|\mathbf{r} - \mathbf{r}'|) &= -\operatorname{div}_{\mathbf{r}'} \mathbf{a}(|\mathbf{r} - \mathbf{r}'|), \\ \operatorname{curl} \mathbf{a}(|\mathbf{r} - \mathbf{r}'|) &= -\operatorname{curl}_{\mathbf{r}'} \mathbf{a}(|\mathbf{r} - \mathbf{r}'|), \\ \nabla^2 \phi(|\mathbf{r} - \mathbf{r}'|) &= \nabla_{\mathbf{r}'}^2 \phi(|\mathbf{r} - \mathbf{r}'|).\end{aligned}$$

Why bother?

Reciprocity; except for sign it does not matter if we exchange the source and field points

Interrupt: Diracs δ function



Greens Functions of Free Space

$$\mathcal{L}_{\mathbf{r}'} \phi(\mathbf{r}') = -f(\mathbf{r}')$$



$$\mathcal{L}_{\mathbf{r}'} G(\mathbf{r}, \mathbf{r}') = -\delta(\mathbf{r} - \mathbf{r}'),$$

$$\int_{\mathcal{V}} \mathcal{L}_{\mathbf{r}'} G(\mathbf{r}, \mathbf{r}') f(\mathbf{r}) dV = - \int_{\mathcal{V}} \delta(\mathbf{r} - \mathbf{r}') f(\mathbf{r}) dV = -f(\mathbf{r}').$$

$$\mathcal{L}_{\mathbf{r}'} \phi(\mathbf{r}') = \int_{\mathcal{V}} \mathcal{L}_{\mathbf{r}'} G(\mathbf{r}, \mathbf{r}') f(\mathbf{r}) dV = \mathcal{L}_{\mathbf{r}'} \int_{\mathcal{V}} G(\mathbf{r}, \mathbf{r}') f(\mathbf{r}) dV,$$

$$\phi(\mathbf{r}') = \int_{\mathcal{V}} G(\mathbf{r}, \mathbf{r}') f(\mathbf{r}) dV.$$

$$G_2(\mathbf{r}, \mathbf{r}') = \frac{1}{2\pi} \ln \left(\frac{|\mathbf{r} - \mathbf{r}'|}{r_{\text{ref}}} \right), \quad G_3(\mathbf{r}, \mathbf{r}') = \frac{1}{4\pi |\mathbf{r} - \mathbf{r}'|}$$



Green's Functions of Free Space

$$\phi(\mathbf{r}') = \int_{\mathcal{V}} G(\mathbf{r}, \mathbf{r}') f(\mathbf{r}) dV.$$

$$\phi(\mathbf{r}) = \int_{\mathcal{V}} G(\mathbf{r}, \mathbf{r}') f(\mathbf{r}') dV'.$$

But what if boundaries are present?

$$\begin{aligned} \phi(\mathbf{r}) &= \int_{\mathcal{V}} G(\mathbf{r}, \mathbf{r}') f(\mathbf{r}') dV' \\ &\quad + \int_{\partial\mathcal{V}} \left(-\phi(\mathbf{r}') \partial_{\mathbf{n}'} G(\mathbf{r}, \mathbf{r}') + G(\mathbf{r}, \mathbf{r}') \partial_{\mathbf{n}'} \phi(\mathbf{r}') \right) da'. \end{aligned}$$



Biot-Savart's Law

$$\nabla^2 \mathbf{A} = -\mu_0 \mathbf{J},$$

$$G_3(\mathbf{r}, \mathbf{r}') = \frac{1}{4\pi |\mathbf{r} - \mathbf{r}'|}$$

$$A_i(\mathbf{r}) = \frac{\mu_0}{4\pi} \int_{\mathcal{V}} \frac{J_i(\mathbf{r}')}{|\mathbf{r} - \mathbf{r}'|} dV',$$

$$\mathbf{A}(\mathbf{r}) = A_x \mathbf{e}_x + A_y \mathbf{e}_y + A_z \mathbf{e}_z = \frac{\mu_0}{4\pi} \int_{\mathcal{V}} \frac{\mathbf{J}(\mathbf{r}')}{|\mathbf{r} - \mathbf{r}'|} dV'.$$

This works only in Cartesian Coordinates

$$\mathbf{B}(\mathbf{r}) = \operatorname{curl} \mathbf{A}(\mathbf{r}) = \frac{\mu_0}{4\pi} \int_{\mathcal{V}} \operatorname{curl} \left(\frac{\mathbf{J}(\mathbf{r}')}{|\mathbf{r} - \mathbf{r}'|} \right) dV'$$

$$A_i(\mathbf{r}) = \frac{\mu_0}{4\pi} \int_{\mathcal{V}} \frac{1}{|\mathbf{r} - \mathbf{r}'|} \sum_{k=1}^3 J_k(\mathbf{r}') (\mathbf{e}_i(\mathbf{r}) \cdot \mathbf{e}_k(\mathbf{r}')) dV'. dV'$$

$$= \frac{\mu_0}{4\pi} \int_{\mathcal{V}} \frac{\mathbf{J}(\mathbf{r}') \wedge (\mathbf{r} - \mathbf{r}')}{|\mathbf{r} - \mathbf{r}'|^3} dV'.$$



Biot Savart's Law

But wait a minute: Are we finished? Are we sure that the divergence ~~of the vector potential is zero as it was required for the Laplace equation?~~ is zero as it was required for the Laplace equation?

$$\operatorname{div} \mathbf{A}(\mathbf{r})$$

$$= -\frac{\mu_0}{4\pi} \int_{\partial\mathcal{V}} \frac{\mathbf{J}(\mathbf{r}')}{|\mathbf{r} - \mathbf{r}'|} \cdot d\mathbf{a}' .$$

Current loops must always be closed and must not leave the problem domain



Biot-Savart's Law for Line Currents

$$\mathbf{A}(\mathbf{r}) = A_x \mathbf{e}_x + A_y \mathbf{e}_y + A_z \mathbf{e}_z = \frac{\mu_0}{4\pi} \int_{\mathcal{V}} \frac{\mathbf{J}(\mathbf{r}')}{|\mathbf{r} - \mathbf{r}'|} dV'.$$

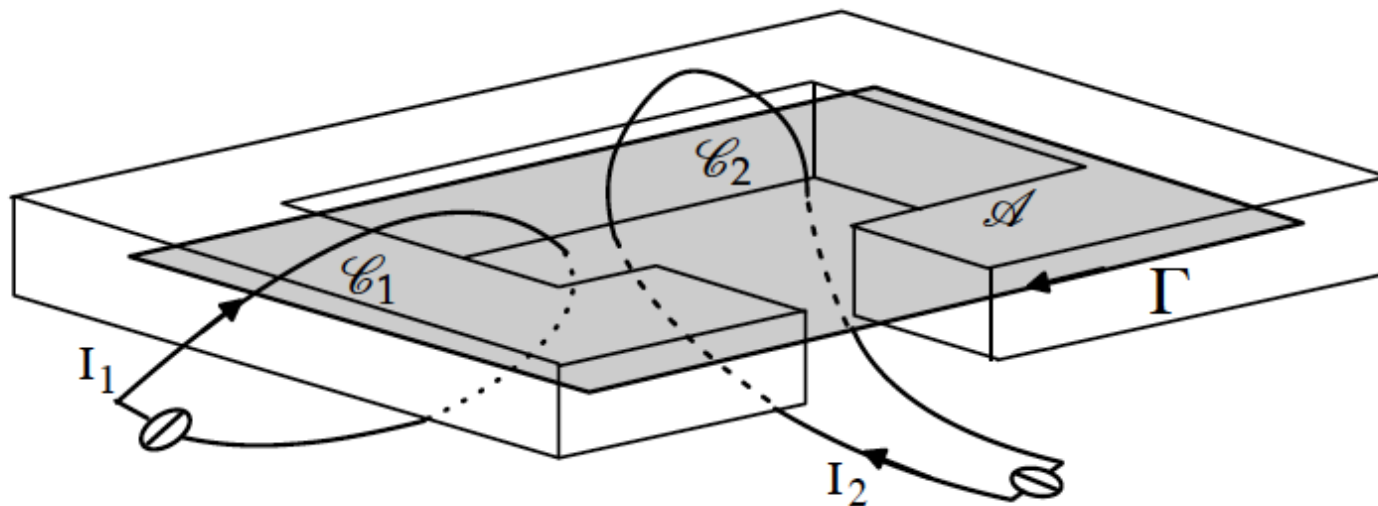
$$\mathbf{A}(\mathbf{r}) = \frac{\mu_0 I}{4\pi} \int_{\mathcal{C}} \frac{d\mathbf{r}'}{|\mathbf{r} - \mathbf{r}'|}$$

$$\mathbf{B}(\mathbf{r}) = \frac{\mu_0 I}{4\pi} \int_{\mathcal{C}} \frac{d\mathbf{r}' \times (\mathbf{r} - \mathbf{r}')}{|\mathbf{r} - \mathbf{r}'|^3},$$



Biot-Savart's Law and the Linking Number

$$NI = I \sum_{k=1}^K \text{link}(\partial\mathcal{A}, \mathcal{C}_k) = I \sum_{k=1}^K \text{int}(\mathcal{A}, \mathcal{C}_k),$$

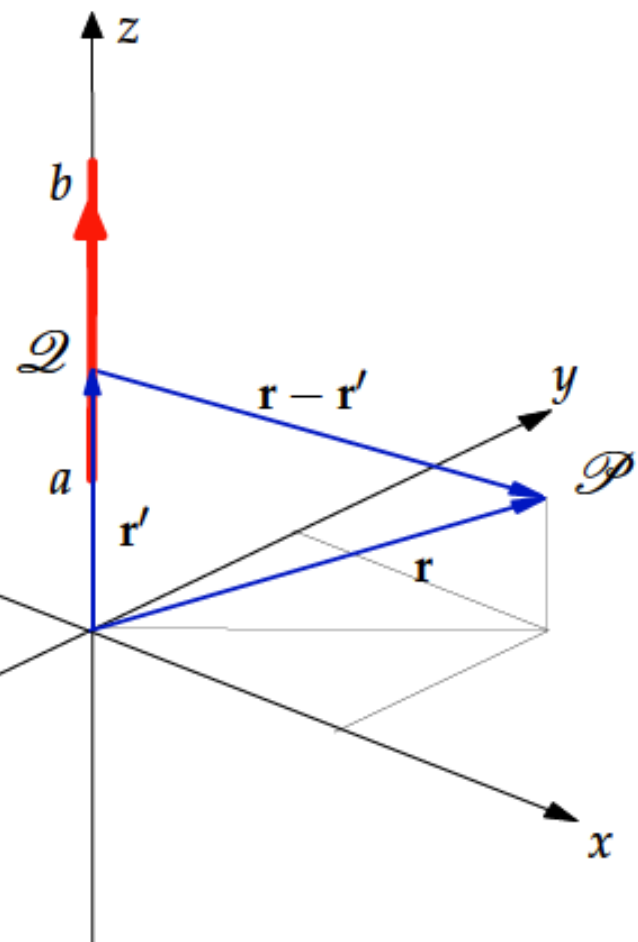


$$\text{int}(\mathcal{A}, \mathcal{C}_k) = \sum_{\mathcal{A} \cap \mathcal{C}_k} \pm 1$$

$$\text{link}(\partial\mathcal{A}, \mathcal{C}_k) = \frac{1}{4\pi} \int_{\partial\mathcal{A}} \int_{\mathcal{C}_k} \frac{d\mathbf{r}' \times (\mathbf{r} - \mathbf{r}')}{|\mathbf{r} - \mathbf{r}'|^3} \cdot d\mathbf{r},$$

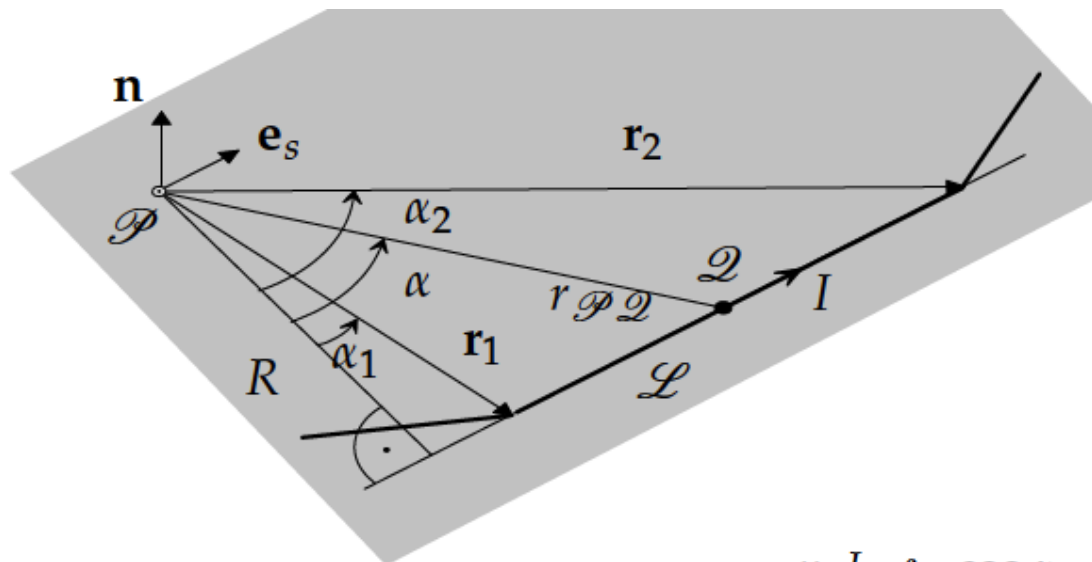
Vector Potential of a Line Current

$$A_z(x, y, z) = \frac{\mu_0 I}{4\pi} \int_a^b \frac{dz_c}{|\mathbf{r} - \mathbf{r}'|} = \frac{\mu_0 I}{4\pi} \int_a^b \frac{dz_c}{\sqrt{x^2 + y^2 + (z - z_c)^2}}$$
$$\left. \frac{-\mu_0 I}{4\pi} \ln \left((z - z_c) + \sqrt{x^2 + y^2 + (z - z_c)^2} \right) \right|_a^b$$
$$\frac{\mu_0 I}{4\pi} \ln \frac{z - a + \sqrt{x^2 + y^2 + (z - a)^2}}{z - b + \sqrt{x^2 + y^2 + (z - b)^2}}.$$



Caution: Infinitely long line currents have infinite energy

Field of a Line Current Segment



$$\begin{aligned}
 \mathbf{B}(\mathcal{P}) &= \frac{\mu_0 I}{4\pi} \int_{\mathcal{L}} \frac{\cos \alpha}{r_{\mathcal{P}\mathcal{Q}}} d\mathbf{r}' = \frac{\mu_0 I}{4\pi R} \mathbf{n} \int_{\alpha_1}^{\alpha_2} \cos \alpha d\alpha = \frac{\mu_0 I}{4\pi R} (\sin \alpha_2 - \sin \alpha_1) \mathbf{n} \\
 &= \frac{\mu_0 I}{4\pi} \frac{\cos \alpha_2 + \cos \alpha_1}{R} \frac{\sin \alpha_2 - \sin \alpha_1}{\cos \alpha_2 + \cos \alpha_1} \mathbf{n} \\
 &= \frac{\mu_0 I}{4\pi} \left(\frac{1}{|\mathbf{r}_1|} + \frac{1}{|\mathbf{r}_2|} \right) \frac{\sin(\alpha_2 - \alpha_1)}{1 + \cos(\alpha_2 - \alpha_1)} \mathbf{n} \\
 &= \frac{\mu_0 I}{4\pi} \left(\frac{1}{|\mathbf{r}_1|} + \frac{1}{|\mathbf{r}_2|} \right) \frac{\sin(\alpha_2 - \alpha_1)}{1 + \frac{\mathbf{r}_1 \cdot \mathbf{r}_2}{|\mathbf{r}_1| |\mathbf{r}_2|}} \frac{\mathbf{r}_1 \times \mathbf{r}_2}{|\mathbf{r}_1| |\mathbf{r}_2| \sin(\alpha_2 - \alpha_1)} \\
 &= \frac{\mu_0 I}{4\pi} \frac{|\mathbf{r}_1| + |\mathbf{r}_2|}{|\mathbf{r}_1| |\mathbf{r}_2| + \mathbf{r}_1 \cdot \mathbf{r}_2} \frac{\mathbf{r}_1 \times \mathbf{r}_2}{|\mathbf{r}_1| |\mathbf{r}_2|},
 \end{aligned}$$

Field of a Line Current

$$\begin{aligned}
 \lim_{a,b \rightarrow \pm\infty} \ln \frac{z-a+\sqrt{x^2+y^2+(z-a)^2}}{z-b+\sqrt{x^2+y^2+(z-b)^2}} &= \lim_{a,b \rightarrow \pm\infty} \ln \frac{-a+|a|\sqrt{1+\frac{x^2+y^2}{a^2}}}{-b+|b|\sqrt{1+\frac{x^2+y^2}{b^2}}} \\
 &= \lim_{a,b \rightarrow \pm\infty} \ln \frac{-a-a(1+\frac{x^2+y^2}{2a^2}+\dots)}{-b+b(1+\frac{x^2+y^2}{2b^2}+\dots)} = \lim_{a,b \rightarrow \pm\infty} \ln \frac{-2a}{-b+b+\frac{x^2+y^2}{2b}} \\
 &= \lim_{a,b \rightarrow \pm\infty} \ln \frac{-4ab}{x^2+y^2}.
 \end{aligned}$$

$$A_z(x, y) = \lim_{a,b \rightarrow \pm\infty} \frac{\mu_0 I}{4\pi} \ln \left(\frac{-4ab}{x_0^2 + y_0^2} \right) - \frac{\mu_0 I}{4\pi} \ln \left(\frac{x^2 + y^2}{x_0^2 + y_0^2} \right).$$

$$\mathbf{A}(x, y) = -\frac{\mu_0 I}{4\pi} \ln \left(\frac{x^2 + y^2}{x_0^2 + y_0^2} \right) \mathbf{e}_z = -\frac{\mu_0 I}{2\pi} \ln \left(\frac{r}{r_{\text{ref}}} \right) \mathbf{e}_z,$$

**Problem solved, but reference radius has physical significance:
Return path for sum-currents**



Field of a Line Current

$$A_\phi(r, z) = \frac{\mu_0 I r_c}{\pi \sqrt{(r + r_c)^2 + z^2}} \int_0^{\pi/2} \frac{2 \sin^2 \psi - 1}{\sqrt{1 - k^2 \sin^2 \psi}} d\psi.$$

Appearance of elliptic integrals:
To be solved numerically.

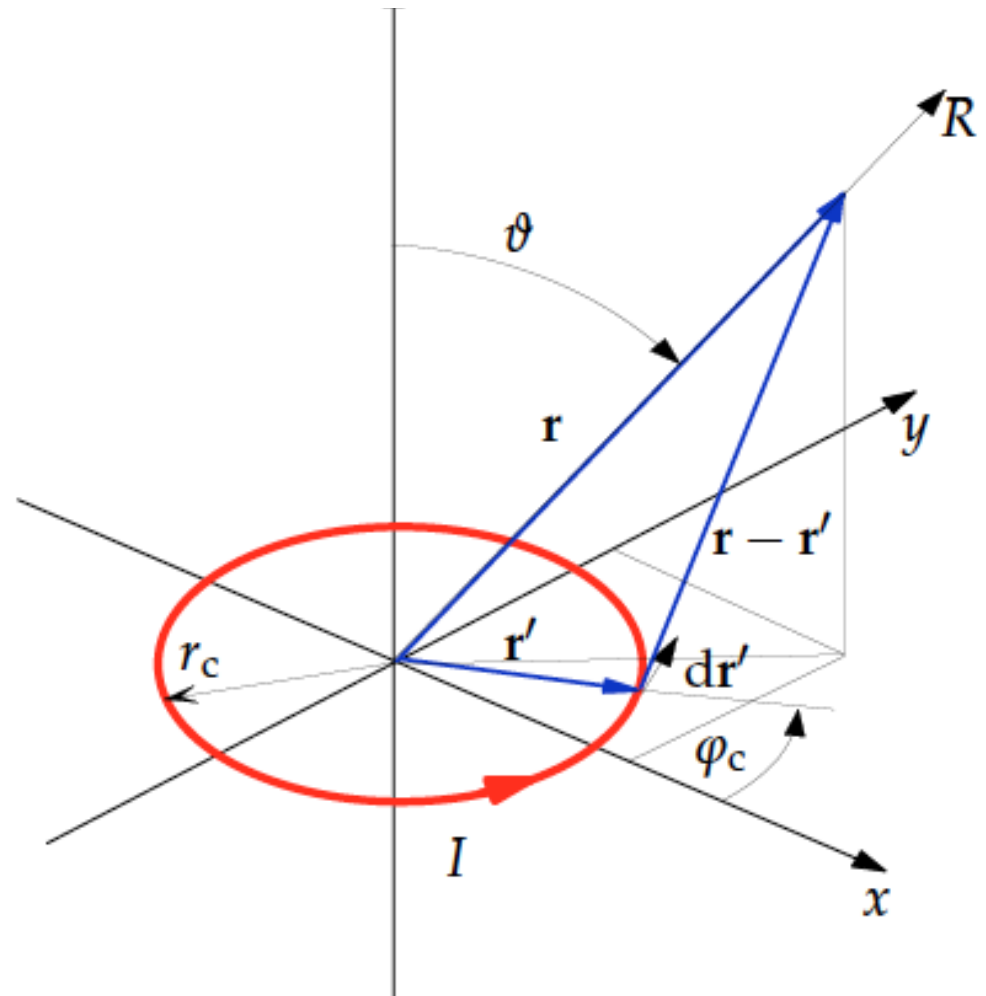
On axis:

$$A_\phi(r, z) = \frac{\mu_0 I r_c^2}{4} \frac{r}{(r_c^2 + z^2)^{\frac{3}{2}}},$$

$$B_z(z) = \frac{\mu_0 I}{2} \frac{r_c^2}{(r_c^2 + z^2)^{\frac{3}{2}}}.$$

In the center:

$$B_z(z=0) = \frac{\mu_0 I}{2r_c}.$$



Magnetic Dipole Moment

Far field approximation

$$A_\varphi(R, \vartheta) \approx \frac{\mu_0 I r_c^2 \pi}{4\pi} \frac{\sin \vartheta}{R^2} = \frac{\mu_0 m}{4\pi} \frac{\sin \vartheta}{R^2},$$

$$R = \sqrt{r^2 + z^2} \text{ and } \sin \vartheta = r/R,$$

$$[m] = 1 \text{ A m}^2. \quad \text{Definition} \quad m := I r_c^2 \pi$$

$$\mathbf{m} = I \mathbf{a},$$

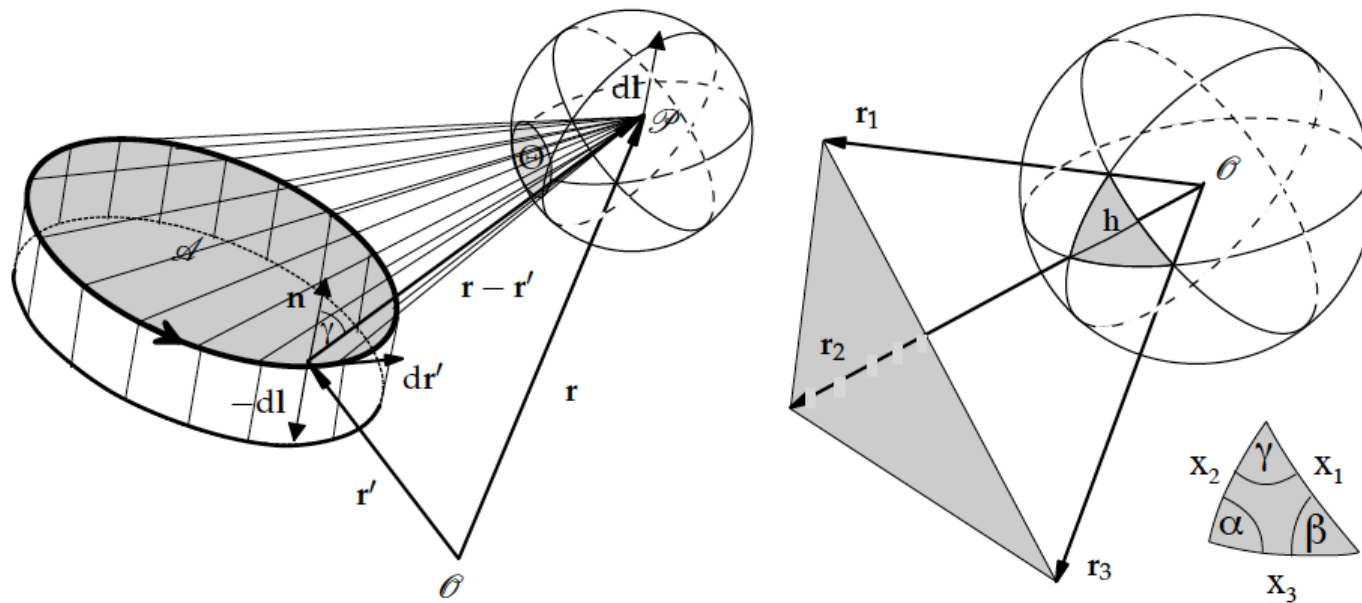
$$\mathbf{m} = \frac{I}{2} \int_{\mathcal{C}} \mathbf{r} \times d\mathbf{r},$$

$$\mathbf{M}(\mathbf{r}) := \frac{d\mathbf{m}}{dV} = \frac{1}{2} \mathbf{r} \times \mathbf{J}(\mathbf{r}),$$



Solid Angle and Magnetic Scalar Potential

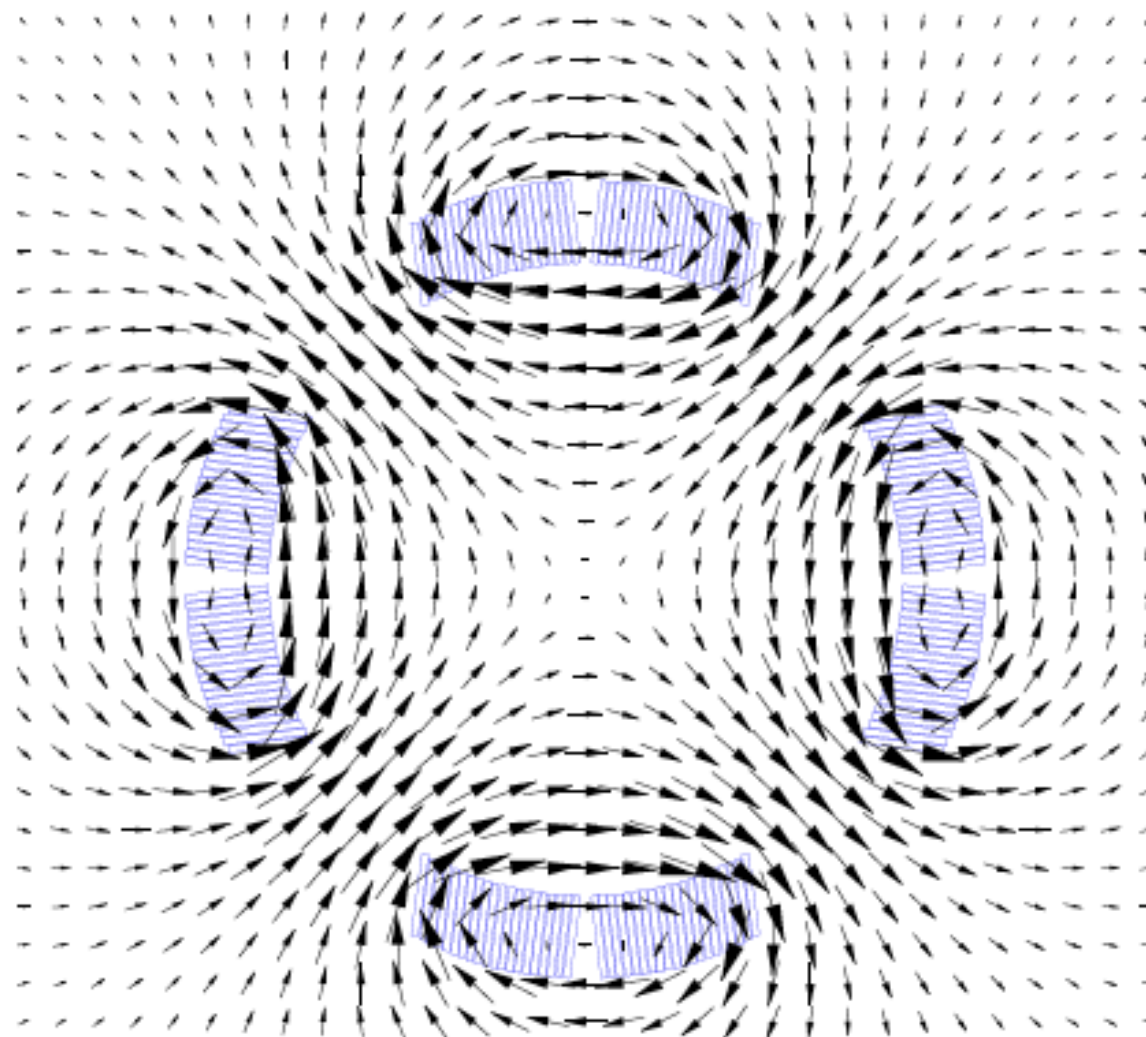
Solid angle (easy to compute) gives the magnetic scalar potential of a current loop



$$\phi_m(\mathbf{r}) = \frac{I}{4\pi} \Theta .$$

$$\tan\left(\frac{\Theta}{2}\right) = \frac{\mathbf{r}_1 \cdot (\mathbf{r}_2 \times \mathbf{r}_3)}{r_1 r_2 r_3 + (\mathbf{r}_1 \cdot \mathbf{r}_2)r_3 + (\mathbf{r}_1 \cdot \mathbf{r}_3)r_2 + (\mathbf{r}_2 \cdot \mathbf{r}_3)r_1} .$$

The Imaging Current Method



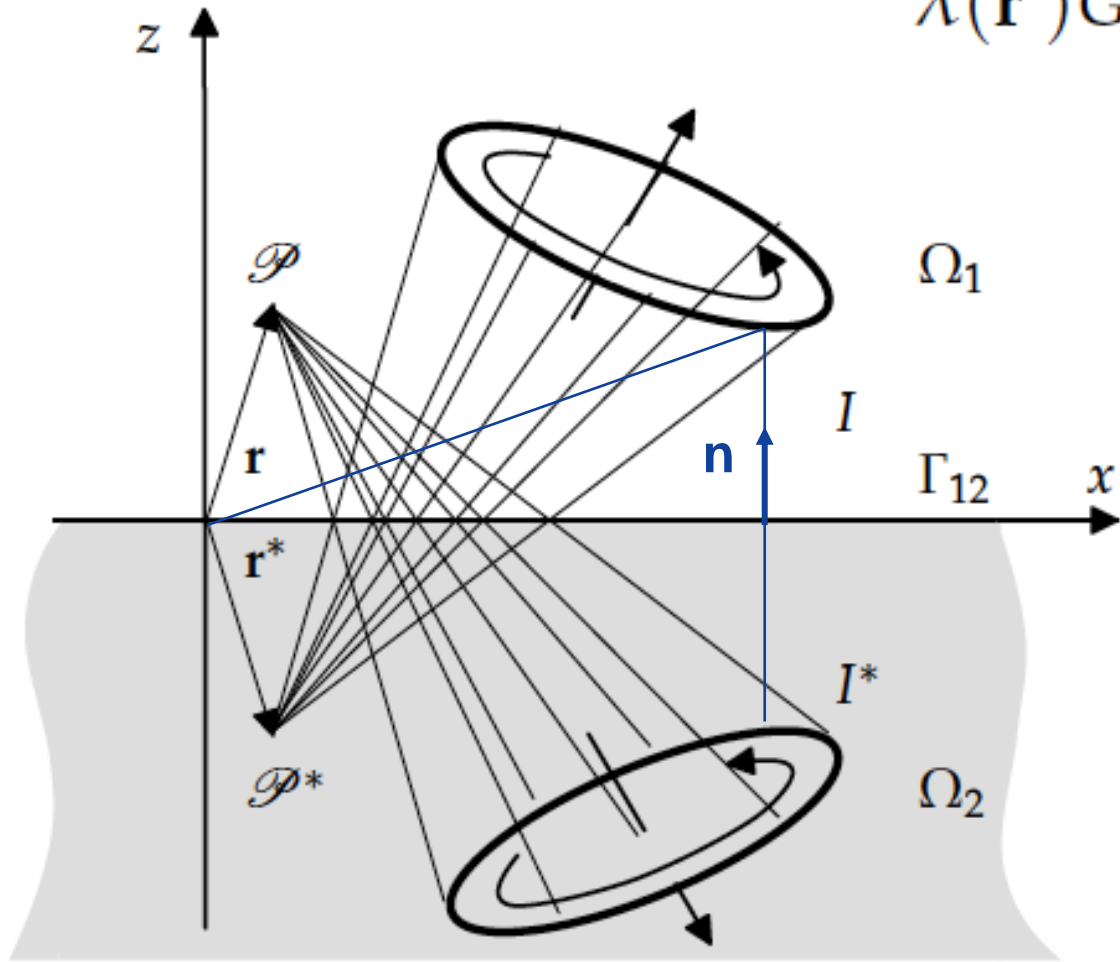
Notes on the Imaging Method

- Domain 1: Domain with current sources
- Domain 2: Highly permeable material
 - All imaging currents must be in domain 2
 - The sources and the images must create a field that satisfies the continuity conditions at the interface between domains 1 and 2
 - The image of the image must be the original source
 - The field generated in domain 1 is identical to the source field plus the field from the (iron) magnetization.
 - The field generated in domain 2 has no physical significance



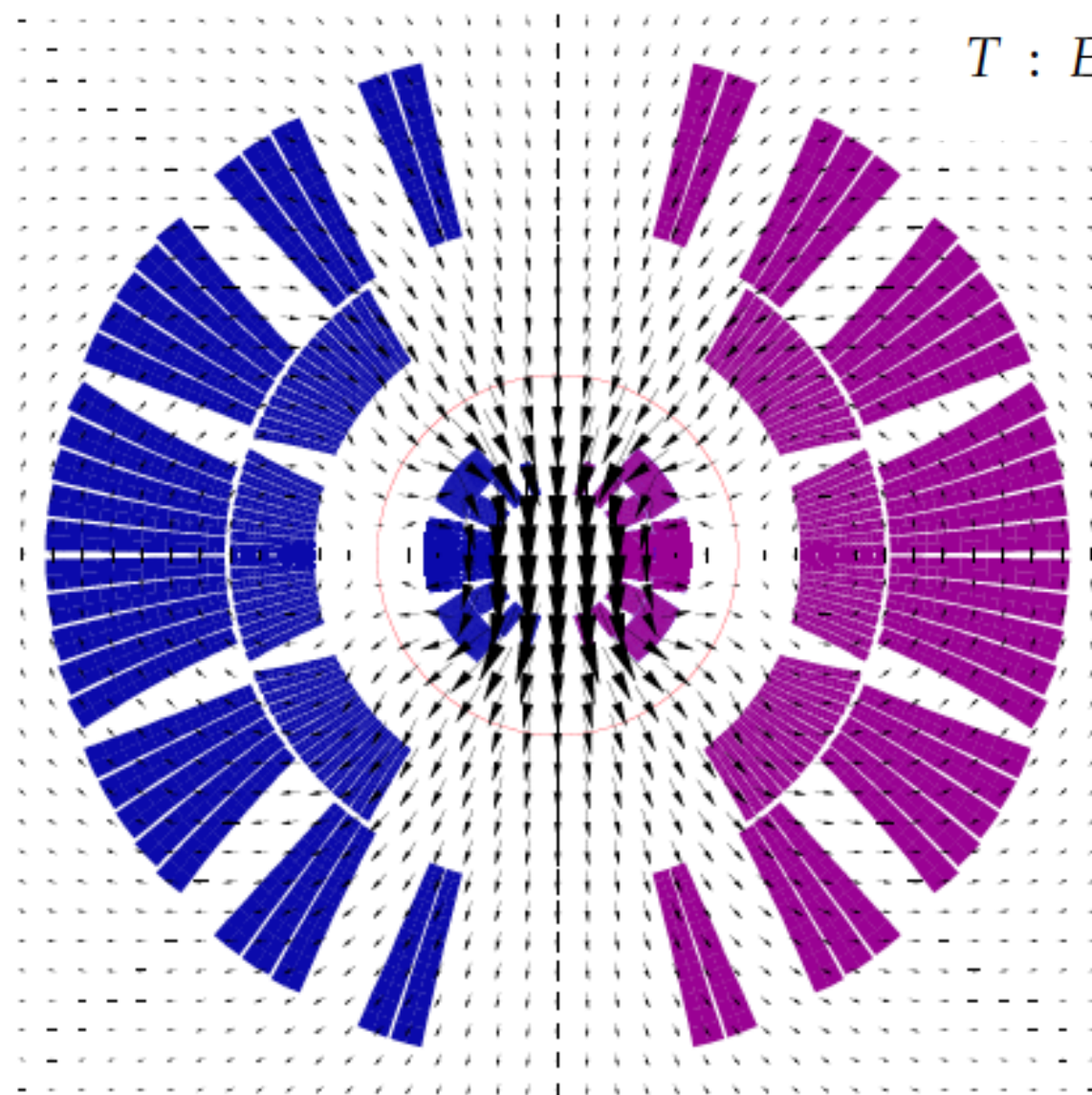
The Imaging Current Method

$$\lambda(\mathbf{r}')G(\mathbf{r}, T\mathbf{r}') = \lambda(\mathbf{r})G(T\mathbf{r}, \mathbf{r}')$$



$$T : E_3 \rightarrow E_3 : \mathbf{r}' \mapsto T\mathbf{r}' = \mathbf{r}' - 2\mathbf{n} (\mathbf{n} \cdot \mathbf{r}'),$$

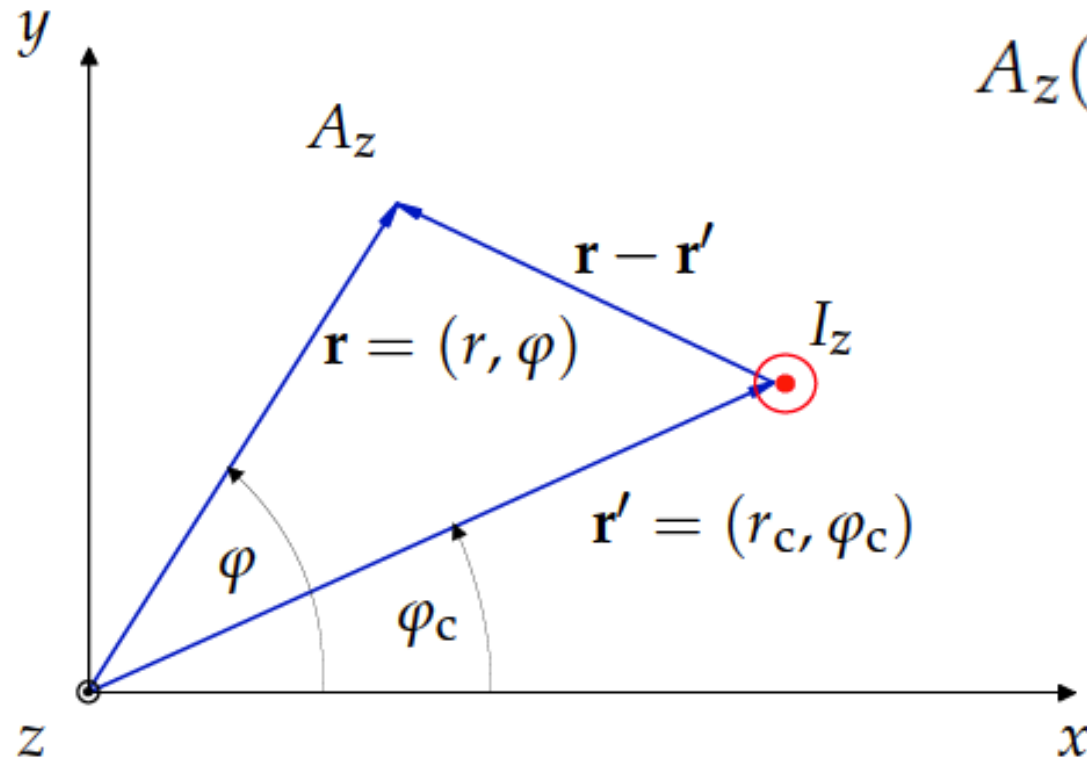
The Imaging Current Method



$$T : E_2 \rightarrow E_2 : \mathbf{r}' \mapsto T\mathbf{r}' = \frac{r_y^2}{|\mathbf{r}'|^2} \mathbf{r}',$$

$$I^* = \lambda_\mu I := \frac{\mu_r - 1}{\mu_r + 1} I.$$

The Field of a Line Current (2D)



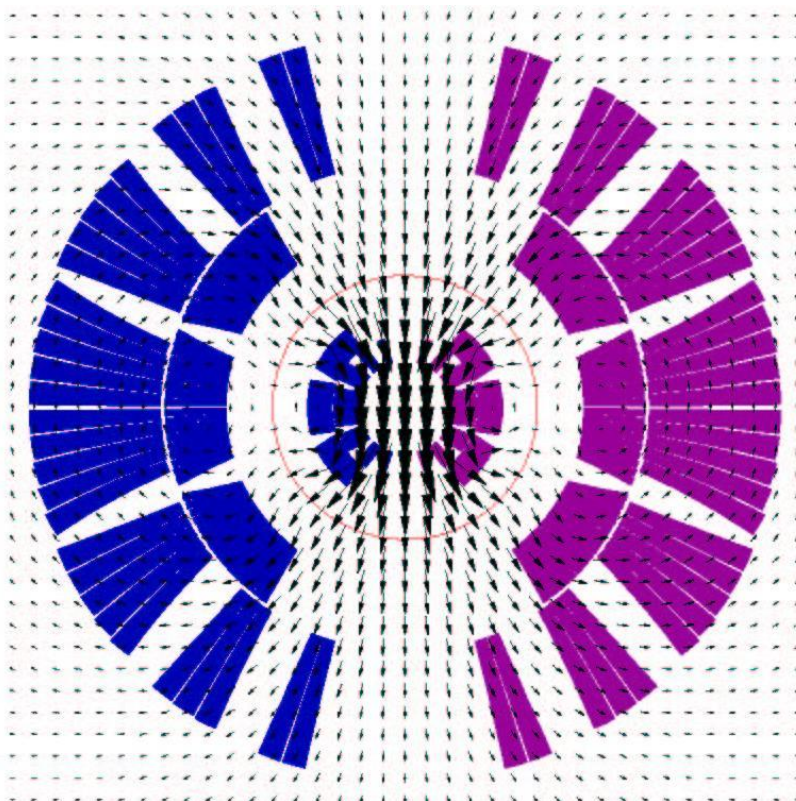
$$A_z(\mathbf{r}) = -\frac{\mu_0 I}{2\pi} \ln \left(\frac{|\mathbf{r} - \mathbf{r}'|}{r_{\text{ref}}} \right)$$

$$A_z(r, \varphi) = -\frac{\mu_0 I}{2\pi} \ln \left(\frac{r_c}{r_{\text{ref}}} \right) + \frac{\mu_0 I}{2\pi} \sum_{n=1}^{\infty} \frac{1}{n} \left(\frac{r}{r_c} \right)^n \cos n(\varphi - \varphi_c)$$

$$B_n(r_0) = -\frac{\mu_0 I}{2\pi r_c} \left(\frac{r_0}{r_c} \right)^{n-1} \cos n\varphi_c, \quad A_n(r_0) = \frac{\mu_0 I}{2\pi r_c} \left(\frac{r_0}{r_c} \right)^{n-1} \sin n\varphi_c.$$

Imaging Method

$$B_n(r_0) = - \sum_{k=1}^K \frac{\mu_0 I_k}{2\pi} \frac{r_0^{n-1}}{r_{c,k}^n} \left(1 + \lambda_\mu \left(\frac{r_{c,k}}{r_y} \right)^{2n} \right) \cos n \varphi_{c,k},$$



$$\lambda_\mu I := \frac{\mu_r - 1}{\mu_r + 1} I.$$

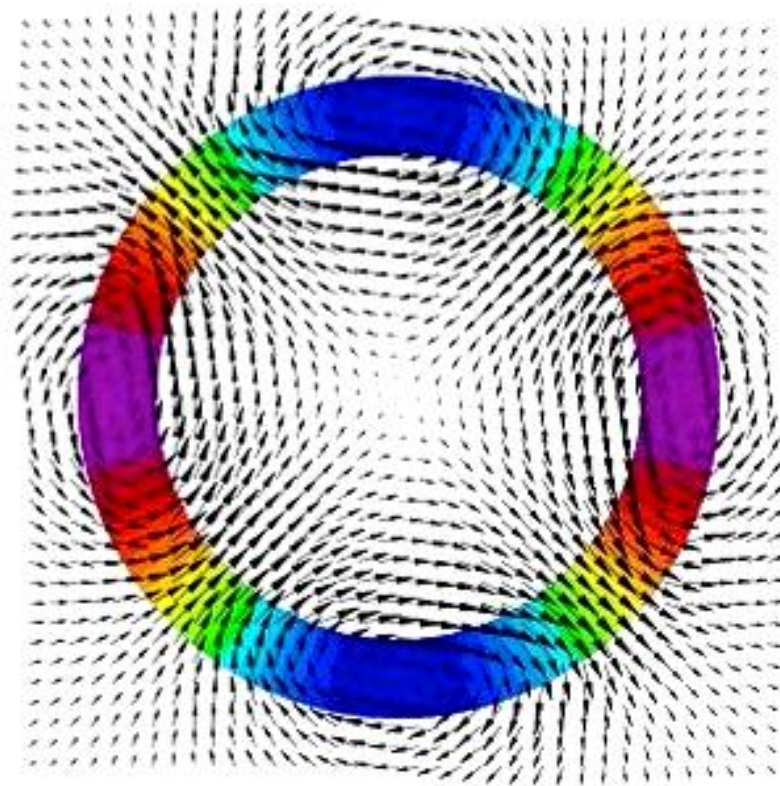
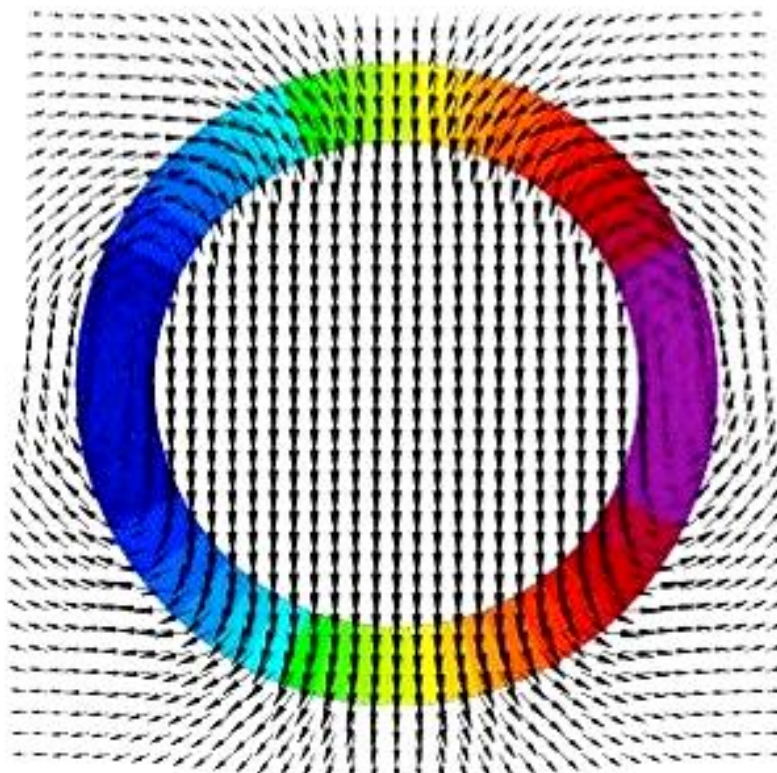
$$\frac{B_N^{\text{imag}}}{B_N + B_N^{\text{imag}}} \approx \left(1 + \left(\frac{r_y}{r} \right)^{2N} \right)^{-1}.$$

Interrupt: Numerical example

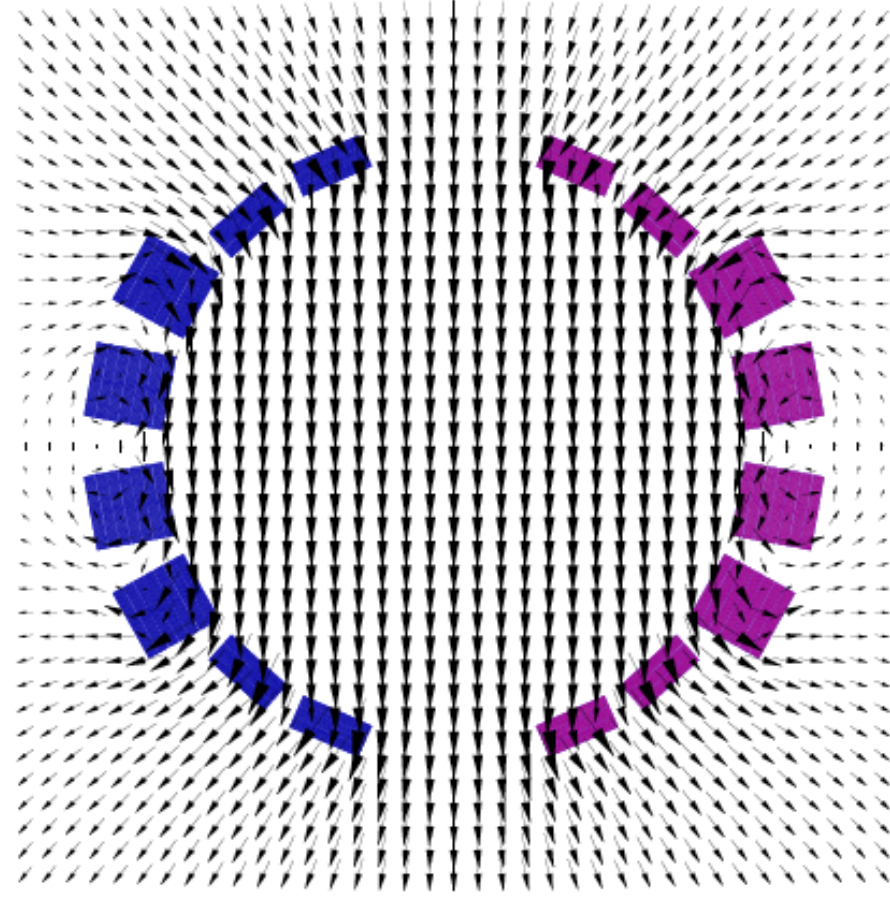
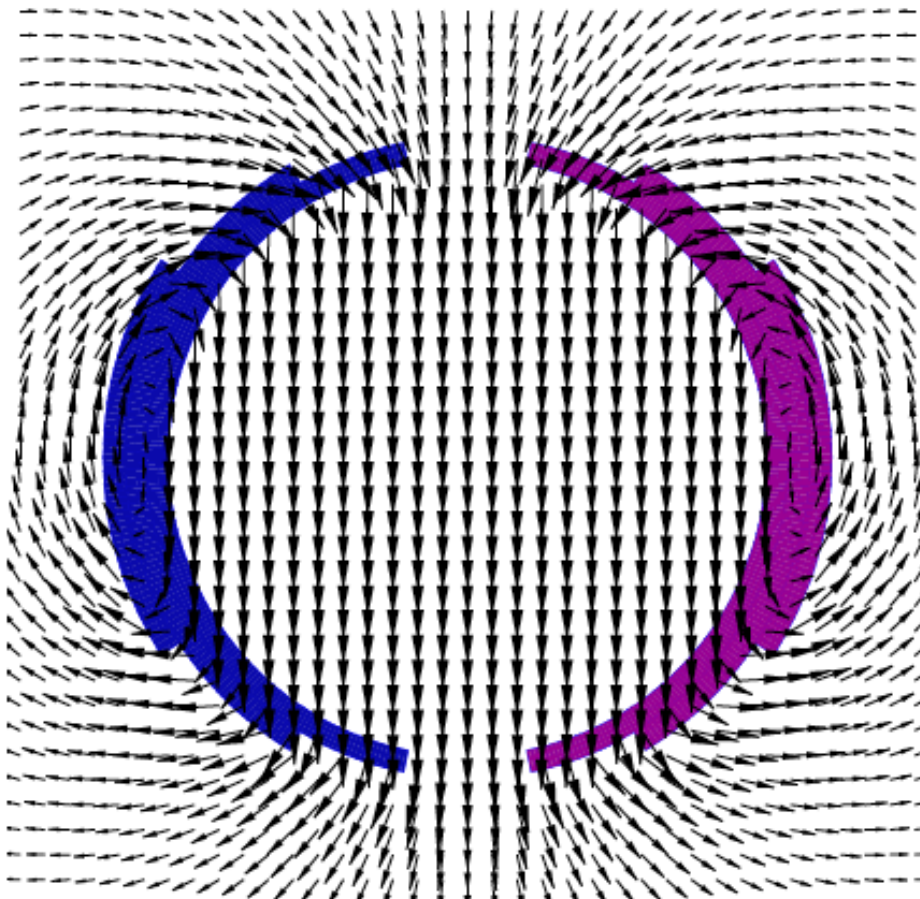
Ideal Current Distributions

$$B_n(r_0) = \int_{r_a}^{r_e} \int_0^{2\pi} -\frac{\mu_0 J_E}{2\pi} J_c(B) d\varphi_c dr_c \cos n\varphi_c r_c d\varphi_c dr_c$$

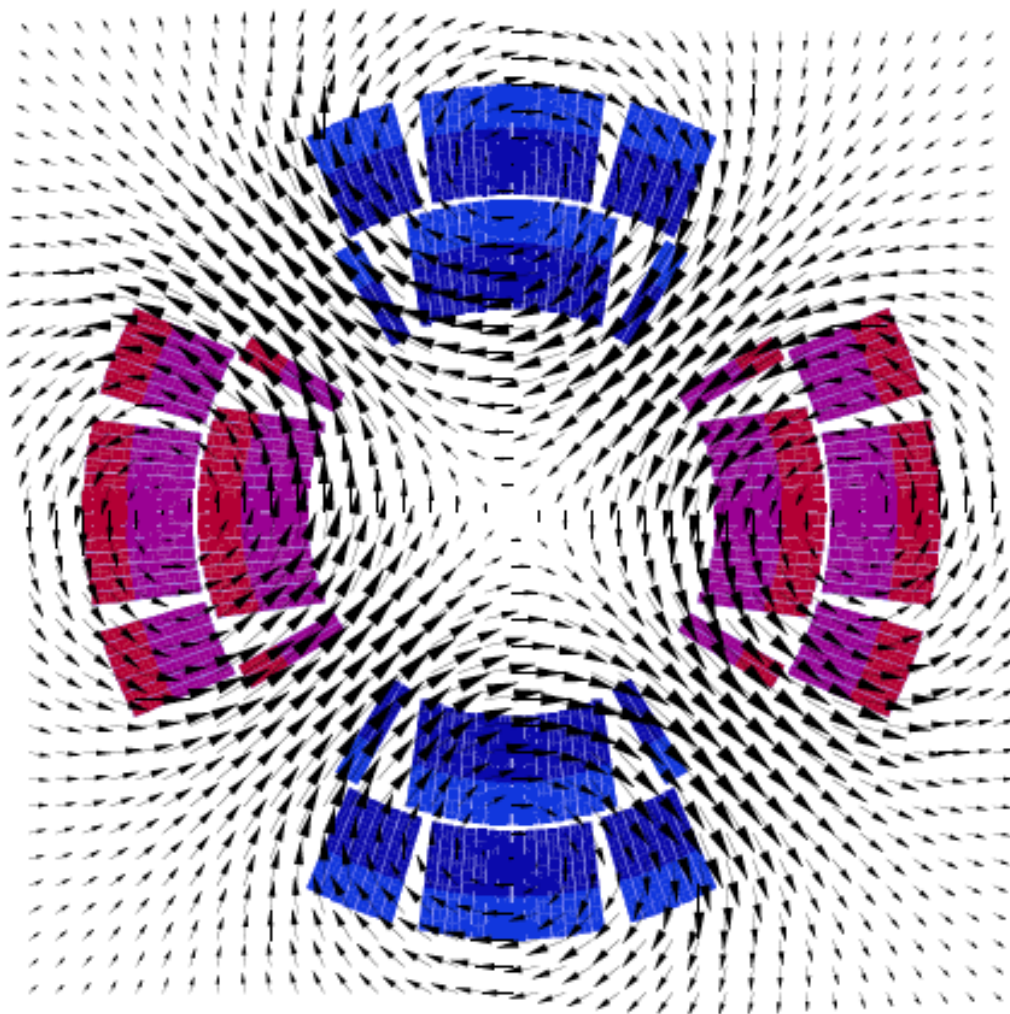
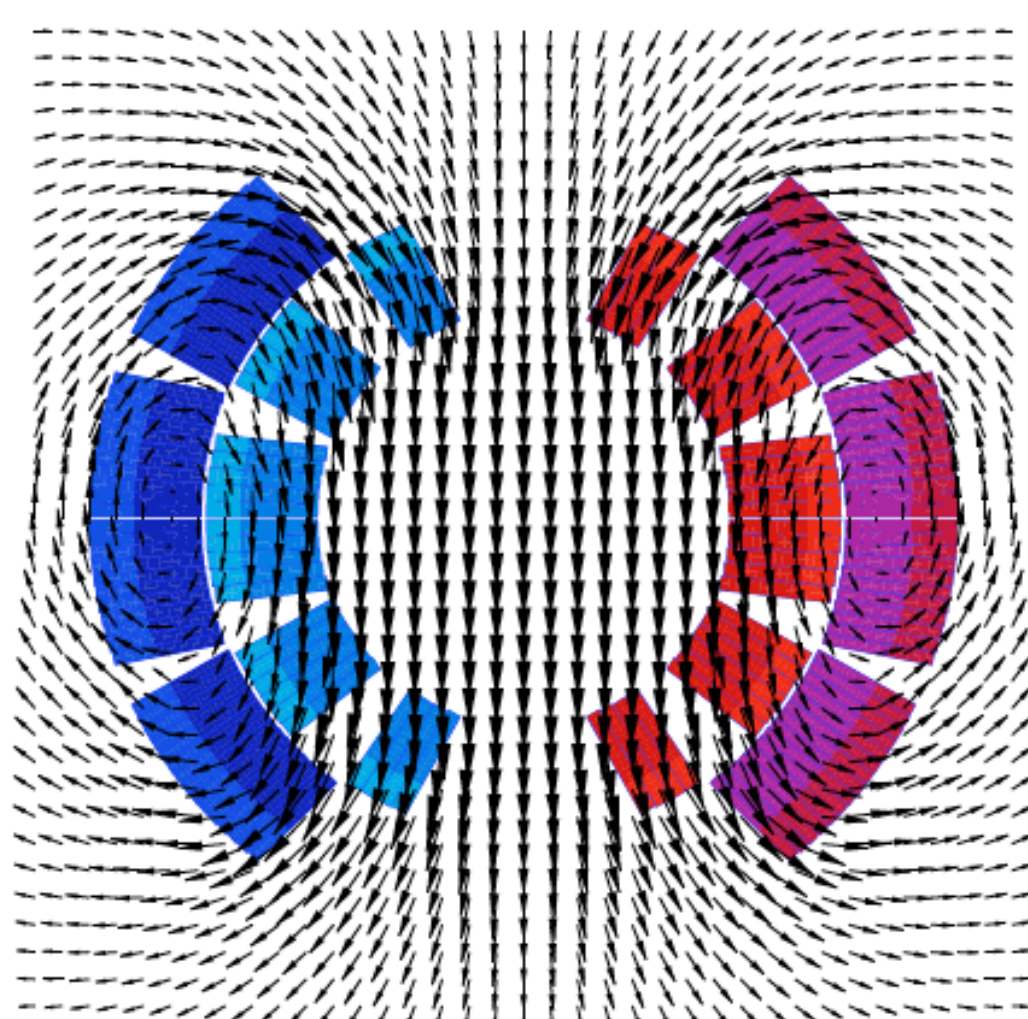
$$B = \frac{\mu_0}{2} \lambda_{\text{tot}} J_c (r_e - r_a) = \frac{\mu_0}{2} \lambda_{\text{tot}} d (B_{c2} - B) (r_e - r_a),$$



Coil-Block Approximations



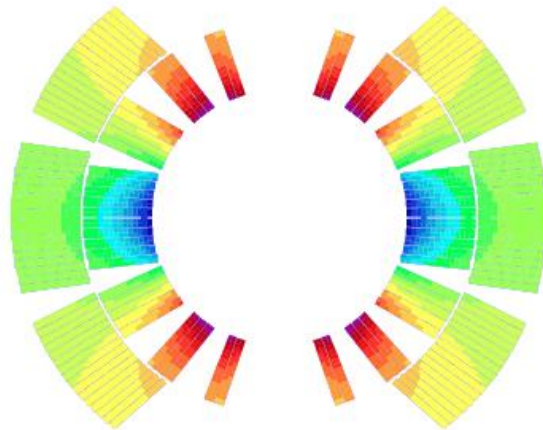
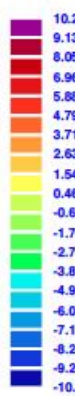
Coil-Block Approximations



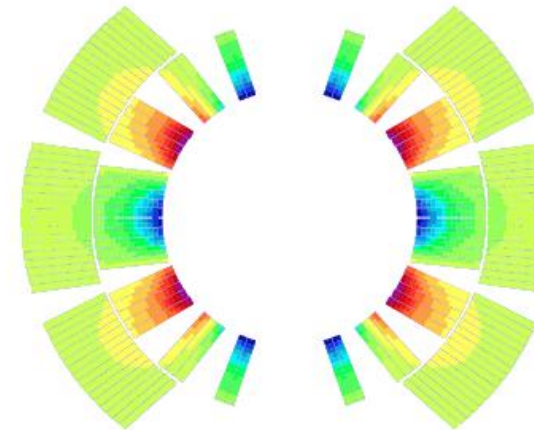
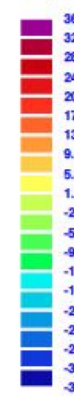
Generation of Multipole Field Errors

$$B_n(r_0) = - \sum_{k=1}^K \frac{\mu_0 I_k}{2\pi} \frac{r_0^{n-1}}{r_{c,k}^n} \left(1 + \lambda_\mu \left(\frac{r_{c,k}}{r_y} \right)^{2n} \right) \cos n\varphi_{c,k},$$

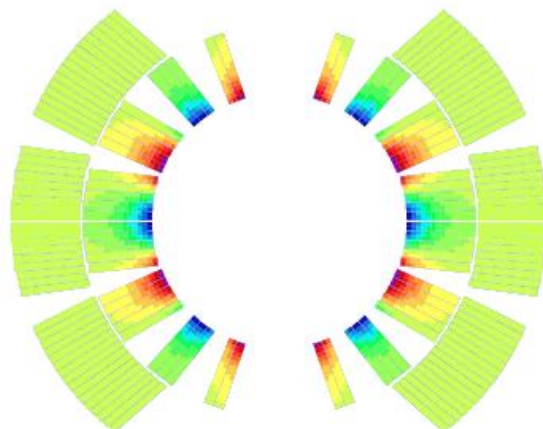
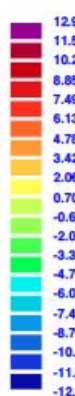
B3 (10E-4 T)



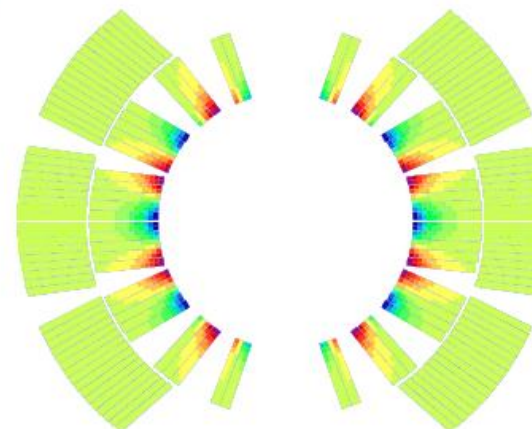
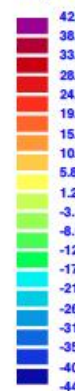
B5 (10E-5 T)



B7 (10E-5 T)



B9 (10E-6 T)



Sensitivity to Manufacturing Errors

$$B_n(r_0) = - \sum_{k=1}^K \frac{\mu_0 I_k}{2\pi} \frac{r_0^{n-1}}{r_{c,k}^n} \left(1 + \lambda_\mu \left(\frac{r_{c,k}}{r_y} \right)^{2n} \right) \cos n\varphi_{c,k},$$

$$\frac{\partial B_n(r_0)}{\partial \varphi_c} = - \frac{\mu_0 I_k}{2\pi} \frac{n r_0^{n-1}}{r_c^n} \left(1 + \left(\frac{r_c}{r_y} \right)^{2n} \right) \sin n\varphi_c,$$

$$\frac{\partial B_n(r_0)}{\partial r_c} = \frac{\mu_0 I_k}{2\pi} \frac{n r_0^{n-1}}{r_c^{n+1}} \left(1 - \left(\frac{r_c}{r_y} \right)^{2n} \right) \cos n\varphi_c.$$

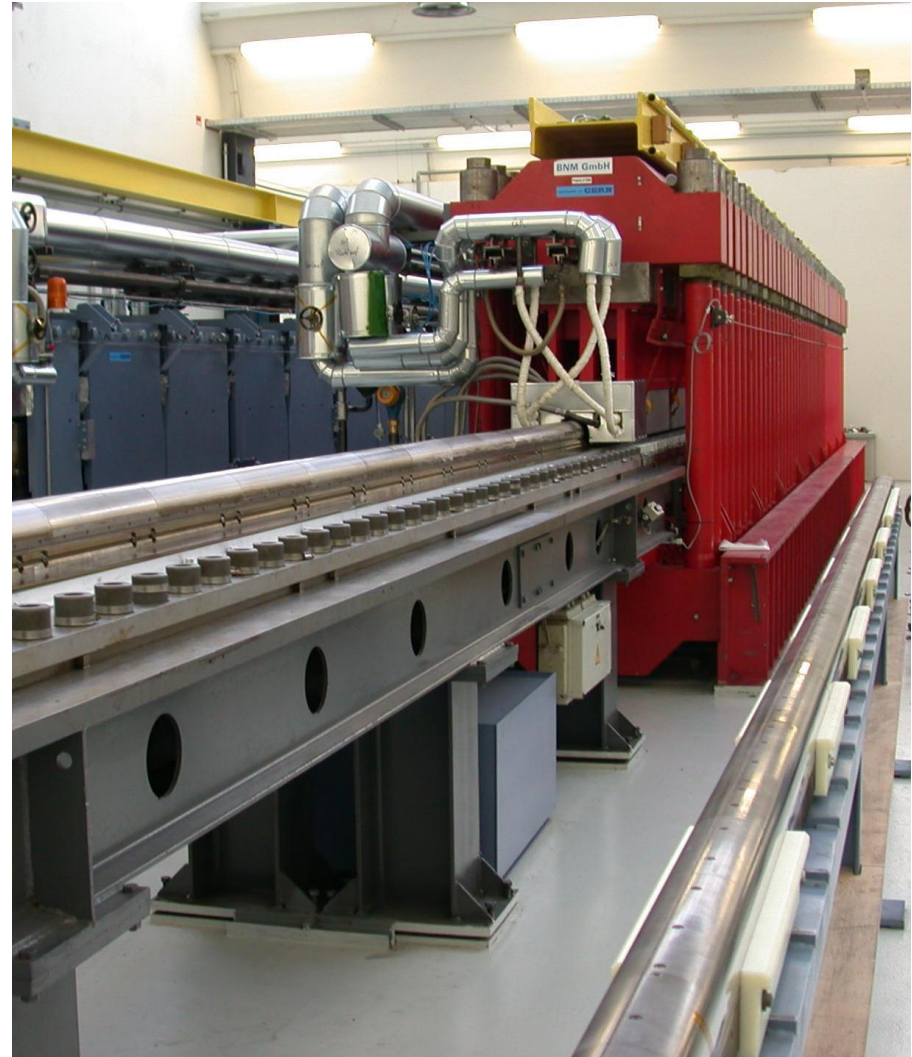
Increase of the azimuthal coil size by 0.1 mm produces (in units of 10^{-4}):

$$b_1 = -14, \quad b_3 = 1.2 \quad b_5 = 0.03$$

Specified tolerances on coils: ± 0.025 mm



Coil Winding and Curing



Field of a Ring Current

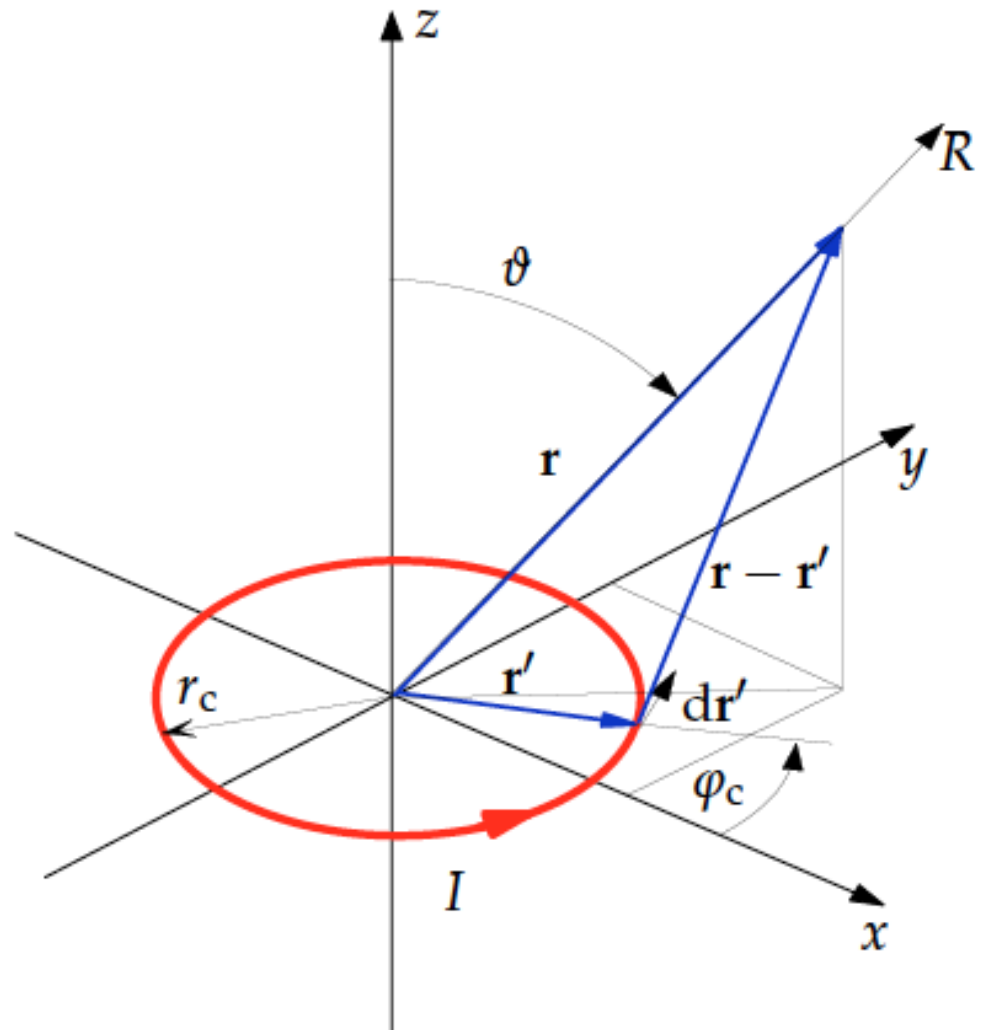
On axis:

$$A_\phi(r, z) = \frac{\mu_0 I r_c^2}{4} \frac{r}{(r_c^2 + z^2)^{\frac{3}{2}}},$$

$$B_z(z) = \frac{\mu_0 I}{2} \frac{r_c^2}{(r_c^2 + z^2)^{\frac{3}{2}}}.$$

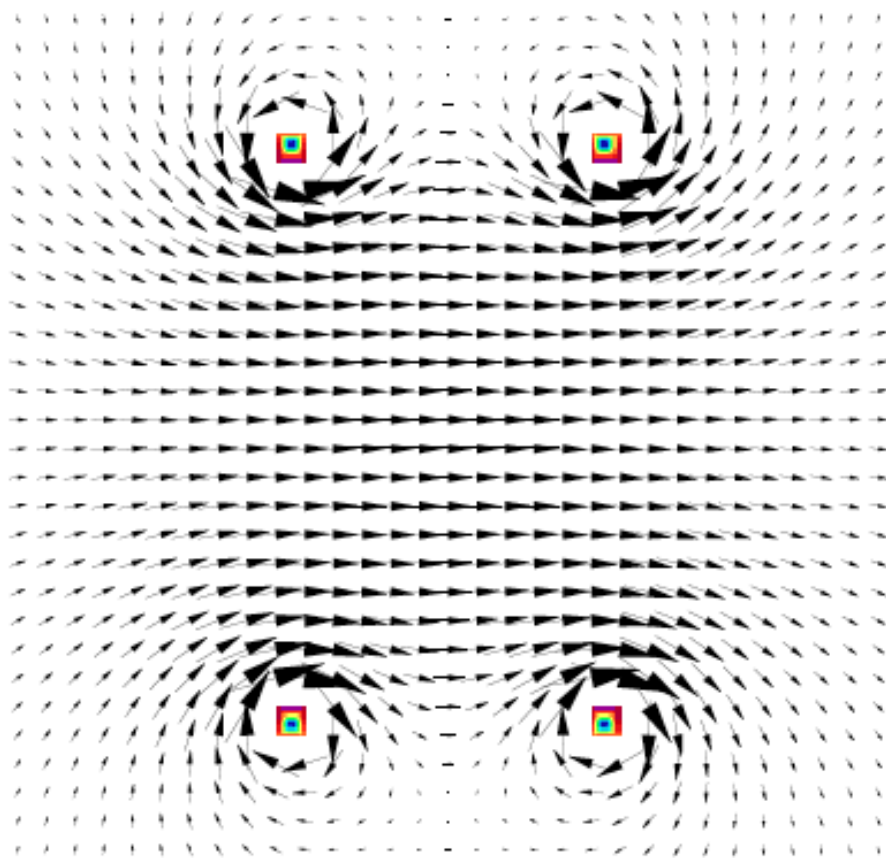
In the center:

$$B_z(z=0) = \frac{\mu_0 I}{2r_c}.$$



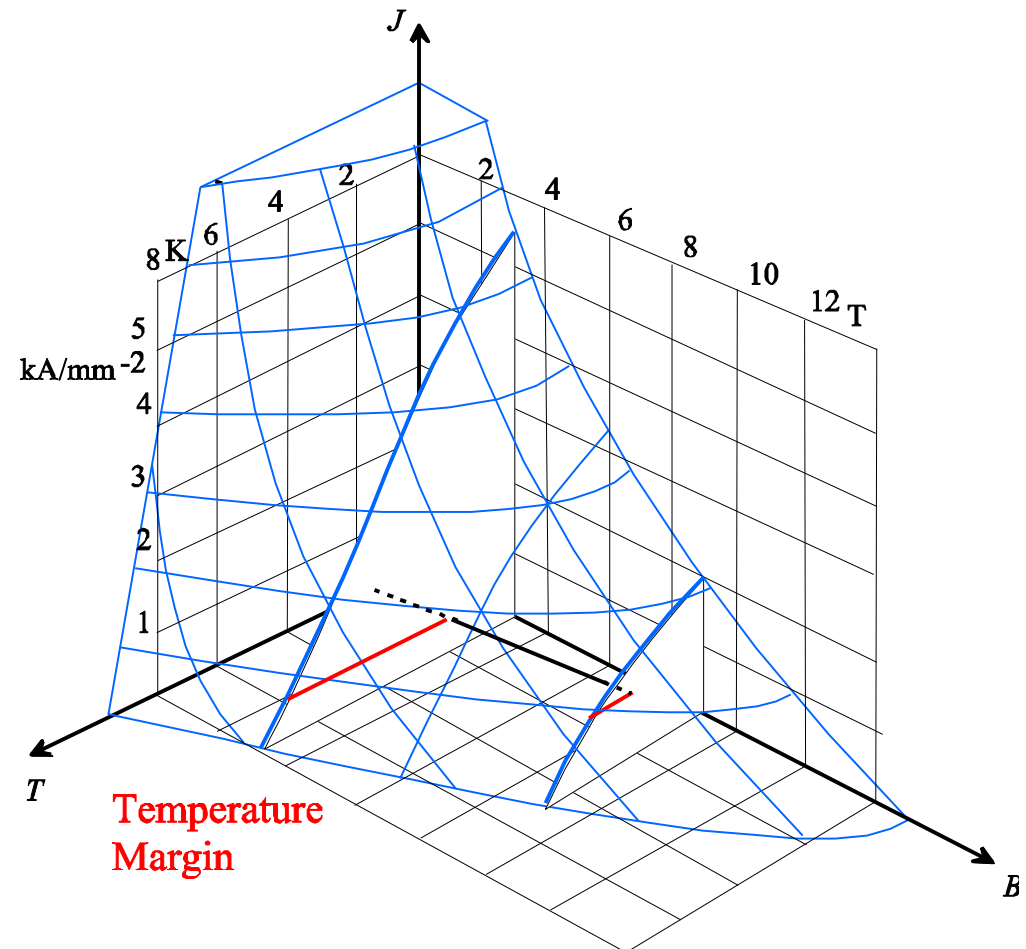
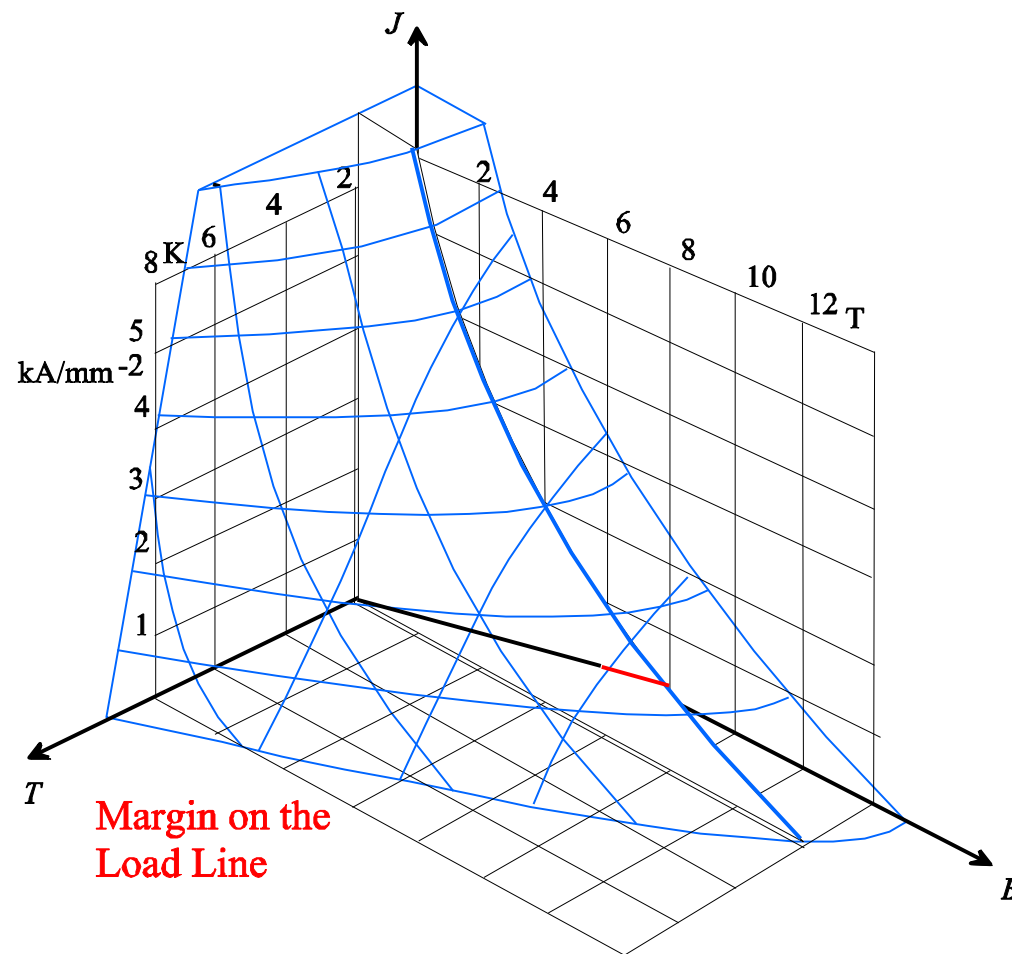
Helmholtz Coils

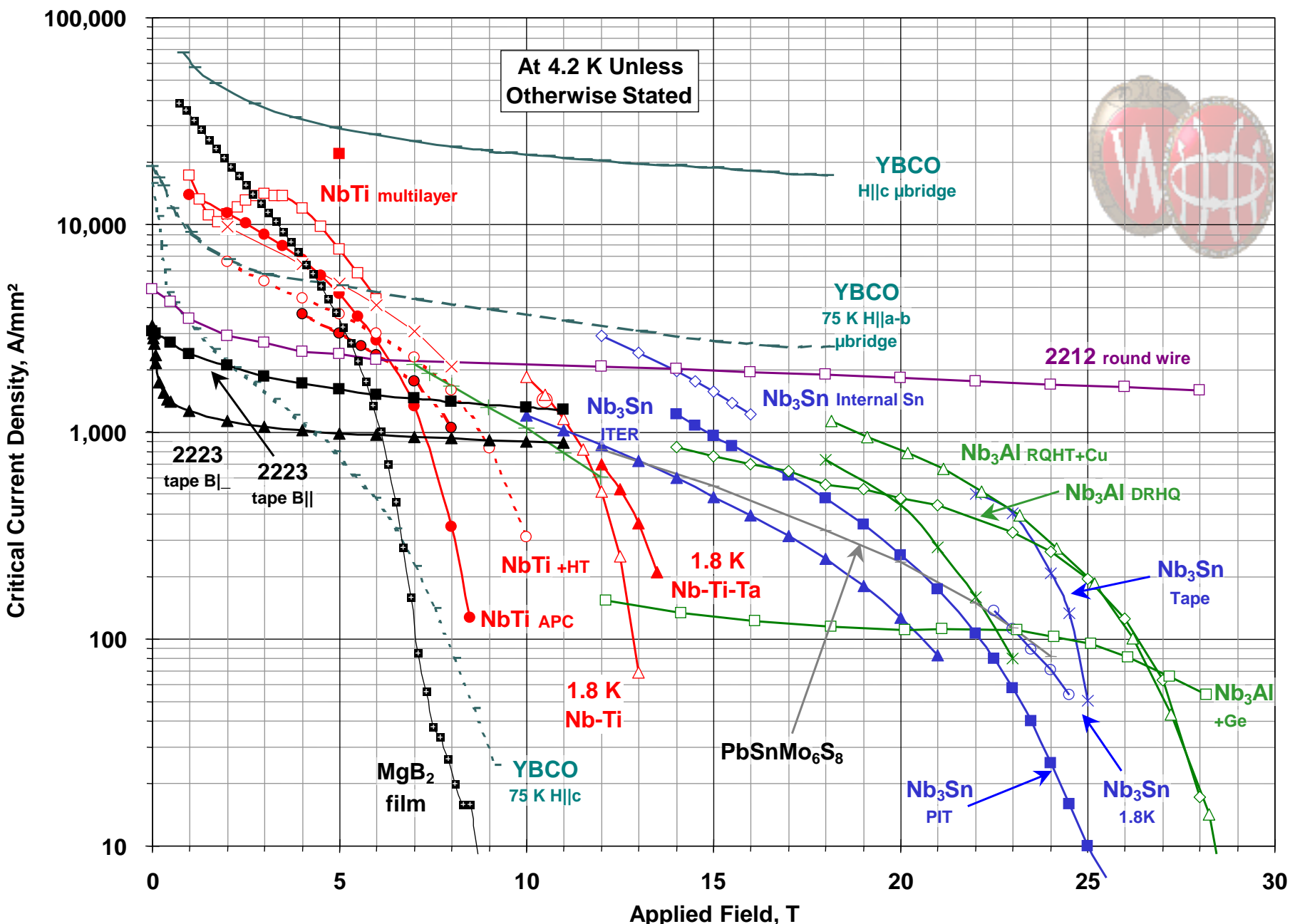
$$\frac{dB_z}{dz} = \frac{-3\mu_0 I r_c^2}{2} \left(\frac{z + z_c}{\sqrt{r_c^2 + (z + z_c)^2}^5} + \frac{z - z_c}{\sqrt{r_c^2 + (z - z_c)^2}^5} \right),$$



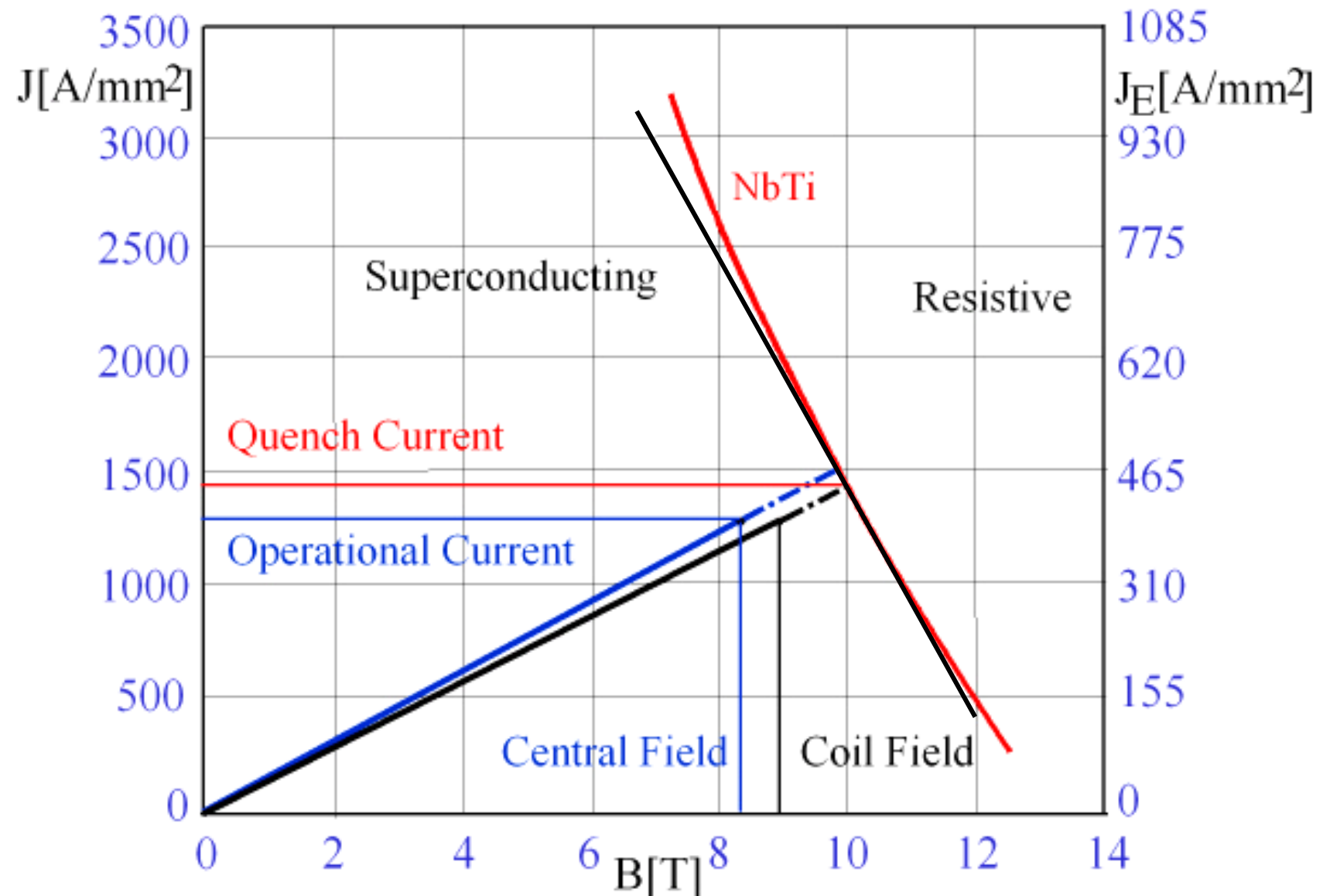
zero at $z = 0$ only if $z_c = r_c/2$.

Critical Surface of NbTi

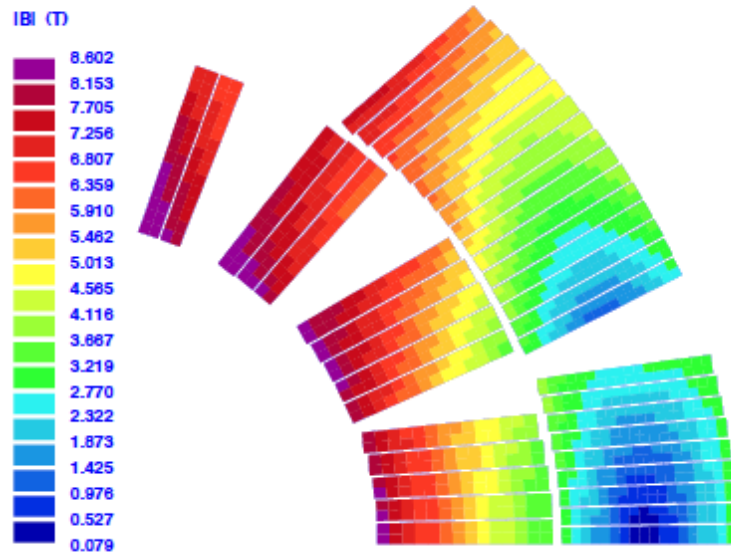
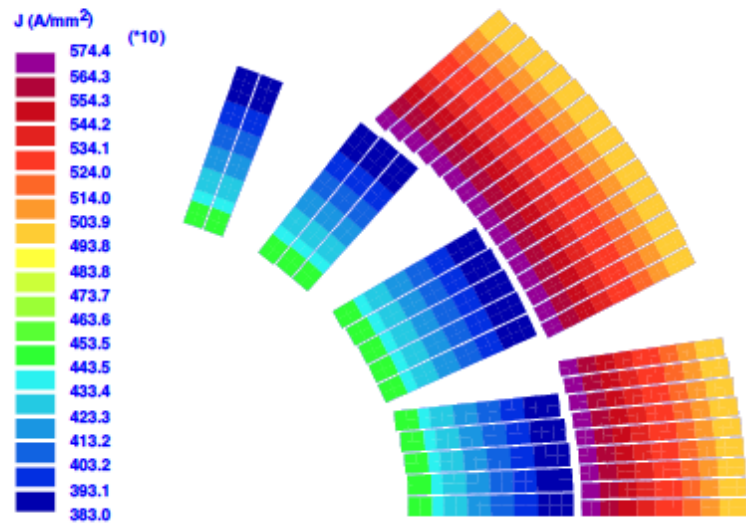
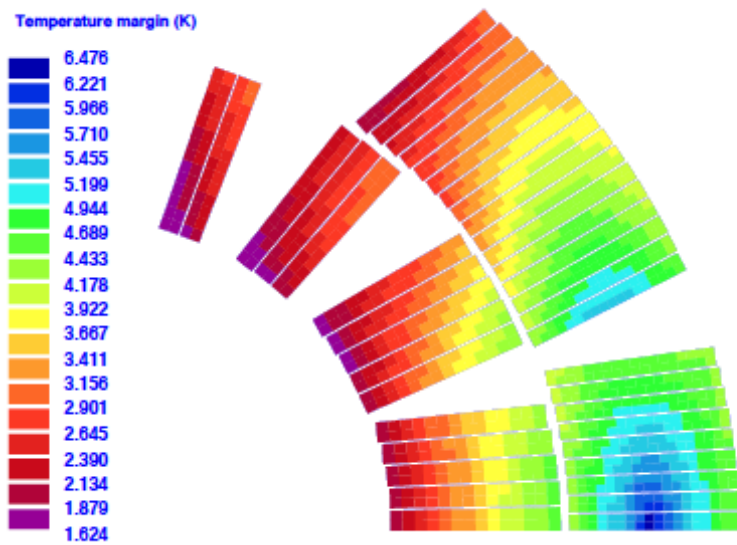
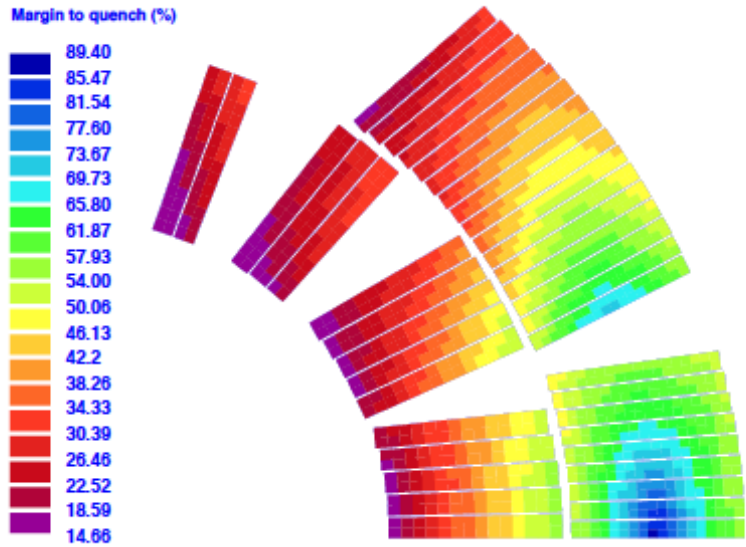




Working Point of LHC Dipole Magnets

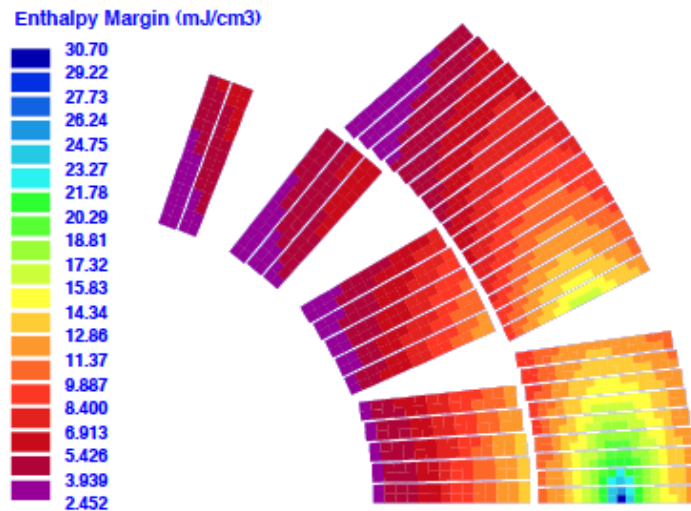


Margins

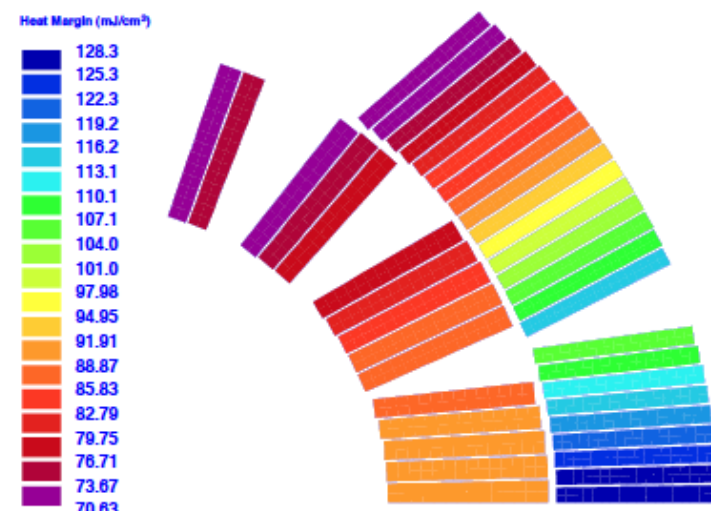


Margins

$$\Delta h := \int_{T_b}^{T_c(J,B)} \rho c_p(T) dT,$$

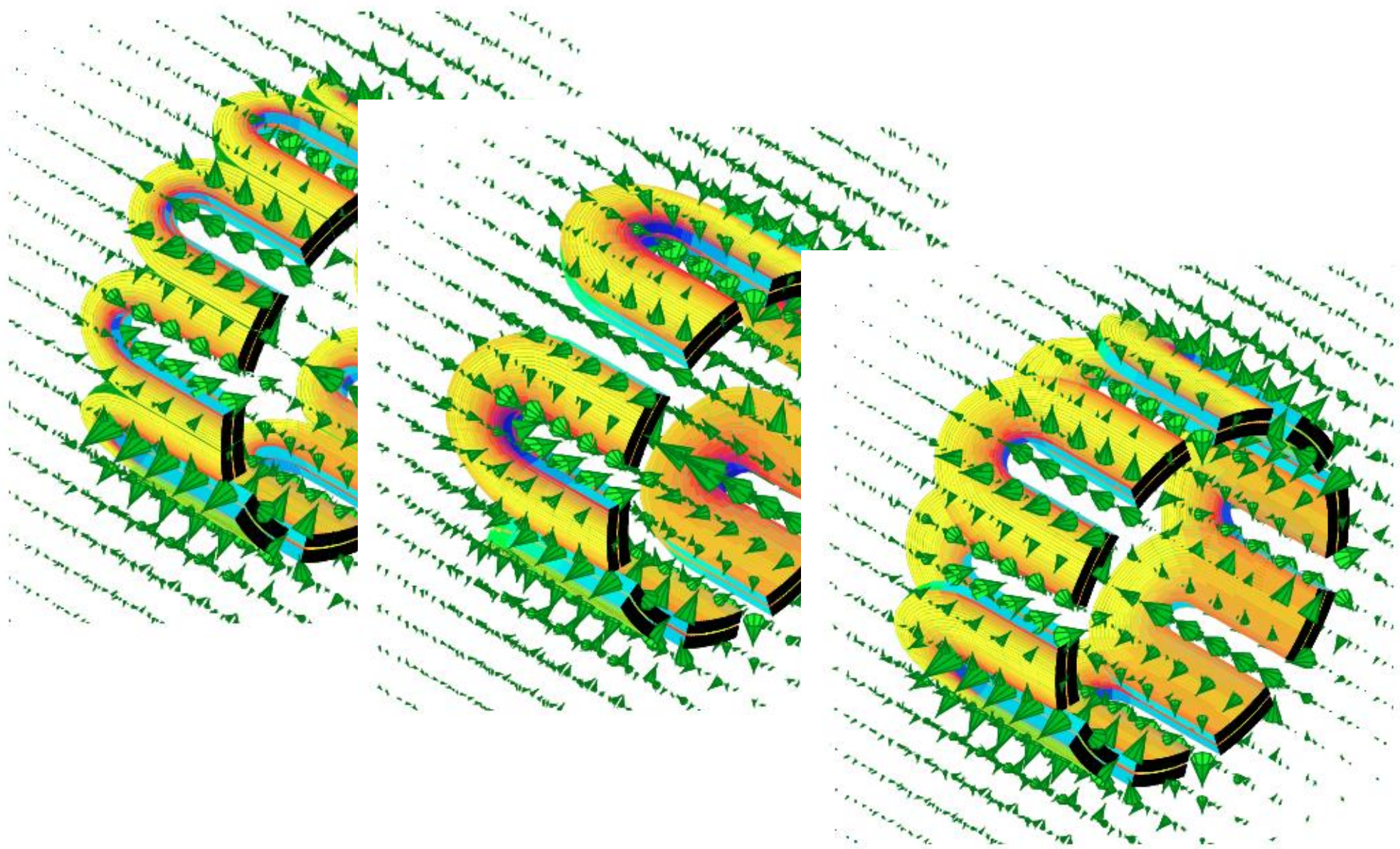


Enthalpy margin

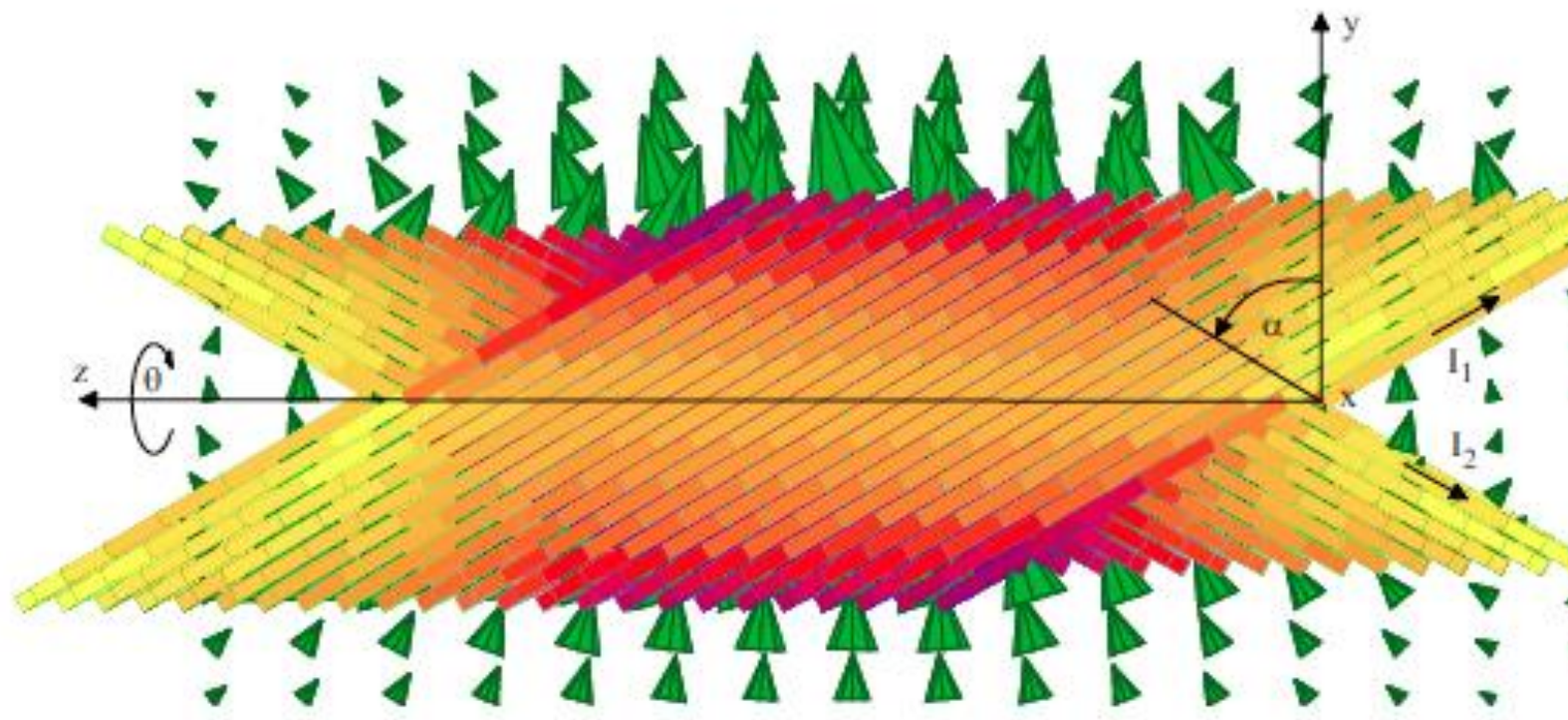


Heat reserve (copper, SC and helium)

Margins

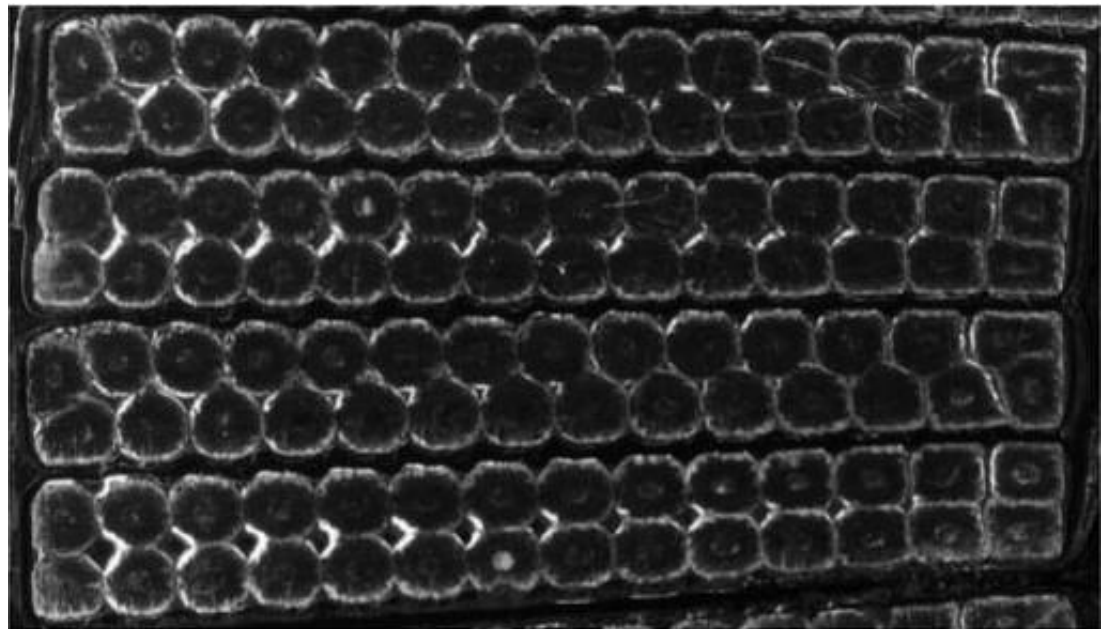


Nested Helices



Coil Block, Pinning Centers in Filaments

Magnetization



Grading of current density

Superconductor Properties

→ Hard Superconductors (Type 2)

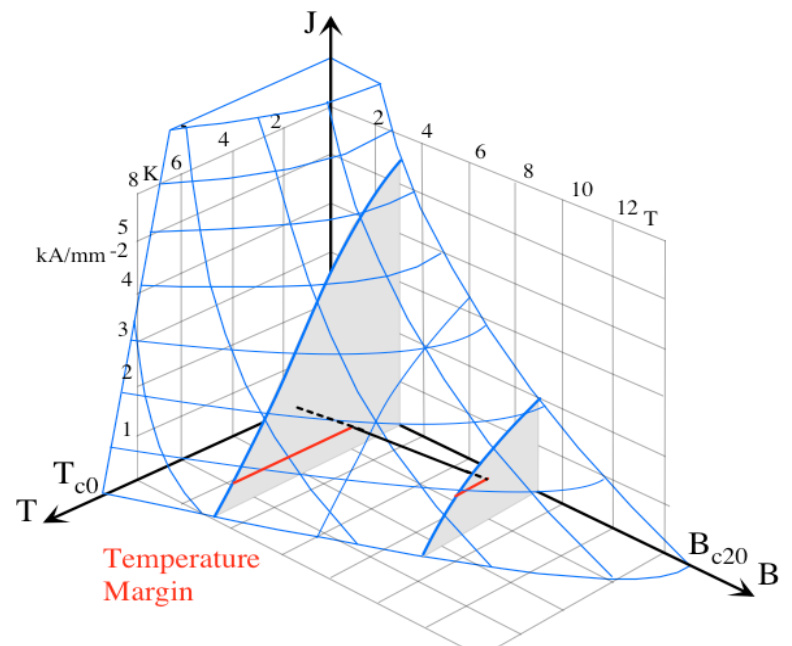
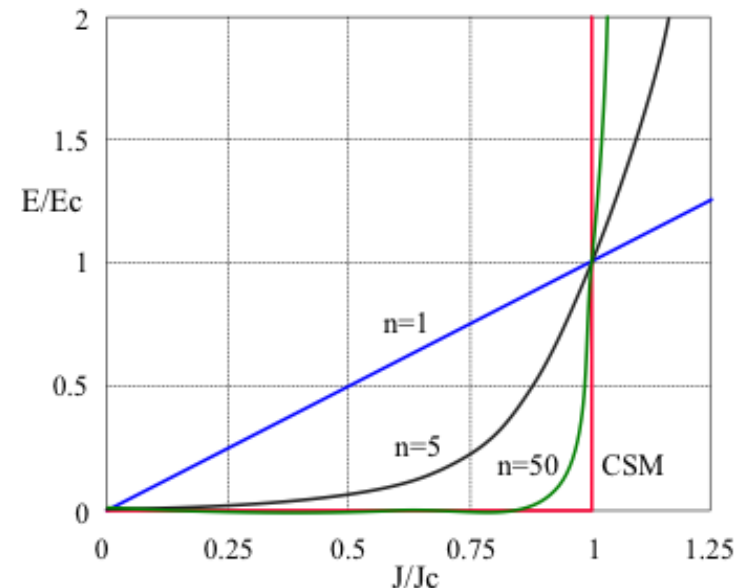
- Magnetic field can penetrate
- Magnetization with hysteresis

→ Critical current density J_c

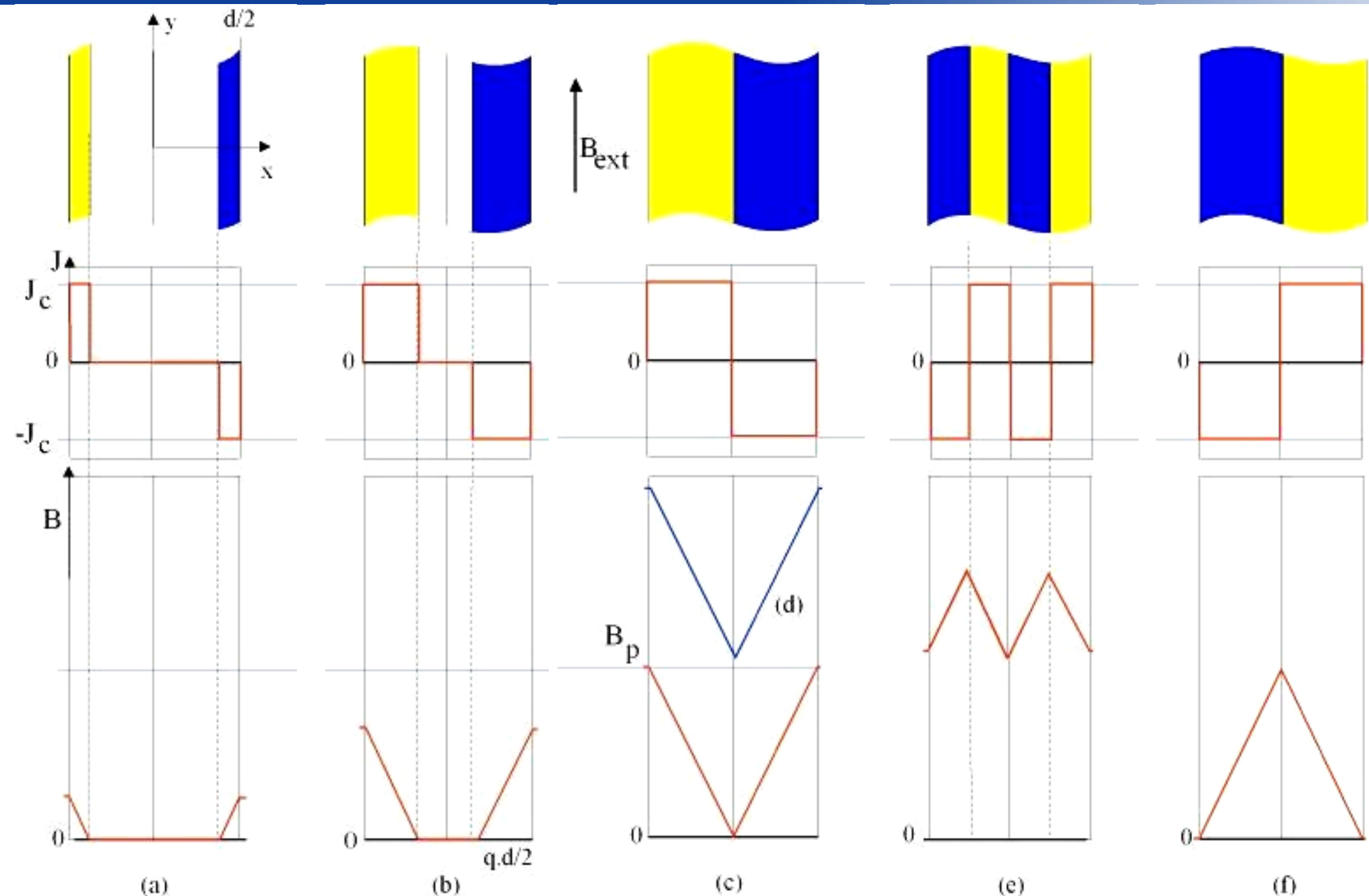
- Current density at spec. electric field ($E_c = 1 \mu\text{V}/\text{cm}$)

→ Critical surface

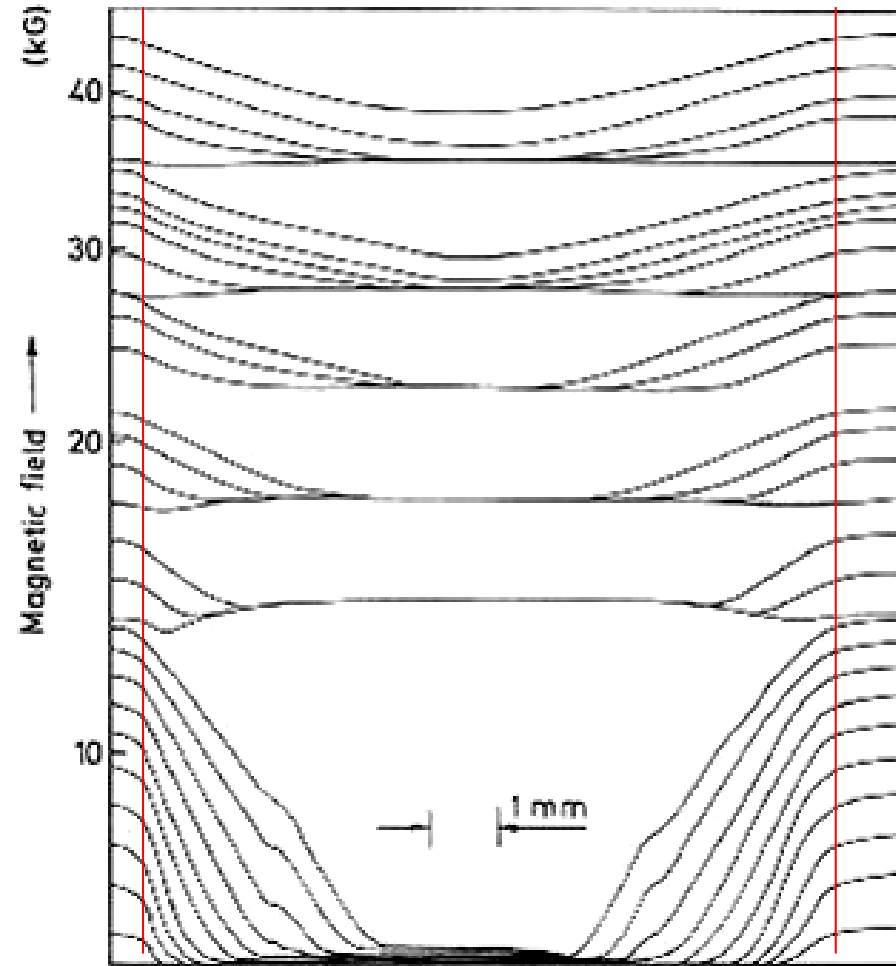
- Dependence of J_c on T and B



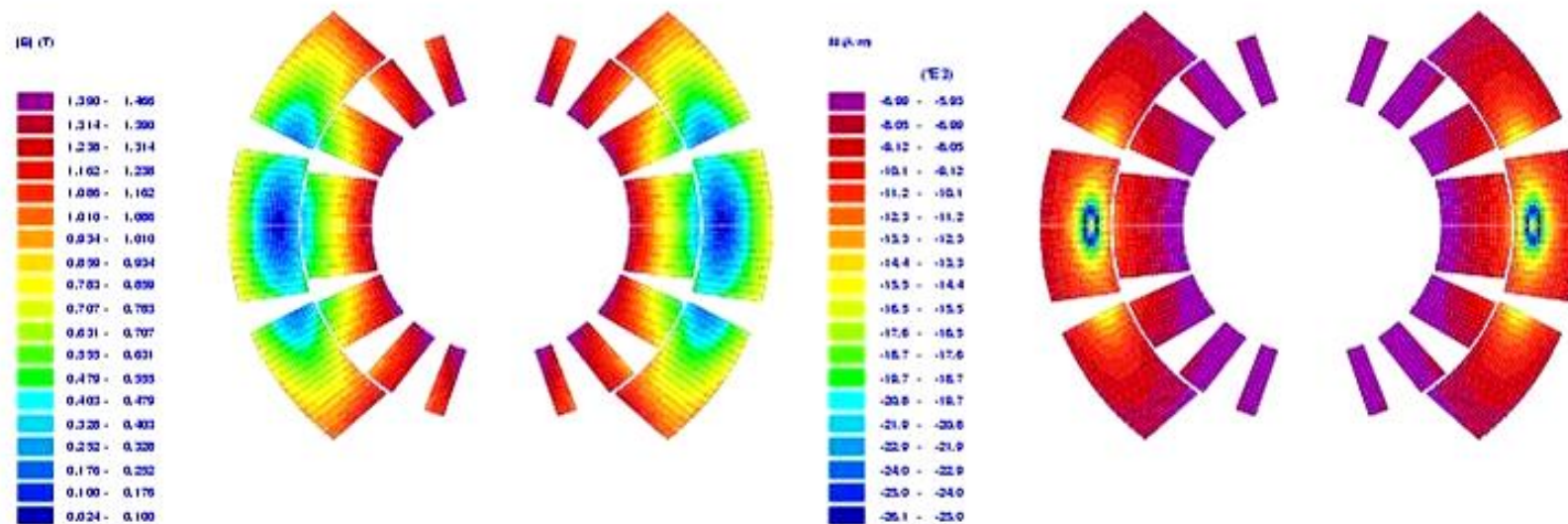
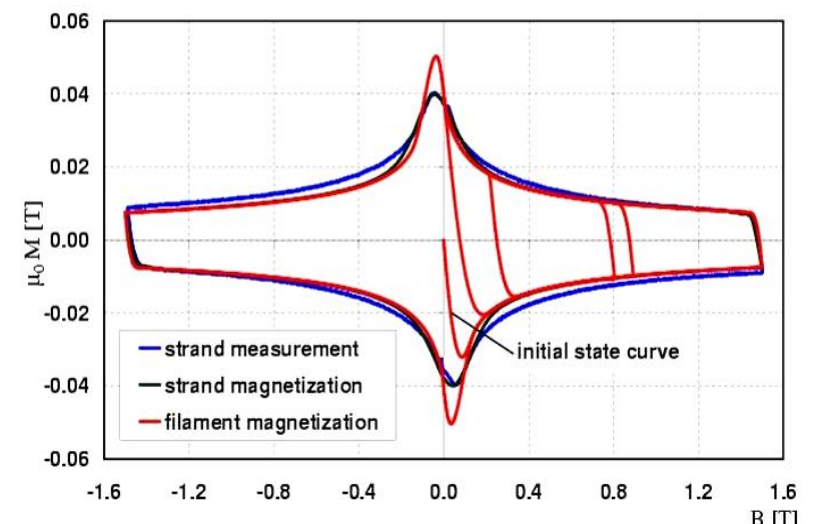
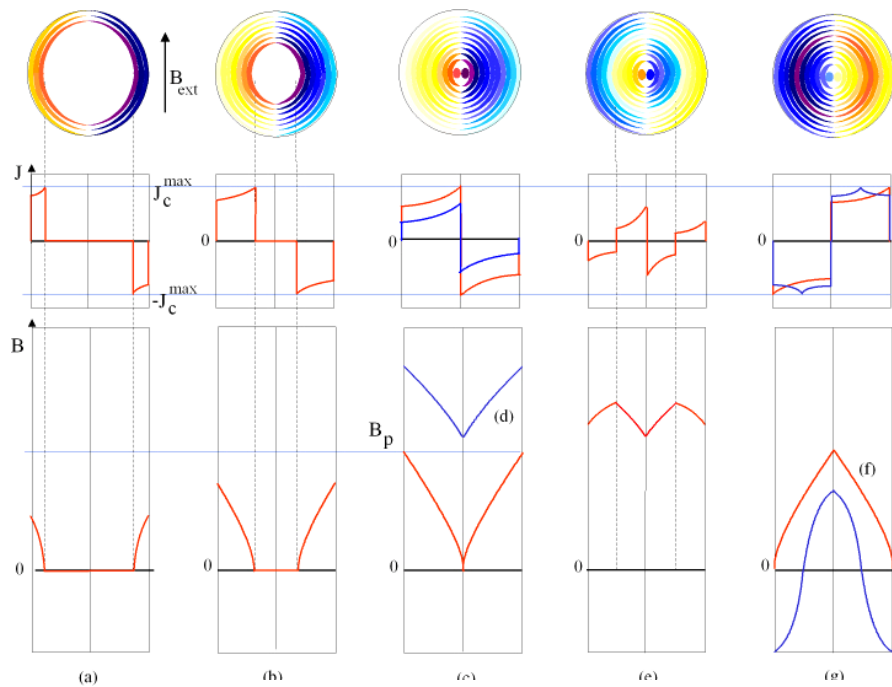
Bean's Critical State Model (CSM)



Screening Field in a Slab



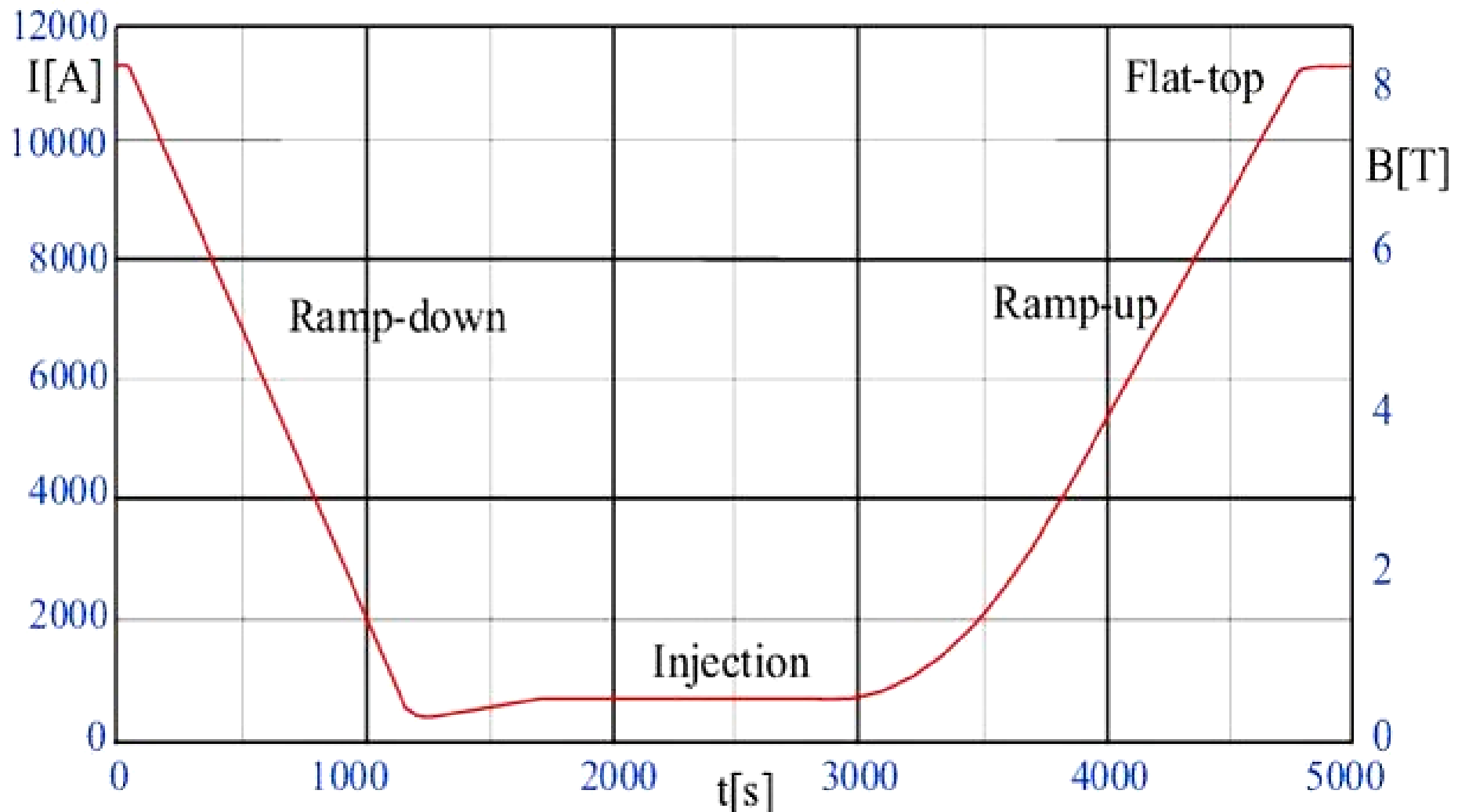
Superconducting Magnetization (Hysteresis Model)



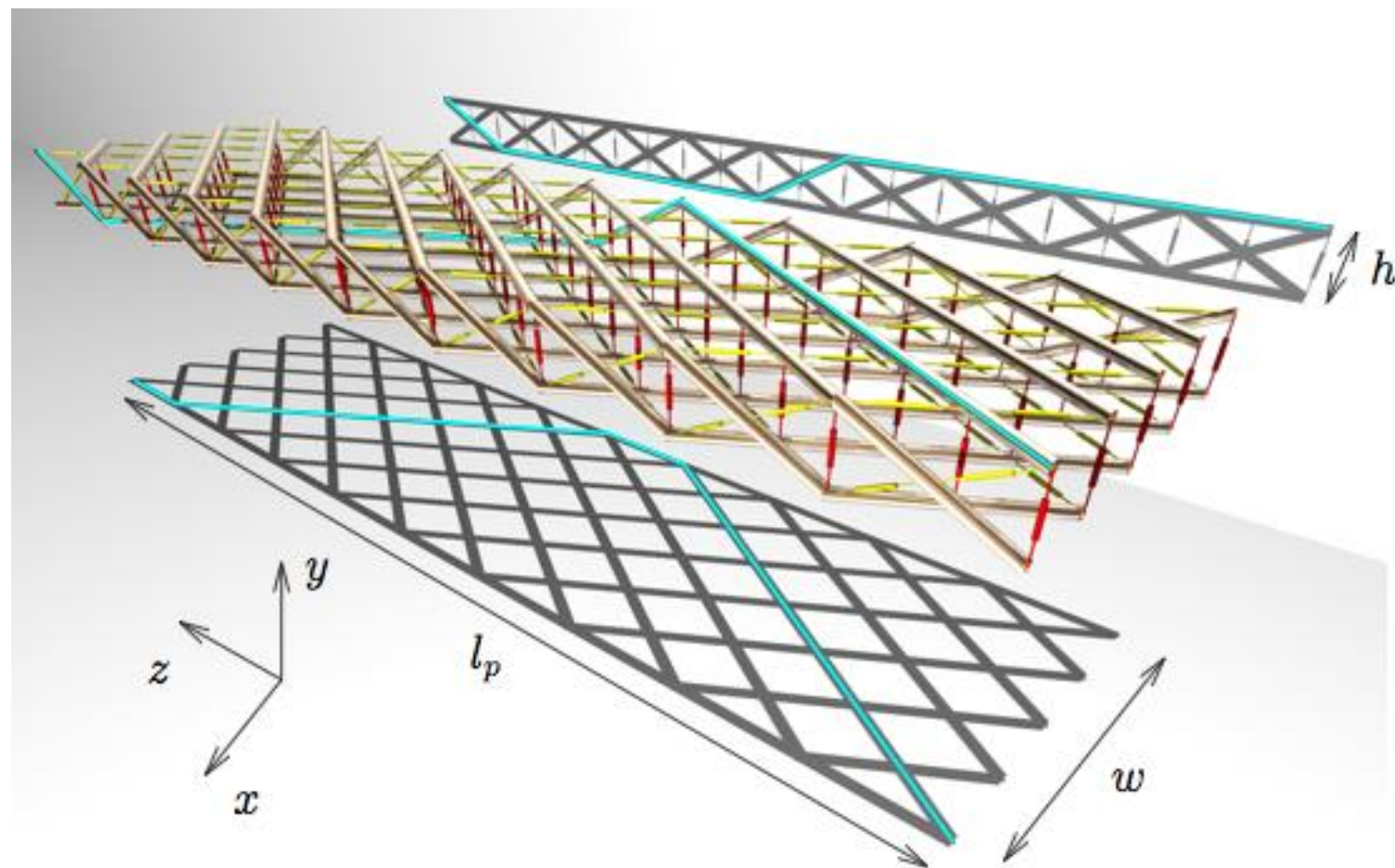
The LHC Excitation Cycle

$$V \approx 2 E / I t$$

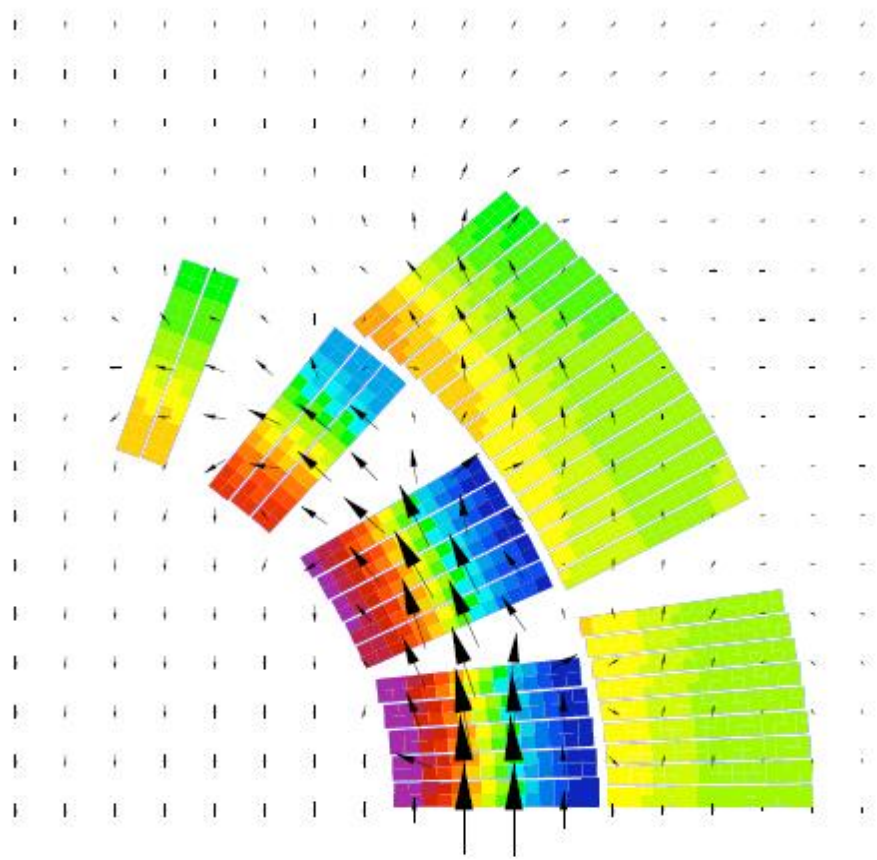
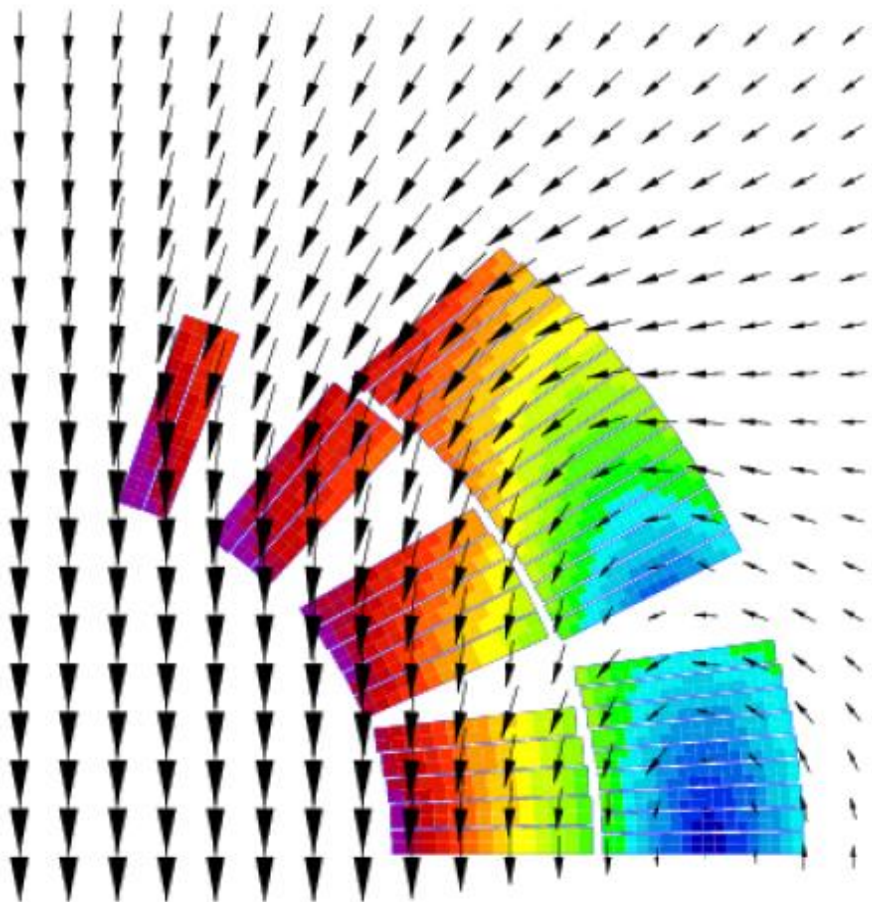
$E = 1.15 \text{ TJ}$ (320 kWh), $I = 11800 \text{ A}$, Ramp rate 10 A/s, 155 V



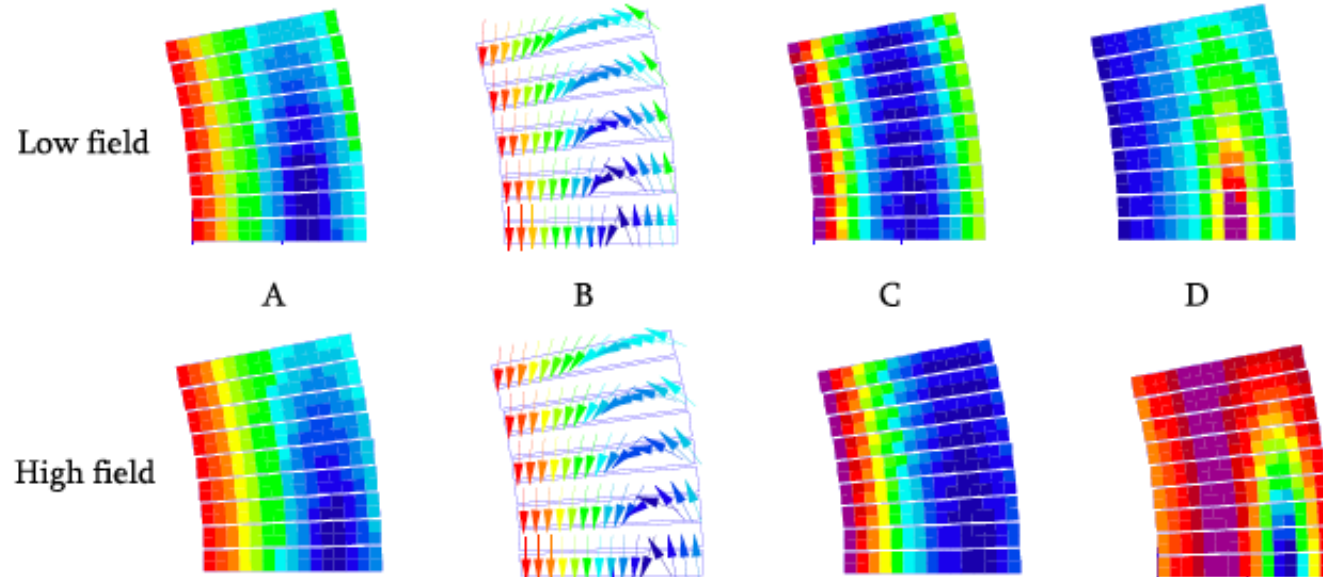
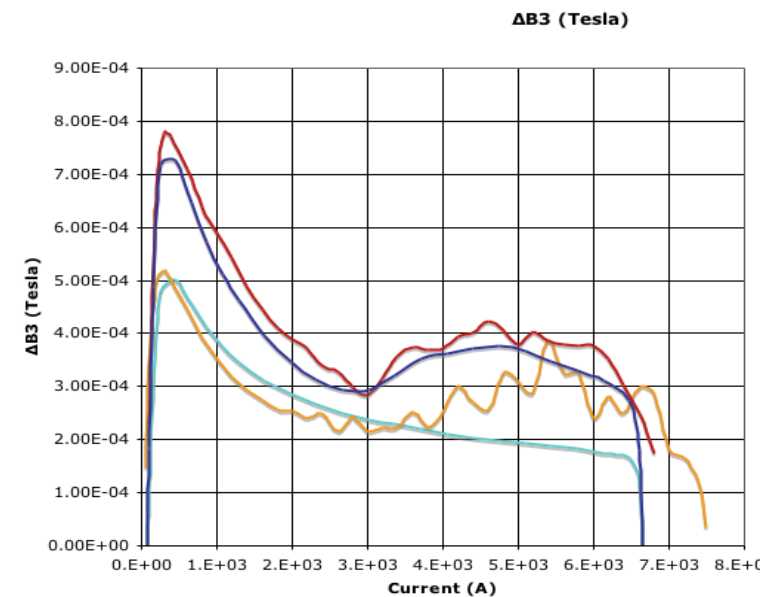
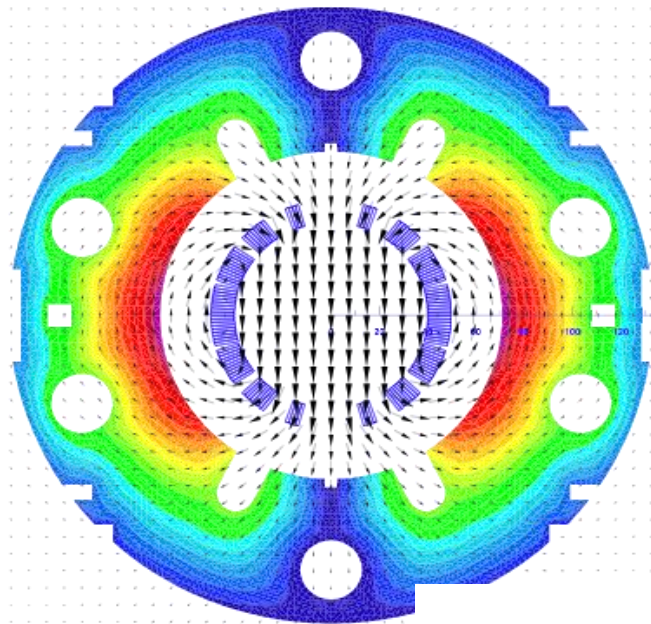
Eddy Currents in Rutherford Cables



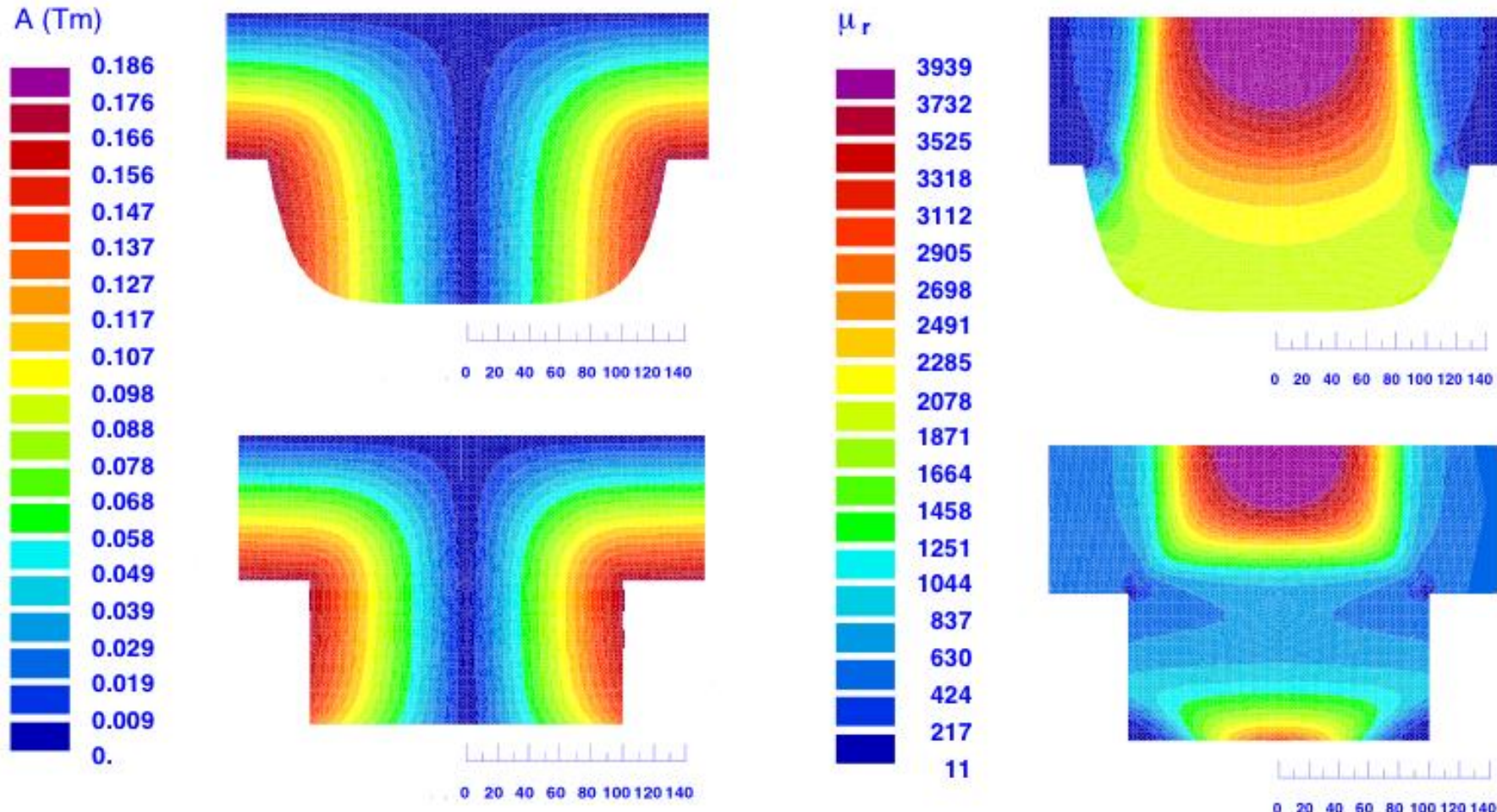
Field Generated by ISCC



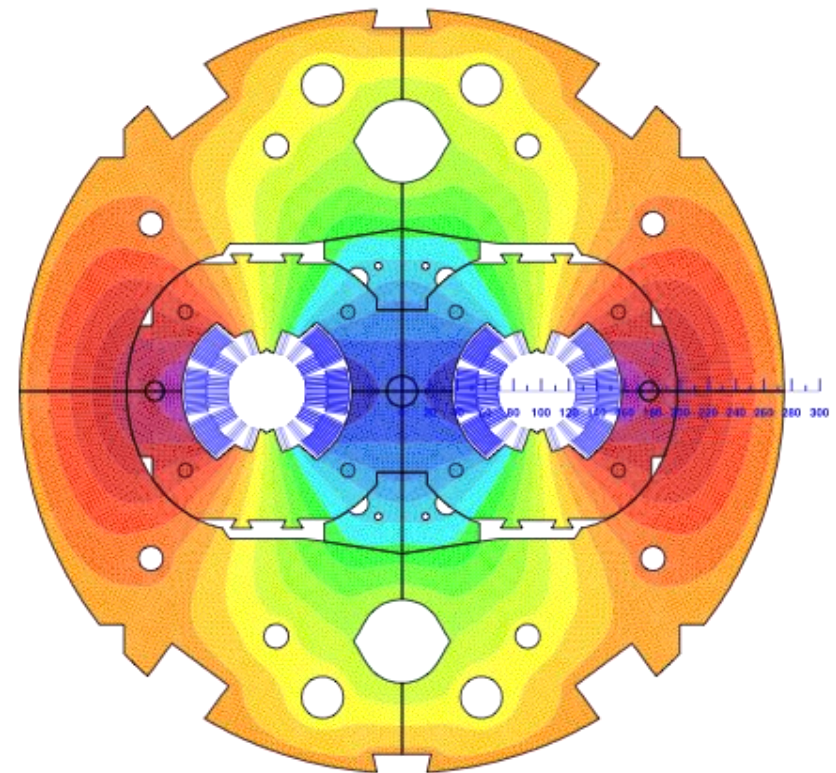
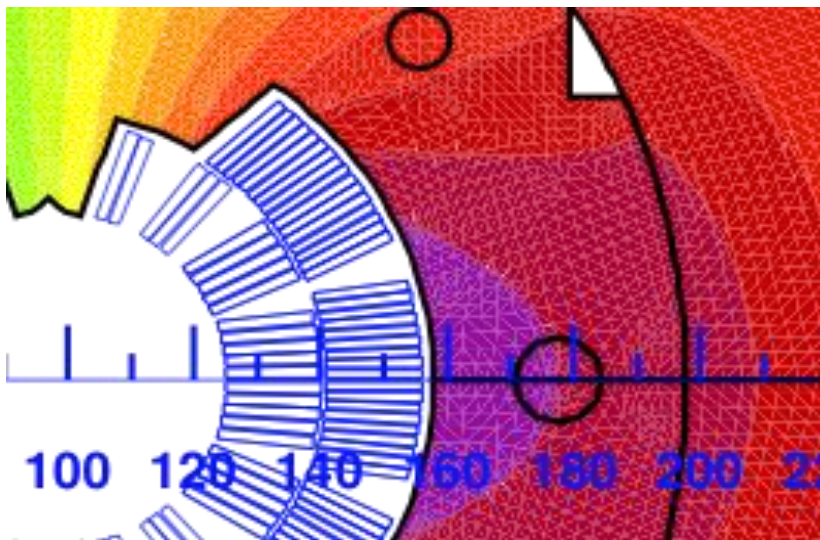
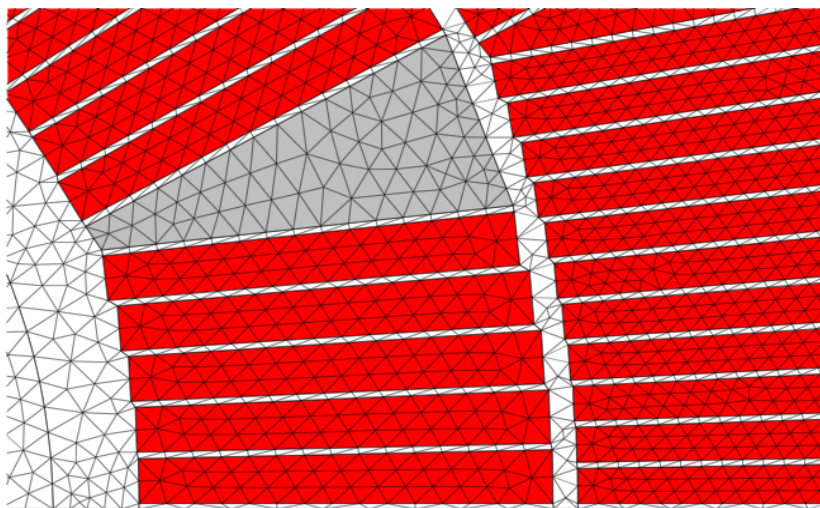
2-D Transient Field Computation for GSI-001



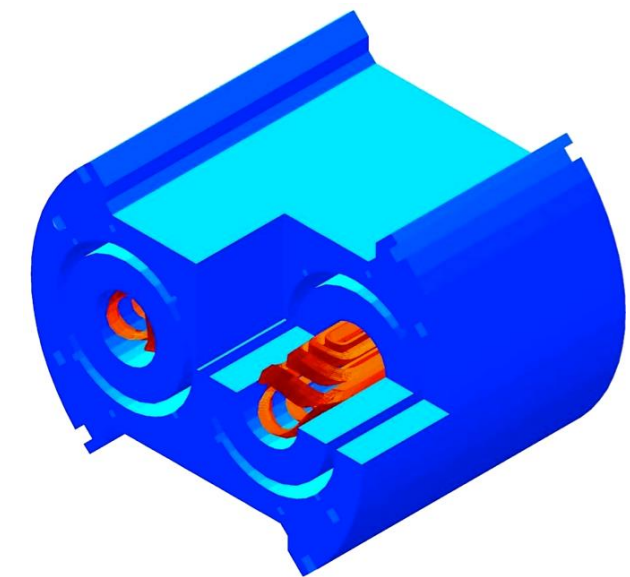
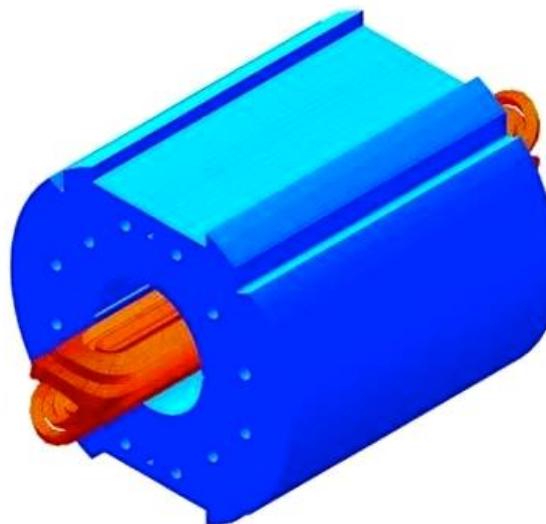
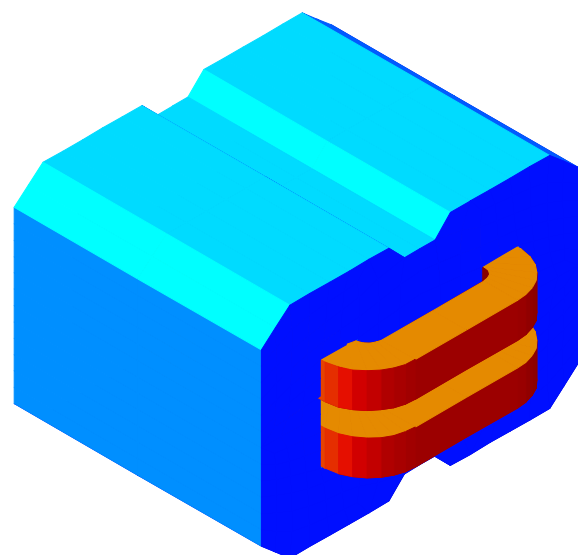
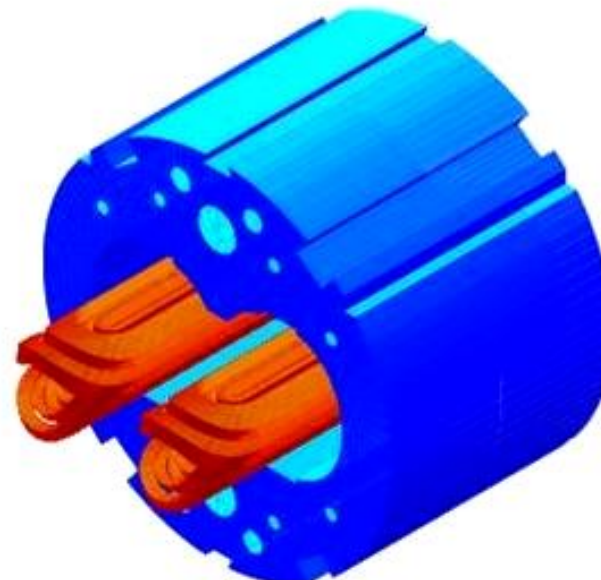
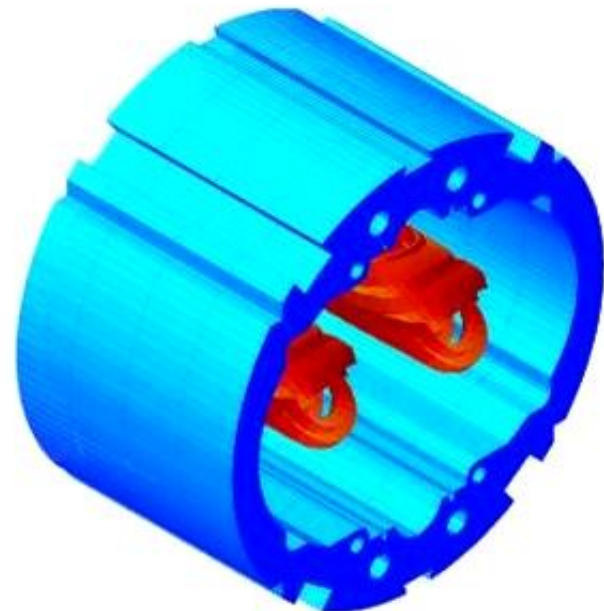
Rogoswki Profiles



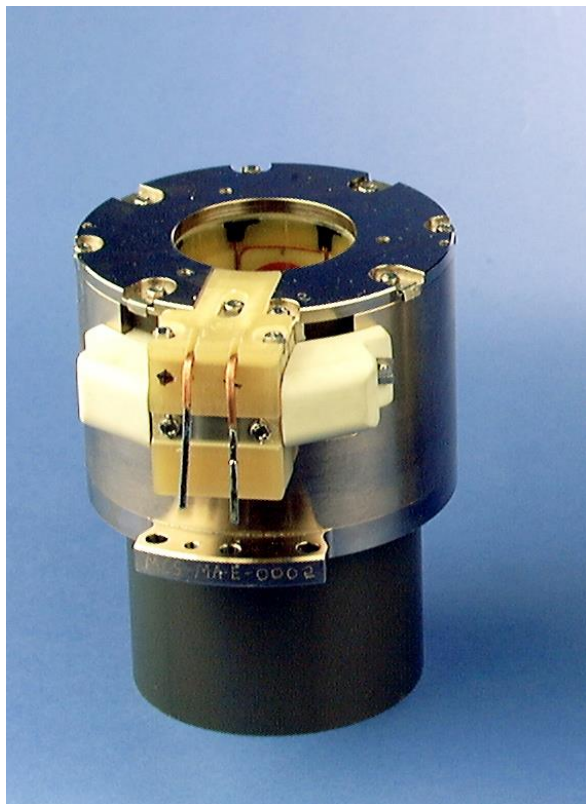
Finite-Element / Boundary-Element Coupling



Magnet Extremities

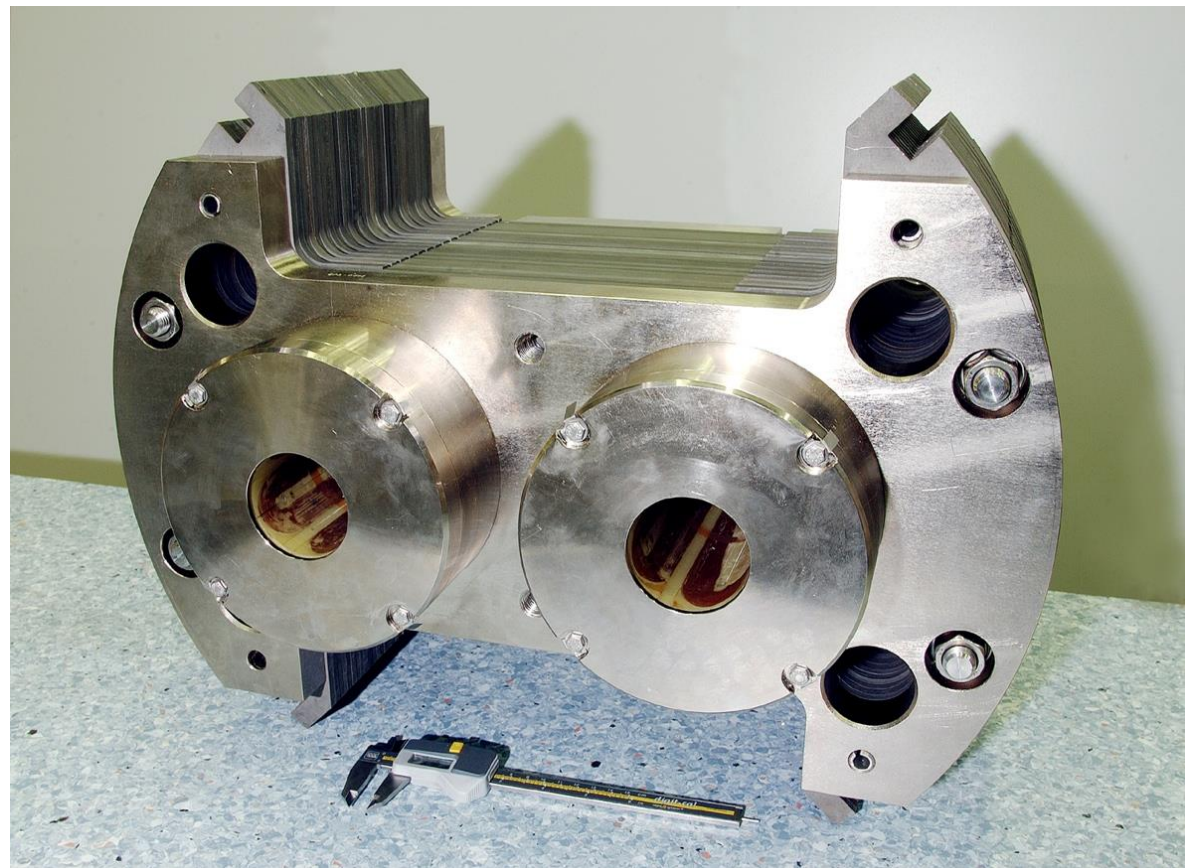


Corrector Magnets

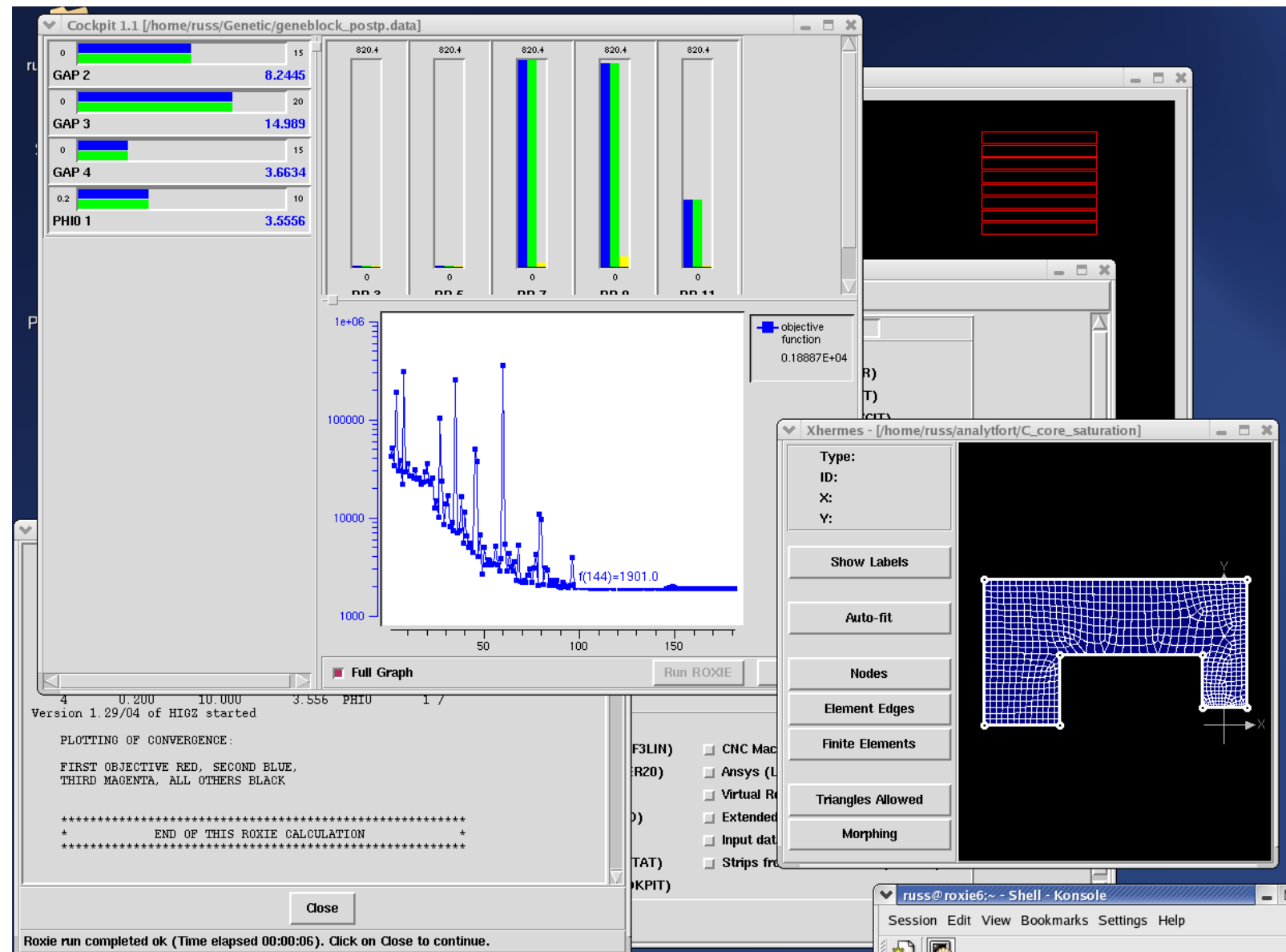


Sextupole-spool pieces

Octupole



The CERN Field Computation Program ROXIE



Objectives for the ROXIE Development

- Automatic generation of coil and yoke geometries
 - Features: Layers, coil-blocks, conductors, strands, holes, keys
- Field computation specially suited for magnet design (Ar, BEM-FEM)
 - No meshing of the coil
 - No artificial boundary conditions
 - Higher order quadrilateral meshes, Parametric mesh generator
 - Modeling of superconductor magnetization
- Mathematical optimization techniques
 - Genetic optimization, Pareto optimization, Search algorithms
- CAD/CAM interfaces
 - Drawings, End-spacer design and manufacture

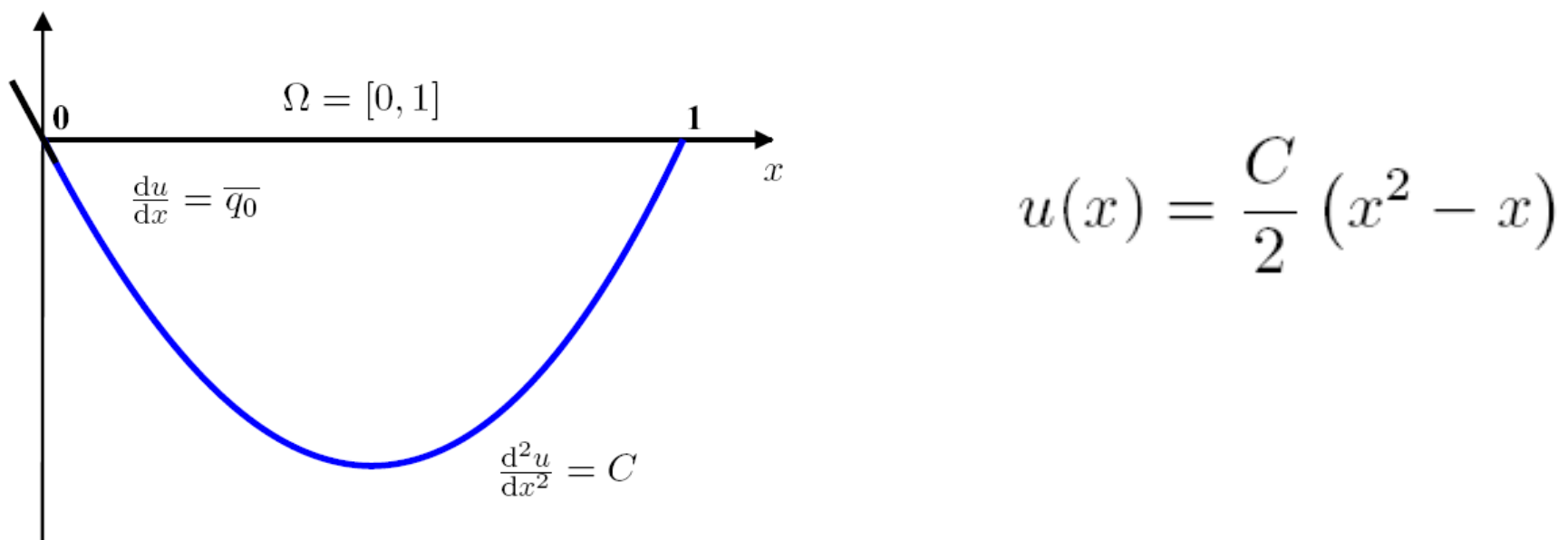


- Feature based geometry modeling
- Conceptual design using genetic optimization
- Minimization of iron saturation effects (BEM-FEM)
- Calculation of superconductor magnetization
- Eddy-currents in Rutherford cables
- Quenchsimulation
- 3D-Coil geometry and yoke optimization
- Sensitivity analysis
- Making of drawings, rapid prototyping
- Inverse field computation

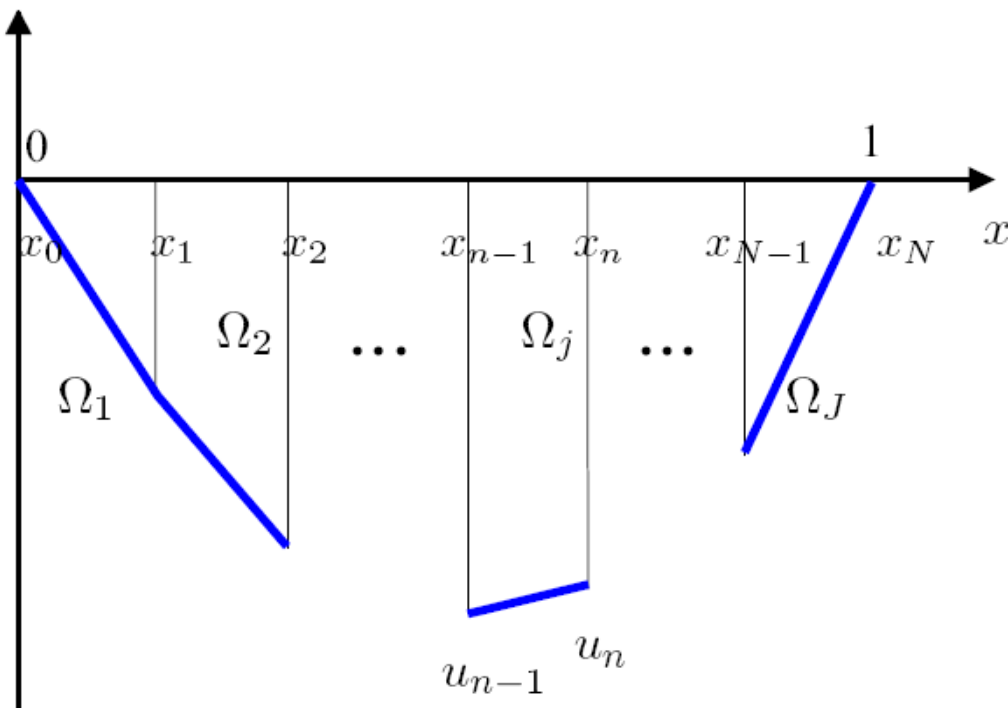
The Model Problem (1-D)

$$\frac{d^2u(x)}{dx^2} = f(x), \quad x \in \Omega$$

$$u(x)|_{x=0} = \bar{u}_0 \quad u(x)|_{x=1} = \bar{u}_1 \quad \text{or} \quad \left. \frac{du}{dx} \right|_{x=1} = \bar{q}_1$$



Shape Functions



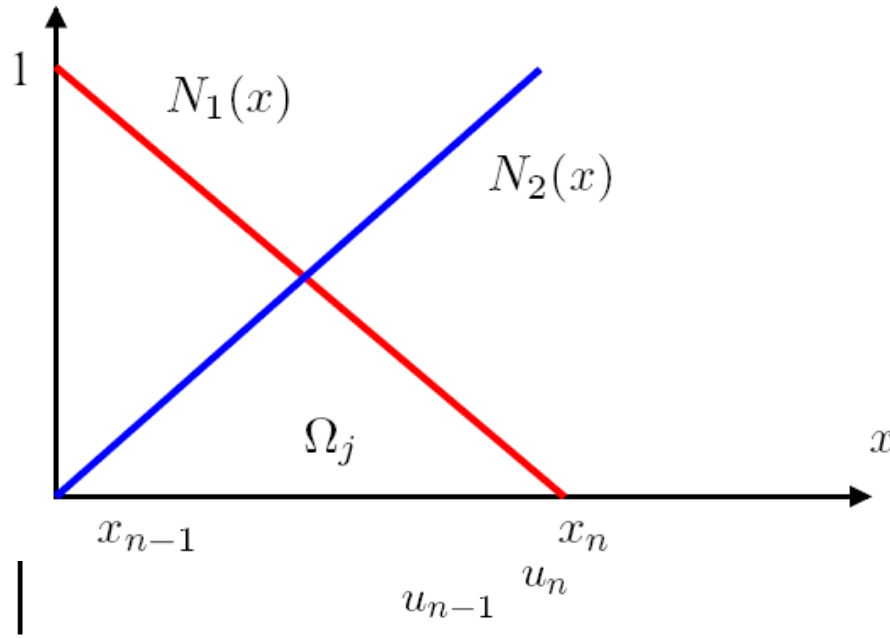
$$\Omega = \bigcup_{j=1}^J \Omega_j$$

$$\Omega_j = [x_{n-1}, x_n]$$

$$u_j(x) = \alpha_{j1} + \alpha_{j2}x \quad x \in \Omega_j$$

$$u_{n-1} = \alpha_{j1} + \alpha_{j2}x_{n-1} \qquad \qquad u_n = \alpha_{j1} + \alpha_{j2}x_n$$

Shape Functions



$$\alpha_{j1} = \frac{\begin{vmatrix} u_{n-1} & x_{n-1} \\ u_n & x_n \end{vmatrix}}{\begin{vmatrix} 1 & x_{n-1} \\ 1 & x_n \end{vmatrix}}$$

Cramer's rule

$$\alpha_{j1} = \frac{x_n u_{n-1} - x_{n-1} u_n}{x_n - x_{n-1}}$$

$$\alpha_{j2} = \frac{u_n - u_{n-1}}{x_n - x_{n-1}}$$

$$u_j(x) = \alpha_{j1} + \alpha_{j2}x = \frac{x_n - x}{x_n - x_{n-1}} u_{n-1} + \frac{-x_{n-1} + x}{x_n - x_{n-1}} u_n$$

What have we won? We can express the field in the element as a function of the node potentials using known polynomials in the spatial coordinates

The Weighted Residual

$$R(x) := \frac{d^2u(x)}{dx^2} - f(x)$$

$$\int_{\Omega} w(x) R(x) d\Omega = \int_{\Omega} w(x) \frac{d^2u(x)}{dx^2} d\Omega - \int_{\Omega} w(x) f(x) d\Omega = 0.$$

$$\int_a^b \phi \psi' dx = [\phi \psi]_a^b - \int_a^b \phi' \psi dx \quad w(x) = \phi \quad \frac{du(x)}{dx} = \psi$$

$$-\int_{\Omega} \frac{dw(x)}{dx} \frac{du(x)}{dx} d\Omega + \left[w(x) \frac{du(x)}{dx} \right]_0^1 - \int_{\Omega} w(x) f(x) d\Omega = 0$$

What have we won? Removal of the second derivative, a way to incorporate Neumann boundary conditions



Galerkin's Method

$$\int_{\Omega} \frac{dw(x)}{dx} \frac{du(x)}{dx} d\Omega = - \int_{\Omega} w(x) f(x) d\Omega$$

$$\int_{\Omega_j} \frac{dw_l(x)}{dx} \sum_{k=1,2} \frac{dN_{jk}(x)}{dx} u^{(k)} d\Omega_j = - \int_{\Omega_j} w_l(x) f(x) d\Omega_j, \quad l = 1, 2.$$

$$\int_{\Omega_j} \frac{dN_{jl}(x)}{dx} \sum_{k=1,2} \frac{dN_{jk}(x)}{dx} u^{(k)} d\Omega_j = - \int_{\Omega_j} N_{jk}(x) f(x) d\Omega_j, \quad l = 1, 2$$

$$\int_{x_{n-1}}^{x_n} \left(\frac{dN_{j1}}{dx} \frac{dN_{j1}}{dx} u_{n-1} + \frac{dN_{j1}}{dx} \frac{dN_{j2}}{dx} u_n \right) dx = - \int_{x_{n-1}}^{x_n} N_{j1} f(x) dx$$

$$\int_{x_{n-1}}^{x_n} \left(\frac{dN_{j2}}{dx} \frac{dN_{j1}}{dx} u_{n-1} + \frac{dN_{j2}}{dx} \frac{dN_{j2}}{dx} u_n \right) dx = - \int_{x_{n-1}}^{x_n} N_{j2} f(x) dx$$

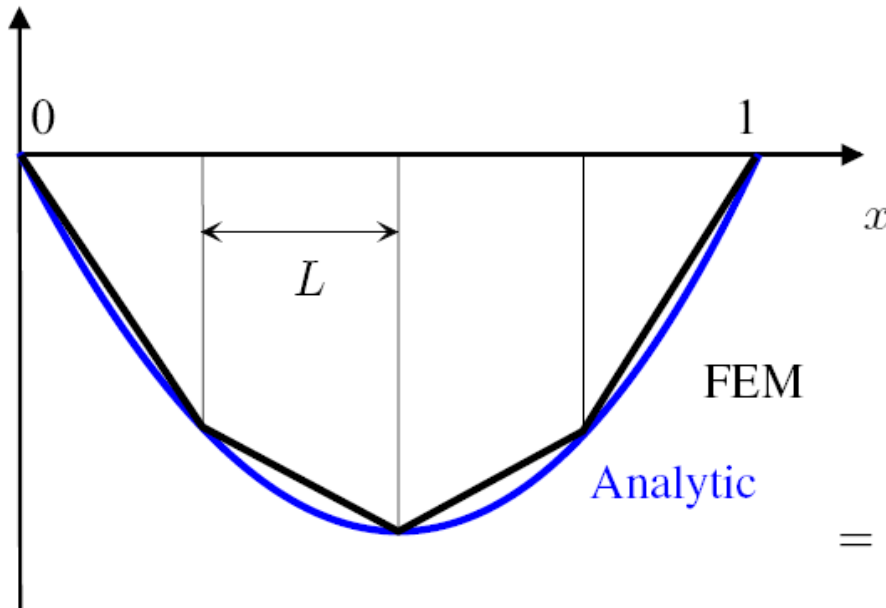
$$[k_j] \{u_j\} = \{f_j\}$$

Linear equation system for the node potentials



Numerical Example

4 finite elements $\Omega_j, j = 1, \dots, 4$ of equidistant length L



$$[k_j] = \int_{x_{n-1}}^{x_n} \begin{pmatrix} \frac{dN_{j1}}{dx} \frac{dN_{j1}}{dx} & \frac{dN_{j1}}{dx} \frac{dN_{j2}}{dx} \\ \frac{dN_{j2}}{dx} \frac{dN_{j1}}{dx} & \frac{dN_{j2}}{dx} \frac{dN_{j2}}{dx} \end{pmatrix} dx$$

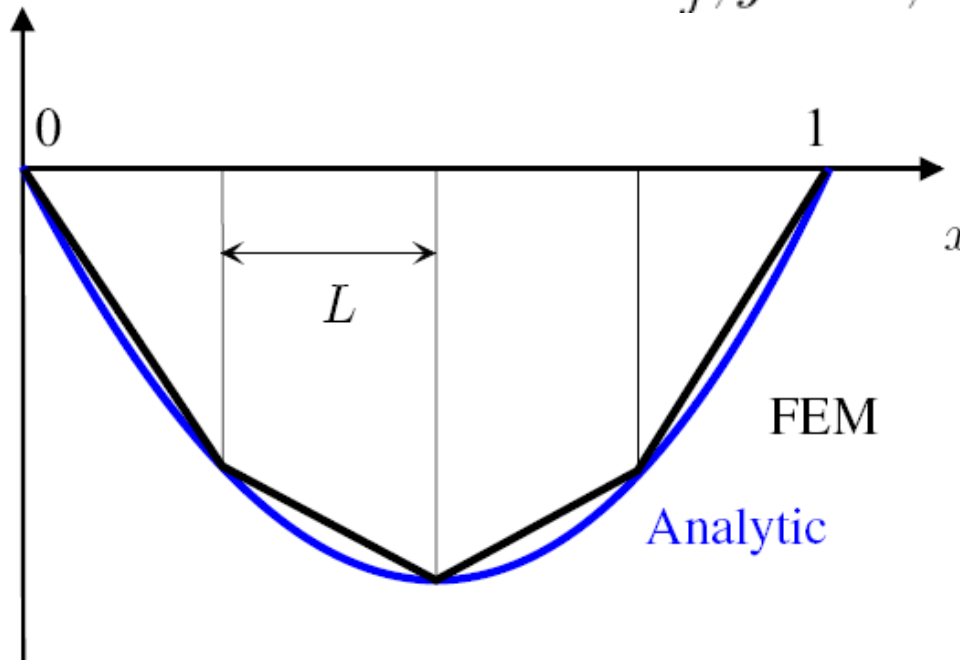
$$= \int_{x_{n-1}}^{x_n} \begin{pmatrix} \frac{1}{(x_n - x_{n-1})^2} & \frac{-1}{(x_n - x_{n-1})^2} \\ \frac{-1}{(x_n - x_{n-1})^2} & \frac{1}{(x_n - x_{n-1})^2} \end{pmatrix} dx = \begin{pmatrix} \frac{1}{L} & \frac{-1}{L} \\ \frac{-1}{L} & \frac{1}{L} \end{pmatrix}$$

$$\{f_j\} = - \int_{x_{n-1}}^{x_n} \begin{pmatrix} N_{j1} \\ N_{j2} \end{pmatrix} C dx = -C \int_{x_{n-1}}^{x_n} \begin{pmatrix} \frac{x_n - x}{x_n - x_{n-1}} \\ \frac{-x_{n-1} + x}{x_n - x_{n-1}} \end{pmatrix} dx$$

$$= -\frac{C}{2L} \begin{pmatrix} 2x_n x - x^2 \\ -2x_{n-1} x + x^2 \end{pmatrix} \Big|_{x_{n-1}}^{x_n} = -\frac{C}{2L} \begin{pmatrix} (x_n - x_{n-1})^2 \\ (x_{n-1} - x_n)^2 \end{pmatrix} = -\begin{pmatrix} 0.5 CL \\ 0.5 CL \end{pmatrix}$$

Numerical Example

4 finite elements $\Omega_j, j = 1, \dots, 4$ of equidistant length L



$$\begin{pmatrix} \frac{1}{L} & -\frac{1}{L} & 0 & 0 & 0 \\ \frac{1}{L} & \frac{2}{L} & -\frac{1}{L} & 0 & 0 \\ 0 & -\frac{1}{L} & \frac{2}{L} & -\frac{1}{L} & 0 \\ 0 & 0 & -\frac{1}{L} & \frac{2}{L} & -\frac{1}{L} \\ 0 & 0 & 0 & -\frac{1}{L} & \frac{1}{L} \end{pmatrix} \begin{pmatrix} u_1 \\ u_2 \\ u_3 \\ u_4 \\ u_5 \end{pmatrix} = - \begin{pmatrix} 0.5CL \\ CL \\ CL \\ CL \\ 0.5CL \end{pmatrix}$$

Essential boundary conditions (Dirichlet)

$$\begin{pmatrix} \frac{2}{L} & -\frac{1}{L} & 0 \\ -\frac{1}{L} & \frac{2}{L} & -\frac{1}{L} \\ 0 & -\frac{1}{L} & \frac{2}{L} \end{pmatrix} \begin{pmatrix} u_2 \\ u_3 \\ u_4 \end{pmatrix} = - \begin{pmatrix} CL \\ CL \\ CL \end{pmatrix}$$

$$\begin{pmatrix} u_2 \\ u_3 \\ u_4 \end{pmatrix} = - \begin{pmatrix} \frac{3L}{4} & \frac{L}{2} & \frac{L}{4} \\ \frac{L}{2} & L & \frac{L}{2} \\ \frac{L}{4} & \frac{L}{2} & \frac{2L}{4} \end{pmatrix} \begin{pmatrix} CL \\ CL \\ CL \end{pmatrix} = \begin{pmatrix} -0.375 \\ -0.5 \\ -0.375 \end{pmatrix}$$

Higher order elements

$$u^{(1)} = \alpha_{j1} + \alpha_{j2}x_1 + \alpha_{j3}x_1^2$$

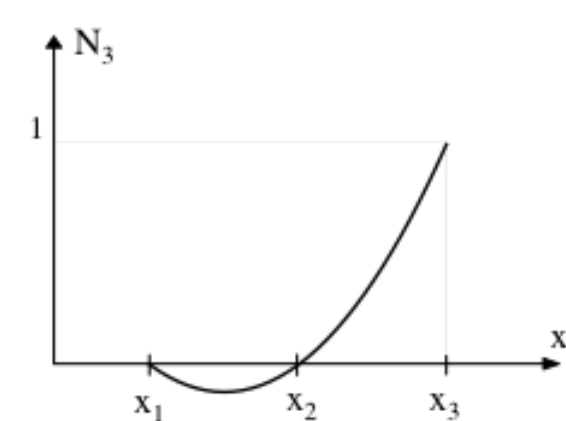
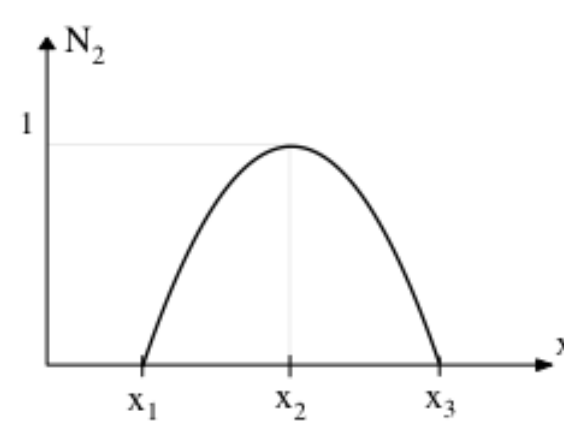
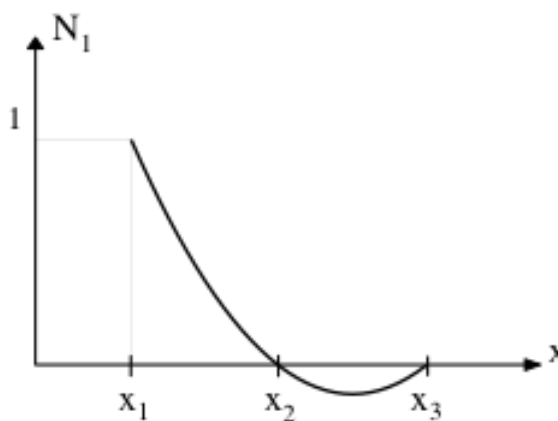
$$u^{(2)} = \alpha_{j1} + \alpha_{j2}x_2 + \alpha_{j3}x_2^2$$

$$u^{(3)} = \alpha_{j1} + \alpha_{j2}x_3 + \alpha_{j3}x_3^2$$

$$u_j(x) = \sum_{k=1}^3 N_{jk}(x) u^{(k)}$$

$$N_{j1}(x) = \frac{(x - x_2)(x - x_3)}{(x_1 - x_2)(x_1 - x_3)},$$

$$N_{j2}(x) = \frac{(x - x_1)(x - x_3)}{(x_2 - x_1)(x_2 - x_3)}$$



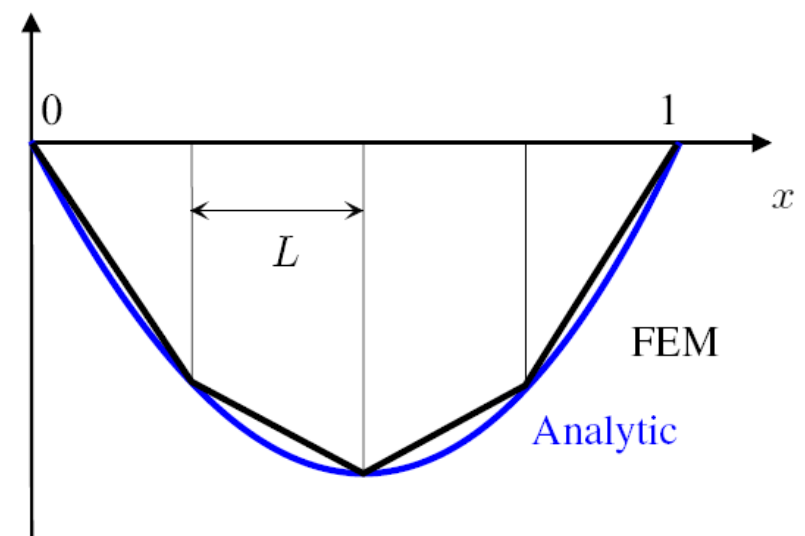
Two Quadratic Elements ($l = 2 L$)

$$[k_j] = \begin{pmatrix} \frac{7}{6l} & \frac{-8}{6l} & \frac{1}{6l} \\ \frac{-8}{6l} & \frac{16}{6l} & \frac{-8}{6l} \\ \frac{1}{6l} & \frac{-8}{6l} & \frac{7}{6l} \end{pmatrix}$$

$$\{f_j\} = -\frac{1}{3}c \begin{pmatrix} l \\ 4l \\ l \end{pmatrix}$$

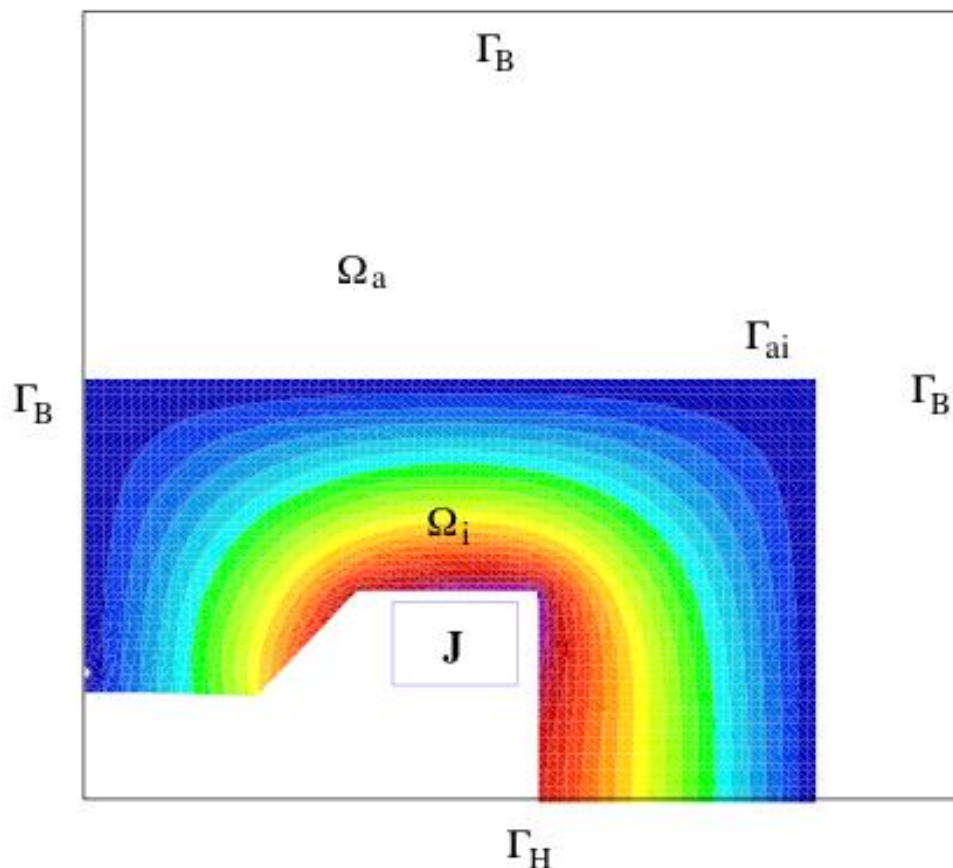
$$\begin{pmatrix} \frac{2}{l} & \frac{-1}{l} & 0 \\ \frac{-1}{l} & \frac{2}{l} & \frac{-1}{l} \\ 0 & \frac{-1}{l} & \frac{2}{l} \end{pmatrix} \begin{pmatrix} u_2 \\ u_3 \\ u_4 \end{pmatrix} = - \begin{pmatrix} cl \\ cl \\ cl \end{pmatrix}$$

$$\begin{pmatrix} u_2 \\ u_3 \\ u_4 \end{pmatrix} = - \begin{pmatrix} \frac{3l}{4} & \frac{l}{2} & \frac{l}{4} \\ \frac{l}{2} & l & \frac{l}{2} \\ \frac{l}{4} & \frac{l}{2} & \frac{3l}{4} \end{pmatrix} \begin{pmatrix} cl \\ cl \\ cl \end{pmatrix} = \begin{pmatrix} -0.375 \\ -0.5 \\ -0.375 \end{pmatrix}$$



Weak Form in the FEM Problem

$$\operatorname{curl} \frac{1}{\mu} \operatorname{curl} \mathbf{A} - \operatorname{grad} \frac{1}{\mu} \operatorname{div} \mathbf{A} = \mathbf{J} \quad \text{in } \Omega$$



$$\begin{aligned}\mathbf{A} \cdot \mathbf{n} &= 0 && \text{on } \Gamma_H, \\ \frac{1}{\mu} \operatorname{div} \mathbf{A} &= 0 && \text{on } \Gamma_B, \\ \mathbf{n} \times (\mathbf{A} \times \mathbf{n}) &= \mathbf{0} && \text{on } \Gamma_B, \\ \mathbf{n} \times \left(\frac{1}{\mu} (\operatorname{curl} \mathbf{A}) \times \mathbf{n} \right) &= \mathbf{0} && \text{on } \Gamma_H, \\ \left[\frac{1}{\mu} \operatorname{div} \mathbf{A} \right]_{ai} &= 0 && \text{on } \Gamma_{ai}, \\ \left[\frac{1}{\mu} (\operatorname{curl} \mathbf{A}) \times \mathbf{n} \right]_{ai} &= \mathbf{0} && \text{on } \Gamma_{ai}, \\ [\mathbf{A}]_{ai} &= \mathbf{0} && \text{on } \Gamma_{ai}. \end{aligned}$$

Weak Form in the FEM Problem

$$\operatorname{curl} \frac{1}{\mu} \operatorname{curl} \mathbf{A} - \operatorname{grad} \frac{1}{\mu} \operatorname{div} \mathbf{A} = \mathbf{J} \quad \text{in } \Omega$$

$$\operatorname{curl} \frac{1}{\mu} \operatorname{curl} \mathbf{A} - \operatorname{grad} \frac{1}{\mu} \operatorname{div} \mathbf{A} - \mathbf{J} = \mathbf{R}$$

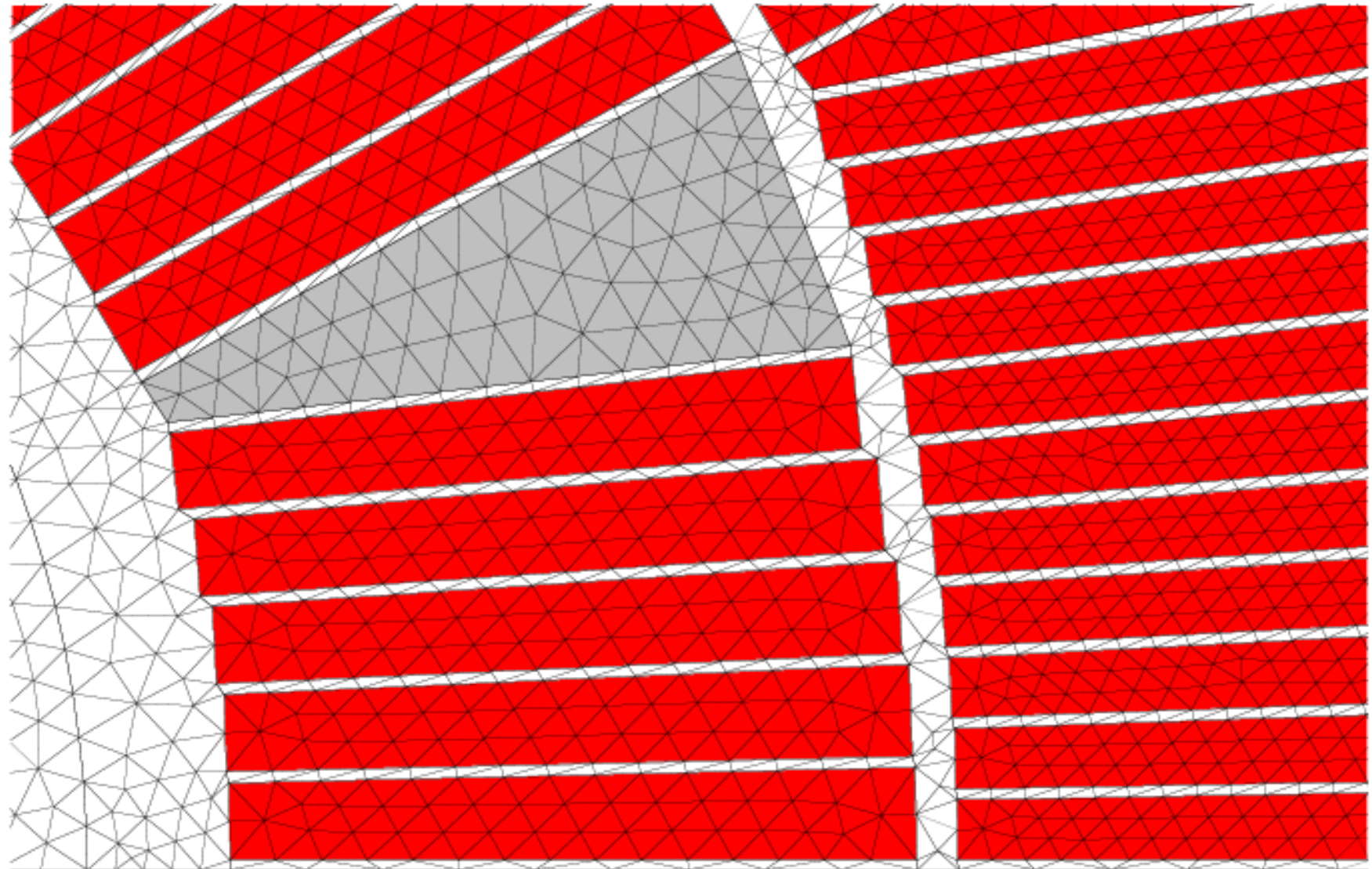
$$\int_{\Omega} \mathbf{w}_a \cdot \left(\operatorname{curl} \frac{1}{\mu} \operatorname{curl} \mathbf{A} - \operatorname{grad} \frac{1}{\mu} \operatorname{div} \mathbf{A} \right) d\Omega = \int_{\Omega} \mathbf{w}_a \cdot \mathbf{J} d\Omega, \quad a = 1, 2, 3.$$

Integration by parts

$$\int_{\Omega} \frac{1}{\mu} \operatorname{curl} \mathbf{w}_a \cdot \operatorname{curl} \mathbf{A} d\Omega + \int_{\Omega} \frac{1}{\mu} \operatorname{div} \mathbf{w}_a \operatorname{div} \mathbf{A} d\Omega = \int_{\Omega} \mathbf{w}_a \cdot \mathbf{J} d\Omega$$

Conclusion: 3-D is more complicated than addition just one dimension in space; it's a different mathematics, and thus often a separate software package

Meshering the Coil

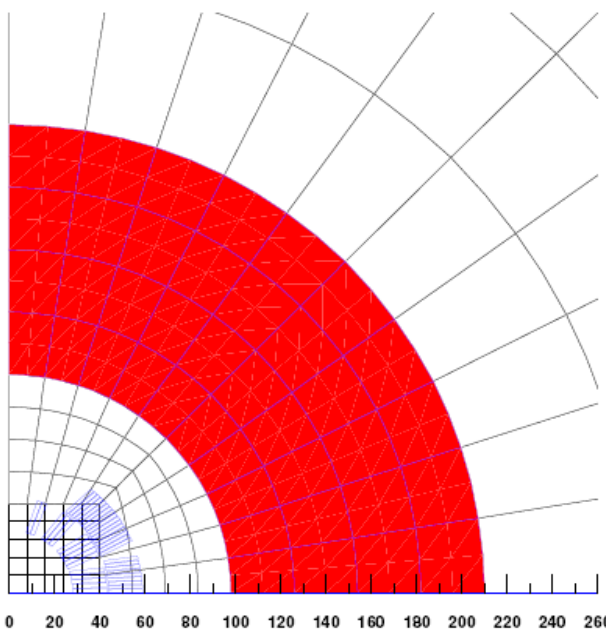


Reduced Vector Potential Formulation

$$\mathbf{A} = \mathbf{A}_s + \mathbf{A}_r$$

$$\mathbf{B} = \mu_0 \mathbf{H}_s + \operatorname{curl} \mathbf{A}_r$$

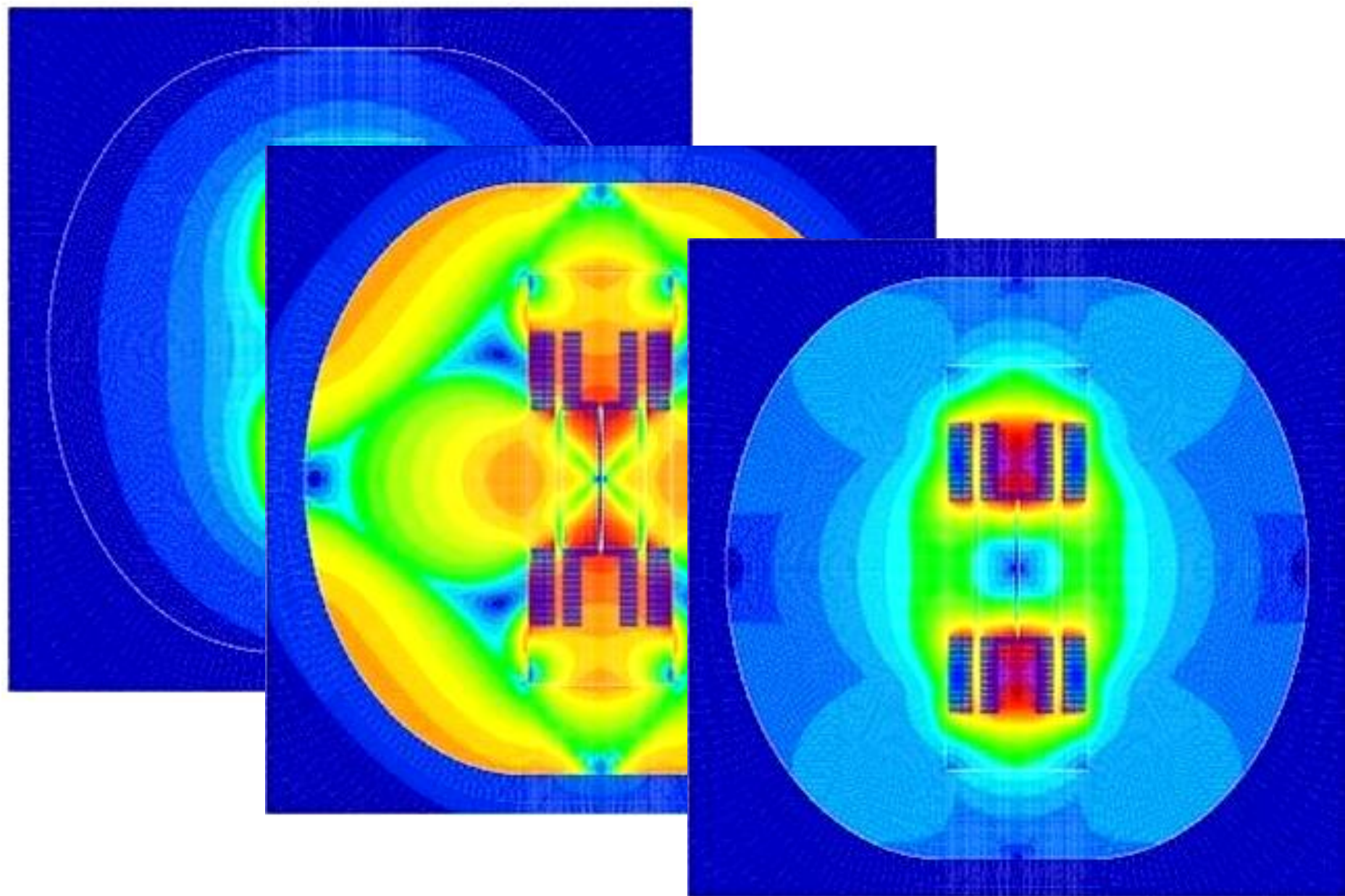
$$\operatorname{curl} \frac{1}{\mu} \operatorname{curl} (\mathbf{A}_r + \mathbf{A}_s) - \operatorname{grad} \frac{1}{\mu} \operatorname{div} (\mathbf{A}_r + \mathbf{A}_s) = \mathbf{J}$$



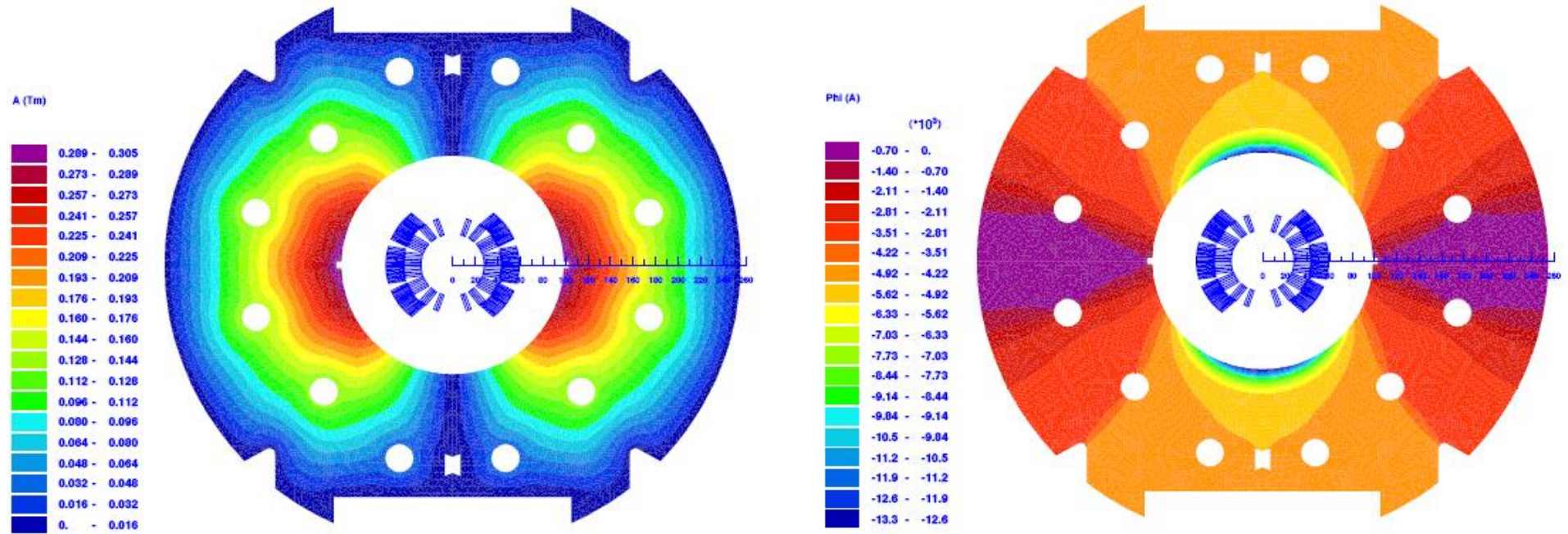
$$\begin{aligned}\operatorname{curl} \frac{1}{\mu} \operatorname{curl} \mathbf{A}_r - \operatorname{grad} \frac{1}{\mu} \operatorname{div} \mathbf{A}_r &= \mathbf{J} - \operatorname{curl} \frac{1}{\mu} \operatorname{curl} \mathbf{A}_s \\ &= \operatorname{curl} \mathbf{H}_s - \operatorname{curl} \frac{\mu_0}{\mu} \mathbf{H}_s \\ &= \operatorname{curl} \left(\mathbf{H}_s - \frac{\mu_0}{\mu} \mathbf{H}_s \right)\end{aligned}$$

Advantages: No meshing of the coil, no cancellation errors, distinction between source field and iron magnetization

Source, Reduced, Total Field

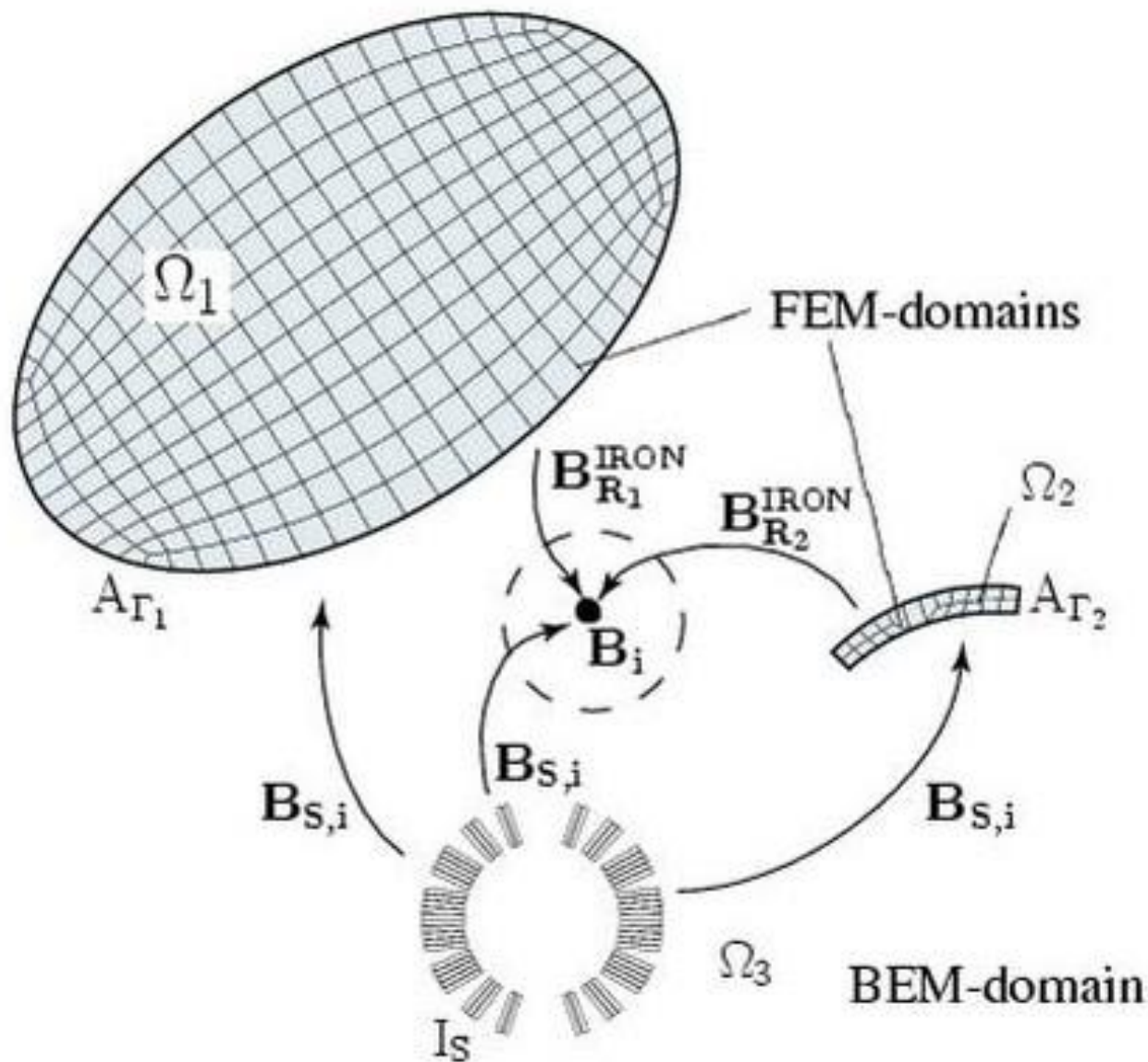


Vector Potential and Total Scalar Potential

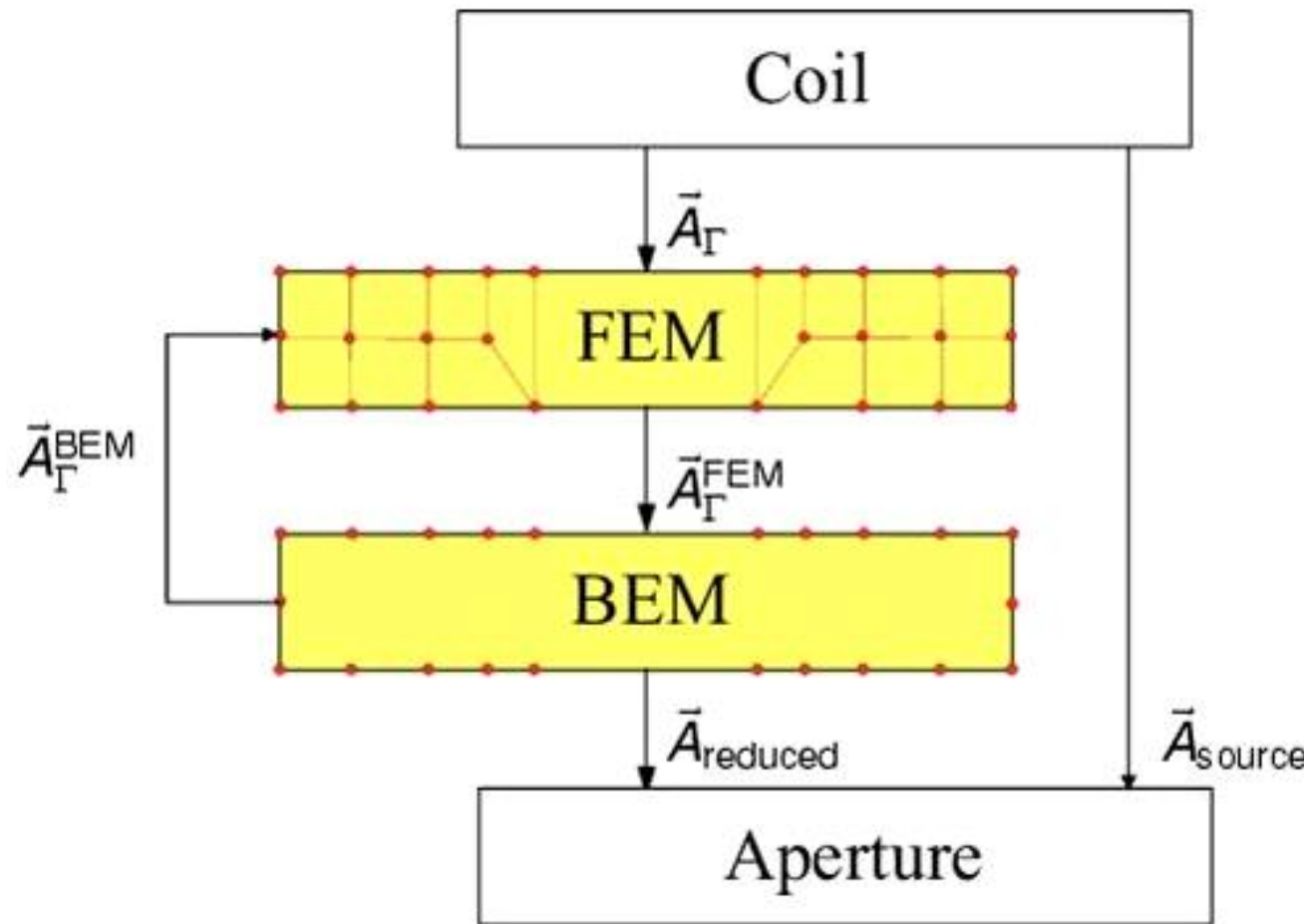


Number of finite elements	60	178	449	787	2799	6233
Total scalar potential	65.8	72.1	13.0	5.0	3.8	15.7
Vector potential	-40.5	-27.4	-7.4	-4.8	-3.8	25.0

BEM-FEM Coupling (Elementary Model Problem)

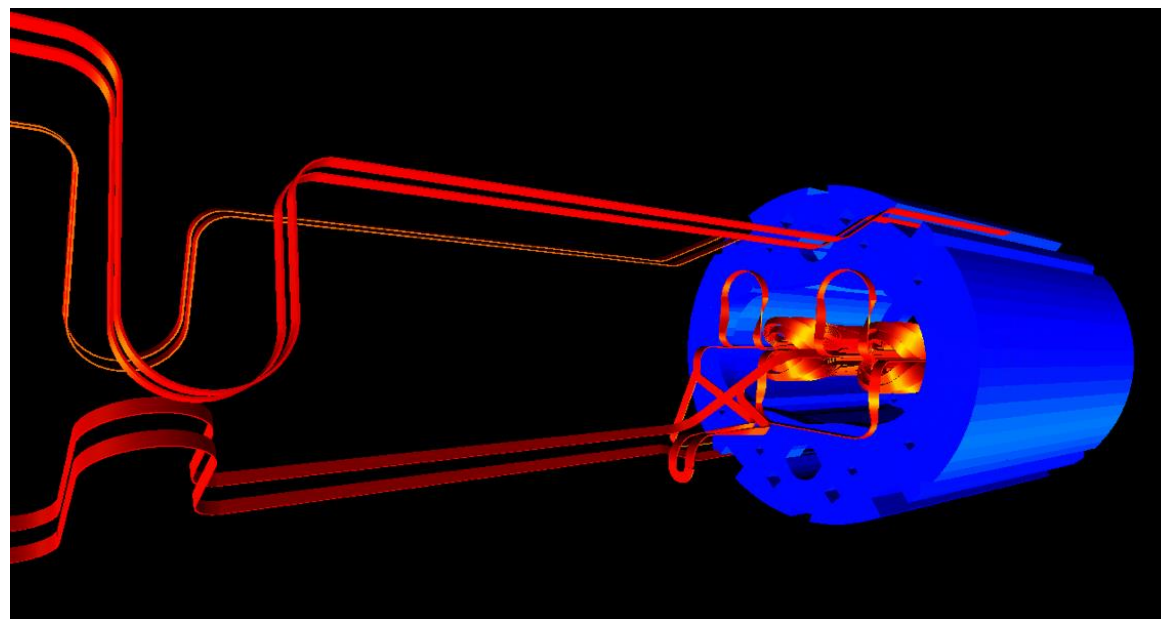
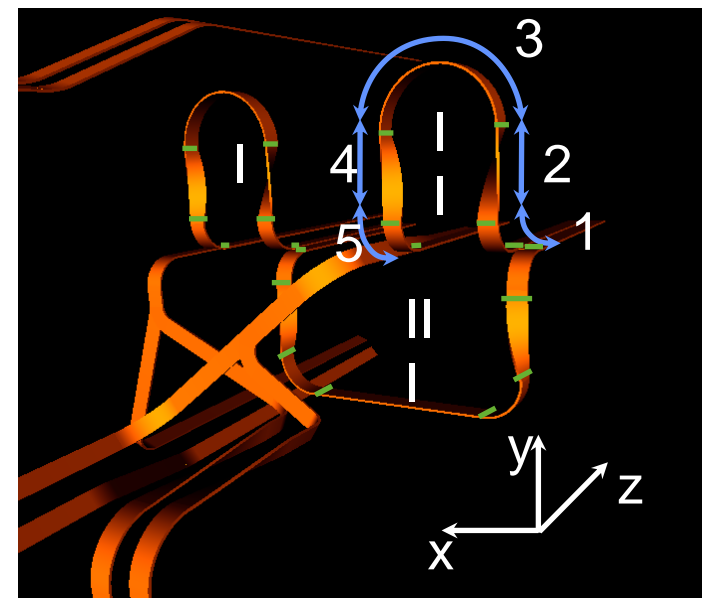


BEM-FEM Coupling



Forces (N) in the Connection Ends of the LHC Main Dipole

I	Fx	Fy	Fz
1	-39.7	-44.0	-45.4
2	-6.5	3.7	-41.7
3	-6.1	88.3	-38.2
4	1.25	3.9	-28.5
5	48.1	-46.7	-48.5
Sum	-2.95	5.2	-202.3

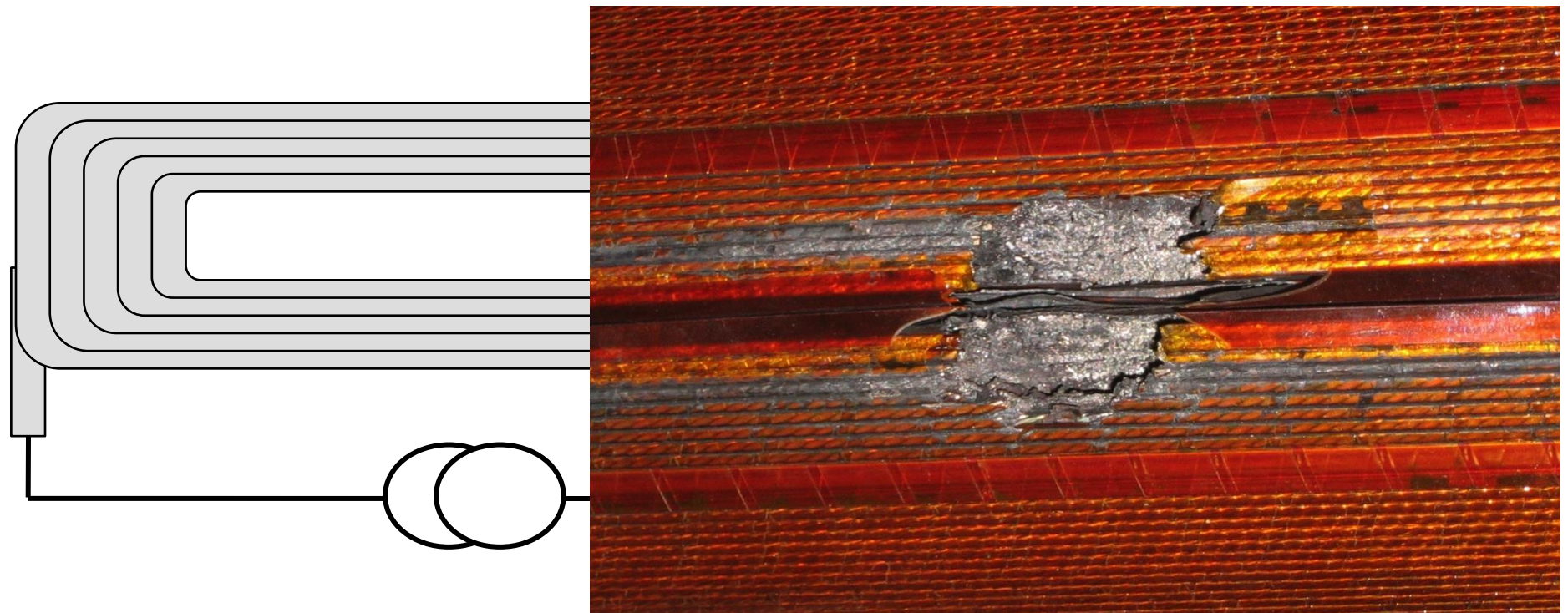


Quench

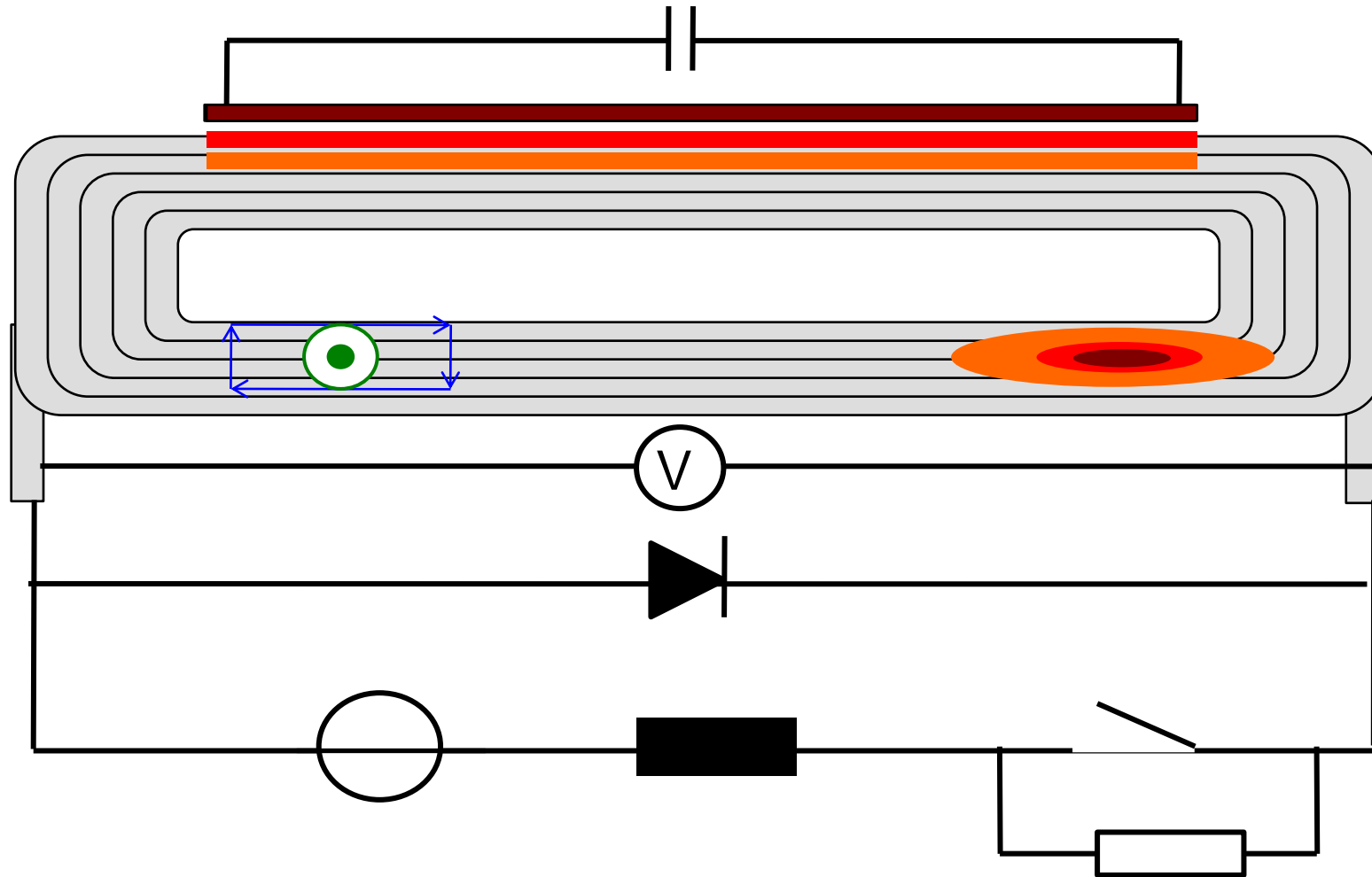
→ **Quench:** Transition from SC to normal conducting state caused by beam losses, conductor movement, eddy currents etc.

→ **Propagation:**

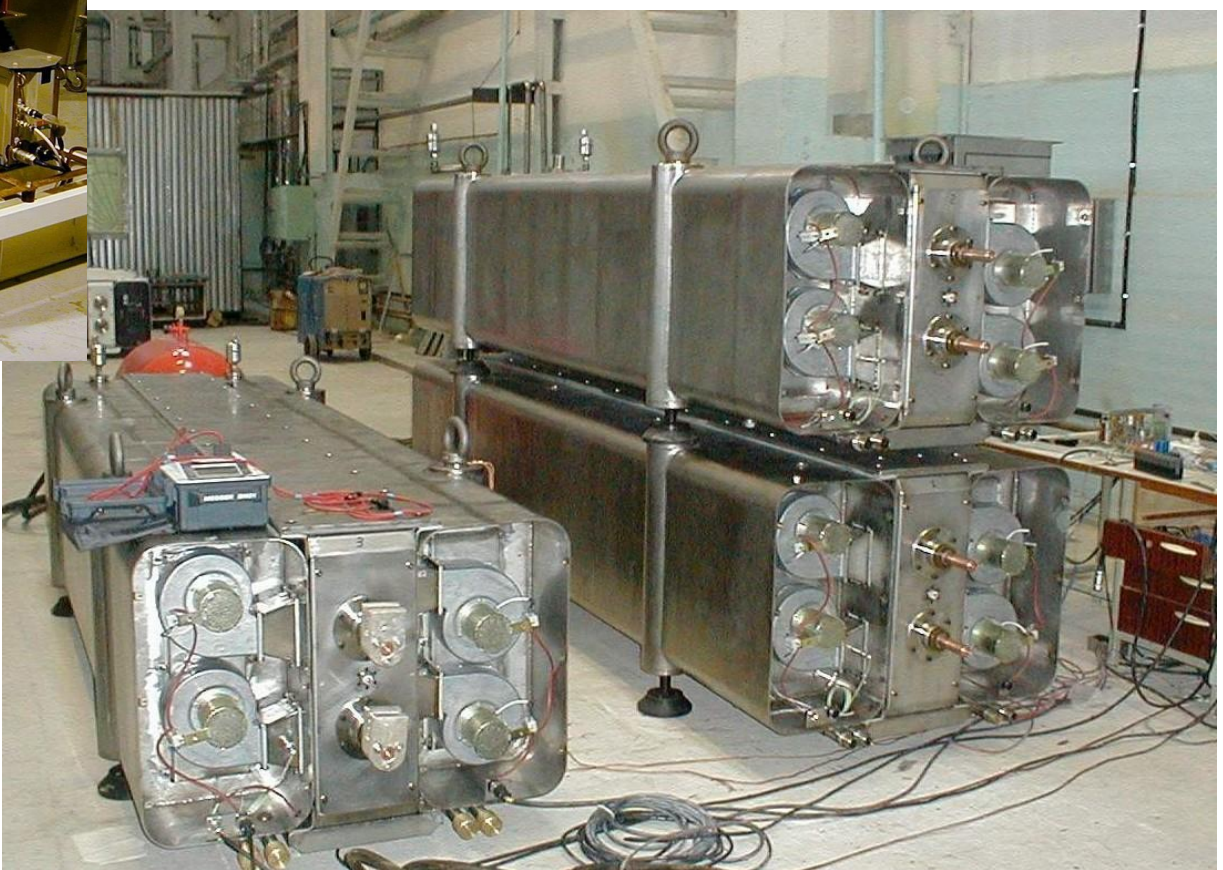
- Normal conducting zone generates Ohmic heat
- Quench- und temperature distribution determined by loss-mechanisms and cooling capacity



Quench Mechanism and Magnet Protection

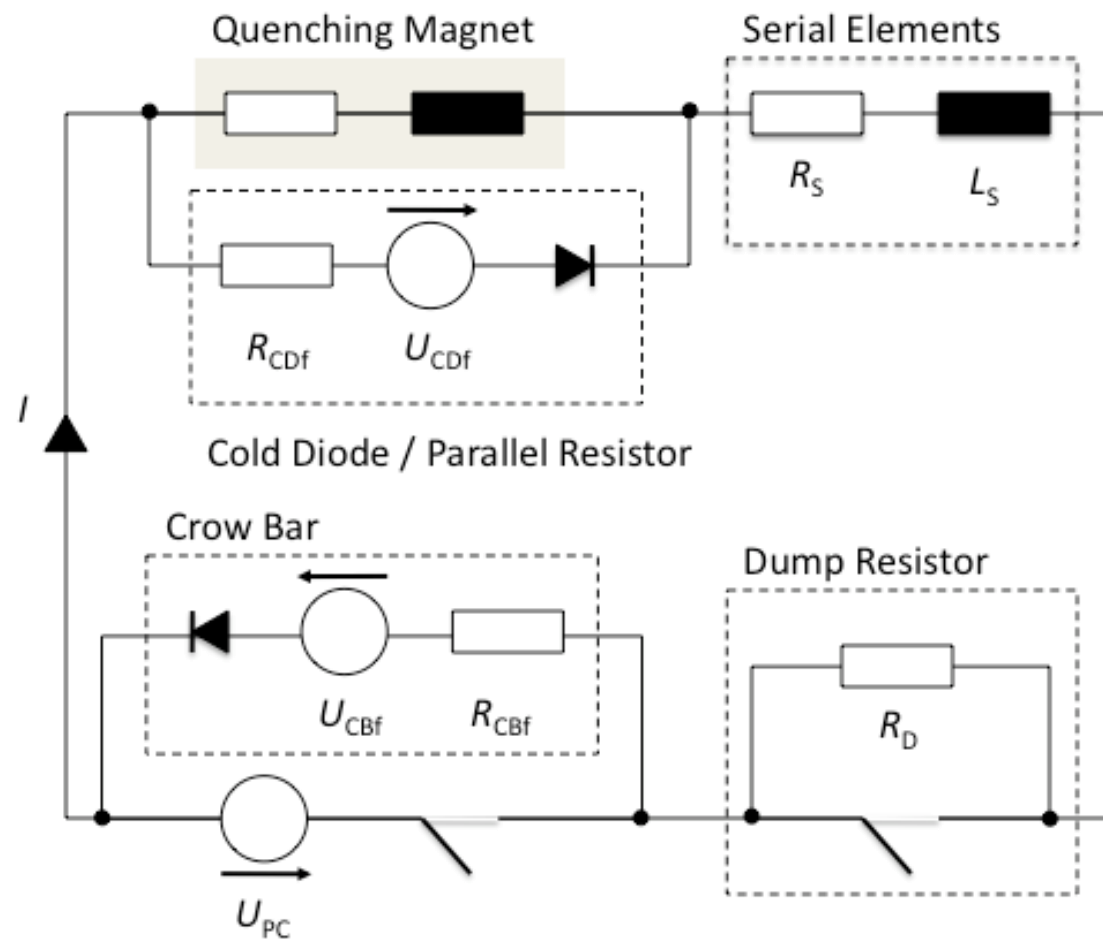


Switches and Dump Resistors



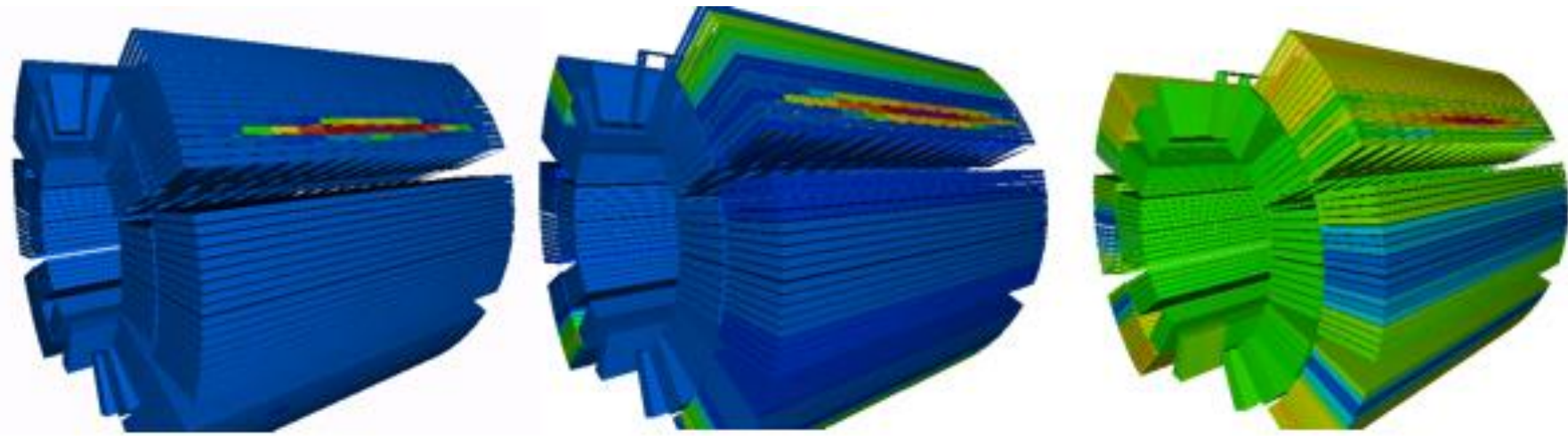
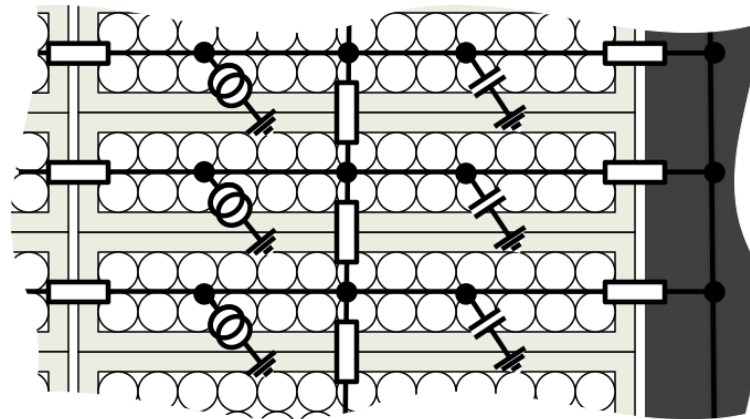
Electrical (External) Network

$$L_d(B) \frac{dI}{dt} = U_{\text{Diode}} - (R_Q(B, T) + R_P(t))I$$

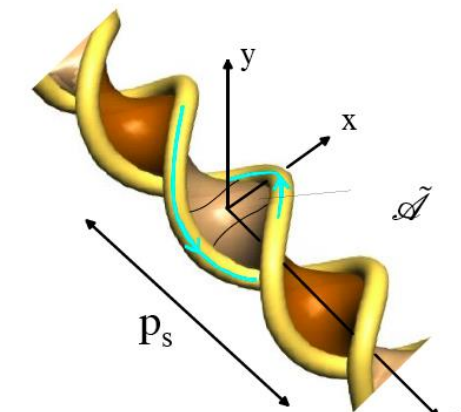
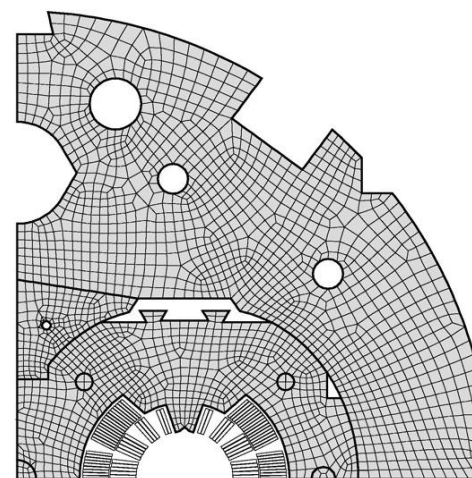
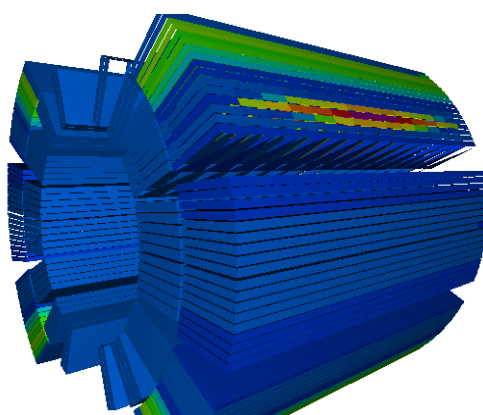
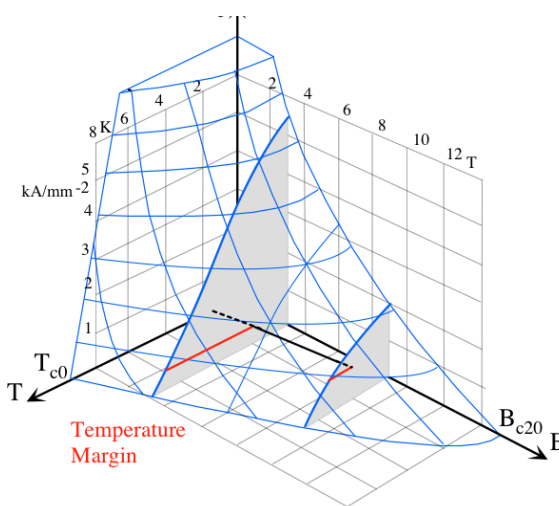
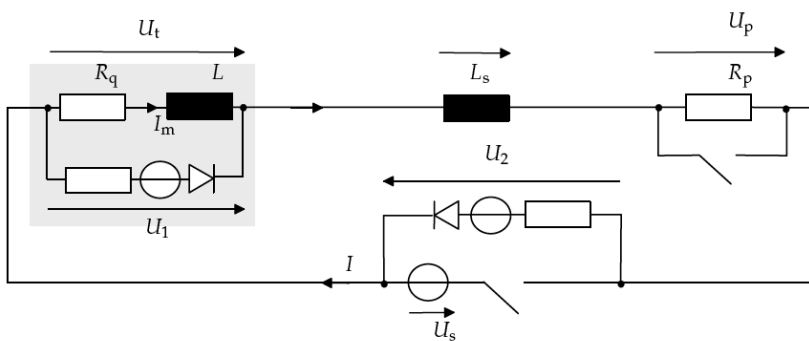


Thermal Model

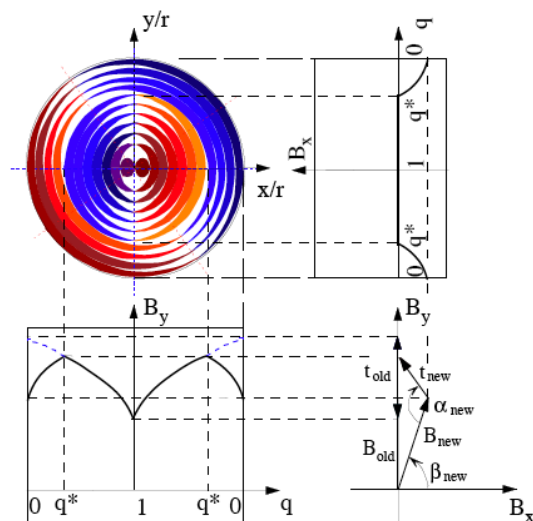
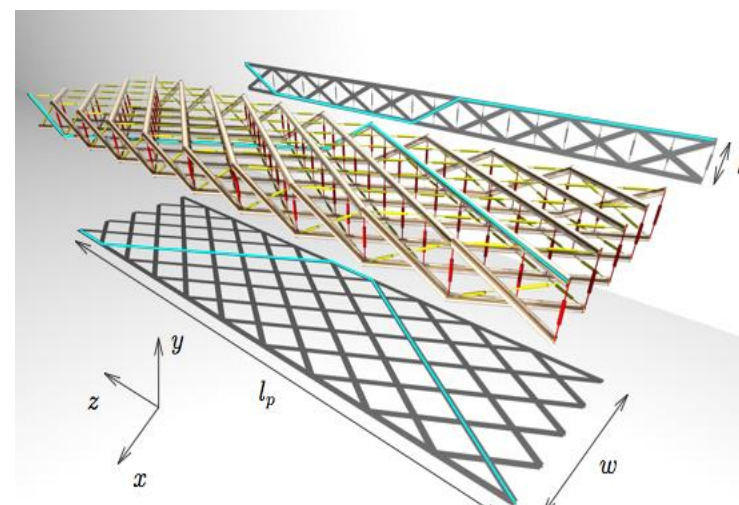
$$c(T) \frac{dT}{dt} = p - \vec{\nabla} \cdot (\kappa(T, B) \vec{\nabla} T)$$



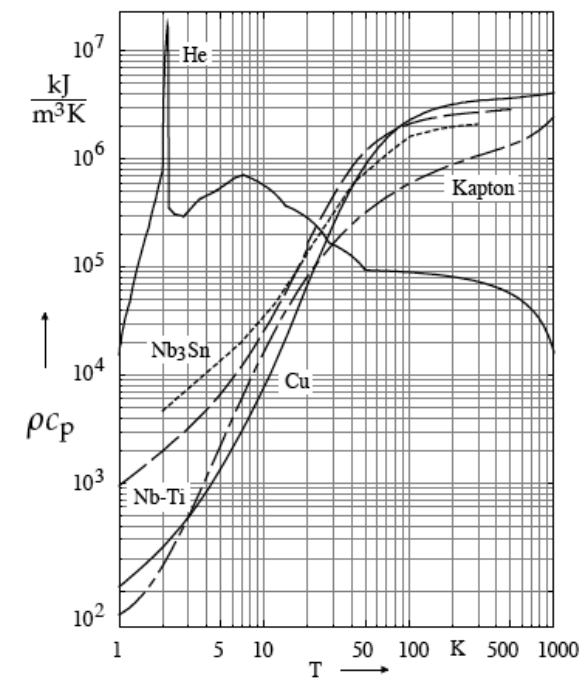
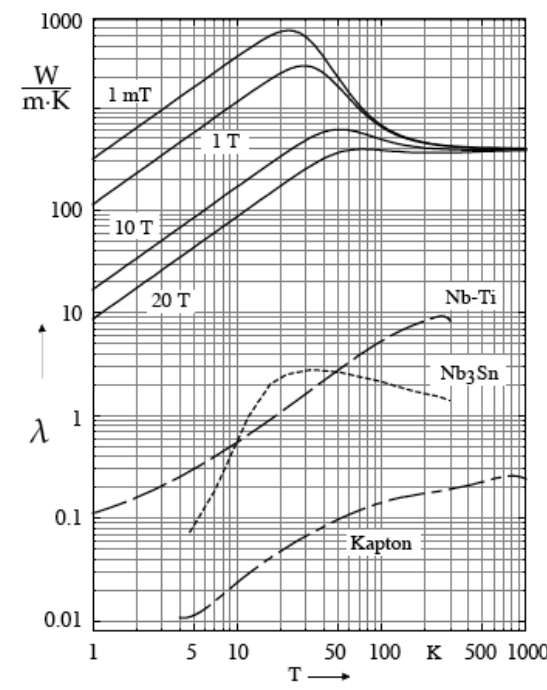
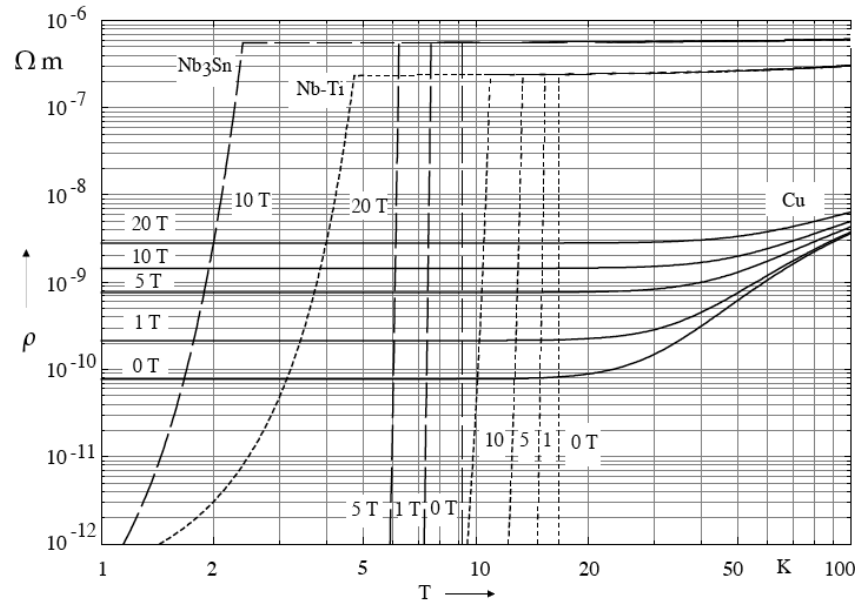
Quench Simulation (Multi-Physics, Multi-Scale)



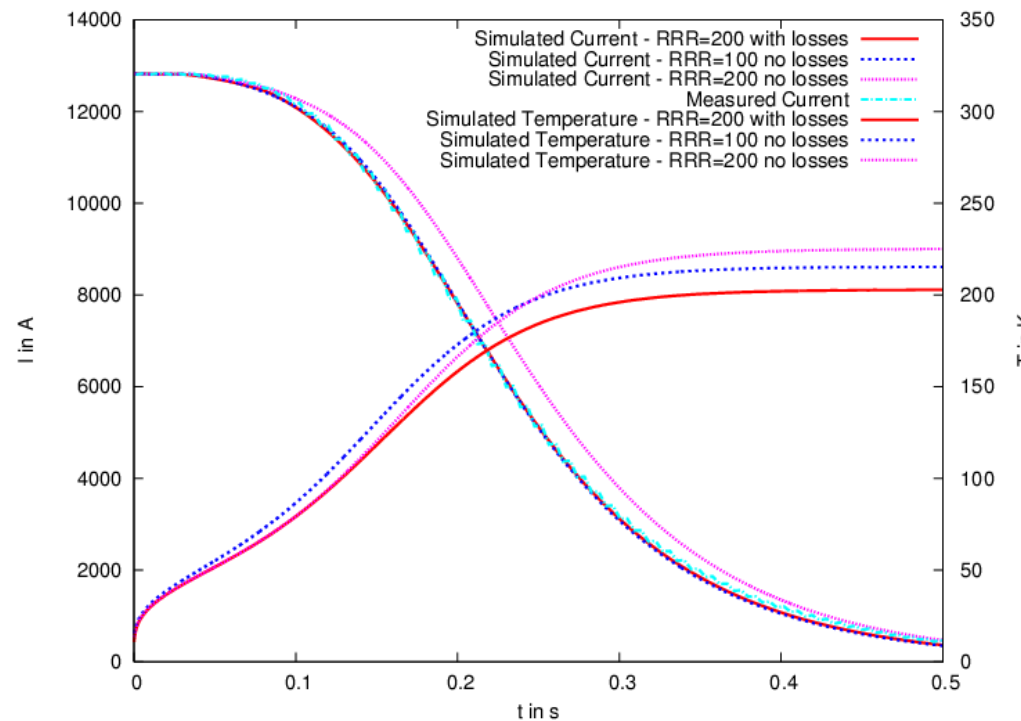
Quench Simulation in ROXIE



Material Parameters



Validation



Empirical parameters:

- RRR
- Ra/Rc
- IFCC effective res.
- heat conductivity
- heat capacity

- Different families of parameters yield exactly the same observable $I(t)$.
- More than one solution exists.
- Great care must be taken to model
 - all relevant phenomena,
 - using realistic material parameters.

Quench Simulation

The challenge of quench simulation:

Model **all relevant physical phenomena** with **adequate accuracy** so that we can be confident to **simulate internal states** of a quenching magnet and understand its behavior.

Validation:

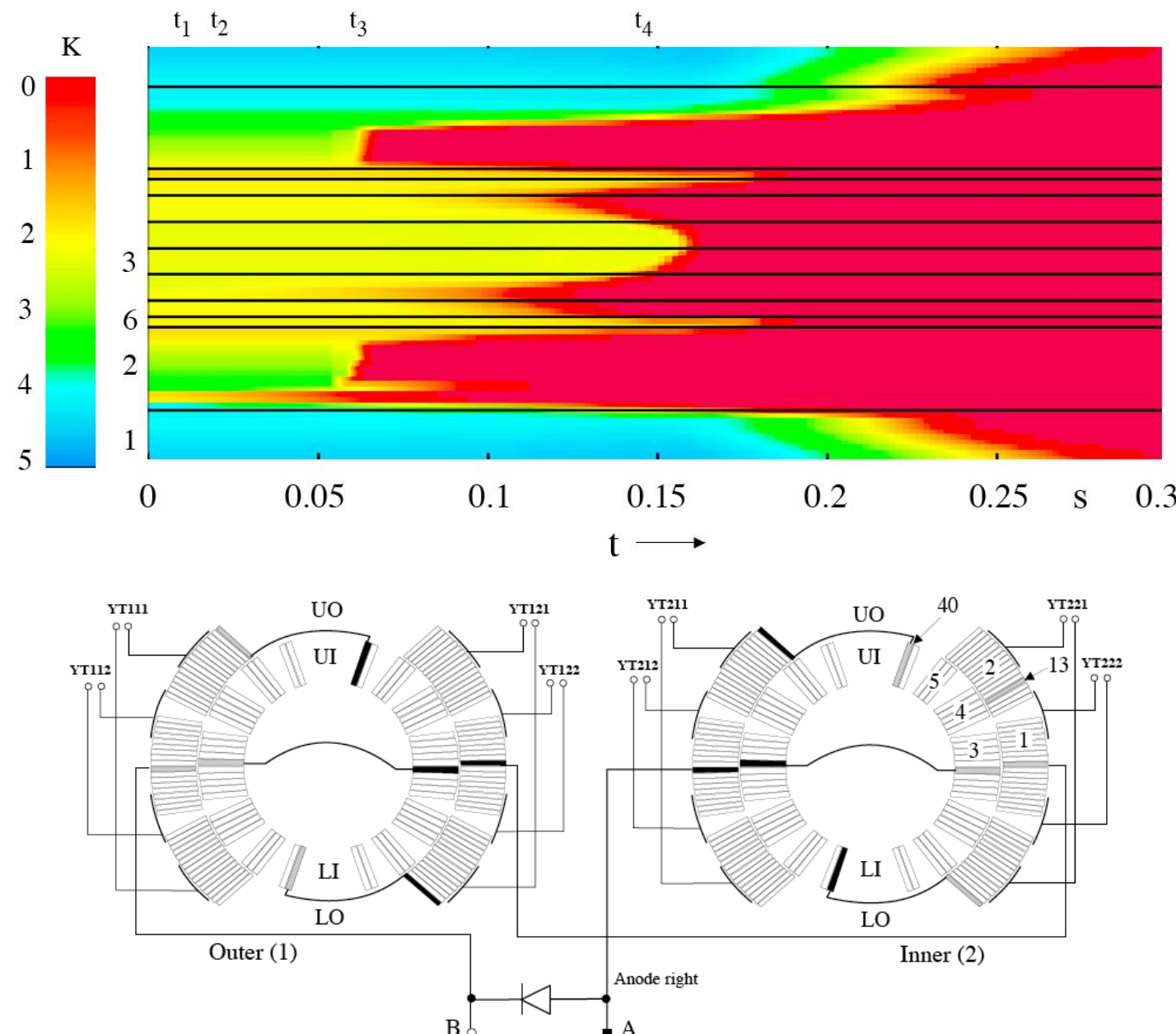
Measured quantities can be reproduced with all material- and model-parameters **within their range of uncertainty**,

Extrapolation and Introspection

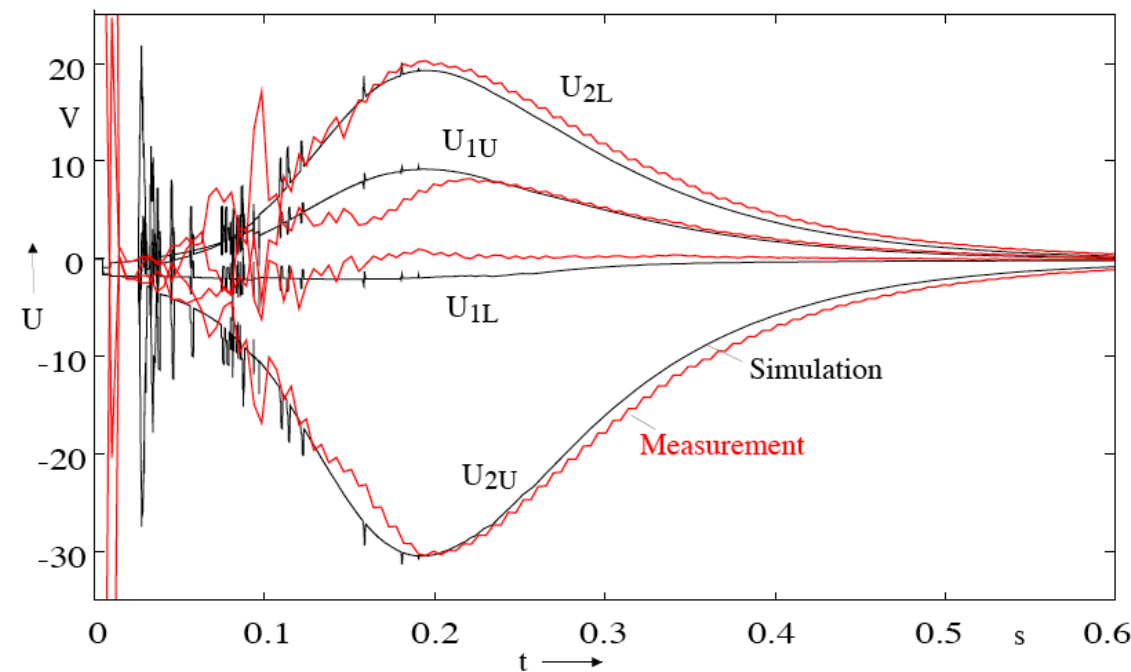
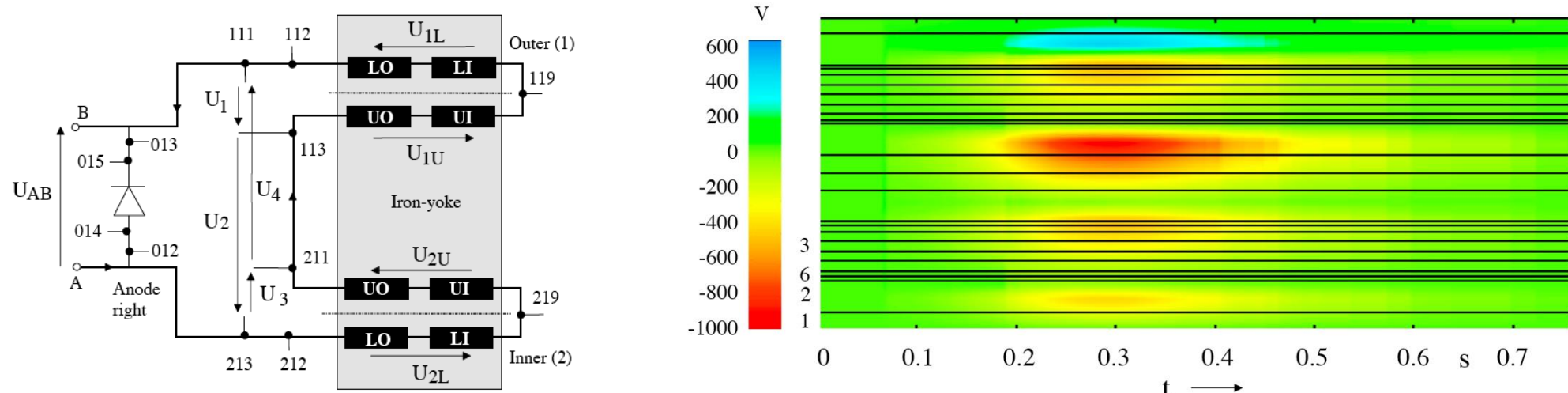
If the above criteria are reached, **extrapolated** results will match measurements **without adaptation of material- and model parameters**. It is then also possible to **simulate internal states** of the magnet that escape measurements.



Introspection (Quench Margin)



Introspection (Voltage Ripples)



Mathematical Formulation of Optimization Problems

$$X \subseteq \mathbb{R}^n$$

$$(x_1, x_2, \dots, x_n)^T \in X$$

$$\min\{f(\mathbf{x})\}$$

$$f : X \rightarrow \mathbb{R}$$

Subject to

$$g_i(\mathbf{x}) \leq 0, \quad i = 1, 2, \dots, m,$$

$$h_j(\mathbf{x}) = 0, \quad j = 1, 2, \dots, p,$$

$$x_{l,\text{lower}} < x_l < x_{l,\text{upper}}, \quad l = 1, 2, \dots, n$$



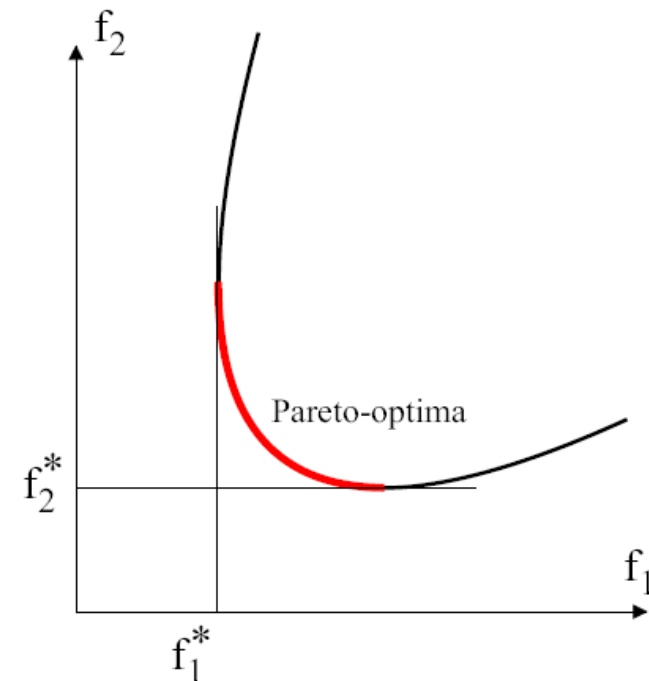
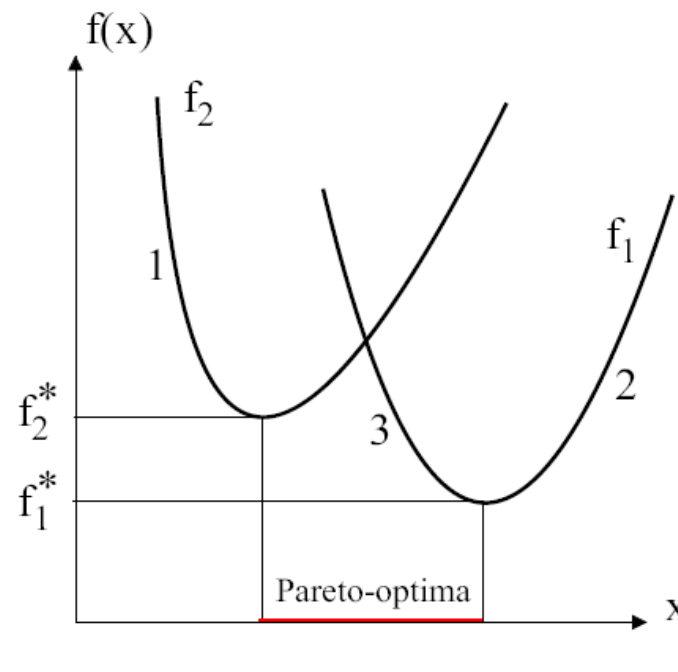
Pareto Optimality

$$\text{MIN } \{\mathbf{f}(\mathbf{x})\} = \text{MIN } \{f_1(\mathbf{x}), f_2(\mathbf{x}), \dots, f_K(\mathbf{x})\}$$

A Pareto optimal solution \mathbf{X}^* is given if there exists no solution with

$$f_k(\mathbf{x}) \leq f_k(\mathbf{x}^*) \quad \forall k \in [1, K],$$

$$f_k(\mathbf{x}) < f_k(\mathbf{x}^*) \quad \text{for at least one } k \in [1, K]$$

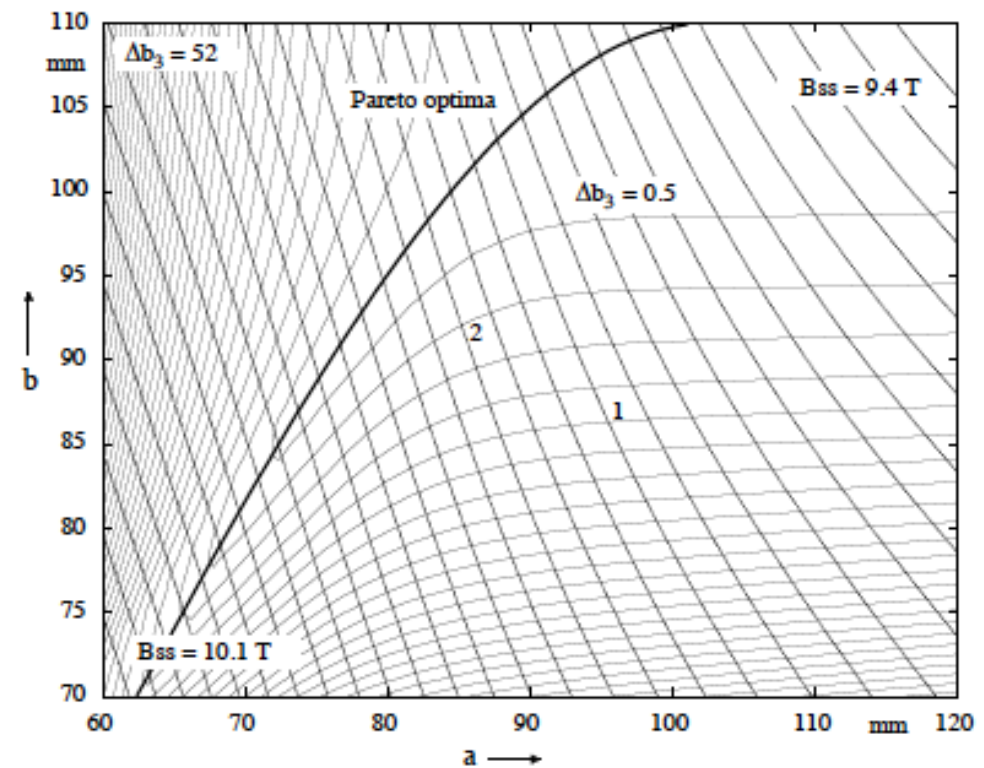
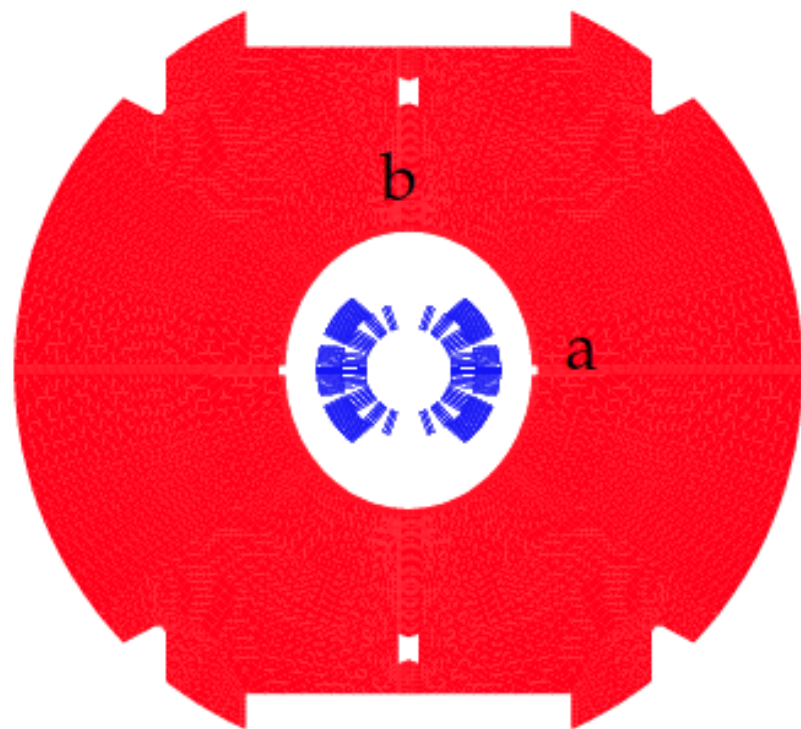


Real World Optimization Problems

- There are only Pareto-optimal solutions
 - Decision making
 - Treatment of nonlinear constraints
 - Optimization algorithms
- The objective conflict is the characteristic of real world optimization problems
- Fuzzy objectives in the concept phase



Objective Conflict Superconducting Magnets

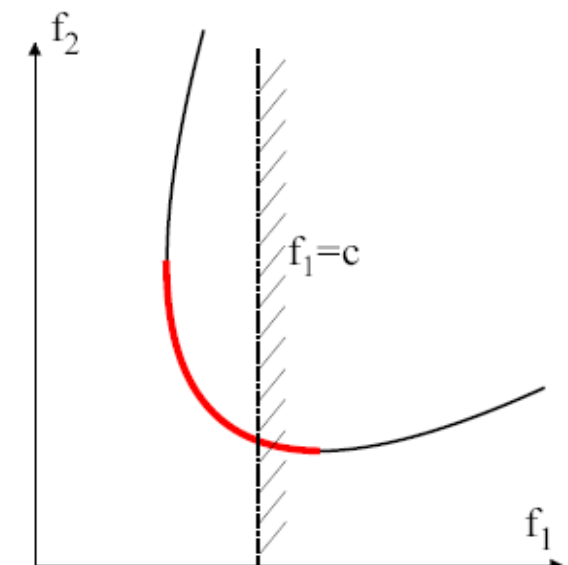
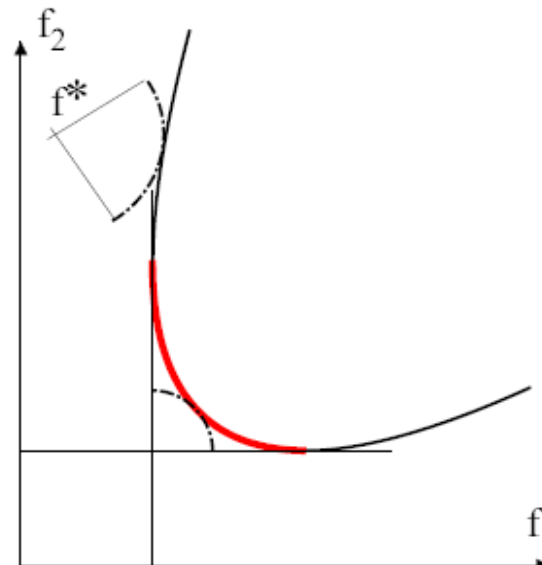
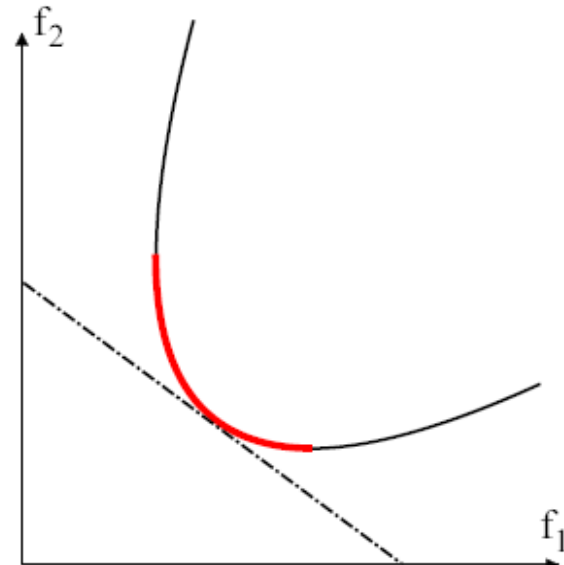


Objective Weighting, Distance Func., Constraint Form.

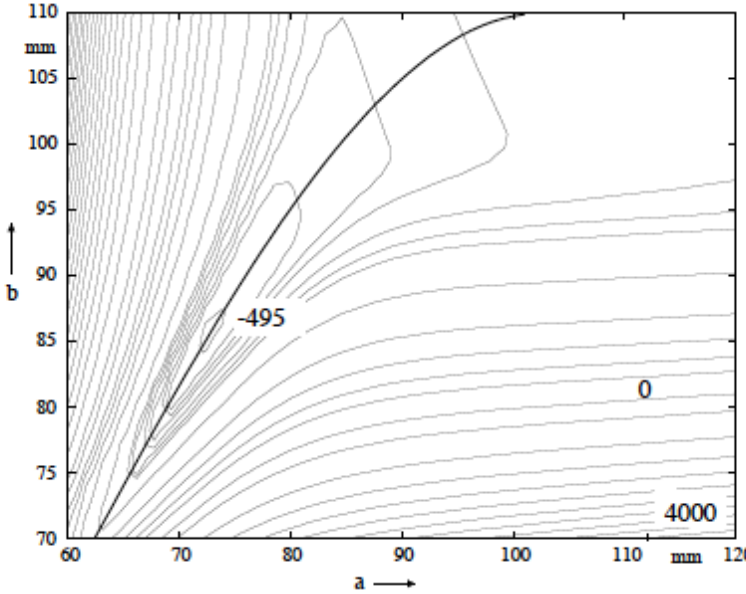
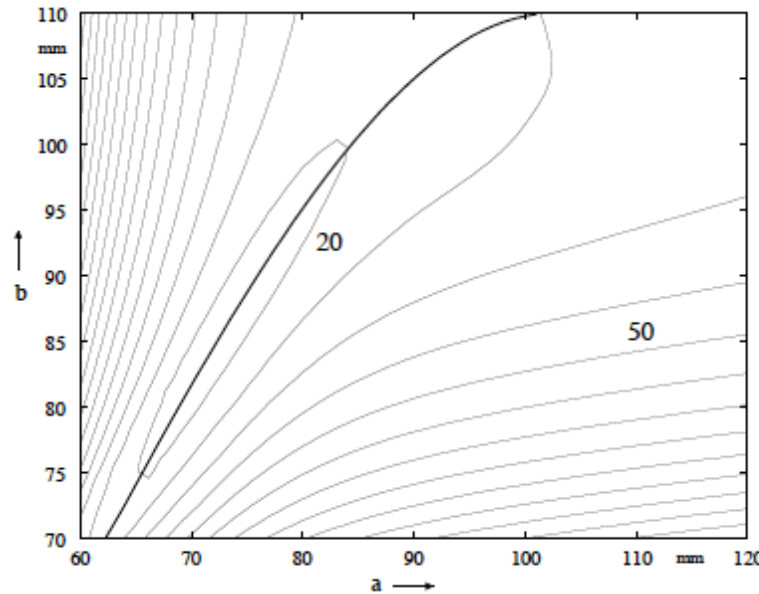
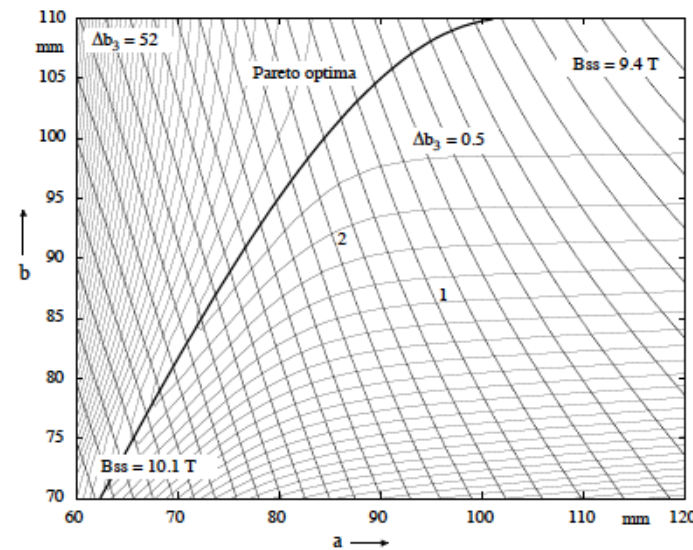
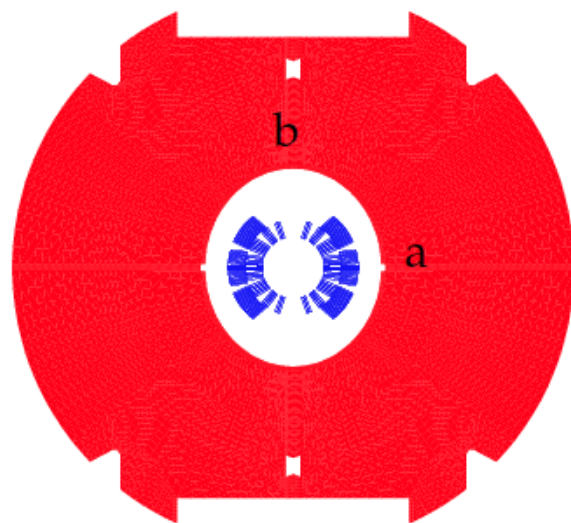
$$\min \left\{ u(\mathbf{f}(\mathbf{x})) := \sum_{k=1}^K t_k f_k(\mathbf{x}) \mid \mathbf{x} \in M \right\}$$

$$\min \left\{ \| \mathbf{z}(\mathbf{x}) \|_2^2 := \sum_{k=1}^K (t_k(f_k^*(\mathbf{x}) - f_k(\mathbf{x})))^2 \mid \mathbf{x} \in M \right\}$$

$$\min \{ f_i(\mathbf{x}) \} \quad \text{s.t.} \quad f_k(\mathbf{x}) - r_k \leq 0$$



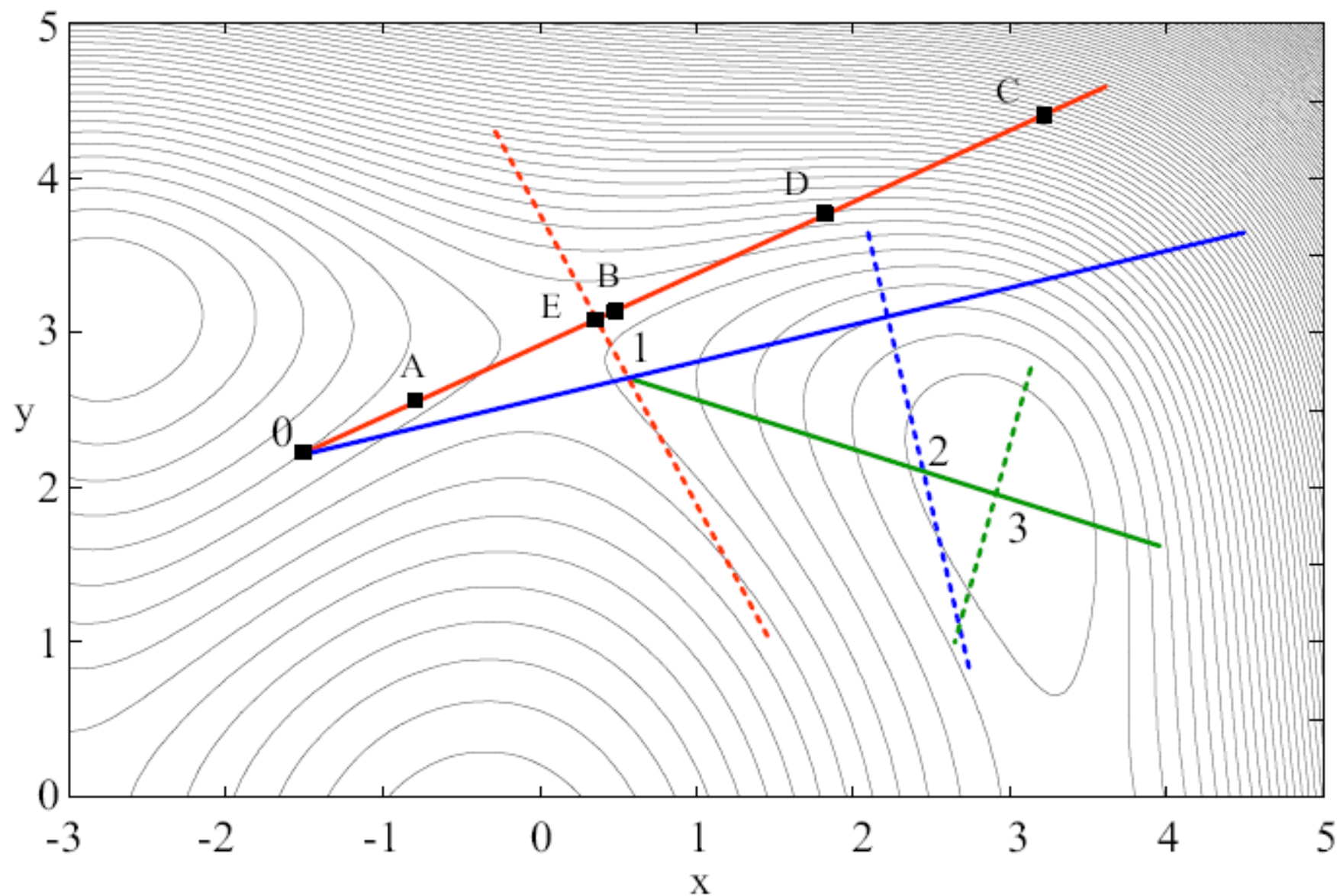
Objective Weighting and L2 Distance Function



Optimization Algorithms

Search methods		
Direct search	Gauss-Seidel	
EXTREM	Jacob	1982
Rosenbrock	Rosenbrock	1960
Powell	Powell	1965
Flexible Polyhedron search	Nelder-Mead	1964
Hooke-Jeeves	Hooke-Jeeves	1962
Gradient methods		
Steepest descend	Cauchy	1847
Newton's method	Newton	1700
Levenberg-Marquard	Levenberg Marquard	1963
Conjugate gradient (CG)	Fletcher-Reeves	1964
Quasi-Newton	Davidon-Fletcher-Powell	1959
Stochastic and neural computing		
Evolutionary	Rechenberg	1964
Genetic algorithms	Fogel-Holland	1987
Neural computing (ANN)	Aarts-Korst	1989





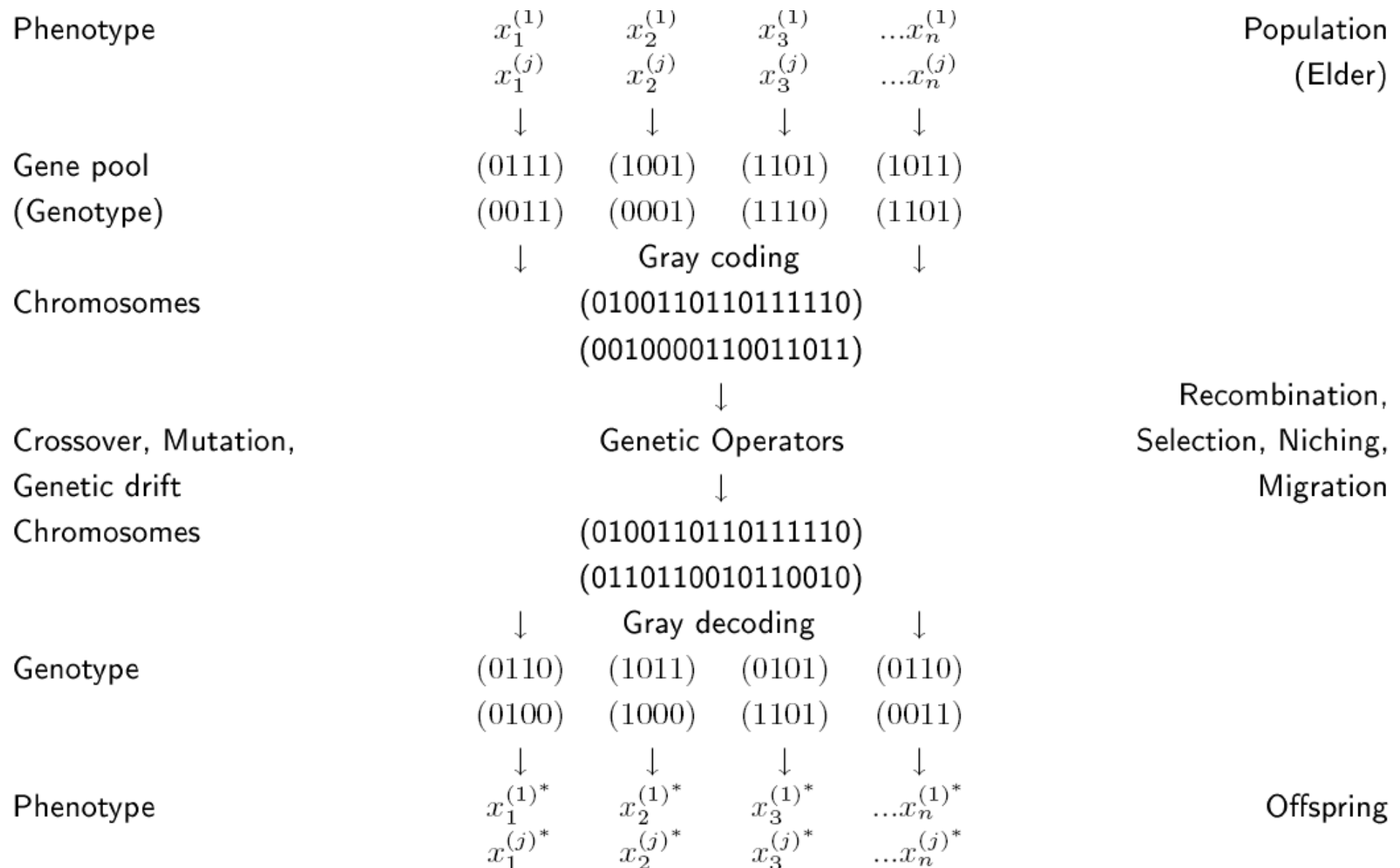
→ Darwin (1860)

- Survival of the fittest
- Variations between individuals of species
- Reproductive populations
- Evolutionary computation (Rechenberg, Schwefel 1964)

→ Mendel (1850)

- Genetic basis of variation
- Coding (Discrete units)
- Genetic algorithms (Holland 1970)
- Niching decreases selective pressure
- Niching genetic algorithms (Mahfoud 1995)

Genetic Algorithms



Encoding

$$g_i = \begin{cases} b_i & \text{if } i = 1 \\ b_{i-1} \oplus b_i & \text{if } i \geq 2 \end{cases}$$
$$\mathbf{b}(13) = (1101)$$
$$(1101) \oplus (\bar{0110}) = (1011)$$

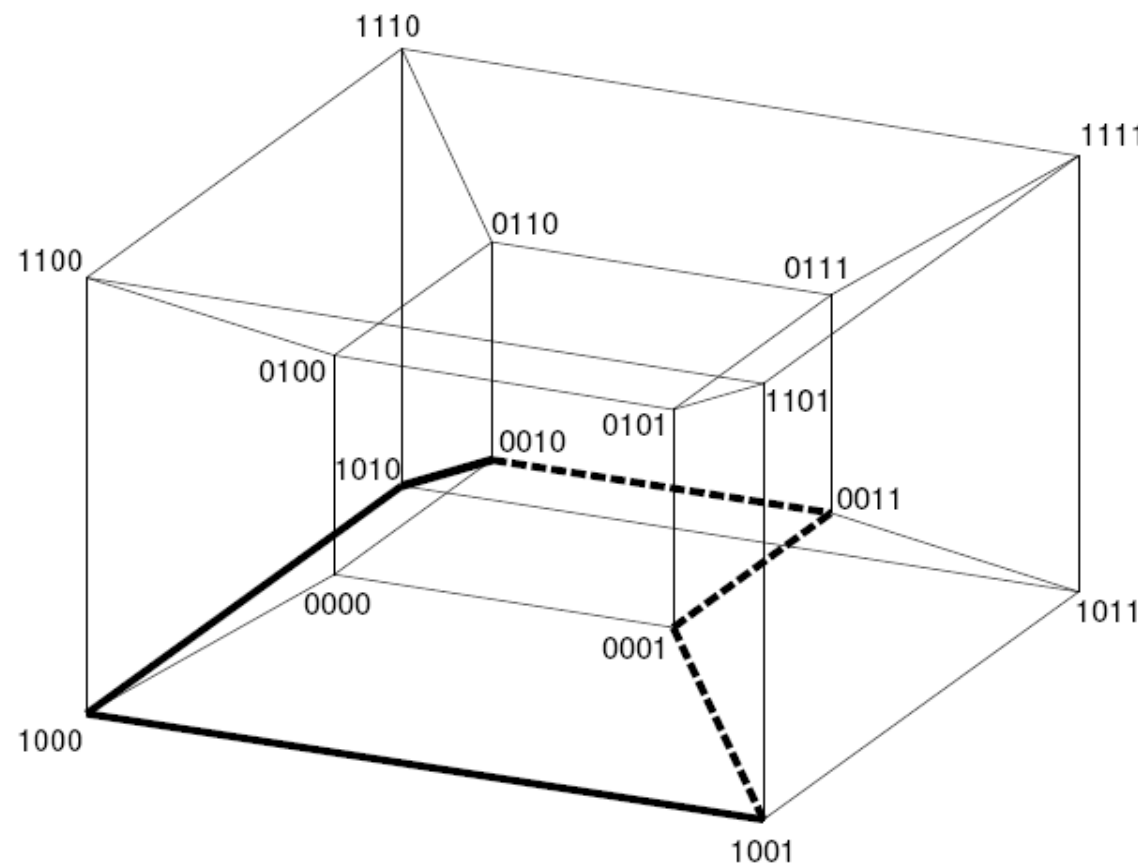
Decimal	Binary	Gray	Decimal	Binary	Gray		
0	(0000)	\leftrightarrow	(0000)	7	(0111)	\leftrightarrow	(0100)
1	(0001)		(0001)	8	(1000)		(1100)
2	(0010)		(0011)	9	(1001)		(1101)
3	(0011)		(0010)	10	(1010)		(1111)
4	(0100)		(0110)	11	(1011)		(1110)
5	(0101)		(0111)	12	(1100)		(1010)
6	(0110)	\leftrightarrow	(0101)	13	(1101)	\leftrightarrow	(1011)

$$b_i = \bigoplus_{j=1}^i g_j$$
$$\mathbf{g} = (1011)$$
$$(1011) \oplus (0101) \oplus (0010) \oplus (0001) = (1101)$$



Genetic Operators: Crossover

Chromosome A:	(0101001 101)	(0101001)	(011)	(0101001 011)
Chromosome B:	(1011010 011)	(1011010)	(101)	(1011010 101)

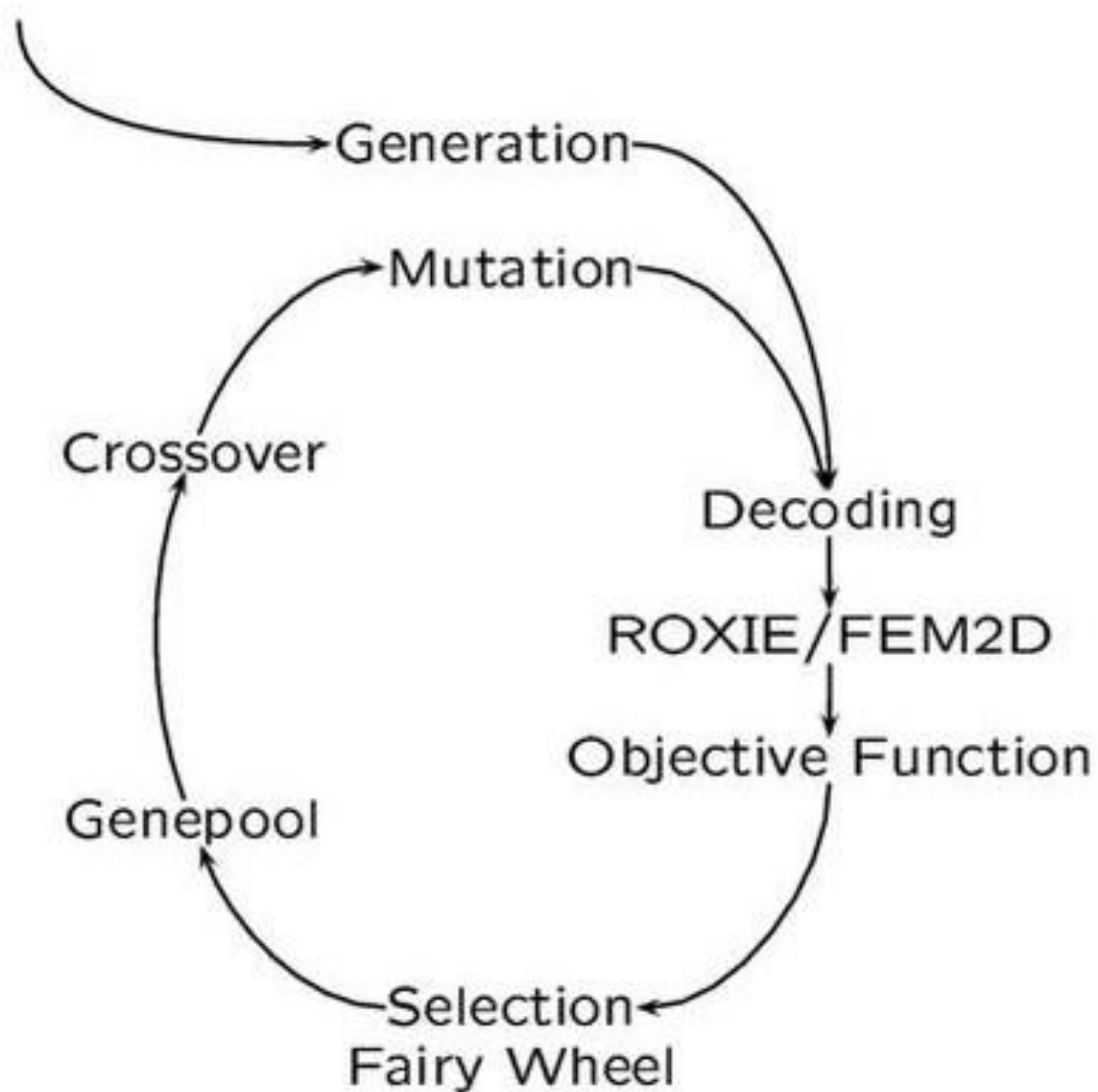


Genetic Operators: Mutation

	10	7	2	1	1	0	Phenotype, k
	1111	0100	0011	0001	0001	0000	Genotype, $g(k)$
a)	10	8	2	1	1	0	Phenotype, k
	1111	1100	0011	0001	0001	0000	Genotype, $g(k)$
b)	13	7	2	1	1	0	Phenotype, k
	1011	0100	0011	0001	0001	0000	Genotype, $g(k)$



Royal Road Algorithm



Fairy Wheel Selection

Index	Parent Population	Objective func. val.	Fitness value		Index of selected Chromosome	Child Population
1	(1000111010)	0.3	0.30		3	(1001101101)
2	(1110101101)	0.4	0.22		1	(1000111010)
3	(1001101101)	0.5	0.18		4	(1011010010)
4	(1011010010)	0.8	0.11	:	1	(1000111010)
5	(0111001100)	0.9	0.10		2	(1110101101)
6	(0111011010)	1.7	0.05		3	(1001101101)
7	(0011000101)	2.6	0.04		1	(1000111010)

Fitness

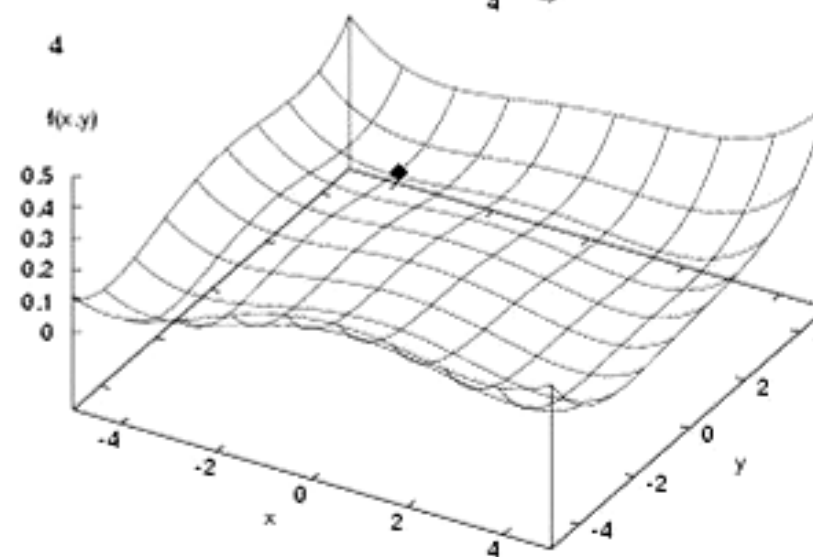
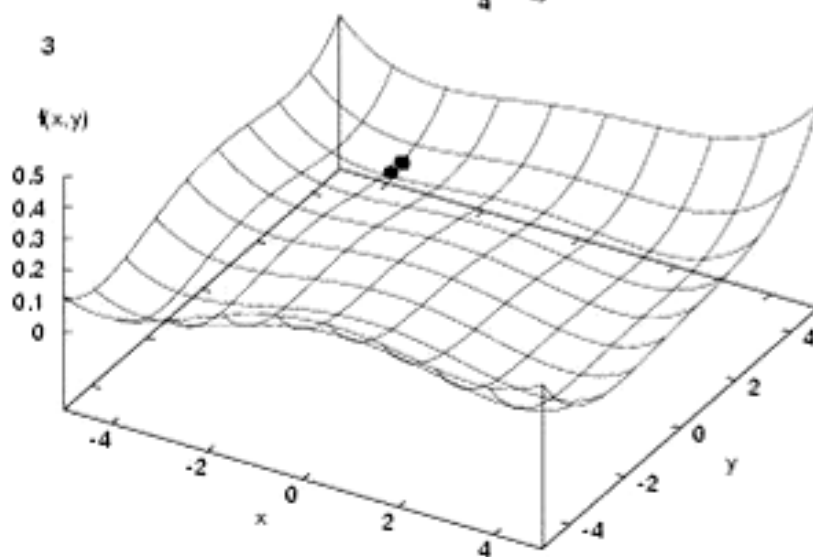
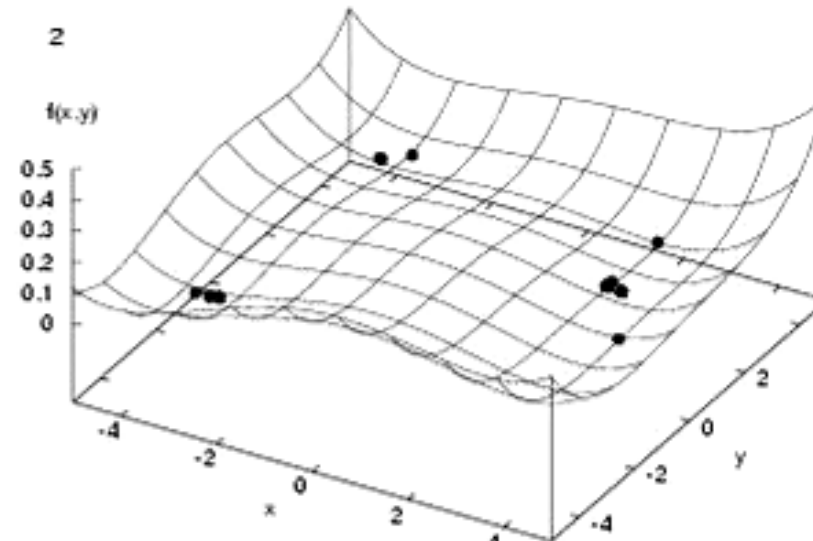
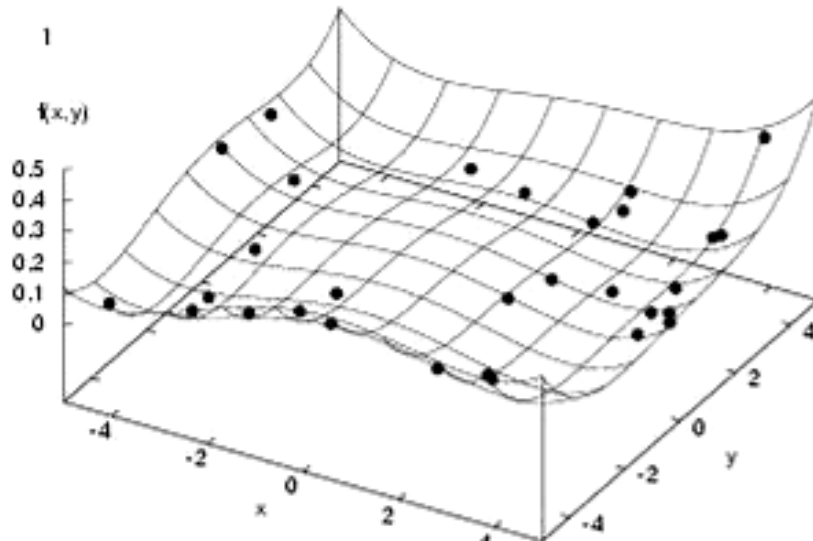
$$e(\mathbf{b}) = f(\mathbf{x}) + c$$

Likelihood of reproduction

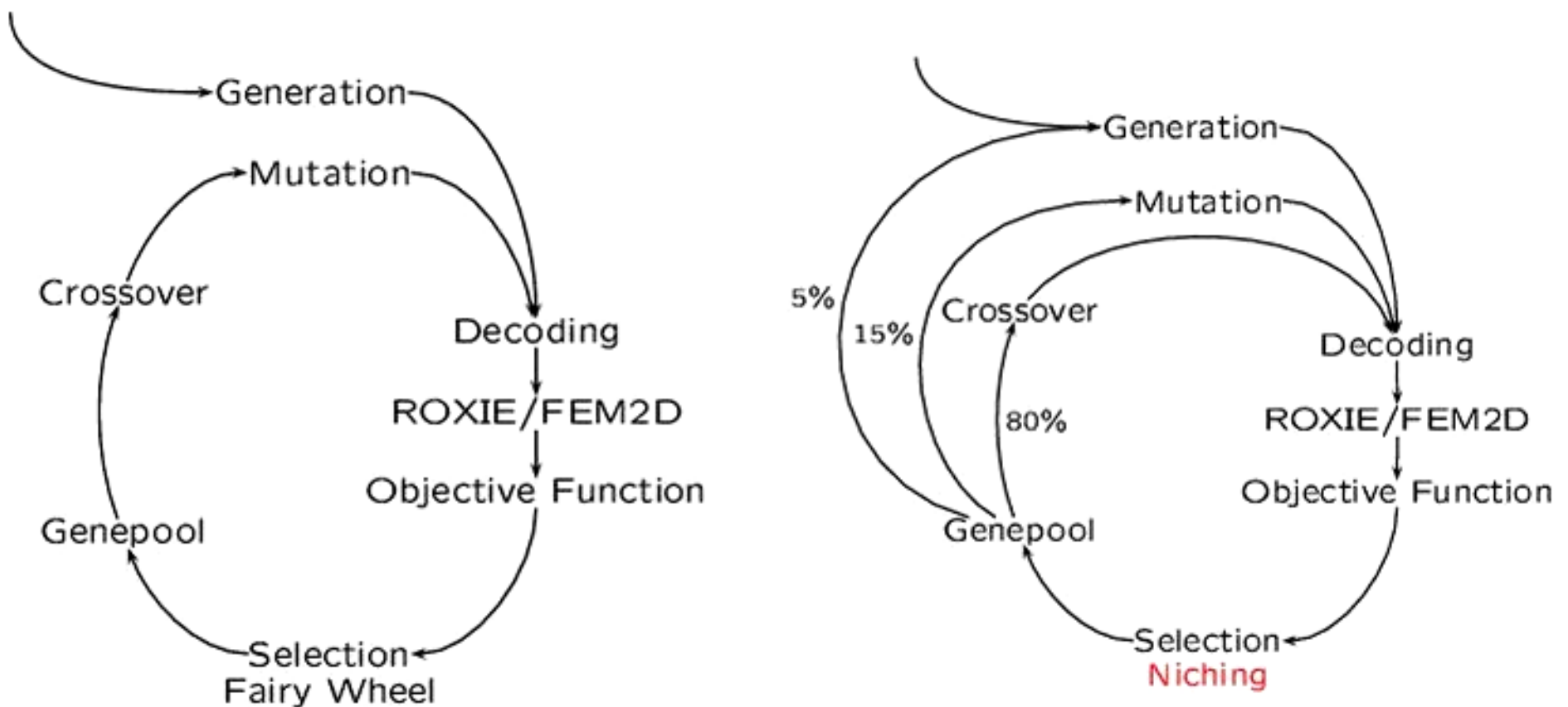
$$p_i := \frac{e(\mathbf{b}_i)}{\sum_{j=1}^n e(\mathbf{b}_j)}$$



Local Properties



Niching Genetic Algorithm



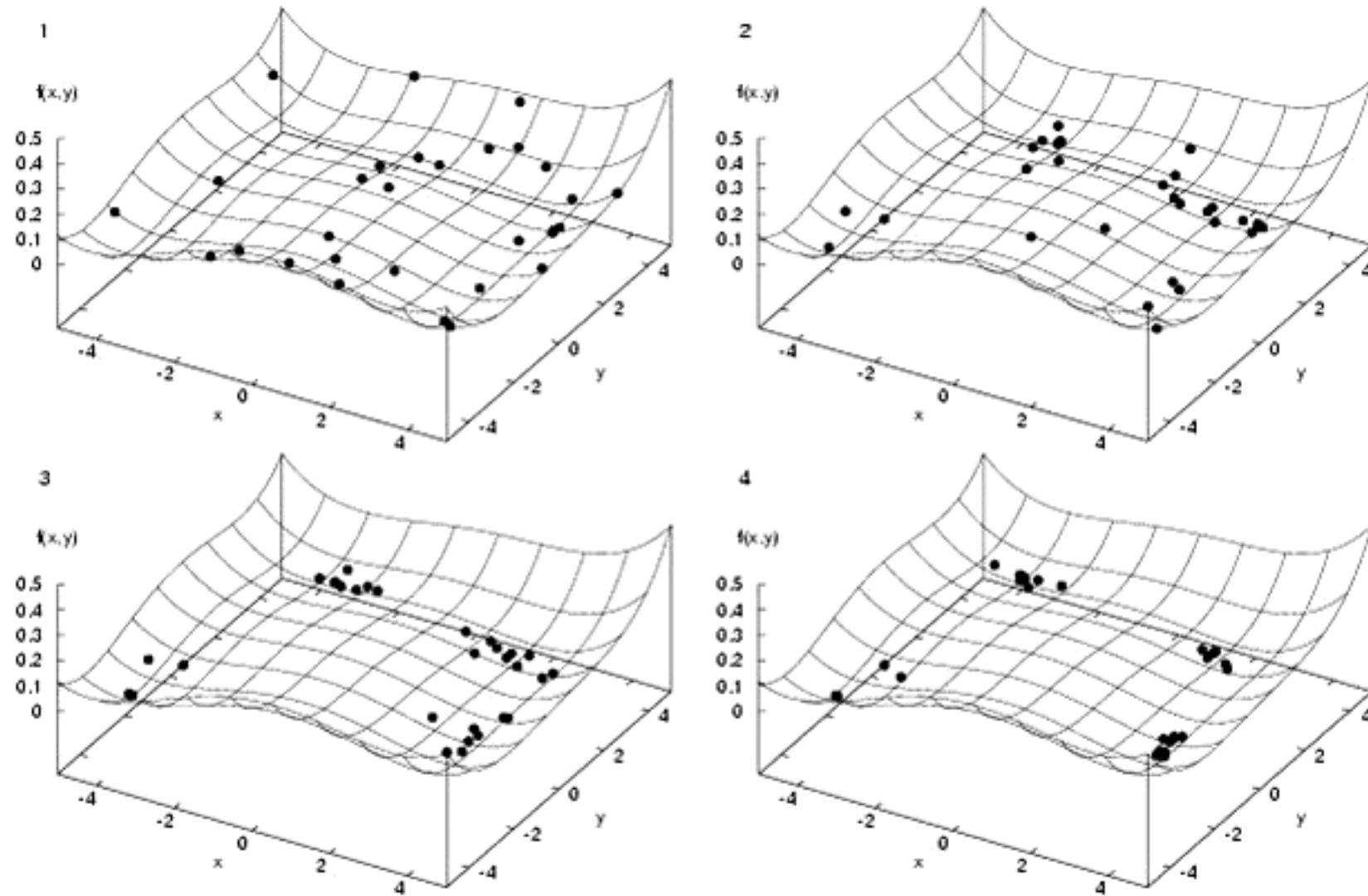
Niching Selection

Index	Parent Population	Objective func. val.	Hamming distance		Index of selected Chromosome	Child Population
1	(1000111010)	0.3	5		1	(1001101101)
2	(1110101101)	0.4	7		2	(1000111010)
3	(1001101101)	0.5	6		3	(1011010010)
4	(1011010010)	0.8	3	:	4	(1000111010)
5	(0111001100)	0.9	3		5	(0111011010)
6	(0111011010)	1.7	2		New	(0011001010)
7	(0011000101)	2.6	4		7	(1000111010)
New	(0011001010)	1.1	0			

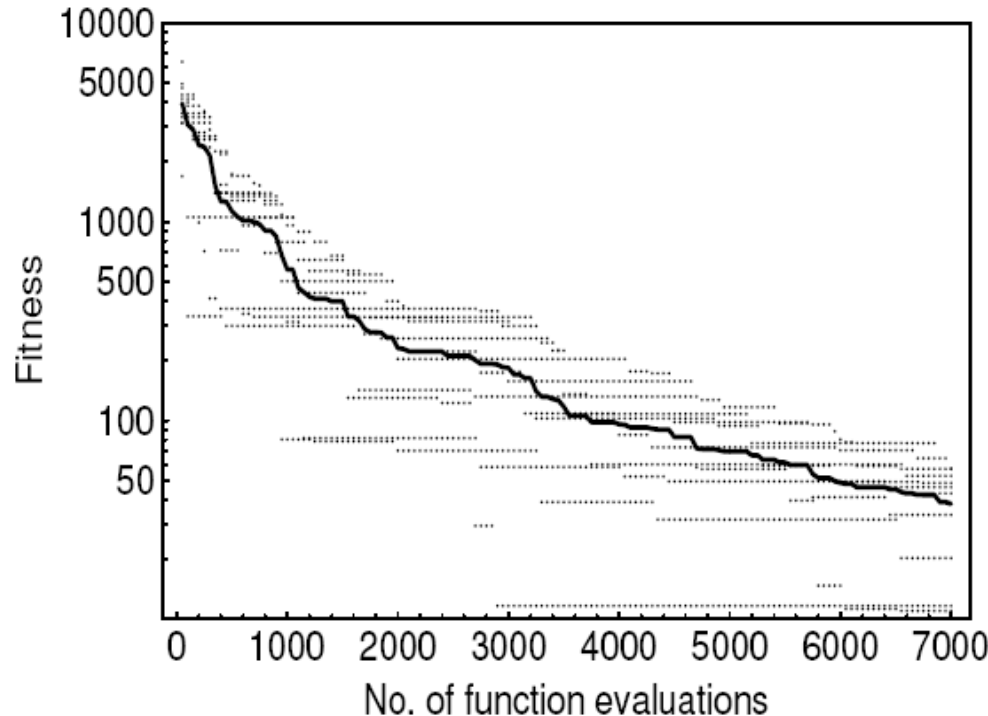
Fitness value

$$F_s(\mathbf{x}_i) := \frac{f(\mathbf{x}_i)}{\sum_{j=1}^n s(d(\mathbf{x}_i, \mathbf{x}_j))}$$

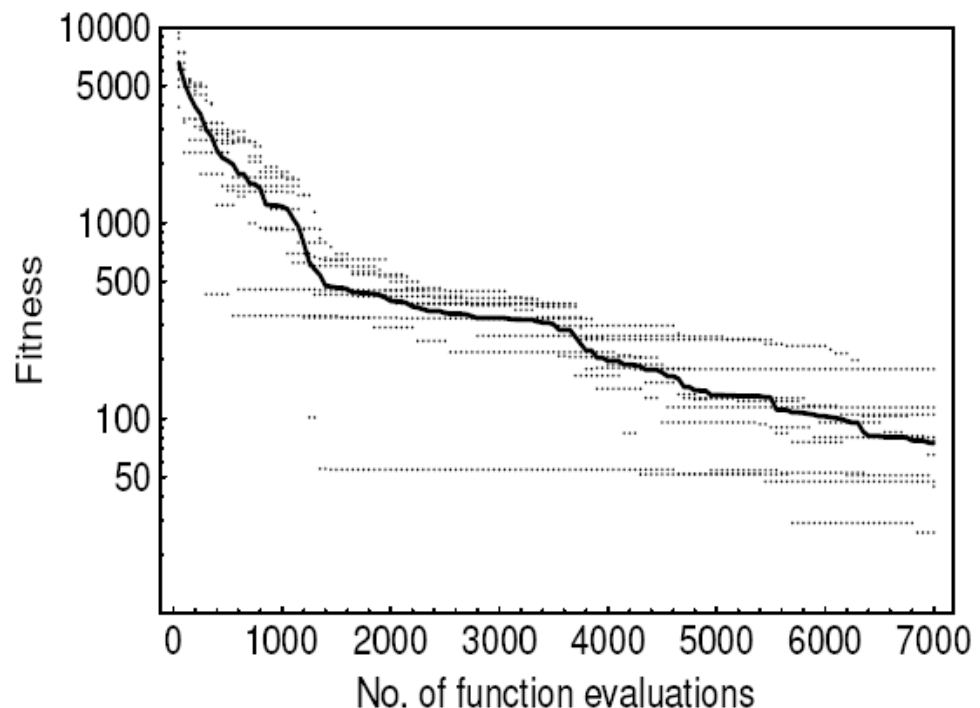
Global Properties



Convergence



Crossover rate 0.8
Mutation rate 0.15
Generation rate 0.05



Crossover rate 0.6
Mutation rate 0.35
Generation rate 0.05

Different Solutions found by Niching Genetic Algorithms

